INFORMATION RECOVERY-BASED MODEL REFERENCE ADAPTIVE
CONTROL FOR FAST ADAPTATION AND IMPROVED TRANSIENTS WITH
AEROSPACE APPLICATIONS

A THESIS SUBMITTED TO
THE GRADUATE SCHOOL OF NATURAL AND APPLIED SCIENCES
OF
MIDDLE EAST TECHNICAL UNIVERSITY

BY

METEHAN YAYLA

IN PARTIAL FULFILLMENT OF THE REQUIREMENTS
FOR
THE DEGREE OF DOCTOR OF PHILOSOPHY
IN
AEROSPACE ENGINEERING

FEBRUARY 2023

Approval of the thesis:

INFORMATION RECOVERY-BASED MODEL REFERENCE ADAPTIVE CONTROL FOR FAST ADAPTATION AND IMPROVED TRANSIENTS WITH AEROSPACE APPLICATIONS

submitted by **METEHAN YAYLA** in partial fulfillment of the requirements for the degree of **Doctor of Philosophy in Aerospace Engineering Department, Middle East Technical University** by,

Prof. Dr. Halil Kalıpçılar
Dean, Graduate School of **Natural and Applied Sciences** _____

Prof. Dr. Serkan Özgen
Head of Department, **Aerospace Engineering** _____

Assist. Prof. Dr. Ali Türker Kutay
Supervisor, **Aerospace Engineering, METU** _____

Examining Committee Members:

Prof. Dr. Ozan Tekinalp
Aerospace Engineering, METU _____

Assist. Prof. Dr. Ali Türker Kutay
Aerospace Engineering, METU _____

Assoc. Prof. Dr. İlkay Yavrucuk
Aerospace Engineering, METU _____

Prof. Dr. Coşku Kasnakoğlu
Electrical and Electronics Engineering, TOBB ETU _____

Assist. Prof. Dr. Yıldıray Yıldız
Mechanical Engineering, Bilkent University _____

Date:13.02.2023

I hereby declare that all information in this document has been obtained and presented in accordance with academic rules and ethical conduct. I also declare that, as required by these rules and conduct, I have fully cited and referenced all material and results that are not original to this work.

Name, Surname: Metehan Yayla

Signature   :

ABSTRACT

INFORMATION RECOVERY-BASED MODEL REFERENCE ADAPTIVE CONTROL FOR FAST ADAPTATION AND IMPROVED TRANSIENTS WITH AEROSPACE APPLICATIONS

Yayla, Metehan

Ph.D., Department of Aerospace Engineering

Supervisor: Assist. Prof. Dr. Ali Türker Kutay

February 2023, 152 pages

This thesis proposes improvements to Filter-based Model Reference Adaptive Control (MRAC) architectures for uncertain dynamical systems. Standard MRAC cannot guarantee closed-loop stability in the presence of bounded perturbations without restrictive persistent excitation of system signals. Robust modifications have been introduced to increase the robustness of standard MRAC and/or guarantee stability without persistent excitation, but little improvement has been achieved in guaranteed transient response. Recently, filter-based solutions have been introduced, among which CMRAC has gained a significant reputation due to its simplicity in application, superior adaptation performance to external disturbances, and improvements on transient performance. However, filter-based methods suffer from losing information during filtering, which can degrade adaptation performance, and assume the uncertainty lies in the span of the control input, which may not hold for many practical systems. This thesis proposes a method to recover information lost during filtering in filter-based adaptive controllers, extending it to cover systems with unknown control effectiveness, and introducing a command governor-based adaptive controller architecture to guarantee strict tracking performance in the presence of

unmatched uncertainty. The proposed information recovery-based model reference adaptive controller (IR-MRAC) is illustrated with an energy-based longitudinal flight controller architecture, which successfully decouples velocity and altitude responses while benefiting from all the advantages of an energy-based controller. The proposed command governor-based adaptive controller is extended to the lateral flight control problem to achieve the desired tracking performance in the presence of both matched and unmatched uncertainties. Closed-loop stability analyses of all proposed methods are illustrated through rigorous Lyapunov's stability analysis, with numerical examples and software-in-the-loop simulations used to validate the proposed methods in a more realistic environment.

ÖZ

HIZLI ADAPTASYON VE GELİŞTİRİLMİŞ GEÇİŞ PERFORMANSI İÇİN BİLGİ KURTARMA TABANLI MODEL REFERANS UYARLAMALI KONTROL VE HAVACILIKTAKİ UYGULAMALARI

Yayla, Metehan

Doktora, Havacılık ve Uzay Mühendisliği Bölümü

Tez Yöneticisi: Dr. Öğr. Üyesi. Ali Türker Kutay

Şubat 2023 , 152 sayfa

Bu tez, belirsiz dinamik sistemler için filtre tabanlı Model Referans Uyarlamalı Kontrol (MRUK) mimarilerinde iyileştirmeler önermektedir. Standart MRUK, bozucu etkilerin varlığında sistem sinyallerinin sürekli uyarımını gerektirmeden kapalı döngü kararlılığını garanti edemez. Gürbüz modifikasyonlar, standart MRUK'un gürbüzlük seviyesini artırmak ve sürekli uyarım gerektirmeden kararlılığı garanti etmek için tanıtılmıştır, ancak garanti edilen geçiş performansına az bir iyileştirme sağlanmıştır. Son zamanlarda filtre tabanlı çözümler tanıtılmıştır. Bunların arasında Kompozit MRUK (KMRUK), basit uygulama, harici bozuculara karşı üstün adaptasyon ve başarılı geçiş performansı noktalarında iyileştirmeler sağladığı için önemli bir itibar kazanmıştır. Ancak, filtreleme sırasında kaybedilen bilgi nedeniyle adaptasyon performansının azalabileceği ve belirsizliğin kontrol girdisi aralığında olduğunu varsaydığından, filtre tabanlı yöntemler birçok pratik sistem için geçerli olmayabilir.

Bu tez, filtre tabanlı uyarlamalı kontrolcülerde filtreleme sırasında kaybedilen bilgiyi

kurtarmak için bir yöntem önermektedir. Bu yöntem, bilinmeyen kontrol etkililiği olan sistemleri de kapsayacak şekilde genişletilmiştir. Ayrıca, eşleşmeyen belirsizlik durumunda üstün takip performansını garanti etmek için bir komut yöneticisi tabanlı uyarlamalı kontrol mimarisi tanıtmaktadır. Önerilen bilgi kurtarma tabanlı model referans uyarlamalı kontrolcü (BK-MRUK), enerji tabanlı bir uzunlamasına uçuş kontrol mimarisi ile gösterilmekte olup, hız ve irtifa yanıtlarını başarıyla ayırmakta ve enerji tabanlı bir kontrolörün tüm avantajlarından yararlanmaktadır. Önerilen komut yöneticisi tabanlı uyarlamalı kontrolcü, eşleşen ve eşleşmeyen belirsizliklerin birlikte olduğu durumlarda, istenen takip performansını elde etmek için yanlamasına uçuş kontrolü problemine genişletilmiştir. Tüm önerilen yöntemlerin kapalı döngü kararlılık analizleri, Lyapunov kararlılık analizi ile gösterilmekte olup, önerilen yöntemlerin daha gerçekçi bir ortamda doğrulanması için sayısal örnekler ve yazılım-döngü simülasyonları kullanılmaktadır.

Anahtar Kelimeler: filtre tabanlı uyarlamalı kontrol, kapalı döngü kararlılık, geçiş performansı, alçak geçirgen filtre, gürbüzlük, eşleşmemiş belirsizlik, komut düzenleyici

to 46104+ victims of Gaziantep-Kahramanmaras-Hatay earthquakes

for three years. I appreciate the attitude of my director Suha Ozgur Dincer, lead engineer Aykut Kutlu, and project manager Hakan Cem Özkara; the best colleagues one can have. Their tolerance during my Ph.D. studies is felt me more comfortable, and encouraged me further.

Finally, I would like to express my deepest gratitudes to my mother, my father, and my brothers Furkan and Oğuzhan for their never ending support. My deepest gratitude is also to my beloved wife Ayşe for her never ending love, for being supportive and understanding. Without them, I would not have achieved this dissertation like many other great things that I have in my life.

TABLE OF CONTENTS

xiv

APPENDICES

LIST OF TABLES

TABLES

LIST OF FIGURES

FIGURES

LIST OF ABBREVIATIONS

2D	2 Dimensional
3D	3 Dimensional
MRAC	Model Reference Adaptive Control
CMRAC	Composite/Combined Model Reference Adaptive Control
CL-MRAC	Concurrent Learning Model Reference Adaptive Control
IR-CMRAC	Information Recovery-based CMRAC
RBF	Radial Basis Function
PE	Persistent Excitation
TECS	Total Energy Control System
RLS	Recursive Least Squares
SISO	Single Input Single Output
MIMO	Multi Input Multi Output
LPV	Linear Parameter Varying
AFCS	Automatic Flight Control System

CHAPTER 1

INTRODUCTION

1.1 Problem Definition and Literature

In this section, three main issues are highlighted in adaptive control to be addressed in the thesis; i) Lost information during low-pass filtering in Composite/Combined Model Reference Adaptive Control, ii) High adaptive learning rates for better tracking performance, iii) Control of uncertain systems with a state-dependent unmatched uncertainty.

1.1.1 Filter-based Adaptive Controller

Model Reference Adaptive Control (MRAC) architectures achieve a desired level of closed-loop stability and performance for uncertain dynamical systems with online adaptive weight update laws. Without restrictive persistent excitation (PE) of system signals, Standard MRAC framework cannot guarantee closed-loop stability in the presence of bounded perturbations using only instantaneous data [1, 2]. To increase the robustness of standard MRAC and/or guarantee stability without PE, well-established robust modifications are introduced in literature [3–9]. Although these modifications improve the robustness of the adaptive controller, little improvements are achieved in the guaranteed transient response. This is an expected result as most of these modifications accommodate only the tracking error in the adaptation. However, it has been widely studied that including the uncertainty estimation error in the adaptive law enhances the transient performance significantly. A few modifications extracting additional information on the uncertainty estimation error are introduced in the literature such as Composite MRAC [10] with its

extension to MIMO systems [11], Concurrent Learning MRAC (CL-MRAC) [12], and q-modification [13]. Motivating from these studies, many other modified adaptive laws have been introduced in the literature. Specifically, Glushchenko et al [14] employs Recursive Least Squares (RLS)-based system identification algorithm in adaptive control architecture. Yet, they assume the existence of state derivative information as direct measurement, which is usually not available for feedback. It is also the main deficiency of Concurrent Learning Model Reference Adaptive Control (CL-MRAC) [12]. In order to overcome this drawback, filter-based solutions are utilized, and information about uncertainty estimation error is extracted using low-pass filters [15–23]. In addition, filter-based methods can successfully limit the frequency range in the control signals. However, it is important to note that filtering methods may suffer from losing information during filtering if the low-pass filters are poorly designed. Hence, the designer should be careful about selecting the bandwidth of the filters.

1.1.2 High Adaptive Gain for Better Tracking

It is well practiced that high-adaptation gains in the adaptive control improve the tracking performance. Thus, it is always desired to set the adaptive gain as high as possible. However, high adaptation gains also decrease the robustness of the closed-loop system in the presence of time-delays, unmodeled dynamics, actuation constraints, and external disturbances with relatively high-frequency (e.g. turbulence, gust). Many studies are introduced in the literature to highlight this fact and suppress the resultant undesired behavior. Yucelen and Haddad [24] introduced a low-frequency learning modification to the standard model reference adaptive control so that the estimated parameters are enforced to stay bounded around their low-pass filtered signals. In this way, high-frequency oscillations in the adaptive input are limited in control, which allows using higher adaptation gains. In the optimal control modification [6], high adaptive gains are allowed at the expense of sacrificed performance. The authors illustrated the efficacy of the proposed method with larger time-delay margins in the presence of high adaptive gains. Unlike these modifications having constant learning rate, there are studies in which the adaptation gain is adjusted with time [14, 25] that improves the tracking performance for uncertain systems

2

with input delay and unmodeled dynamics. In these methods, however, learning rate vanishes if the basis is not sufficiently and/or persistently exciting. Thus, the adaptation is terminated.

1.1.3 Systems with Unmatched Uncertainty

Many MRAC frameworks in the literature (e.g. [3–10, 13]), including all the aforementioned studies, have been restricted to systems with uncertainties lying on the span of the control input, which are called *matched* uncertainties. However, this assumption may not hold for many practical systems with unmatched uncertainties (e.g. magnetic levitation [26]). Although the original nonlinear system does not have an unmatched uncertainty, a nominal linear system (possibly obtained by linearization of the nonlinear model) may introduce an unmatched content if the nominal system is incorrect. In fact, this scenario is highly likely to occur if the the actual plant is not modeled using high-fidelity tools. For instance, in case the system matrix A and input matrix B are unknown for a linear system $\dot{x} = Ax + Bu$, it is not possible to guarantee the matching conditions hold, which might induce unmatched uncertainty to be handled in the controller. In practice, if the nature of the uncertainty upon the system is not only matched but also *unmatched* (e.g., a portion of the uncertainties that are not reachable with the control input), then vast majority of the works on adaptive control does not necessarily guarantee stability (unless the effect of unmatched uncertainties are sufficiently small and/or ignorable), and hence, desired performance cannot be strictly achieved. A few notable contributions are available addressing this point including, for example, [27–38]. Specifically, the authors of [27] and [28] utilize the controller gain optimization using the linear matrix inequality (LMI) tools in the controller design to satisfy the desired boundedness constraints of the tracking errors. Similarly, the authors of [29] use LMI tools to analyze the performance and stability of the adaptive control framework. They investigate the tolerable unmatched uncertainty by the control input and degradation in the performance due to unmatched uncertainty upon the system. The authors of [30] combine the adaptive backstepping technique with the sliding mode control method for output tracking in semi-strict feedback systems. Furthermore, the authors of [31] propose an integral sliding surface that benefits from the radial

basis functions (RBF) neural networks. With the proposed method, their integral sliding mode controller partially suppresses the effects of the unmatched uncertainty and enhances overall system robustness. The authors of [32] utilize a different adaptive control framework based on low-pass filtered input command and fast state estimation scheme. The authors of [33] present an indirect certainty equivalence adaptive control (CEAC) framework that uses fast identification model and command filtered backstepping controller. Authors of [39] claim that they achieved guaranteed parameter convergence for the systems with an unmatched uncertainty. However, their results are far-fetched from the truth as so-called 'unmatched uncertainty' lies in the range space of control input in their system description. In study [40], another CEAC solution is proposed to deal with unmatched uncertainties. Yet, their solution is restricted to nonlinear systems with relative degree two. In studies [32] and [33], high adaptation gains may need to be employed to effectively suppress the effects of uncertainties since they only rely on instantaneous data, which can be highly prone to issues such as poor closed-loop system performance or even instability in the presence of unmodeled dynamics, actuation constraints, or measurement noise to name but a few examples. Authors of [34] introduce an uncertainty identification method for both matched and unmatched uncertainties. They utilize a hybrid adaptive control architecture for a class of unmatched uncertainties. However, tracking performance is not guaranteed before the identification phase. Furthermore, in studies [32] and [34], there are no performance recovery mechanisms which leads to performance degradation as the unmatched uncertainty is increased. In addition, the proposed method in [33] covers the systems with single input, only. Authors of [35] proposed a command governor-based adaptive controller to suppress the undesired effects of unmatched disturbances using backstepping control method. Similarly, authors of [37] proposes a disturbance observer-based hybrid control system to deal with unmatched disturbances. In both studies [35] and [37], authors considered only bounded time-varying unmatched disturbances, which is a simpler and easier problem to solve compared to state-dependent unmatched uncertainties. Lastly, authors of [38] introduces a robust control method to deal with unmatched uncertainties using fuzzy-set theory with deterministic control robust control input. As there is no performance recovery mechanism in this study, performance degradation may arise in the presence of large unmatched uncertainties.

4

1.1.4   Energy-based Longitudinal Flight Control

For the last decades, many automatic flight control systems (AFCS) have been designed relying on the classical control theory which uses Single Input-Single Output (SISO) design methods (see [41–46]). In traditional SISO controllers, each control channel is reserved to the control of one flight variable. Hence, the overall control approach is able to realize only one function at a time. Furthermore, SISO design methods inherently assume that the controlled states are barely coupled. In a conventional longitudinal flight controller, autothrottle is assigned to control the airspeed using thrust and autopilot is responsible for the flight path angle control (or altitude hold) using the elevator. Such a task sharing causes a basic conceptual flaw in autothrottle control system that one of the most important state variables -flight path angle- is left out in determining the required thrust. In addition, the autopilot control system has the basic deficiency of not knowing the airplane's steady state climb and descent limits. One solution to suppress the effects of cross-couplings could be using high feedback gains which may result in excessive control activity and high fuel consumption [47]. Yet, under certain flight conditions, autopilot may cause speed instabilities during flight path control at constant throttle. Similarly, autothrottle may result in unstable flight path response at constant elevator deflection. Because of these reasons, a desired flight path and airspeed responses can only be achieved if both autothrottle and autopilot work in coordination. However, it requires a significant amount of man-hours and flight testing to the coordinated co-operation of autopilot and autothrottle [48]. Another issue with the SISO AFCS designs is their inability to control the energy-state of the aircraft. Satisfactory energy-management is possible with fully integrated longitudinal flight control algorithm taking the aircraft performance and flight envelope into account. As depicted earlier, traditional SISO AFCS designs suffer from coordination between autothrottle and autopilot control systems, and insufficiency of envelope protection covering the entire flight regime. Sadly, this was a contributing factor in an Airbus A330 crash (see [49,50] for details). Even the latest generation SISO designs have not satisfactorily solved the energy management, flight envelope protection, and control coupling issues. Recognizing that, NASA and Boeing has developed an energy based flight controller, Total Energy Control System (TECS), to offer solutions to these problems [51].

Unlike conventional SISO AFCS designs, TECS employs Multi Input-Multi Output (MIMO) control to achieve the desired flight performance in a much simpler manner. MIMO TECS strategy relies on the Hamiltonian and Lagrangian of the aircraft. Note that the Hamiltonian corresponds to total mechanical energy of the aircraft if the generalized coordinates are expressed in the inertial frame. In that case, the Hamiltonian can be stated as the summation of kinetic energy and potential energy of the aircraft. It can be depicted from the aircraft performance considerations that the engine is the only source to adjust the required power, which is necessary to realize the desired longitudinal acceleration and flight path commands. Hence, the throttle channel is assigned to the control of the total energy of the aircraft. Assuming that the additional drag due to elevator deflection is negligible, the elevator has a conservative effect on the aircraft total energy. So, the elevator is assigned to distribute the total energy between kinetic and potential energy. Since the elevator has a conservative effect on the aircraft energy whereas the thrust directly affects it, it can be inferred that the elevator and throttle command responses are orthogonal to each other in terms of total energy and its distribution. Therefore, it becomes quite possible to achieve desired decoupled speed and flight path responses as the control of the aircraft total energy and its distribution are decoupled, as well. A few success of the TECS architecture over the conventional SISO AFCS design can be listed as follows: *i*) Functional overlap is eliminated. *ii*) generic and reusable design with minimal aircraft specific information is achieved. *iii*) Consistent operation at each flight condition and over combination of flight modes is ensured. *iv*) Pilot-like control strategy is achieved with efficient energy management strategy. Block diagram representation of TECS core architecture is shown in Figure 1.1.

Total Energy-based Control System (TECS) first introduced by Lambregts to address the problems with conventional SISO AFCS designs [52]. In the later studies, the author described the engine control unit integration into TECS architecture [53]. Also in [54], operational aspects of the TECS such as operational design objectives, operational features, operation with limited control variables are discussed. Unlike other energy based flight control methods (e.g. [55]), TECS does not require aircraft specific information at its core part. Efficiency, simplicity, and success of the TECS has been shown experimentally with several studies. Specifically, a small UAV
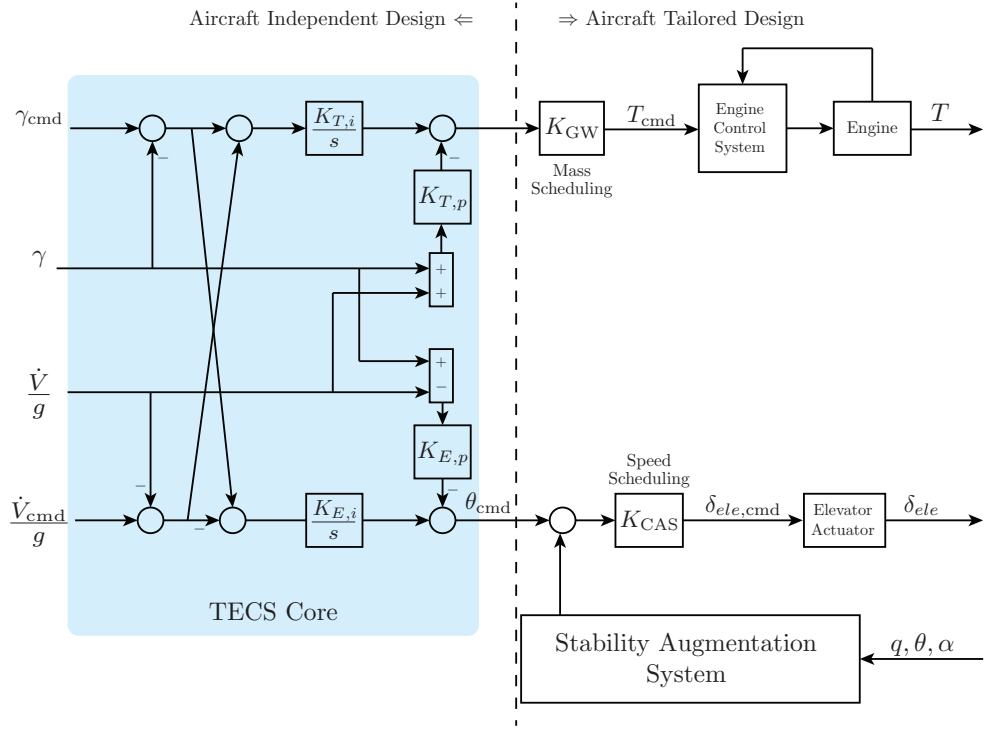
Figure 1.1: TECS Core Architecture

platform is used in [56] to validate the performance of the basic TECS architecture. Furthermore, flight test results for Boeing 737 has been presented in [57]. Wang et al. employed TECS algorithm in a fault-tolerant control scheme [58]. Brigido et al. uses TECS in conjunction with adaptive control to compensate the discrepancy in trimmed thrust values due to erroneous drag estimation [59], and present their experiment results in [60]. They are able to achieve better throttle management with their proposed architecture. Lamp et al. accommodate the airbrakes into TECS concept, and tested the modified scheme on a motor glider [61]. Another experimental study is conducted by Chudy et al. on a general aviation aircraft [62] to show the simplicity of implementation of the basic TECS architecture over the conventional SISO AFCS. Lamp et al. modified the fundamental TECS Core by adding an airbrake, changing the speed and flight path prioritization, and converting the structure from PI-control to P-control to improve the automatic landing performance via maintaining the desired glide slope [63]. Apart from these experimental studies, Lai and Ting proposed an optimal energy control system for a fixed wing UAV [64]. They combine the the pilot-like energy management property of TECS scheme and LQG optimal control

theory, and presented their results on a flight simulator software X-plane. Shevchenko integrated a drag correction unit into TECS structure [65] through energy balance equation. With their modified TECS structure, a better energy-management strategy under atmospheric disturbances is achieved which reduces the risks at terminal flight phases such as takeoff and landing. Kurdjukov et al proposed a modified TECS core architecture with a correction unit to handle the cases with highly nonlinear aerodynamics such as presence of substantial wind gusts [47]. Degaspare and Kienitz successfully extended the basic TECS structure by incorporating the engine parameters into throttle control channel, and investigates the robustness and performance characteristics of their architecture in the presence of engine model uncertainties [66]. Lastly, Argyle and Beard extends the standard linear TECS formulation to the nonlinear formulation [67]. Furthermore, they include an adaptive element to improve the accuracy of the aerodynamics model.

Although TECS started a new era of the flight control solutions, designing controller gains are usually performed using classical design methodologies. Yet, there exist few works on designing TECS more systematically. Voth and Ly proposed constrained parameter optimization based low-order robust and optimal controller design method for the inner loop of the TECS [68]. Nuriwati and Sasongko investigate the effects of TECS Core gains on the altitude and velocity tracking performances, and compared their results on the simulation with a conventional SISO AFCS [69]. Faleiro and Lambregts applied the eigenstructure assignment method to the TECS core [49]. Viswanathan et al. proposed an adaptive TECS architecture by combining the L_1-adaptive output feedback control and basic TECS architecture [70]. Although desired transient performance in the energy rate is achieved in [70], their solution suffers from the high filter gains in L_1-adaptive control. This can also be observed from unacceptably high rates in the throttle and elevator control commands. Looye proposed a multi-objective optimization based robust controller design using nonlinear dynamic inversion for the TECS [71,72]. Rysdyk and Agarwal proposed an approximate dynamic inversion based adaptive TECS in which they apply adaptation to eliminate the effects of residual errors due to approximate inversion [73].

Decoupled altitude and velocity control over the entire flight regime is attainable with TECS architecture if and only if the Hamiltonian and Lagrangian control loops

8

operate at the same bandwidth. Otherwise, energy will be added and subtracted due to asynchronous control from the variable that is commanded to be held constant. If this point is addressed properly, the elevator and thrust control becomes perfectly coordinated, which yields fully decoupled velocity and altitude command responses. Although in theory, the TECS gains can be selected freely so that the energy and energy distribution dynamics are identical, it is evident that these will alter from their nominal values during the operation due to presence of unmodeled dynamics, uncertainties in the plant model, external disturbances (e.g. wind, turbulence, gust). Briefly, for an ideal energy state management of an aircraft in the presence of uncertainties, the controller should

- successfully suppress the effects of uncertainties on the energy states of the aircraft
- ensure the Hamiltonian and Lagrangian control loops operate at the same bandwidth

Although there exist several works incorporating adaptive control in TECS architecture [59, 70, 73], the attention was on the compensation of the erroneous drag estimation, not on the coordinated longitudinal control.

1.2 Motivation

In general, desired tracking performance in standard model reference adaptive control is achievable with high adaptive gains. However, robustness of the closed-loop system against time-delay and unmodeled dynamics is usually degraded. Filter-based MRAC approaches offer a solution to this problem by incorporating the uncertainty estimation into adaptive law provided that the low-pass filter bandwidth is properly adjusted. If not, the lost information during filtering will cause degradation in the tracking and adaptation performances. Furthermore, a vast majority of the adaptive control studies in the literature focus on the systems with matched uncertainties, only. Hence, the motivation of the thesis becomes to introduce an adaptive controller that

- recovers the lost information in filter-based adaptive controllers
- achieves the desired tracking performance without high adaptation gains

9

- handles the systems with both matched and unmatched uncertainties

with illustrations on the aerospace applications. Furthermore, the coordinated longitudinal flight problem with energy-based controllers is addressed. As mentioned earlier, no controller architecture is studied in the literature that ensures the coordinated aircraft energy management in the presence of system uncertainties.

1.3 Contributions and Novelties

To this extent, an information recovery-based model reference adaptive controller (IR-MRAC) is proposed that achieves better tracking even if the low-pass filter is poorly designed with an inadequate bandwidth in filter-based methods. With the proposed architecture, the high frequency content of the uncertainty estimation is included into the adaptation to recover the lost information due to low-pass filtering. Simultaneously, a non-vanishing time-varying learning rate is introduced to eliminate the adverse effects of included high-frequency signals. In this respect, time-varying learning rate works as a stability augmentation system that suppresses the undesired high-frequency oscillations in the adaptive control input. One may include the high-frequency content by simply increasing the bandwidth of the low-pass filter in the conventional filter-based adaptive controllers. In that case, the signals with high frequencies have the same level of importance as those with low frequencies, which might result in undesired oscillations in the closed-loop response. On the other hand, IR-MRAC allows to adjust the contributions from low-frequency and high-frequency contents, separately. Hence, high-frequency signals are included in the adaptation in a frequency-selective framework. With this flexibility, the designer may adjust the weight of high-frequency signals on the adaptation. To the best knowledge of the author, there is no study addressing the lost information recovery in filter-based adaptive controllers.

In addition, a new Command Governor-based Model Reference Adaptive Control architecture is introduced and analyzed for uncertain dynamical systems with not only matched but also *unmatched* uncertainties. Using the unmatched uncertainty approximation obtained through RBF neural networks, the command governor

10

signal is designed to achieve the desired command following performance of the user-defined subset of the accessible states. With this Command Governor-based MRAC, the tracking error of the selected states can be made arbitrarily small by judiciously tuning the design parameters. In addition to the analysis of the closed-loop system stability using methods from Lyapunov theory, findings are also illustrated through numerical examples. Specifically, the major contribution is the guaranteed tracking performance for arbitrary state-dependent matched and unmatched uncertainties.

Next, an adaptive energy-based longitudinal flight control framework is proposed. Uncertainties on the Lagrangian channel is eliminated with an adaptive element in the pitch stability augmentation system, in which the fast system states are regulated. Thus, uncertainties in the energy distribution channel is successfully removed, and short period mode characteristics are improved. For the coordination between Hamiltonian and Lagrangian controls, an adaptive outer energy management loop is designed. Remaining uncertainties on the energy sources and/or energy draining components are addressed in this controller. Furthermore, bandwidth of both Lagrangian and Hamiltonian control loops are determined with a reference model. As a result, proper suppression of uncertainties immediately results in the desired decoupled airspeed and altitude responses. The main contribution is to introduce an adaptive energy management module ensuring that the energy is added to (or subtracted from) the system and remaining energy is distributed properly to achieve the desired and decoupled tracking performance.

Lastly, the aircraft lateral flight control problem is re-visited. Specifically, it is allowed that the nominal system to be freely chosen without any concern on the matching assumption in model reference adaptive controller. Proposed command governor-based MRAC approach is utilized to eliminate the effects of matched and unmatched uncertainties. As a result, the same command tracking performance is achieved throughout the entire flight envelope with a single reference model and nominal controller. Thus, necessity for the gain scheduling is eliminated and the effects of uncertainties are suppressed successfully. Specifically, with this form of lateral flight controller, assumptions on the system reduce to: $i)$ Controllability of the system and $ii)$ Sign of the control gain.

1.4   The Outline of the Thesis

Chapter 2 presents the notation and definitions used in the thesis. Furthermore, a review for standard MRAC is included. In addition, Composite/Combined MRAC architecture is revisited as the contributions of the thesis are mainly based on these two frameworks. In Chapter 3, a new adaptive control architecture is proposed to recover the lost information in filter-based adaptive controllers. Chapter 4 extends the Information Recovery-based MRAC (IR-MRAC) to cover the systems with unknown control effectiveness. In Chapter 5, a command-governor based adaptive control framework is introduced for the dynamical systems with matched and unmatched uncertainties. In Chapter 6, a nonlinear energy-based flight controller is presented. Well-known Total Energy Control System (TECS) is extended to nonlinear formulation for coordinated longitudinal flight. In Chapter 7, lateral flight control problem is re-visited with relaxed matching assumption, and hence, allowing unmatched content in the adaptive control system. Command governor-based MRAC, which is proposed in Chapter 5, is utilized as a command following performance recovery mechanism. Lastly, Chapter 8 concludes the thesis.

CHAPTER 2

PRELIMINARIES

2.1 Notation and Definitions

Notation used in this thesis is fairly standard. Specifically, $\mathbb{R}_+$ denotes the set of strictly positive real numbers, '$\triangleq$' denotes equality by definition, $A \succ 0$ denotes that A is a positive definite matrix, $(\cdot)^{-1}$ denotes inverse, $(\cdot)^T$ denotes transpose, $(\cdot)^\dagger$ denotes the Moore–Penrose inverse, '$\text{vec}(\cdot)$' denotes the column stacking operator, '$\text{tr}(\cdot)$' denotes the trace operator, $\lambda_{\min}(A)$ returns the minimum eigenvalue of matrix A, and $\sigma_{\max}(A)$ returns the maximum singular value of matrix A. Furthermore, for the vector $x = \begin{bmatrix} x_1 & \cdots & x_n \end{bmatrix}^T \in \mathbb{R}^n$ and matrix $A = [a_{ij}]\big|_{\substack{i=1,\cdots,m \\ j=1,\cdots,n}} \in \mathbb{R}^{m \times n}$ with $a_{ij} \in \mathbb{R}$, the Euclidean vector norm $\|x\|$, the induced matrix norm $\|A\|$, and Frobenius matrix norm $\|A\|_{\text{F}}$ are defined as

$$\|x\| \triangleq \sqrt{\sum_{i=1}^{n} x_i^2}, \qquad \|A\|_{\text{F}} \triangleq \sqrt{\text{tr}(A^T A)}.$$

$$\|A\| \triangleq \sqrt{\lambda_{\max}(A^T A)} = \sigma_{\max}(A)$$

Kronecker product is denoted by '$\otimes$' and '$\wedge$' denotes the logical *'AND'* operator. For the vector $\theta \in \mathbb{R}^k$ and convex function $f : \mathbb{R}^k \to \mathbb{R}$, the gradient operator $\nabla f(\theta)$ is $\nabla f(\theta) = \begin{bmatrix} \frac{\partial f(\theta)}{\partial \theta_1} & \cdots & \frac{\partial f(\theta)}{\partial \theta_k} \end{bmatrix}^T$. Lastly, '$\blacksquare$' indicates the completion of a mathematical proof. $\mathcal{N}(\cdot)$ denotes the null space, for $\delta \in \mathbb{R}_+$, the set $N_\delta(y(t))$ denotes the δ-neighborhood of the signal $y(t) \in \mathbb{R}^n$

$$N_\delta(y(t)) = \{x(t) \in \mathbb{R}^n : \|x(t) - y(t)\| \leq \delta\}.$$

Finally, definition of the projection operator is presented. For this purpose, let the Boolean L_{pr} be $L_{\text{pr}} \triangleq f(\theta) > 0 \wedge y^T \nabla f(\theta) > 0$. Then, the projection operator for

the vectors $\theta, y \in \mathbb{R}^k$ is

$$\text{Proj}(\theta, y) \triangleq \begin{cases} y - \frac{\nabla f(\theta)(\nabla f(\theta))^T}{\|\nabla f(\theta)\|^2} y f(\theta) & \text{if } L_{\text{pr}} \text{ is true} \\ y & \text{otherwise} . \end{cases}$$

In this thesis, the convex function $f(\cdot)$ is taken as

$$f(\theta) \triangleq \frac{(\varepsilon_\theta + 1) \theta^T \theta - \theta_{\max}^2}{\varepsilon_\theta \theta_{\max}^2},$$

where $\theta_{\max} \in \mathbb{R}_+$ is a projection norm bound imposed on $\theta \in \mathbb{R}^n$ and $\varepsilon_\theta \in \mathbb{R}_+$ is a projection tolerance bound.

$\mathcal{F}_b\big(C; \vec{u}_1^{(b)}, \vec{u}_2^{(b)}, \vec{u}_3^{(b)}\big)$ denotes the frame $\mathcal{F}_b$ with its unit vectors $\vec{u}_1^{(b)}, \vec{u}_2^{(b)}, \vec{u}_3^{(b)}$ which has an origin at point C. $\vec{u}_i^{(b)}$ denotes i^{th} unit vector of frame $\mathcal{F}_b$. $\widehat{C}^{(a,b)}$ denotes the transformation matrix from frame $\mathcal{F}_b$ to frame $\mathcal{F}_a$. Representation of vector $\vec{X}$ in frame $\mathcal{F}_b$ is denoted by $\big[\vec{X}\big]^{(b)} = \bar{X}^{(b)}$. $\bar{u}_j^{(a/b)} = \big[\vec{u}_j^{(a)}\big]^{(b)}$ corresponds to representation of jth unit vector of frame $\mathcal{F}_a$ in frame $\mathcal{F}_b$. Representation of every unit vector in its own frame is always the same; i.e. $\bar{u}_j^{(a/a)} = \bar{u}_j^{(b/b)} = \bar{u}_j$. $\vec{V}_{A/\mathcal{F}_o(B)} = D_o \vec{r}_{A/B}$ denotes the derivative of position vector $\vec{r}_{A/B}$ with respect to frame $\mathcal{F}_o$. $\text{cpm}(\bar{\omega}^{(b)}) = \widetilde{\omega}^{(b)}$ denotes the cross-product matrix generated by $\bar{\omega}^{(b)}$ which is column-matrix representation of vector $\vec{\omega}$ in frame $\mathcal{F}_b$. $\sigma_{\min}(\cdot)$ and $\sigma_{\max}(\cdot)$ return the minimum and maximum singular value of inside argument, respectively.

Definition 2.1. *[Persistent Excitation] The signal $\omega(t) \in \mathbb{R}^n$ is said to be persistently exciting over an excitation period of τ if and only if there exist positive constants $\tau, \beta \in \mathbb{R}_+$ such that the following inequality holds:*

$$\int_{t-\tau}^{t} \omega(s)\omega^T(s)ds \succeq \beta I_{n \times n}, \qquad \forall t \in \mathbb{R}_+$$

for $\forall t \in \mathbb{R}_+$ where $I_{n \times n}$ is the $n \times n$ identity matrix.

Definition 2.2. *[Sufficient Excitation] The signal $\omega(t) \in \mathbb{R}^n$ is said to be sufficiently exciting at time $t = T_e$ if there exists a positive constant $\beta \in \mathbb{R}_+$ such that the following inequality holds:*

$$\int_{t_0}^{t} \omega(s)\omega^T(s)ds \succeq \beta I_{n \times n}, \qquad t = T_e \in \mathbb{R}_+$$

2.2 Standard Model Reference Adaptive Control

In this section, mathematical background of the standard model reference adaptive control is briefly described. Consider the following nonlinear uncertain system:

$$\dot{x}(t) = Ax(t) + B\left[u(t) + \Delta\big(x(t)\big)\right], \quad x(t_0) = x_0 \tag{2.1}$$

where $x(t) \in \mathcal{D}_x \subset \mathbb{R}^n$ denotes the state vector, $u(t) \in \mathcal{D}_u \subset \mathbb{R}^m$ is the control input, system matrix $A \in \mathbb{R}^{n \times n}$ and input matrix $B \in \mathbb{R}^{n \times m}$ are known constant matrices. Furthermore, the pair (A, B) is assumed to be controllable and input matrix B has full column rank. $\mathcal{D}_x$ is sufficiently large compact set, $\mathcal{D}_u$ is admissible control set, and $\Delta : \mathbb{R}^n \to \mathbb{R}^m$ is the mapping for the unknown matched uncertainty. In addition, full state measurement is available for feedback control, and the plant is not over-actuated; that is $n \geq m$.

The main objective in model reference adaptive controllers is to achieve the desired state tracking performance, which is characterized by the reference model:

$$\dot{x}_r(t) = A_r x_r(t) + B_r r(t), \quad x_r(t_0) = x_{r0} \tag{2.2}$$

where $x_r(t) \in \mathbb{R}^n$ is the reference state vector, $r(t) \in \mathbb{R}^q$ is the bounded and piecewise continuous reference command signal with its dimension being less than or equal to that of the control input; i.e. $q \leq m$. $B_r \in \mathbb{R}^{n \times q}$ denotes the reference model input matrix, and system matrix $A_r \in \mathbb{R}^{n \times n}$ is designed to be Hurwitz.

Assumption 2.1. *[Matching Condition] Reference model system matrix A_r and input matrix B_r satisfies the relations:*

$$A_r = A - BK_x$$

$$B_r = BK_r$$

with $K_x \in \mathbb{R}^{m \times n}$ and $K_r \in \mathbb{R}^{m \times q}$ being feedback and feedforward controller gains, respectively.

Remark 2.1. *Assumption 2.1 is a well-known and widely accepted assumption in model reference adaptive control theory [1, 74, 75]. Since the system matrices A and B are known, it is possible to design feedback gain K_x and feedforward gain K_r so*

that the desired closed-loop system performance is achieved for the nominal system.

Assumption 2.2. *[Structured Matched Uncertainty] The uncertainty $\Delta(x)$ in the plant dynamics in Eq 2.1 can be represented by the linear combination of known basis vector-function $\phi : \mathbb{R}^n \to \mathbb{R}^s$ as:*

$$\Delta(x) = W^T \phi(x)$$

where $W \in \mathbb{R}^{s \times m}$ is the unknown constant weight matrix.

Remark 2.2. *Many uncertainties in physical systems can be parametrized as in Assumption 2, (e.g. nonlinear wing-rock dynamics [76]). However, for the case where the basis vector-function $\phi(x)$ is unknown, Assumption 2.2 can be relaxed using universal approximators such as Radial Basis Functions (RBF) [77] as follows:*

$$\Delta(x) = W^T \phi(x) + \varepsilon(x)$$

where the residual $\varepsilon(x)$ can be made arbitrarily small by increasing the size of the regressor RBF vector-function $\phi(x)$; i.e. $\|\varepsilon(x)\| \leq \varepsilon_0$, $\forall x \in \mathcal{D}_x$ with arbitrarily small residual bound of ε_0. Thus, the proposed algorithm can be readily extended for unstructured matched uncertainties.

As the reference model system matrix A_r is Hurwitz, the following Lyapunov equation holds for any given positive definite matrix $Q = Q^T \succ 0$:

$$A_r^T P + P A_r = -Q \tag{2.3}$$

with $P = P^T \succ 0$ being positive definite solution [78].

Nominal control input $u_n(t)$ has feedback and feedforward parts given as follows:

$$u_n(t) = -K_x x(t) + K_r r(t) \tag{2.4}$$

The overall control input consists of the nominal controller in Eq 2.4 and adaptive controller to be in the following form:

$$u(t) = u_n(t) - u_{ad}(t) \tag{2.5}$$

where the adaptive control input $u_{ad}(t)$ is given by

$$u_{ad}(t) = \hat{W}^T(t) \phi(x) \tag{2.6}$$

with $\hat{W}(t) \in \mathbb{R}^{s \times m}$ being online estimation of unknown constant weight $W \in \mathbb{R}^{s \times m}$. Combining Eq 2.4, Eq 2.5, and Eq 2.6 yields the resultant control input as follows:

$$u(t) = -K_x x(t) + K_r r(t) - \hat{W}^T(t)\phi(x) \tag{2.7}$$

Substituting the control input in Eq 2.7 into the uncertain system dynamics with Assumption 2.2 results in the following closed-loop system dynamics:

$$\dot{x}(t) = Ax(t) + B\left[u(t) + \Delta(x(t))\right]$$
$$\dot{x}(t) = Ax(t) + B\left[-K_x x(t) + K_r r(t) - \hat{W}^T(t)\phi(x) + W^T\phi(x)\right] \tag{2.8}$$
$$\dot{x}(t) = A_r x(t) + B_r r(t) + B\tilde{W}^T(t)\phi(x)$$

where $\tilde{W}(t) \triangleq W - W(t)$ is the online weight estimation error. State tracking error $e(t)$ is defined to be the difference between the reference model states and plant states; that is, $e(t) \triangleq x_r(t) - x(t), \forall t \geq t_0$. Then, the state tracking error dynamics can be obtained using Eq 2.2 and Eq 2.8 as the following:

$$\dot{e}(t) = \dot{x}_r(t) - \dot{x}(t)$$
$$\dot{e}(t) = A_r e(t) - B\tilde{W}^T(t)\phi(x) \tag{2.9}$$

Finally, the weight update law in standard model reference adaptive control formulation is given by:

$$\dot{\hat{W}}(t) = \dot{\hat{W}}_b(t) = -\Gamma\phi(x)e(t)^T PB \tag{2.10}$$

where $\Gamma = \Gamma^T \succ 0$ is the user-defined learning rate matrix with $\Gamma \in \mathbb{R}^{s \times s}$.

Remark 2.3. *The closed-loop stability of the standard model reference adaptive control system can be shown using radially unbounded Lyapunov function $\mathcal{V}_b(e, \tilde{W}) = e^T Pe + tr(\tilde{W}^T \Gamma^{-1}\tilde{W}) > 0$ with $\dot{\mathcal{V}}_b(e, \tilde{W}) = -e^T Qe \leq 0$ using the system trajectories along Eq 2.9 and Eq 2.10. Note that $\mathcal{V}_b(0, 0) = 0$ and $\mathcal{V}_b(e, \tilde{W}) > 0$, for all $(e, \tilde{W}) \neq (0, 0), \forall t \in \mathbb{R}_+$. Since $\mathcal{V}_b(e, \tilde{W})$ is lower-bounded by zero, and its derivative $\dot{\mathcal{V}}_b(e, \tilde{W}) \leq 0$ is less than or equal to zero, Lyapunov function $\mathcal{V}_b(e, \tilde{W})$ approaches to a finite limit as $t \to \infty$. Hence, the boundedness of tracking error $e(t)$ and weight estimation error $\tilde{W}(t)$ is guaranteed. Since $e(t)$ and $x_r(t)$ are bounded, system states $x(t)$ and basis vector-function $\phi(x)$ immediately become bounded. With bounded $e(t), x(t), \phi(x),$ and $\tilde{W}(t),$ time derivative of tracking error dynamics $\dot{e}(t)$*

17

becomes bounded which ensures the boundedness of $\ddot{\mathcal{V}}_b(e, \tilde{W}) = -2e^T Q \dot{e}, \forall t \in \mathbb{R}_+$. It then follows from Barbalat's Lemma [79] that $\lim_{t\to\infty} \dot{\mathcal{V}}_b(e(t), \tilde{W}(t)) = 0$ which implies the asymptotic stability of tracking error $e(t)$; that is, $\lim_{t\to\infty} e(t) = 0$. If the basis vector-function $\phi(x)$ is persistently exciting, then the estimated parameters converge to their ideal values, as well; that is, $\hat{W}(t) \to W$ as $t \to \infty$. Readers may refer to Ref [74] for the details.

Remark 2.4. *If the structure of the uncertainty is unknown and universal approximators are used to parametrize the uncertainty as suggested in Remark 2.2, the boundedness of the online weight estimations is not guaranteed by the standard MRAC. To increase the robustness (e.g. in the unstructured uncertainty case), many robust modifications are introduced in the literature including but not limited to σ-modification [3], e-modification [4], optimal control based modification [6], Kalman filter modification [9], and q-modification [13]. Furthermore, it is common practice to include the projection operator [80] to bound the parameters within the prescribed convex set.*

2.3 Combined/Composite Model Reference Adaptive Control

It is well known that the standard MRAC requires high learning rates for fast adaptation. Although adaptive control with high gains enables fast adaptation, it might degrade the transient performance by inducing high-frequency oscillations in the system and even cause instabilities in the presence of large uncertainties and sudden changes in the system dynamics. That's why improving the transient performance in adaptive control has always been an attractive problem [6, 11, 24, 81–85]. As seen from these studies, and references therein, including the uncertainty estimation error in the adaptation law enhances the transient performance significantly. This fact was first utilized in the study of Slotine and Li [10], called '*Composite Model Reference Adaptive Control*'. Almost at the same time, quite a similar approach was introduced by Duarte and Narendra [86] as '*Combined Model Reference Adaptive Control*'. Later in Lavretsky's work [11], these two approaches are generalized to cover the multi-input multi-output systems. In this section, improved formulation of Composite/Combined MRAC proposed by Lavretsky [11]

is revisited. As Lavretsky does in his study, these two methods are called as CMRAC to acknowledge both studies.

2.3.1 Filtering System Dynamics

Basically, CMRAC starts with filtering the uncertain system dynamics in Eq 2.1 as:

$$\dot{x}_f(x,t) = Ax_f(x,t) + B\left[u_f(t) + \Delta_f(x,t)\right] \tag{2.11}$$

with subscript 'f' indicating that the signal is filtered through the low-pass filters:

$$
\begin{aligned}
\dot{x}_f &= \omega_f\big(x - x_f\big), & x_f(t_0) &= x(t_0) \\
\dot{u}_f &= \omega_f\big(u - u_f\big), & u_f(t_0) &= u(t_0) \\
\dot{r}_f &= \omega_f\big(r - r_f\big), & r_f(t_0) &= r(t_0) \\
\dot{\phi}_f &= \omega_f\big(\phi - \phi_f\big), & \phi_f(t_0) &= \phi(x_0) \\
\dot{\psi}_f &= \omega_f\big(\psi - \psi_f\big), & \psi_f(t_0) &= \psi(x_0)
\end{aligned}
\tag{2.12}
$$

where $\omega_f \in \mathbb{R}_+$ is the cut-off frequency that determines the bandwidth of the low-pass filters, $r(t)$ is bounded and piecewise continuous exogenous reference signal. Basis function ψ_f is introduced in Chapter 5. Wherever appropriate, the arguments 't' for time dependency and 'x' for state dependency are dropped consistently for ease of exposition. Rearranging Eq 2.11 yields:

$$B^\dagger\left[\dot{x}_f - Ax_f\right] - u_f = \Delta_f = W^T\phi_f \tag{2.13}$$

with $B^\dagger$ denoting the left-pseudo inverse of input matrix B. Note that the signals x_f, u_f, ϕ_f, $\dot{x}_f$ and $\dot{\phi}_f$ are all accessible through Eq 2.12.

2.3.2 CMRAC Update Law

Once the low-pass filters are applied to the uncertain system dynamics, the low-frequency content of uncertainty, Δ_f, becomes an available signal for control purposes as all the signals in the left-hand side of Eq 2.13 are available. The idea in CMRAC is to use the low-frequency content of the matched uncertainty in the update

19

law by constructing its estimation as follows:

$$\Delta_f = W^T \phi_f = B^\dagger [\dot{x}_f - A x_f] - u_f$$

$$\hat{\Delta}_f = \hat{W}^T \phi_f$$

(2.14)

where $\hat{W}(t)$ is the online estimation of unknown constant weight matrix W. Then, one can define the low-frequency uncertainty estimation error as the following:

$$\tilde{\Delta}_f \triangleq \Delta_f - \hat{\Delta}_f = W^T \phi_f - \hat{W}^T \phi_f = \tilde{W}^T \phi_f \qquad (2.15\text{a})$$

$$\tilde{\Delta}_f = B^\dagger [\dot{x}_f - A x_f] - u_f - \hat{W}^T \phi_f \qquad (2.15\text{b})$$

The modified update law in CMRAC is given by

$$\dot{\hat{W}} = \Gamma\big[-\phi e^T P B + \gamma_c \phi_f \tilde{\Delta}_f^T\big] \qquad (2.16)$$

where $\tilde{\Delta}_f$ is available with Eq 2.15b and $\gamma_c \in \mathbb{R}_+$ is a positive scalar learning rate.

Remark 2.5. *Asymptotic stability of the closed-loop system with CMRAC weight update law in Eq 2.16 can be shown as the following. Time derivative of the radially unbounded Lyapunov function $\mathcal{V}_c(e, \tilde{W}) = \frac{1}{2} e^T P e + \frac{1}{2} tr(\tilde{W}^T \Gamma^{-1} \tilde{W})$ along the system trajectories in Eq 2.9 and Eq 2.16 is given by $\dot{\mathcal{V}}_c(e, \tilde{W}) = -\frac{1}{2} e^T Q e - \gamma_c tr(\tilde{W}^T \phi_f \phi_f^T \tilde{W})$ which is also equal to $\dot{\mathcal{V}}_c(e, \tilde{W}) = -\frac{1}{2} e^T Q e - \gamma_c \|\tilde{\Delta}_f\|_F^2 \leq -\frac{1}{2} e^T Q e - \gamma_c \|\tilde{\Delta}_f\|^2$. With this result, boundedness of the Lyapunov function $\mathcal{V}_c$ is guaranteed which implies the boundedness of the state tracking error $e(t)$ and weight estimation error $\tilde{W}(t)$. Next, following the similar discussions made in Remark 2.3, one can show the boundedness of $\ddot{\mathcal{V}}_c(e, \tilde{W}) = -\frac{1}{2} e^T Q \dot{e} - \gamma_c \tilde{\Delta}_f^T\big(-\dot{\hat{W}}^T \phi_f + \tilde{W}^T \dot{\phi}_f\big)$ using Eq 2.12 and Eq 2.16. It then follows from Barbalat's Lemma [79] that $\lim_{t \to \infty} \dot{\mathcal{V}}_c(e(t), \tilde{W}(t)) = 0$ which implies the asymptotic stability of the state tracking error $e(t)$ and filtered uncertainty estimation error $\tilde{\Delta}_f(t)$; that is, $\lim_{t \to \infty} e(t) = 0$ and $\lim_{t \to \infty} \tilde{\Delta}_f(t) = 0$. Comparing CMRAC result with that of standard adaptive control in Remark 2.3, it can be realized that CMRAC modification enhances the stability since $\dot{\mathcal{V}}_c \leq \dot{\mathcal{V}}_b \leq 0$. However, it should be emphasized that the parameter convergence is still not guaranteed with CMRAC since the asymptotic stability of $\tilde{\Delta}_f$ does not imply the asymptotic stability of weight estimation error $\tilde{W}$ unless the basis function ϕ is persistently exciting.*

Remark 2.6. *Contribution of the CMRAC weight update law in Eq 2.16 is three fold:*

- *Adaptive parameters are updated in the direction that minimizes the low-frequency estimation of the uncertainty Δ_f. In that respect, the CMRAC modification can be considered analogous to q-modification [13].*

- *CMRAC update law enforces the adaptive estimation to be a low-frequency signal. Hence, CMRAC works similar to low-frequency learning-based adaptive control [24] as the high frequency content in the adaptive parameters is suppressed in both frameworks.*

- *Since the signals in CMRAC mainly contain low-frequency content, it allows to use relatively high gains in the modification term which accelerates the adaptation as in the optimal control based adaptive control modification [6] and low-frequency learning MRAC [24].*

2.3.3 CMRAC Extension to Systems with Unknown Control Effectiveness

In this case, the nonlinear uncertain dynamical system of interest is as follows:

$$\dot{x}(t) = Ax(t) + B\Lambda\left[u(t) + \Delta\big(x(t)\big)\right], \quad x(t_0) = x_0 \tag{2.17}$$

where Λ is a diagonal positive definite constant matrix that represents the unknown control effectiveness. The matched uncertainty is assumed to be structured and can be represented as in Assumption 2.2. For the same reference model in Eq 2.2, the tracking error dynamics becomes:

$$\dot{e}(t) = A_r e(t) - B\Lambda\tilde{W}^T(t)\phi(x) \tag{2.18}$$

Filtering the uncertain system dynamics yields:

$$\dot{x}_f(x,t) = Ax_f(x,t) + B\Lambda\big[u_f(t) + \Delta_f(x,t)\big]$$
$$= Ax_f(x,t) + B\Lambda\big[u_f(t) + W^T\phi_f(x,t)\big]$$

Manipulating and rearranging the resultant equation gives:

$$Y \triangleq \Lambda\big[u_f + W^T\phi_f\big] = B^\dagger\big[\dot{x}_f - Ax_f\big]$$

with $B^\dagger$ being pseudo-inverse of B. Its estimated form is defined as:

$$\hat{Y} \triangleq \hat{\Lambda}\big[u_f + \hat{W}^T \phi_f\big]$$

where $\hat{\Lambda}$ and $\hat{W}$ are being online estimations of unknown control effectiveness matrix Λ and unknown ideal matched weight matrix W, respectively. Corresponding error is

$$
\begin{aligned}
e_Y \triangleq Y - \hat{Y} &= \Lambda\big[u_f + W^T \phi_f\big] - \hat{\Lambda}\big[u_f + \hat{W}^T \phi_f\big] \\
&= \tilde{\Lambda}u_f + \Lambda W^T \phi_f - \hat{\Lambda}\hat{W}^T \phi_f \pm \Lambda\hat{W}^T \phi_f \\
&= \tilde{\Lambda}\big(u_f + \hat{W}^T \phi_f\big) + \Lambda\tilde{W}^T \phi_f
\end{aligned}
$$

Then, the update laws for the evolution of $\hat{\Lambda}$ and $\hat{W}$ are given as in the following bilinear predictor form [11]:

$$
\begin{aligned}
\dot{\hat{W}} &= -\Gamma\big[\phi e^T PB - \gamma_c \phi_f e_Y^T\big] \\
\dot{\hat{\Lambda}} &= \Gamma_\Lambda \gamma_c e_Y \big(u_f + \hat{W}^T \phi_f\big)^T
\end{aligned}
\tag{2.19}
$$

with $\gamma_c \in \mathbb{R}_+$ being positive scalar constant and Γ_Λ being a positive definite matrix.

Remark 2.7. *Stability of the closed-loop system with dynamics in Eq 2.17, control input in Eq 2.7, and adaptive weight update laws in Eq 2.19 can be illustrated using the following Lyapunov function:*

$$\mathcal{V} = \frac{1}{2}e^T Pe + \frac{1}{2}tr\big(\tilde{W}^T \Gamma^{-1}\tilde{W}\Lambda\big) + \frac{1}{2}tr\big(\tilde{\Lambda}^T \Gamma_\Lambda^{-1}\tilde{\Lambda}\big)$$

Its time derivative along the system trajectories in Eq 2.18 and Eq 2.19 results in:

$$
\begin{aligned}
\dot{\mathcal{V}} =& e^T PA_r e - e^T PB\Lambda\tilde{W}^T \phi + tr\big(\tilde{W}^T \Gamma^{-1}\dot{\tilde{W}}\Lambda\big) + tr\big(\tilde{\Lambda}^T \Gamma_\Lambda^{-1}\dot{\tilde{\Lambda}}\big) \\
=& -\frac{1}{2}e^T Qe - tr\big(\Lambda\tilde{W}^T \phi e^T PB\big) - tr\big(\Lambda\tilde{W}^T \Gamma^{-1}\dot{\hat{W}}\big) - tr\big(\tilde{\Lambda}^T \Gamma_\Lambda^{-1}\dot{\hat{\Lambda}}\big) \\
=& -\frac{1}{2}e^T Qe - tr\big(\Lambda\tilde{W}^T \phi e^T PB\big) + tr\big\{\Lambda\tilde{W}^T\big[\phi e^T PB - \gamma_c \phi_f e_Y^T\big]\big\} - tr\big(\tilde{\Lambda}^T \Gamma_\Lambda^{-1}\dot{\hat{\Lambda}}\big) \\
=& -\frac{1}{2}e^T Qe - \gamma_c tr\big(\Lambda\tilde{W}^T \phi_f e_Y^T\big) - tr\big(\tilde{\Lambda}^T \Gamma_\Lambda^{-1}\dot{\hat{\Lambda}}\big) \\
=& -\frac{1}{2}e^T Qe - \gamma_c tr\big(e_Y e_Y^T\big) \\
\leq& -\frac{1}{2}\lambda_{\min}(Q)\|e\|_2^2 - \gamma_c\|e_Y\|_2^2 \leq 0
\end{aligned}
$$

which implies the uniform ultimate boundedness of the error signals $e(t)$, $\tilde{W}(t)$, and $\tilde{\Lambda}(t)$, $\forall t \geq t_0$. It can also be shown using Barbalat's Lemma [79, 87] that $e(t)$ and $e_Y(t)$ converge to zero asymptotically; that is, $e(t), e_Y(t) \to 0$ as $t \to \infty$. Since the Lyapunov function is radially unbounded, these results hold globally. Readers may also refer to Ref [11] for the detailed proof.

2.4 The Projection Operator

Definition 2.3. *A set $\mathcal{D} \subset \mathbb{R}^k$ is a convex set if:*

$$\lambda x + (1 - \lambda)y \in \mathcal{D}, \qquad \forall x \in \mathcal{D}, \ \forall y \in \mathcal{D}, \ 0 \leq \lambda \leq 1$$

Thus, for any chosen points $x, y \in \mathcal{D}$, all the points on the line connecting x and y are also in the set $\mathcal{D}$.

Definition 2.4. *A function $f : \mathbb{R}^k \to \mathbb{R}$ is convex function if:*

$$f\left(\lambda x + (1 - \lambda)y\right) \leq \lambda f(x) + (1 - \lambda)f(y), \qquad 0 \leq \lambda \leq 1$$

Lemma 2.1. *Let $f : \mathbb{R}^k \to \mathbb{R}$ be a convex function. Then, the subset Ω_β is convex for any constant $\beta > 0$ such that $\Omega_\beta := \left\{\theta \in \mathbb{R}^k : f(\theta) \leq \beta\right\}$ (Lemma 3 in [88]).*

The projection operator for vectors $\theta, y \in \mathbb{R}^k$ is given by [80]:

$$\text{Proj}(\theta, y, f) = \begin{cases} y & \text{if } f(\theta) < 0 \\ y & \text{if } f(\theta) \geq 0 \wedge y^T \nabla f(\theta) \leq 0 \\ y - \frac{\nabla f(\theta)(\nabla f(\theta))^T}{\|\nabla f(\theta)\|^2} y f(\theta) & \text{otherwise} \end{cases} \qquad (2.20)$$

where $\nabla f(\theta_b) := \left(\begin{array}{cccc} \frac{\partial f(\theta)}{\partial \theta_1} & \frac{\partial f(\theta)}{\partial \theta_2} & \cdots & \frac{\partial f(\theta)}{\partial \theta_k} \end{array} \right)^T$ is evaluated at θ_b. It can equivalently be expressed as:

$$\text{Proj}(\theta, y, f) = \begin{cases} y - \frac{\nabla f(\theta)(\nabla f(\theta))^T}{\|\nabla f(\theta)\|^2} y f(\theta) & \text{if } f(\theta) > 0 \wedge y^T \nabla f(\theta) > 0 \\ y & \text{otherwise} \end{cases} \qquad (2.21)$$

Lemma 2.2. *Let $\theta \in \mathbb{R}^k$ be a vector, $f : \mathbb{R}^k \to \mathbb{R}$ be a convex function, Ω_0 be a convex set such that $\Omega_0 := \left\{\theta \in \mathbb{R}^k : f(\theta) \leq 0\right\}$, Ω_1 be a convex set given by $\Omega_1 := \left\{\theta \in \mathbb{R}^k : f(\theta) \leq 1\right\}$. Projection operator is given as in Eqn. (2.20). Further, let $\theta_0 := \theta(t = 0)$ be the initial value for $\theta(t)$ such that $\theta_0 \in \Omega_0$. If the vector $\theta(t)$ is updated according to the law $\dot{\theta}(t) = Proj\,(\theta, y, f)$, then $\theta(t)$ is bounded and ensured to be $\theta(t) \in \Omega_1$, $\forall t \geq 0$. (Lemma 9 in [80]).*

In this thesis, the convex function $f(\cdot)$ is chosen to be:

$$f(\theta) = \frac{\|\theta\|^2 - \upsilon^2}{2\epsilon\upsilon + \epsilon^2} \tag{2.22}$$

where $\epsilon > 0$ and $\upsilon > 0$ are scalar constants which determine the boundaries of convex sets Ω_0 and Ω_1. An illustrative trajectory for Lemma 2.2 is given in Figure 2.1 where θ^* is a point on the boundary of the convex set Ω_1; i.e. $f(\theta^*) = 1$.
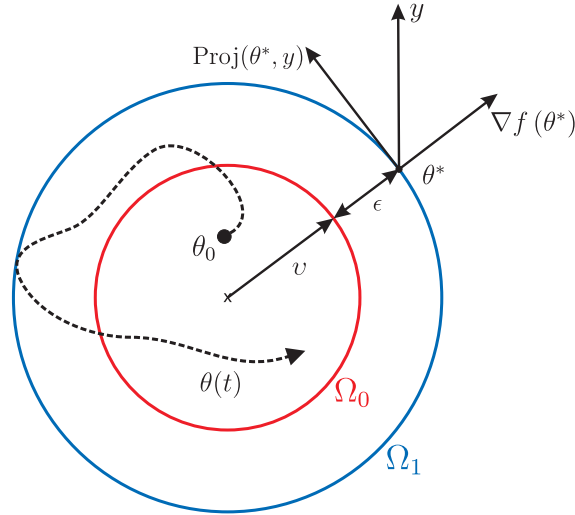
Figure 2.1: An Example to Trajectory Behavior Under Projection

Remark 2.8. *From Lemma 2.2, $\theta(t) \in \mathbb{R}^k$ satisfies the following condition:*

$$\|\theta(t)\| = \|\theta(t)\|_F \le \epsilon + \upsilon, \qquad \forall t \ge 0 \tag{2.23}$$

provided that the initial value θ_0 is such that $\theta_0 \in \Omega_0$. Hence, the vector $\theta(t)$ is uniformly ultimately bounded.

Lemma 2.3. *Let $f(\cdot) : \mathbb{R}^k \to \mathbb{R}$ be a continuously differentiable convex function. Consider the convex set $\Omega_1 := \{\theta \in \mathbb{R}^k : f(\theta) \le 1\}$. Let θ^* be an interior point of the convex set Ω_1; i.e. $f(\theta^*) < 1$. Then,*

$$(\theta^* - \theta)^T (y - \text{Proj}(\theta, y, f)) \le 0, \qquad \forall \theta \in \Omega_1$$

Readers may refer to Ref [80] for the details.

CHAPTER 3

INFORMATION RECOVERY IN FILTER-BASED MODEL REFERENCE ADAPTIVE CONTROL

3.1 Problem Definition

In this chapter, following uncertain dynamical systems are considered:

$$\dot{x}(t) = Ax(t) + B\left[u(t) + \Delta\big(x(t)\big)\right], \quad x(t_0) = x_0$$

Chapter 2 highlighted both Standard MRAC and Combined/Composite MRAC frameworks for the uncertain systems of interest. Superiority of CMRAC over Standard MRAC has been stated in Remark 2.6. Although CMRAC and its further modifications (e.g. Refs [15, 16, 20, 85, 89]) contributed a lot to the robustness and performance , all these filter-based solutions suffer from losing information during filtering. Thus, the adaptation performance might be degraded if the system experiences high-frequency variations such as abrupt changes in the weight (e.g. payload drop for an aircraft), actuator failures, and so on. Furthermore, a relatively small cut-off frequency ω_f for low-pass filters in Eq 2.12 may cause problems such as instabilities due to time-delay because of the nature of low-pass filters. In this chapter, these issues are addressed, and a new model reference adaptive control architecture is proposed that compensates the information lost during filtering by incorporating the high-frequency content of the filtered signals into adaptation.

It is important to note that this chapter builds on Section 2.3. A few definitions and formulations which are already available in Chapter 2 are omitted to avoid the repetitions. Hence, readers strongly advised to visit Chapter 2 before attempting this chapter.

3.2 Proposed Solution

Similar to the aforementioned studies, the low-frequency content of the uncertainty, Δ_f, is utilized in the adaptation to improve the transient behavior. Consider the following optimization problem:

$$\min_{\hat{W}} \mathcal{J}$$
$$\mathcal{J}(\hat{W}) = \frac{1}{2}\|W^T\phi_f(x) - \hat{W}^T(t)\phi_f(x)\|^2 = \frac{1}{2}\|\Delta_f - \hat{\Delta}_f\|^2 = \frac{1}{2}\|\tilde{\Delta}_f\|^2 \tag{3.1}$$

where the gradient of the cost function in Eq 3.1 is given by:

$$\nabla \mathcal{J}_{\hat{W}}(\hat{W}) = -\phi_f\left[\Delta_f(x) - \hat{W}^T(t)\phi_f(x)\right]^T = -\phi_f\phi_f^T\tilde{W} = -\phi_f\tilde{\Delta}_f^T$$

Remark 3.1. *Negative gradient of the cost function constructs the modification term in CMRAC as it is a typical approach in gradient-descent based optimization. That is, the modification term in CMRAC architecture can be written as*

$$\dot{\hat{W}}_{cmrac} = -\gamma\nabla \mathcal{J}_{\hat{W}}(\hat{W}) = \gamma\phi_f\tilde{\Delta}_f^T = \gamma\phi_f\phi_f^T\tilde{W}$$

In that respect, the dynamics of the modification term is analogous to an integrator system with the input being a proportional feedback of the gradient term.

Assumption 3.1. *Basis function $\phi \in \mathbb{R}^s$ is a sufficiently exciting signal. Hence, there exists positive constants $\alpha, T_e \in \mathbb{R}_+$, $t_0 \in \mathbb{R}$ such that the following inequality holds:*

$$\int_{t_0}^{t} \phi(\tau)\phi^T(\tau)d\tau \succeq \alpha I_{s\times s}, \qquad t = T_e > t_0$$

Remark 3.2. *Assumption 3.1 ensures that basis function ϕ contains as many spectral lines as there are unknown parameters. Note that basis function ϕ is an exogenous signal to the low-pass filter system in Eq 2.12 with the transfer function of $\mathcal{G}(s) \triangleq \frac{\omega_f}{s+\omega_f}$. Then, filtered basis function ϕ_f has also the same number of spectral lines with less energy than that of the original basis ϕ since $\mathcal{G}(s)$ is stable, minimum phase, and strictly proper transfer function [87]. This implies the following:*

$$\int_{t_0}^{t} \phi_f(\tau)\phi_f^T(\tau)d\tau \succeq \beta I_{s\times s}, \qquad t = T_e$$

with $0 < \beta \leq \alpha$. The degradation in the richness of the signal (which is equivalent to how small is β than α) depends on the cutoff frequency ω_f and spectrum of the basis ϕ. Let the spectral measure of ϕ is given by $S_\phi([\omega_1 \ \omega_2])$ with $\omega_1 < \omega_2$. Choosing the filter design parameter ω_f to be larger than ω_2 leads to relatively small degradation in the richness of ϕ_f with β being closer to α. To give a practical example, one can consider the longitudinal dynamics of an aircraft with basis being the system states; i.e. $\phi(x) = x$. In this case, choosing the cutoff frequency ω_f to be larger than the natural frequency of the short period mode will be sufficient to preserve the richness of the filtered basis $\phi_f = x_f$. Note that this is generally possible as prior information about possible spectrum of the states are available from the nominal aircraft model.

Low-frequency content of the matched uncertainty Δ_f is manipulated as follows:

$$\Delta_f \phi_f^T = W^T \phi_f \phi_f^T$$

$$\mathcal{M}^T \triangleq \int_{t_0}^{t} \Delta_f \phi_f^T d\xi = \int_{t_0}^{t} W^T \phi_f \phi_f^T d\xi = W^T \int_{t_0}^{t} \phi_f \phi_f^T d\xi$$

Note that the signal $\mathcal{M}$ is accessible as the low-frequency content of the uncertainty Δ_f is available from Eq 2.14. Then, estimated form $\hat{\mathcal{M}}$ and corresponding error $\tilde{\mathcal{M}}$ are defined as:

$$\hat{\mathcal{M}}^T \triangleq \hat{W}^T \int_{t_0}^{t} \phi_f \phi_f^T d\xi$$

$$\tilde{\mathcal{M}} \triangleq \mathcal{M} - \hat{\mathcal{M}} = \underbrace{\left(\int_{t_0}^{t} \phi_f \phi_f^T d\xi \right)}_{\triangleq \Phi} \tilde{W} = \Phi \tilde{W} \tag{3.2}$$

It should also be noted that the signal $\tilde{\mathcal{M}}$ is also available since both $\mathcal{M}$ and $\hat{\mathcal{M}}$ are accessible. Having defined the error signal $\tilde{\mathcal{M}}$, the weight update law is decomposed to have the following form:

$$\dot{\hat{W}} = \dot{\hat{W}}_b + \dot{\hat{W}}_m, \qquad \text{with} \quad \dot{\hat{W}}_b = -\left(\Gamma^{-1} + \gamma_m \phi_f \phi_f^T \right)^{-1} \phi e^T P B$$

where $\dot{\hat{W}}_b$ is the standard adaptive law with time-varying learning rate, $\dot{\hat{W}}_m$ is the proposed modification in the weight update law. Using the auxiliary error signal $\tilde{\mathcal{M}}$ in Eq 3.2, the following modification term is proposed:

$$\dot{\hat{W}}_m = \left(\Gamma^{-1} + \gamma_m \phi_f \phi_f^T \right)^{-1} \left(\gamma_m \dot{\phi}_f \tilde{\Delta}_f^T + \gamma_1 \phi_f \tilde{\Delta}_f^T + \gamma_2 \tilde{\mathcal{M}} \right) \tag{3.3}$$

where $\gamma_1, \gamma_2, \gamma_m \in \mathbb{R}_+$ are user-defined design variables. Constructive proof of the proposed weight update law will be provided in Theorem 3.1. Then, overall weight update law becomes:

$$\dot{\hat{W}} = \left(\Gamma^{-1} + \gamma_m \phi_f \phi_f^T\right)^{-1}\left(-\phi e^T P B + \gamma_m \dot{\phi}_f \tilde{\Delta}_f^T + \gamma_1 \phi_f \tilde{\Delta}_f^T + \gamma_2 \tilde{\mathcal{M}}\right) \qquad (3.4)$$

Theorem 3.1. *Consider the uncertain system dynamics given in Eq 2.1, uncertainty parametrization in Assumption 2.2, reference model dynamics in Eq 2.2, control input in Eq 2.7, filter states in Eq 2.12, and adaptive law in Eq 3.4. Then, the state tracking error $e(t)$ is asymptotically stable for the closed-loop system. Furthermore, all the closed-loop signals are bounded. If the basis function ϕ is sufficiently exciting, then the zero-solution $\left(e, \tilde{W}, \tilde{\Delta}_f\right) = \left(0, 0, 0\right)$ is globally asymptotically stable.*

Proof. Consider the following radially unbounded Lyapunov function:

$$\begin{aligned}
\mathcal{V}\left(e, \tilde{W}, \tilde{\Delta}_f\right) &= \frac{1}{2}e^T P e + \frac{1}{2}\mathrm{tr}\left(\tilde{W}^T \Gamma^{-1} \tilde{W}\right) + \frac{1}{2}\tilde{\Delta}_f^T \gamma_m \tilde{\Delta}_f \\
&= \frac{1}{2}\eta^T \bar{P} \eta
\end{aligned} \qquad (3.5)$$

with $\eta \triangleq \begin{bmatrix} e^T & \mathrm{vec}(\tilde{W})^T & \tilde{\Delta}_f^T \end{bmatrix}^T$ and $\bar{P} \triangleq \mathrm{diag}\left(P, I_{m \times m} \otimes \Gamma^{-1}, \gamma_m\right)$. Note that $\mathcal{V}(0,0,0) = 0$ and $\mathcal{V}\left(e, \tilde{W}, \tilde{\Delta}_f\right) \neq 0$ for all $\left(e, \tilde{W}, \tilde{\Delta}_f\right) \neq \left(0, 0, 0\right)$, $\forall t \in \mathbb{R}_+$. The time derivative of Lyapunov function $\mathcal{V}\left(e, \tilde{W}, \tilde{\Delta}_f\right)$ along the system trajectories in Eq 2.9 and Eq 3.4 is given as the following:

$$\begin{aligned}
\dot{\mathcal{V}} &= e^T P \dot{e} + \mathrm{tr}\left(\tilde{W}^T \Gamma^{-1} \dot{\tilde{W}}\right) + \tilde{\Delta}_f^T \gamma_m \dot{\tilde{\Delta}}_f \\
&= e^T P A_r e - e^T P B \tilde{W}^T \phi + \mathrm{tr}\left(\tilde{W}^T \Gamma^{-1} \dot{\tilde{W}}\right) + \gamma_m \mathrm{tr}\left[\tilde{\Delta}_f^T \left(\dot{\tilde{W}}^T \phi_f + \tilde{W}^T \dot{\phi}_f\right)\right]
\end{aligned}$$

Since the ideal weights are constant, the equality $\dot{\tilde{W}} = -\dot{\hat{W}}$ holds. Then,

$$\begin{aligned}
\dot{\mathcal{V}} &= e^T P A_r e - e^T P B \tilde{W}^T \phi - \mathrm{tr}\left(\tilde{W}^T \Gamma^{-1} \dot{\hat{W}}\right) + \gamma_m \mathrm{tr}\left[\tilde{\Delta}_f^T \left(\dot{\tilde{W}}^T \phi_f + \tilde{W}^T \dot{\phi}_f\right)\right] \\
&= -\frac{1}{2}e^T Q e - \mathrm{tr}\left(\tilde{W}^T \phi e^T P B\right) - \mathrm{tr}\left(\tilde{W}^T \Gamma^{-1} \dot{\hat{W}}\right) \\
&\quad - \gamma_m \mathrm{tr}\left(\tilde{\Delta}_f^T \dot{\hat{W}}^T \phi_f\right) + \gamma_m \mathrm{tr}\left(\tilde{\Delta}_f^T \tilde{W}^T \dot{\phi}_f\right) \\
&= -\frac{1}{2}e^T Q e - \mathrm{tr}\left(\tilde{W}^T \phi e^T P B\right) - \mathrm{tr}\left(\tilde{W}^T \Gamma^{-1} \dot{\hat{W}}\right) \\
&\quad - \gamma_m \mathrm{tr}\left(\tilde{W}^T \phi_f \phi_f^T \dot{\hat{W}}\right) + \gamma_m \mathrm{tr}\left(\tilde{W}^T \dot{\phi}_f \tilde{\Delta}_f^T\right) \\
&= -\frac{1}{2}e^T Q e - \mathrm{tr}\left[\tilde{W}^T \left(\phi e^T P B - \gamma_m \dot{\phi}_f \tilde{\Delta}_f^T\right)\right] - \mathrm{tr}\left[\tilde{W}^T \left(\Gamma^{-1} + \gamma_m \phi_f \phi_f^T\right)\dot{\hat{W}}\right]
\end{aligned}$$

28

Substituting the update law in Eq 3.4 and using Assumption 3.1 and Remark 3.2, the time derivative of the Lyapunov function can be upper-bounded by:

$$
\begin{aligned}
\dot{\mathcal{V}} &= -\frac{1}{2}e^T Q e - \gamma_1 \mathrm{tr}\big(\tilde{W}^T \phi_f \phi_f^T \tilde{W}\big) - \gamma_2 \mathrm{tr}\big(\tilde{W}^T \Phi \tilde{W}\big) \\
&\leq -\frac{1}{2}\lambda_{\min}(Q)\|e\|^2 - \gamma_1 \|\tilde{\Delta}_f\|^2 - \gamma_2 \lambda_{\min}(\Phi)\|\tilde{W}\|^2 \\
&= -\frac{1}{2}\lambda_{\min}(Q)\|e\|^2 - \gamma_1 \|\tilde{\Delta}_f\|^2 - \gamma_2 \beta \|\tilde{W}\|^2 \\
&\leq -\mu_1 \|\eta\|^2 < 0
\end{aligned}
\tag{3.6}
$$

with $\mu_1 \triangleq \min\left\{\frac{1}{2}\lambda_{\min}(Q), \gamma_1, \gamma_2 \beta\right\} \in \mathbb{R}_+$. Positive definite Lyapunov function $\mathcal{V}(\eta) > 0$, $\forall \eta \neq 0$, with its negative definite time derivative $\dot{\mathcal{V}}(\eta) < 0$, $\forall \eta \neq 0$, implies the zero solution $\eta(t) \equiv 0$ is asymptotically stable; i.e. $\eta(t) \to 0$ as $t \to \infty$. Specifically, for the positive definite Lyapunov candidate $\mathcal{V}\big(e, \tilde{W}, \tilde{\Delta}_f\big)$ given in Eq 3.5, the inequality $\dot{\mathcal{V}}\big(e, \tilde{W}, \tilde{\Delta}_f\big) < 0$ holds for all $\big(e, \tilde{W}, \tilde{\Delta}_f\big) \neq \big(0, 0, 0\big)$ ensuring that Lyapunov function $\mathcal{V}\big(e, \tilde{W}, \tilde{\Delta}_f\big)$ approaches to zero as $t \to \infty$. Hence, the asymptotic stability of state tracking error $e(t)$ and weight estimation error $\tilde{W}(t)$ is constructed. Furthermore, asymptotic convergence of the weight estimation error $\tilde{W}$ yields $\tilde{\Delta} = \big(\Delta - \hat{\Delta}\big) \to 0$ as $t \to \infty$. Since the Lyapunov function is radially unbounded, this result is global, and that completes the proof of global asymptotic stability of the zero-solution $\big(e, \tilde{W}, \tilde{\Delta}_f\big) = \big(0, 0, 0\big)$.

∎

Remark 3.3. *If Assumption 3.1 is not satisfied, i.e. $\alpha = \beta = 0$, the closed-loop stability of the proposed adaptive control system can be shown using radially unbounded Lyapunov function given in Eq 3.5. Since $\mathcal{V}\big(e, \tilde{W}, \tilde{\Delta}_f\big)$ is lower-bounded by zero, and inequality $\dot{\mathcal{V}}\big(e, \tilde{W}, \tilde{\Delta}_f\big) \leq 0$ holds for its derivative for $\beta = 0$, Lyapunov function $\mathcal{V}\big(e, \tilde{W}, \tilde{\Delta}_f\big)$ approaches to a finite limit as $t \to \infty$. Hence, the boundedness of tracking error $e(t)$, weight estimation error $\tilde{W}(t)$, and low-frequency uncertainty estimation error $\tilde{\Delta}_f(t)$ is guaranteed. Since $e(t)$ and $x_r(t)$ are bounded, system states $x(t)$ and basis vector-function $\phi(x)$ immediately become bounded. Note that low-pass filters in Eq 2.12 are BIBO stable dynamical systems. Thus, the filtered states $x_f(t)$ and $\phi_f(t)$ are also bounded. With bounded signals $e(t), x(t), \phi(x), x_f(t), \phi_f(t)$, and $\tilde{W}(t)$, state tracking error rate $\dot{e}(t)$ and adaptive weight estimation error rate $\dot{\tilde{W}}(t)$ are bounded, which ensures the boundedness of $\ddot{\mathcal{V}}\big(e, \tilde{W}, \tilde{\Delta}_f\big)$, $\forall t \in \mathbb{R}_+$. It then*

follows from Barbalat's Lemma [79] that $\lim_{t\to\infty}\dot{\mathcal{V}}\big(e(t),\tilde{W}(t),\tilde{\Delta}_f\big) = 0$ *which implies the asymptotic stability of tracking error* $e(t)$ *and low-frequency uncertainty estimation error* $\tilde{\Delta}_f(t)$; *that is,* $\lim_{t\to\infty} e(t) = 0$ *and* $\lim_{t\to\infty}\tilde{\Delta}_f(t) = 0$. *All in all, without sufficient excitation of filtered basis vector-function* ϕ_f, *zero solution* $\big(e(t),\tilde{\Delta}_f(t)\big) = (0,0)$ *is asymptotically stable, and adaptive weight estimation matrix* $\hat{W}(t)$ *is uniformly ultimately bounded. Since the Lyapunov function is radially unbounded, these results hold globally.*

Lemma 3.1. *Convergence rate for the augmented error signal* $\eta(t)$, $\forall t \geq t_0$, *is given by the following inequality:*

$$\|\eta(t)\| \leq e^{-\frac{\min\left\{\frac{1}{2}\lambda_{\min}\left(Q\right),\gamma_1,\gamma_2\beta\right\}}{\max\left\{\lambda_{\max}(P),\lambda_{\max}(\Gamma^{-1}),\gamma_m\right\}}(t-t_0)}\sqrt{\frac{\max\left\{\lambda_{\max}(P),\lambda_{\max}(\Gamma^{-1}),\gamma_m\right\}}{\min\left\{\lambda_{\min}(P),\lambda_{\min}(\Gamma^{-1}),\gamma_m\right\}}}\|\eta(t_0)\|$$

Proof.

Lyapunov function in Eq 3.5 can be bounded as follows:

$$\frac{1}{2}\lambda_{\min}\left(\bar{P}\right)\|\eta(t)\|^2 \leq \mathcal{V}\left(\eta(t)\right) \leq \frac{1}{2}\lambda_{\max}\left(\bar{P}\right)\|\eta(t)\|^2, \qquad \forall t \geq t_0 \qquad (3.7)$$

Wherever appropriate, the arguments 't' for time dependency and 'x' for state dependency are dropped consistently for ease of exposition. Next, using Eq 3.7, lower-bound for the error vector η can be expressed as

$$\|\eta\|^2 \geq \frac{2\mathcal{V}}{\lambda_{\max}\left(\bar{P}\right)}$$

Let $\mu_2 \in \mathbb{R}_+$ be defined as $\mu_2 \triangleq \frac{2\mu_1}{\lambda_{\max}(\bar{P})}$. Also, recall the time derivative of the Lyapunov function in Eq 3.6:

$$\dot{\mathcal{V}} \leq -\mu\|\eta\|^2 \leq -\frac{2\mu}{\lambda_{\max}\left(\bar{P}\right)}\mathcal{V} \qquad \Rightarrow \qquad \dot{\mathcal{V}} \leq -\alpha\mathcal{V}$$

Using Comparison Lemma [79], one can obtain:

$$\mathcal{V}(t) \leq e^{-\alpha(t-t_0)}\mathcal{V}(t_0)$$

30

Eventually, the following inequality is obtained:

$$\frac{1}{2}\lambda_{\min}\left(\bar{P}\right)\|\eta(t)\|^2 \leq \mathcal{V}(t) \leq e^{-\mu_2(t-t_0)}\mathcal{V}(t_0)$$

$$e^{-\mu_2(t-t_0)}\mathcal{V}(t_0) = \frac{1}{2}e^{-\mu_2(t-t_0)}\eta^T(t_0)\bar{P}\eta(t_0) \leq \frac{1}{2}e^{-\mu_2(t-t_0)}\lambda_{\max}\left(\bar{P}\right)\|\eta(t_0)\|^2$$

$$= \frac{1}{2}e^{-\mu_2(t-t_0)}\eta^T(t_0)\bar{P}\eta(t_0) \leq \frac{1}{2}e^{-\mu_2(t-t_0)}\lambda_{\max}\left(\bar{P}\right)\|\eta(t_0)\|^2 \qquad (3.8)$$

$$\lambda_{\min}\left(\bar{P}\right)\|\eta(t)\|^2 \leq e^{-\mu_2(t-t_0)}\lambda_{\max}\left(\bar{P}\right)\|\eta(t_0)\|^2$$

$$\|\eta(t)\| \leq e^{-\frac{\mu_2}{2}(t-t_0)}\sqrt{\frac{\lambda_{\max}\left(\bar{P}\right)}{\lambda_{\min}\left(\bar{P}\right)}}\|\eta(t_0)\|, \qquad \forall t \geq t_0$$

where the positive constants $\lambda_{\max}\left(\bar{P}\right), \lambda_{\min}\left(\bar{P}\right), \mu,$ and μ_2 are given by:

$$\lambda_{\max}\left(\bar{P}\right) = \max\left\{\lambda_{\max}(P), \lambda_{\max}(\Gamma^{-1}), \gamma_m\right\} = \max\left\{\lambda_{\max}(P), \frac{1}{\lambda_{\min}(\Gamma)}, \gamma_m\right\}$$

$$\lambda_{\min}\left(\bar{P}\right) = \min\left\{\lambda_{\min}(P), \lambda_{\min}(\Gamma^{-1}), \gamma_m\right\} = \min\left\{\lambda_{\min}(P), \frac{1}{\lambda_{\max}(\Gamma)}, \gamma_m\right\}$$

$$\mu = \min\left\{\frac{1}{2}\lambda_{\min}(Q), \gamma_1, \gamma_2\beta\right\}$$

$$\mu_2 = \frac{2\min\left\{\frac{1}{2}\lambda_{\min}(Q), \gamma_1, \gamma_2\beta\right\}}{\max\left\{\lambda_{\max}(P), \lambda_{\max}(\Gamma^{-1}), \gamma_m\right\}}$$

$$(3.9)$$

Substituting the variables in Eq 3.9 into Eq 3.8 results in:

$$\|\eta(t)\| \leq e^{-\frac{\min\left\{\frac{1}{2}\lambda_{\min}(Q), \gamma_1, \gamma_2\beta\right\}}{\max\left\{\lambda_{\max}(P), \lambda_{\max}(\Gamma^{-1}), \gamma_m\right\}}(t-t_0)}\sqrt{\frac{\max\left\{\lambda_{\max}(P), \lambda_{\max}(\Gamma^{-1}), \gamma_m\right\}}{\min\left\{\lambda_{\min}(P), \lambda_{\min}(\Gamma^{-1}), \gamma_m\right\}}}\|\eta(t_0)\|$$

That concludes the convergence rate derivation for the augmented error signal $\eta(t)$.

$\blacksquare$

Lemma 3.2. *Transient performance bounds for state tracking error $e(t)$, adaptive weight estimation error $\tilde{W}(t)$, and low-frequency uncertainty estimation error $\tilde{\Delta}_f(t)$ are given for $\forall t \geq t_0$ as follows:*

$$\|e(t)\|^2 \leq \frac{1}{\lambda_{\min}(P)}\left[\lambda_{\max}(P)\|e(t_0)\|^2 + \lambda_{\max}(\Gamma^{-1})\|\tilde{W}(t_0)\|_F^2 + \gamma_m\|\tilde{\Delta}_f(t_0)\|^2\right]$$

$$\|\tilde{W}(t)\|^2 \leq \lambda_{\max}(\Gamma)\left[\lambda_{\max}(P)\|e(t_0)\|^2 + \lambda_{\max}(\Gamma^{-1})\|\tilde{W}(t_0)\|_F^2 + \gamma_m\|\tilde{\Delta}_f(t_0)\|^2\right]$$

$$\|\tilde{\Delta}_f(t)\|^2 \leq \frac{1}{\gamma_m}\left[\lambda_{\max}(P)\|e(t_0)\|^2 + \lambda_{\max}(\Gamma^{-1})\|\tilde{W}(t_0)\|_F^2 + \gamma_m\|\tilde{\Delta}_f(t_0)\|^2\right]$$

Proof.

Lyapunov function in Eq 3.5 can be bounded as follows:

$$\frac{1}{2}\lambda_{\min}\left(P\right)\left\|e(t)\right\|^2 + \frac{1}{2}\lambda_{\min}\left(\Gamma^{-1}\right)\left\|\tilde{W}(t)\right\|^2 + \frac{1}{2}\gamma_m\|\tilde{\Delta}_f(t)\|^2 \leq \mathcal{V}(t), \qquad t \geq t_0$$

which gives the following relations:

$$\frac{1}{2}\lambda_{\min}\left(P\right)\left\|e(t)\right\|^2 \leq \mathcal{V}(t)$$
$$\frac{1}{2}\lambda_{\min}\left(\Gamma^{-1}\right)\|\tilde{W}(t)\|^2 \leq \mathcal{V}(t) \qquad (3.10)$$
$$\frac{1}{2}\gamma_m\|\tilde{\Delta}_f(t)\|^2 \leq \mathcal{V}(t)$$

From Theorem 3.1 and Remark 3.3, if the sufficient excitation condition does not hold (i.e. $\alpha = \beta = 0$), $\dot{\mathcal{V}}(t) \leq 0$ yields $0 \leq \mathcal{V}(t) \leq \mathcal{V}(t_0)$. Note that the initial value of the Lyapunov function satisfies the following:

$$\mathcal{V}(t_0) \leq \frac{1}{2}\lambda_{\max}\left(P\right)\left\|e(t_0)\right\|^2 + \frac{1}{2}\lambda_{\max}\left(\Gamma^{-1}\right)\|\tilde{W}(t_0)\|_F^2 + \frac{1}{2}\gamma_m\|\tilde{\Delta}_f(t_0)\|^2 \quad (3.11)$$

Finally, combining the results from Eq 3.10 and Eq 3.11 with $\lambda_{\max}\left(\Gamma\right) = \frac{1}{\lambda_{\min}\left(\Gamma^{-1}\right)}$ results in:

$$\|e(t)\|^2 \leq \frac{1}{\lambda_{\min}\left(P\right)}\left[\lambda_{\max}\left(P\right)\left\|e(t_0)\right\|^2 + \lambda_{\max}\left(\Gamma^{-1}\right)\|\tilde{W}(t_0)\|_F^2 + \gamma_m\|\tilde{\Delta}_f(t_0)\|^2\right]$$
$$\|\tilde{W}(t)\|^2 \leq \lambda_{\max}\left(\Gamma\right)\left[\lambda_{\max}\left(P\right)\left\|e(t_0)\right\|^2 + \lambda_{\max}\left(\Gamma^{-1}\right)\|\tilde{W}(t_0)\|_F^2 + \gamma_m\|\tilde{\Delta}_f(t_0)\|^2\right]$$
$$\|\tilde{\Delta}_f(t)\|^2 \leq \frac{1}{\gamma_m}\left[\lambda_{\max}\left(P\right)\left\|e(t_0)\right\|^2 + \lambda_{\max}\left(\Gamma^{-1}\right)\|\tilde{W}(t_0)\|_F^2 + \gamma_m\|\tilde{\Delta}_f(t_0)\|^2\right]$$

This concludes the proof of Lemma 2.

∎

Remark 3.4. *This remark elaborates the contributions and important aspects of the proposed modification in Eq 3.4. First, it should be noted that the proposed adaptive law acquires all the benefits of CMRAC listed in Remark 2.6. Additionally, the proposed method exhibits significant improvements in terms of robustness. Specifically,*

- *The term '$\gamma_1\phi_f\tilde{\Delta}_f^T = \gamma_1\phi_f\phi_f^T\tilde{W}$' adds a new update direction that minimizes the low-frequency content of the uncertainty estimation error. One can show*

32

this through the following optimization problem:

$$\min_{\hat{W}} \mathcal{J}, \qquad \mathcal{J}(\hat{W}) = \frac{1}{2}\|W^T\phi_f - \hat{W}^T\phi_f\|^2 = \frac{1}{2}\|\Delta_f - \hat{\Delta}_f\|^2 = \frac{1}{2}\|\tilde{\Delta}_f\|^2$$

Gradient of the cost function to be used in a simple gradient descent optimization framework is given by:

$$\nabla \mathcal{J}_{\hat{W}}(\hat{W}) = \phi_f\left[\Delta_f - \hat{W}^T\phi_f\right]^T = \phi_f\phi_f^T\tilde{W} \tag{3.12}$$

where the signal Δ_f is available with Eq 2.14, $\hat{W}$ is the online estimation of the unknown weight matrix W, and low-pass filtered basis function ϕ_f is computed using Eq 2.12. Note that a few variations of this gradient descent-based term appears in the literature, as well [14, 20, 90, 91].

- *As the design parameter γ_m tends to zero, modification term learning rate $\left(\Gamma^{-1} + \gamma_m^{-1}\phi_f\phi_f^T\right)^{-1}$ tends to Γ. Furthermore, with $\gamma_2 = 0$, the entire proposed modification term approaches to the solution of optimizing solution in Eq 3.12, which results in CMRAC in Eq 2.16. Hence, the proposed adaptive law can be considered as a generalized form of CMRAC. That is,*

$$if \quad \gamma_2 = \gamma_m = 0 \qquad \Rightarrow \qquad \begin{aligned} \dot{\hat{W}}_m &= \gamma_1\Gamma\phi_f\phi_f^T\tilde{W} \\ \dot{\hat{W}} &= \Gamma\left[-\phi e^T PB + \gamma_1\phi_f\phi_f^T\tilde{W}\right] \end{aligned}$$

- *Time derivative of gradient of the cost function in Eq 3.12 is given by*

$$\frac{d}{dt}\left(\nabla\mathcal{J}_{\hat{W}}\right) = 2\dot{\phi}_f\phi_f^T\tilde{W} - \phi_f\phi_f^T\dot{\hat{W}}_b - \phi_f\phi_f^T\dot{\hat{W}}_m \tag{3.13}$$

It can be observed that proposed update law in Eq 3.4 contains the entire derivative information given in Eq 3.13. Adding such a derivative information to the traditional gradient-descent based optimization allows to shape the transient behavior and increases the robustness of the optimization just like the derivative action in traditional PID controllers. Each term contributes to the robustness of the proposed solution in different manners. Specifically, the term in Eq 3.13, '$\dot{\phi}_f\tilde{\Delta}_f^T$', compensates the information lost while filtering the basis function ϕ. Thus, high-frequency content of the basis vector-function ϕ is included in the adaptation. Then, '$\phi_f\phi_f^T\dot{\hat{W}}_b$', regulates the standard adaptive law through design parameter γ_m. In that respect, this term can be considered as proportional feedback control for the standard adaptive law behaving like a

stability augmentation system. This is equivalent to re-adjusting the learning rate Γ so that the large values in the basis function ϕ does not affect the adaptation adversely. The last term, '$\phi_f \phi_f^T \dot{\tilde{W}}_m$', regulates the learning rate of the modification term in a similar way to the regulation in the standard model reference adaptive law. Time varying learning rate in Eq 3.4 contains these regulation information in compact form.

- *Last but not the least, term '$\gamma_2 \tilde{\mathcal{M}}$' plays a vital role in ensuring the parameter convergence; i.e. $\hat{W}(t) \rightarrow W$ as $t \rightarrow \infty$. In that respect, this term acts like an integral action in a traditional PID controllers as it analogously allows to remove the steady state error in the weight estimations.*

3.3 Inverse-free Weight Update Law

One may realize that the proposed update law in Eq 3.4 requires to take the inverse of a (possibly large) matrix during the online operation. Clearly, this will introduce an additional computational cost and cause practical issues. In order to eliminate these drawbacks, an inverse-free form of the learning rate is introduced.

Lemma 3.3. *Given $\Gamma = \Gamma^T \succ 0$ is positive definite matrix, $\gamma_m \in \mathbb{R}_+$ is a positive constant, and $\phi_f \in \mathbb{R}^s$, the matrix $(\Gamma^{-1} + \gamma_m \phi_f \phi_f^T)$ is invertible and its inverse is:*

$$\left(\Gamma^{-1} + \gamma_m \phi_f \phi_f^T \right)^{-1} = \Gamma - \frac{\gamma_m}{1 + tr\left(\gamma_m \phi_f \phi_f^T \Gamma \right)} \Gamma \phi_f \phi_f^T \Gamma \succ 0$$

Proof. Note that $\Gamma = \Gamma^T \succ 0$ and $\gamma_m \phi_f \phi_f^T \succeq 0$ with $\gamma_m > 0$. This fact implies $(\Gamma^{-1} + \gamma_m \phi_f \phi_f^T)$ is also a positive definite matrix; i.e. $(\Gamma^{-1} + \gamma_m \phi_f \phi_f^T) \succ 0$. Then, $(\Gamma^{-1} + \gamma_m \phi_f \phi_f^T)$ is always invertible. Now, let $E \triangleq \gamma_m \phi_f \phi_f^T$. Note that E has rank one. In addition, let the inverse of $(\Gamma^{-1} + E)$ be in the form of $\Gamma - \nu \Gamma \gamma_m \phi_f \phi_f^T \Gamma$.

Then,

$$\left(\Gamma^{-1} + E\right)\left(\Gamma - \nu\Gamma E\Gamma\right) = I$$

$$I - \nu E\Gamma + E\Gamma - \nu E\Gamma E\Gamma = I \qquad (3.14)$$

$$\nu E\Gamma - E\Gamma + \nu E\Gamma E\Gamma = 0$$

Recall that $E\Gamma E = \mathrm{tr}\left(E\Gamma\right)E$. This fact can be shown as follows:

$$E\Gamma E = \gamma_m\phi_f\phi_f^T\Gamma\gamma_m\phi_f\phi_f^T = \gamma_m\phi_f\left[\gamma_m\phi_f^T\Gamma\phi_f\right]\phi_f^T = \left[\gamma_m\phi_f^T\Gamma\phi_f\right]\gamma_m\phi_f\phi_f^T = \left[\gamma_m\phi_f^T\Gamma\phi_f\right]E$$

with $\left(\gamma_m\phi_f^T\Gamma\phi_f\right) = \gamma_m\mathrm{tr}\left(\phi_f^T\Gamma\phi_f\right) = \mathrm{tr}\left(\gamma_m\phi_f\phi_f^T\Gamma\right) = \mathrm{tr}\left(E\Gamma\right)$. Hence,

$$E\Gamma E = \mathrm{tr}\left(E\Gamma\right)E$$

Substituting these results into Eq 3.14 results in:

$$\nu E\Gamma - E\Gamma + \nu\mathrm{tr}\left(E\Gamma\right)E\Gamma = \left[\nu - 1 + \nu\mathrm{tr}\left(E\Gamma\right)\right]E\Gamma = 0$$

which can be satisfied for $\nu \triangleq \frac{1}{1+tr(E\Gamma)}$. Eventually, the inverse of $\left(\Gamma^{-1} + E\right)$ becomes:

$$\left(\Gamma^{-1} + E\right)^{-1} = \Gamma - \nu\Gamma E\Gamma = \Gamma - \frac{1}{1 + \mathrm{tr}\left(E\Gamma\right)}\Gamma E\Gamma$$

Substituting $E = \gamma_m\phi_f\phi_f^T$ yields:

$$\left(\Gamma^{-1} + \gamma_m\phi_f\phi_f^T\right)^{-1} = \Gamma - \frac{\gamma_m}{1 + \mathrm{tr}\left(\gamma_m\phi_f\phi_f^T\Gamma\right)}\Gamma\phi_f\phi_f^T\Gamma$$

This completes the proof. Reader may also refer to Refs [92], [93] for more detailed information.

■

Block diagram of the proposed architecture can be seen in Figure 3.1.

3.4 Numerical Examples

Aircraft wing-rock dynamics [76] is considered as a numerical example:

$$\dot{x} = \begin{bmatrix} 0 & 1 \\ 0 & 0 \end{bmatrix}x + \begin{bmatrix} 0 \\ 1 \end{bmatrix}[u(t) + \Delta(x)]$$

$$\Delta(x) = 0.2314x_1 + 0.6918x_2 - 0.6254|x_1|x_2 + 0.095|x_2|x_2 + 0.214x_1^3$$
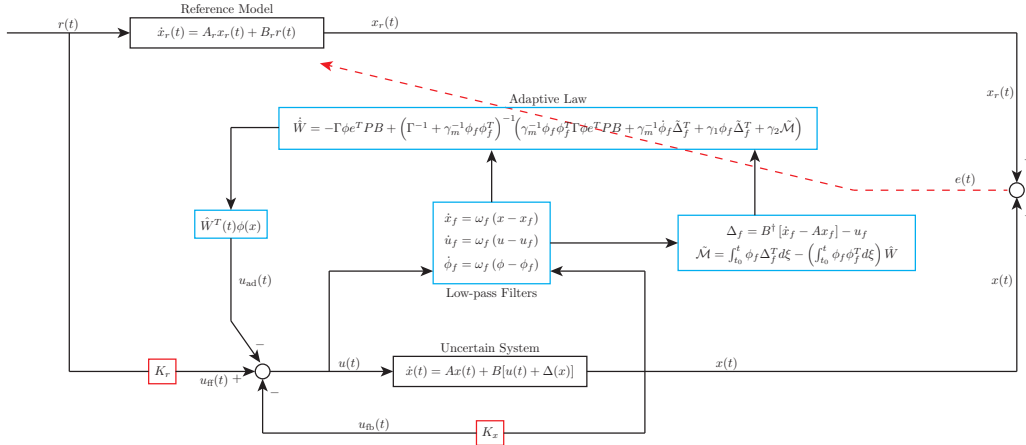
Figure 3.1: Block Diagram of the Proposed Adaptive Controller

where control input u is the aileron deflection, states x_1 and x_2 are roll angle and roll rate, respectively. Reference model is constructed with feedback gain $K_x = \begin{bmatrix} 2.46 & 2.22 \end{bmatrix}$ and feedforward gain $K_r = 2.46$. In addition, simulation parameters are as follows: Lyapunov design matrix $Q = I_{n \times n}$, and low-pass filter cut-off frequency $\omega_f = 8$ rad/s. All the states are initialized from zero. Simulation sampling frequency is set to be 100 Hz.

Nominal controller response in the presence of uncertainties (without time delay) is given in Figure 3.2. As seen from the figure, state tracking performance of the nominal controller is not satisfactory.

In this section, three simulation cases are considered as numerical examples:

1. Simulations with the proposed adaptive controller with no time delay

2. Simulations comparing the proposed adaptive controller with the standard adaptive controller and CMRAC

3. Simulations highlighting the effects of design parameters

3.4.1 Proposed adaptive controller with no time delay

Figure 3.3 illustrates the state tracking performance of the proposed adaptive control architecture. Also, the control input and tracking error norm are given in Figure 3.4.
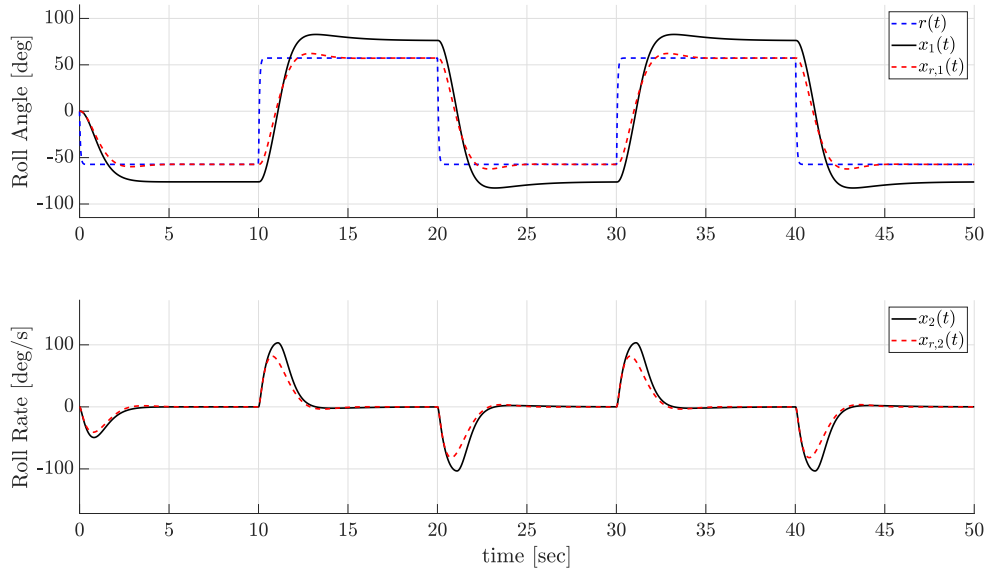
Figure 3.2: State Tracking Performance of the Nominal Controller in Eq 2.4 with no time delay
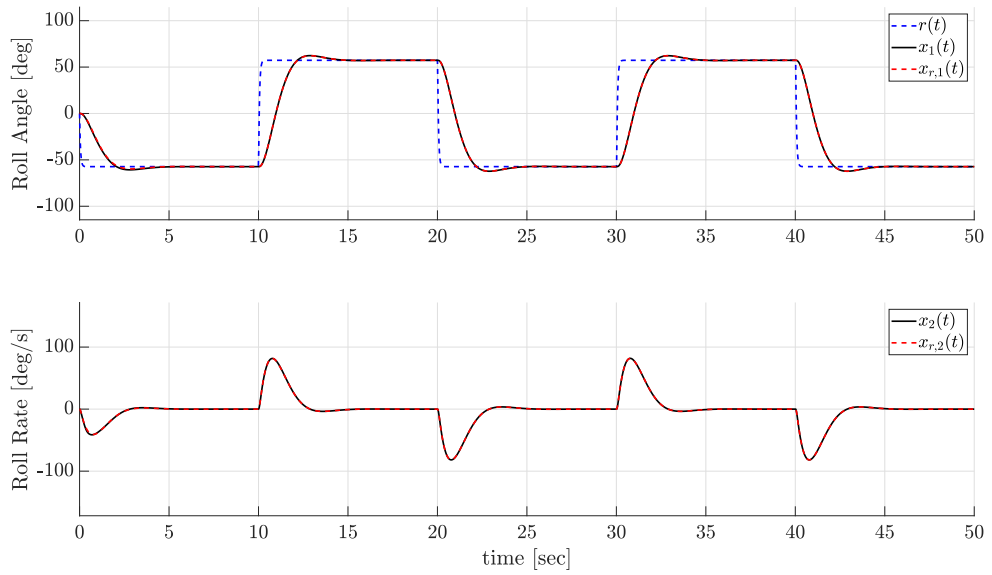
Figure 3.3: State Tracking Performance of the Proposed Method in Eq 3.4 for $\Gamma = 10$, $\gamma_1 = 1$, $\gamma_2 = 40$, and $\gamma_m = 20$ with no time delay

Evolution of the adaptive weights is illustrated in Figure 3.5. As seen clearly, adaptive parameters converge to their ideal values. It can be seen in Figure 3.4 that the tracking error converges to zero. Hence, the results are consistent with Theorem 3.1.

37
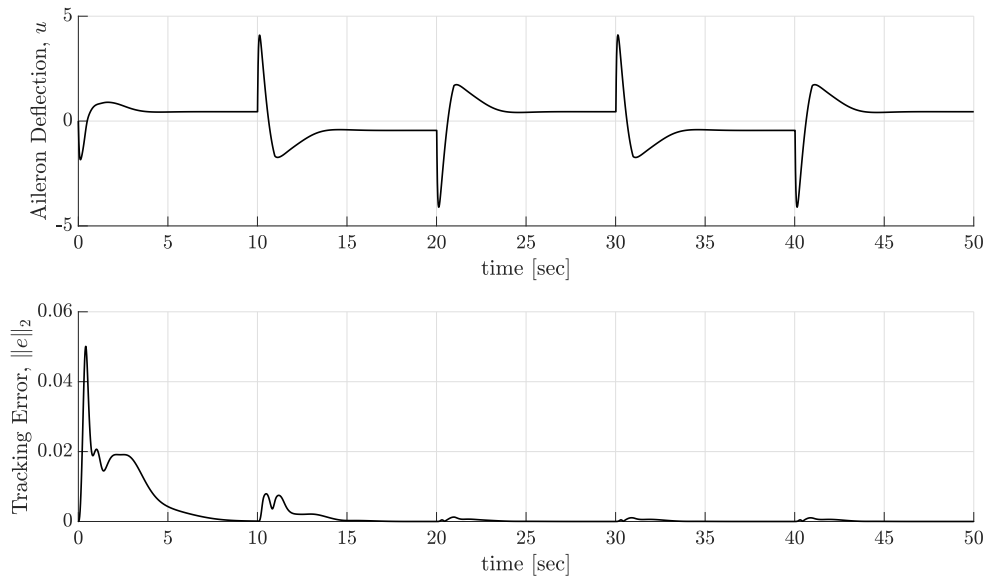
Figure 3.4: Control Input and Tracking Error with the Proposed Method in Eq 3.4 for $\Gamma = 10$, $\gamma_1 = 1$, $\gamma_2 = 40$, and $\gamma_m = 20$ with no time delay
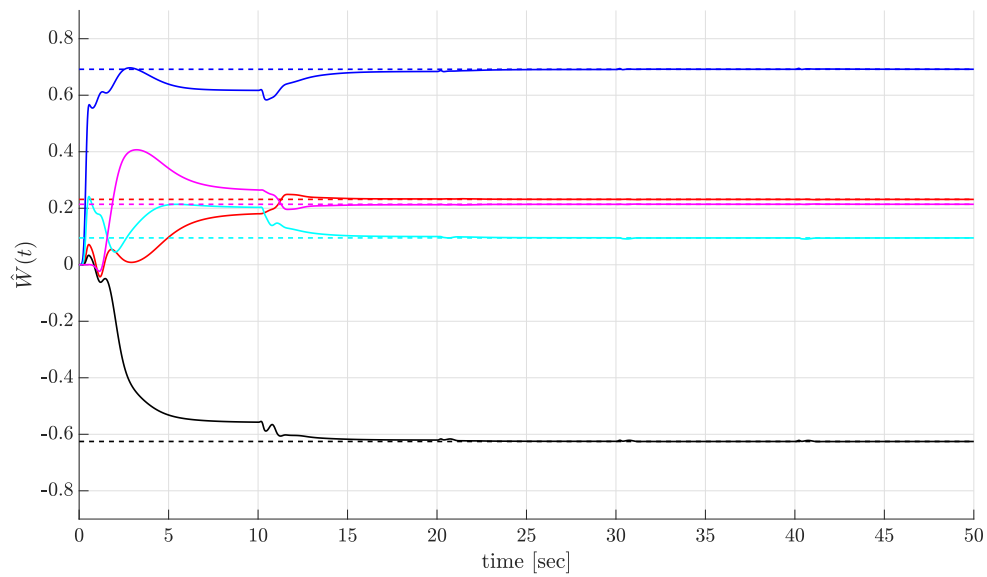
Figure 3.5: Adaptive Weight Estimation Performance of the Proposed Method in Eq 3.4 for $\Gamma = 10$, $\gamma_1 = 1$, $\gamma_2 = 40$, and $\gamma_m = 20$ with no time delay (Dashed lines indicate ideal values of unknown parameters W)

3.4.2 Comparison in the presence of time delay

In this case, an input time delay is introduced so that the system dynamics becomes:

$$\dot{x} = \begin{bmatrix} 0 & 1 \\ 0 & 0 \end{bmatrix} x + \begin{bmatrix} 0 \\ 1 \end{bmatrix} [u(t - t_d) + \Delta(x)]$$

$$\Delta(x) = 0.2314x_1 + 0.6918x_2 - 0.6254|x_1|x_2 + 0.095|x_2|x_2 + 0.214x_1^3$$

with $t_d \in \mathbb{R}_+$ being time-delay.

Standard MRAC update law in Eq 2.10, CMRAC update law in Eq 2.16, and the proposed update law in Eq 3.4 can be re-written as follows:

$$\dot{\hat{W}} = \dot{\hat{W}}_b = -\Gamma\phi e^T PB \tag{3.15a}$$

$$\dot{\hat{W}} = \dot{\hat{W}}_b + \dot{\hat{W}}_c = -\Gamma\phi e^T PB + \Gamma\gamma_c\phi_f\tilde{\Delta}_f^T \tag{3.15b}$$

$$\dot{\hat{W}} = \dot{\hat{W}}_b + \dot{\hat{W}}_c + \dot{\hat{W}}_r = -\Gamma\phi e^T PB + \Gamma\gamma_1\phi_f\tilde{\Delta}_f^T + \mathcal{Y}(x,t) \tag{3.15c}$$

where $\mathcal{Y}(x,t)$ is defined as

$$\mathcal{Y}(x,t) \triangleq -\frac{\gamma_m}{1 + \gamma_m\text{tr}(\phi_f\phi_f^T\Gamma)}\Gamma\phi_f\phi_f^T\Gamma\left(-\phi e^T PB + \gamma_m\dot{\phi}_f\tilde{\Delta}_f^T + \gamma_1\phi_f\tilde{\Delta}_f^T + \gamma_2\tilde{\mathcal{M}}\right)$$

Eqns 3.15a-3.15c illustrate that CMRAC adds a modification term to the standard adaptive law, and the proposed modification adds another term, $\mathcal{Y}(x,t)$, to CMRAC update law. In the comparative Figure 3.6, common adaptive gains in the update laws 3.15a-3.15c are kept the same to make a fair comparison.

In Figure 3.6, state tracking response of the proposed method is compared with those of Standard MRAC and CMRAC in the presence of time delay of $t_d = 0.28$ seconds. As seen from the figure, both CMRAC and Standard MRAC fails whereas the proposed adaptive controller performs quite satisfactorily.

Lastly, for the design parameters $\Gamma = 10$, $\gamma_1 = \gamma_c = 1$, $\gamma_2 = 40$, and $\gamma_m = 20$, time-delay margins of the adaptive control systems composed of weight update laws in Eqns 3.15a-3.15c are given in Table 3.1.

3.4.3 Stabilization with γ_m

In this example, the effect of γ_m on the closed-loop stability is investigated. As shown in Eq 3.4, design parameter γ_m regulates the learning rate of both standard
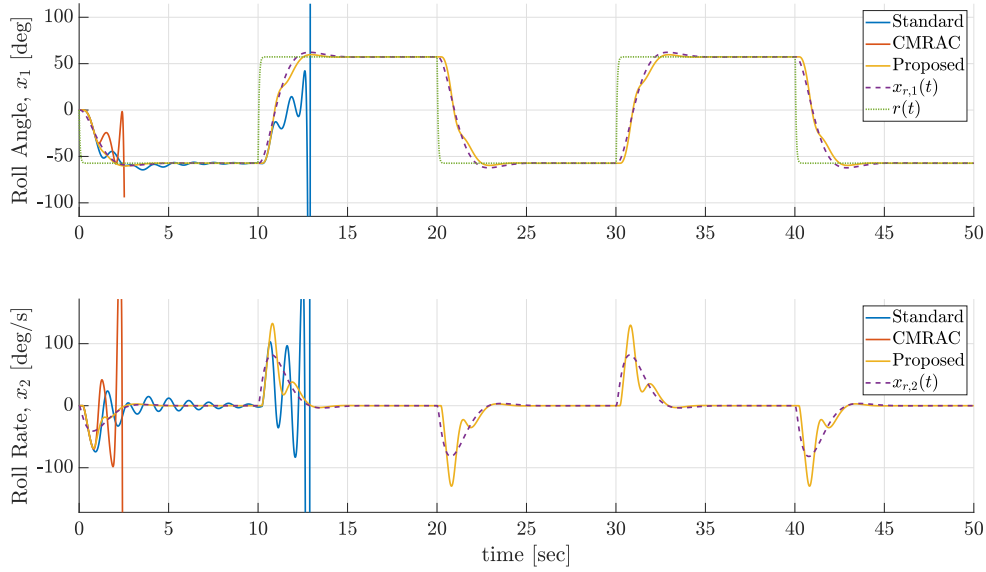
Figure 3.6: State Tracking Performance Comparison for $\Gamma = 10$, $\gamma_1 = \gamma_c = 1$, $\gamma_2 = 40$, and $\gamma_m = 20$ with time delay of $t_d = 0.28$ seconds (Unstable behavior with Standard Adaptive Control in Eq 2.10 and CMRAC in Eq 2.16)

Table 3.1: Time Delay Margins for Adaptive Systems

	Standard	CMRAC	Proposed
$(t_d)_{\max}$	0.0865	0.1241	0.2872

adaptive law and modification term. In that respect, γ_m behaves like a stability augmentation that improves the robustness of the closed-loop system. Furthermore, it is stated in Remark 3.3 that the proposed adaptive architecture converges to CMRAC if $\gamma_m = \gamma_2 = 0$. Thus, two simulations with $\gamma_m = 20$ and $\gamma_m = 50$ are compared to illustrate the contribution that comes with design parameter γ_m. It should be noted that increasing γ_m increases the feedback contribution in the regulated learning rates (see Eq 3.4) as it is proportional to the corresponding feedback gain. Hence, a stable response is achieved with larger γ_m as illustrated in Figure 3.7.

40
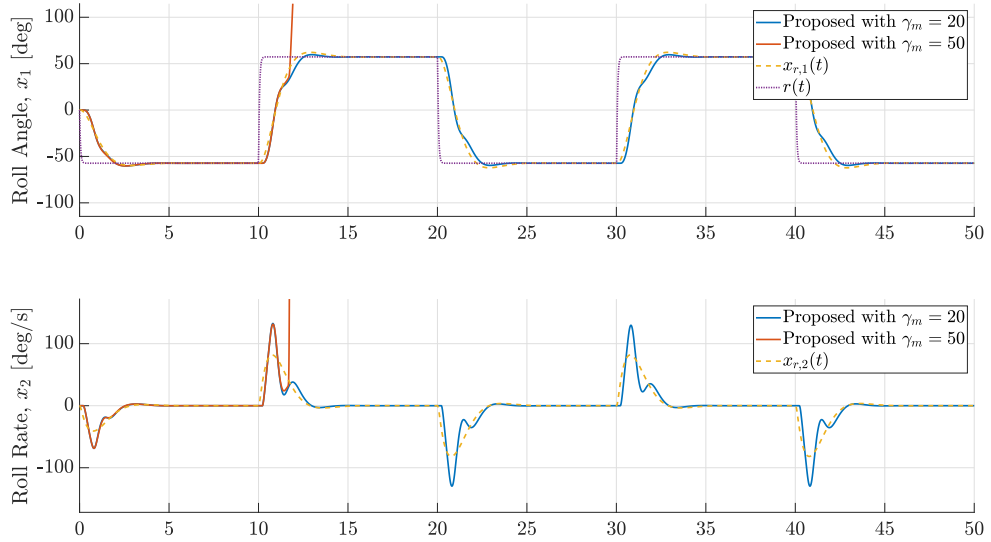
Figure 3.7: Tracking Comparison for $\Gamma = 10$, $\gamma_1 = \gamma_c = 1$, and $\gamma_2 = 40$ with time delay of $t_d = 0.28$ seconds

3.5 Software-in-the-Loop Simulations

In this section, software-in-the-loop (SITL) simulation results are presented to show the efficacy of the proposed method with more realistic examples. To this end, an adaptive flight controller is designed for the lateral dynamics of F-4 Phantom II fighter aircraft, and simulations are performed on X-Plane flight simulator. The flight scenario is to bank to the left and right by 30 degrees, successively.

Left Bank

Right Bank

3.5.1 X-Plane Flight Simulator

The principle of operation of X-Plane is based on the blade element theory. In the physics engine, the velocity components on each blade element are computed. The sources of these velocity components could be rotational motion, free-stream velocity, propeller inflow (propwash), downwash and wake due to aerodynamic surfaces and fuselage. Then, forces and moments on each element are calculated and converted to translational and rotational accelerations which are used to generate the velocity and position responses. As all these complexities are reflected in X-Plane, it makes X-Plane a Federal Aviation Administration (FAA) certified flight simulator [94].

3.5.2 Unstructured Matched Uncertainty with RBF Approximation

In this example, Assumption 2.2 is relaxed with a matched uncertainty parametrization using RBF approximators as noted in Remark 2.2. That is,

$$\Delta(x) = W^T \Phi(x) + \varepsilon(x)$$

with $\|\varepsilon(x)\| \leq \varepsilon_0$, $\forall x \in \mathcal{D}_x$, where the residual bound ε_0 can be made arbitrarily small by increasing the size of RBF Neural Networks. The basis $\Phi : \mathbb{R}^n \to \mathbb{R}^{n+s}$ is constructed by augmenting the state vector and radial basis functions (RBfs) as:

$$\Phi(x) = \begin{bmatrix} x_1 & \ldots & x_n & \phi_1(x) & \phi_2(x) & \ldots & \phi_s(x) \end{bmatrix}^T,$$

where $\phi_i(x) \in \mathbb{R}$ for $i = 1, \ldots, s$ is given by

$$\phi_i(x) = \begin{cases} 1 & \text{, for } i = 1 \\ \exp\left(-\frac{\|x(t) - \bar{c}_i\|^2}{2\bar{\mu}_i^2}\right) & \text{, for } i = 2, \ldots, s \end{cases}$$

with $\bar{c}_i \in \mathbb{R}^n$ being the center of an RBF unit and $\bar{\mu}_i \in \mathbb{R}_+$ being the width of the ith kernel node [77]. State vector is added to the basis function to capture the linear behavior in the uncertainty whereas the Radial Basis Functions are reserved for the nonlinearities. For the unstructured parametrization of the matched uncertainty, 16 RBF elements are used. The centers $\bar{c}_i$ for RBF are uniformly distributed over the expected range of the $x_1 - x_2 - x_3 - x_4$ space $[-2, 2] \times [-2, 2] \times [-2, 2] \times [-2, 2]$, and width of the kernel unit is uniformly set to $\bar{\mu}_i = 1$ for $i = 2, \ldots, s = 16$. The first element $\phi_1(x)$ is reserved for the bias unit; i.e. $\phi_1(x) = 1$.

3.5.3 Linear Lateral Dynamics of F-4 Phantom II

Linear equations of motion for the lateral dynamics of F-4 Phantom II at steady wings-level trim conditions with true airspeed of $V_\infty = 186$ m/s and altitude of $h = 24000$ ft are obtained using '*Athena Vortex Lattice*' [95] as:

$$
\begin{bmatrix} \dot{\beta} \\ \dot{p} \\ \dot{r} \\ \dot{\phi} \end{bmatrix} = \underbrace{\begin{bmatrix} -1.47 & 0.0 & -1.0 & 0.075 \\ -18.85 & -7.52 & 2.89 & 0.0 \\ 15.15 & 0.56 & -7.61 & 0.0 \\ 0.0 & 1.0 & 0.0 & 0.0 \end{bmatrix}}_{\triangleq A_p} \underbrace{\begin{bmatrix} \beta \\ p \\ r \\ \phi \end{bmatrix}}_{\triangleq x_p} + \underbrace{\begin{bmatrix} 0.0 & -0.15 \\ 8.48 & -0.96 \\ -0.18 & 3.94 \\ 0.0 & 0.0 \end{bmatrix}}_{\triangleq B_p} \underbrace{\begin{bmatrix} \delta_a \\ \delta_r \end{bmatrix}}_{\triangleq u}
$$

$$
y_p = \begin{bmatrix} \beta \\ \phi \end{bmatrix} = \begin{bmatrix} 1 & 0 & 0 & 0 \\ 0 & 0 & 0 & 1 \end{bmatrix} x_p = E_p x_p
$$

where β is angle of sideslip $[rad]$, p is roll rate $[rad/s]$, r is yaw rate $[rad/s]$, and ϕ is roll angle $[rad]$. $\delta_a \in [-1, 1]$ and $\delta_r \in [-1, 1]$ are aileron and rudder deflections, respectively. Note that the control surface deflections are normalized using maximum deflection of 20 degrees.

3.5.4 Nominal Controller Design

In order to increase the robustness and improve the tracking performance, integrator states are introduced as follows:

$$
\dot{z}(t) = \begin{bmatrix} \beta_{cmd}(t) \\ \phi_{cmd}(t) \end{bmatrix} - \begin{bmatrix} \beta(t) \\ \phi(t) \end{bmatrix}
$$

$$
\dot{z}(t) = r(t) - y_p(t) = r(t) - E_p x_p(t)
$$

Then, augmented system dynamics can be expressed as follows:

$$
\begin{bmatrix} \dot{x}_p \\ \dot{z} \end{bmatrix} = \underbrace{\begin{bmatrix} A_p & 0 \\ -E_p & 0 \end{bmatrix}}_{\triangleq A} \underbrace{\begin{bmatrix} x_p \\ z \end{bmatrix}}_{\triangleq x} + \underbrace{\begin{bmatrix} B_p \\ 0 \end{bmatrix}}_{\triangleq B} \begin{bmatrix} \delta_a \\ \delta_r \end{bmatrix} + \underbrace{\begin{bmatrix} 0 \\ I \end{bmatrix}}_{\triangleq B_r} \begin{bmatrix} \beta_{cmd} \\ \phi_{cmd} \end{bmatrix}
$$

$$
\dot{x} = Ax + Bu + B_r r
$$

Reference model that captures the desired closed-loop behavior is defined as

$$
\dot{x}_r = A_r x_r + B_r r
$$

where the system matrix A_r satisfies the matching condition $A_r = A - BK$. Feedback gain matrix K in the nominal controller $u_n(t) = -Kx(t)$ is designed to be:

$$K = \begin{bmatrix} 1.14 & 1.15 & -0.81 & 4.14 & -3.25 & -3.02 \\ -0.58 & -0.69 & 0.09 & -1.32 & 4.76 & 0.97 \end{bmatrix}$$

Fastest mode of the lateral dynamics is the roll subsidence with frequency of 7.66 rad/s. Hence, the cutoff frequency of the low-pass filters is chosen to be $\omega_f = 8$ rad/s.

3.5.5 SITL Simulation Results

In this section, SITL simulation results are presented for the lateral dynamics of F-4 Phantom fighter aircraft. The scenario is to perform successive bank maneuvers to the left and right while keeping the sideslip close to zero in order to maintain the coordinated flight. adaptation is not activated for the first 70 seconds, and only nominal controller is employed. The proposed adaptive law is activated at $t = 70\ s$.

In Figure 3.8, state tracking performance is illustrated. It is clear that the coordinated flight is achieved once the desired tracking performance (specifically in roll and yaw rate channels) is maintained with activating the adaptation.
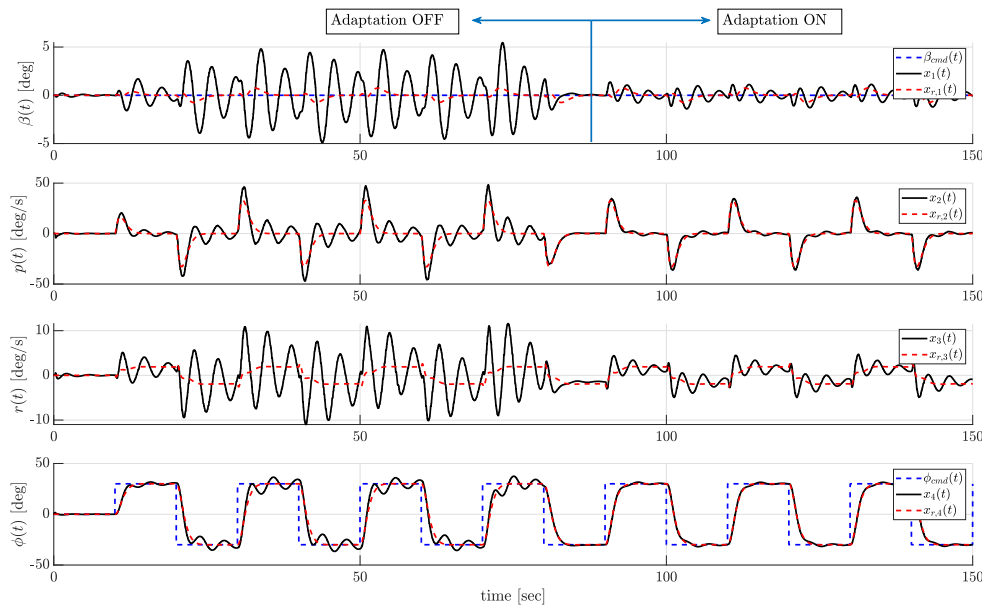
Figure 3.8: State Tracking Performance for X-Plane SITL Simulation with $\Gamma = 2I_{n \times n}$, $\gamma_m = 20$, $\gamma_1 = 1$, and $\gamma_2 = 20$

Note that the exact uncertainty $\Delta(x)$ is not available since the physics engine of the flight simulator is unknown. However, one can still compute its filtered uncertainty $\Delta_f(x,t)$ through Eq 2.14. In Figure 3.9, filtered uncertainty $\Delta_f(x,t)$ and estimated uncertainty $\hat{\Delta}(x,t)$ are presented for comparison purposes. As shown in the figure, the estimated uncertainty successfully captures the filtered uncertainty in all control channels. Furthermore, one can observe that the estimated uncertainty $\hat{\Delta}(x,t)$ is ahead of the filtered uncertainty $\Delta_f(x,t)$ in time, which is an expected result due to time lag nature of the low-pass filter.
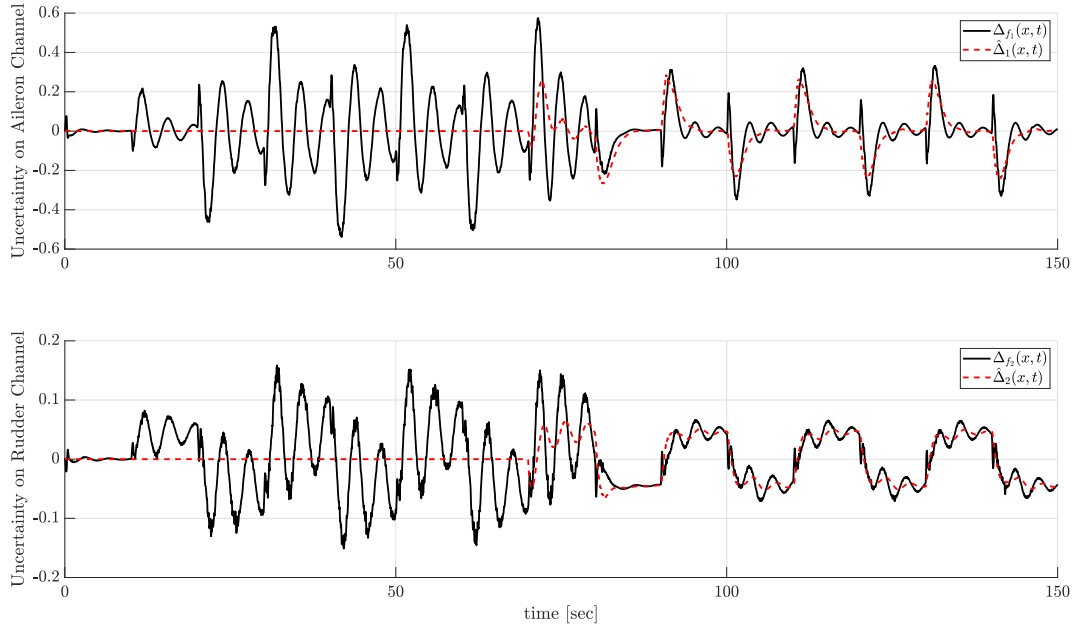
Figure 3.9: Uncertainty Estimation for X-Plane SITL Simulation with $\Gamma = 2I_{n \times n}$, $\gamma_m = 20$, $\gamma_1 = 1$, and $\gamma_2 = 20$

Figure 3.10 illustrates the evolution of the adaptive weight estimations $\hat{W}(t)$. As it can be seen, the adaptive parameters quickly stay bounded around nearly constant values without any high-frequency oscillations thanks to fast adaptation capability of the proposed architecture. Lastly, Figures 3.11-3.12 present the commanded and actuated control history. As the adverse effects of the uncertainties are successfully suppressed, high-frequency content in the aileron input is reduced as shown in Figure 3.11. Thus, one can deduce that the proposed controller performed satisfactorily well in the presence of the actuator dynamics.
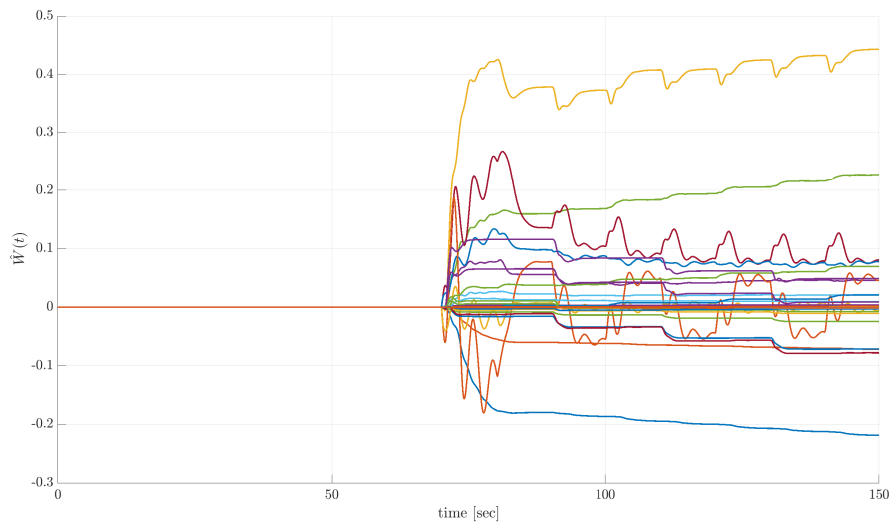
Figure 3.10: RBF NN Weight Estimation for X-Plane SITL Simulation with $\Gamma = 2I_{n \times n}$, $\gamma_m = 20$, $\gamma_1 = 1$, and $\gamma_2 = 20$
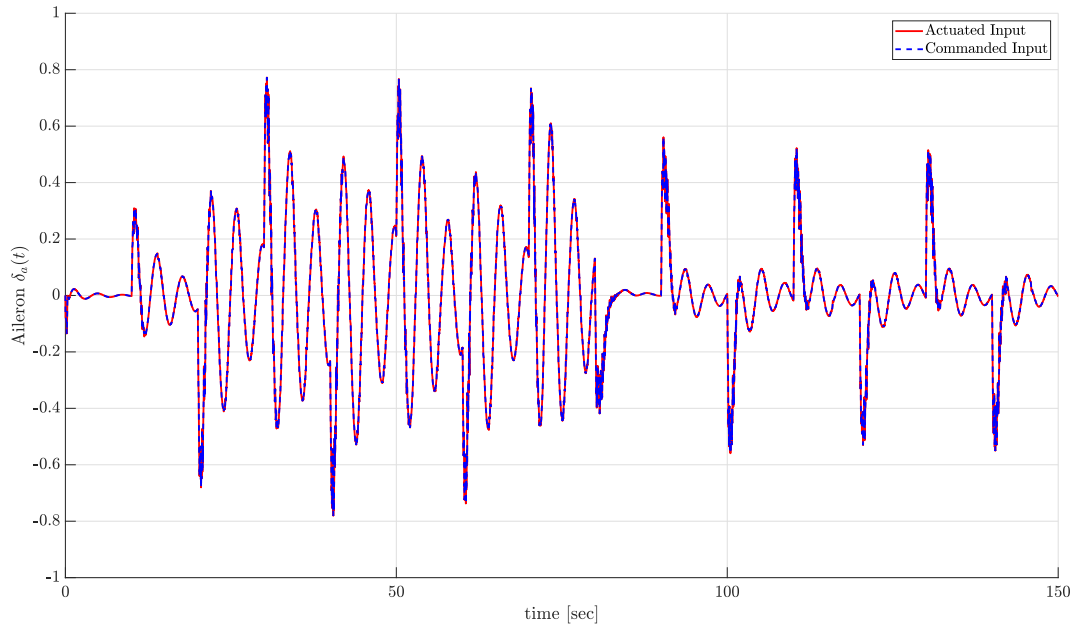
Figure 3.11: Aileron Control for X-Plane SITL Simulation with $\Gamma = 2I_{n \times n}$, $\gamma_m = 20$, $\gamma_1 = 1$, and $\gamma_2 = 20$

46
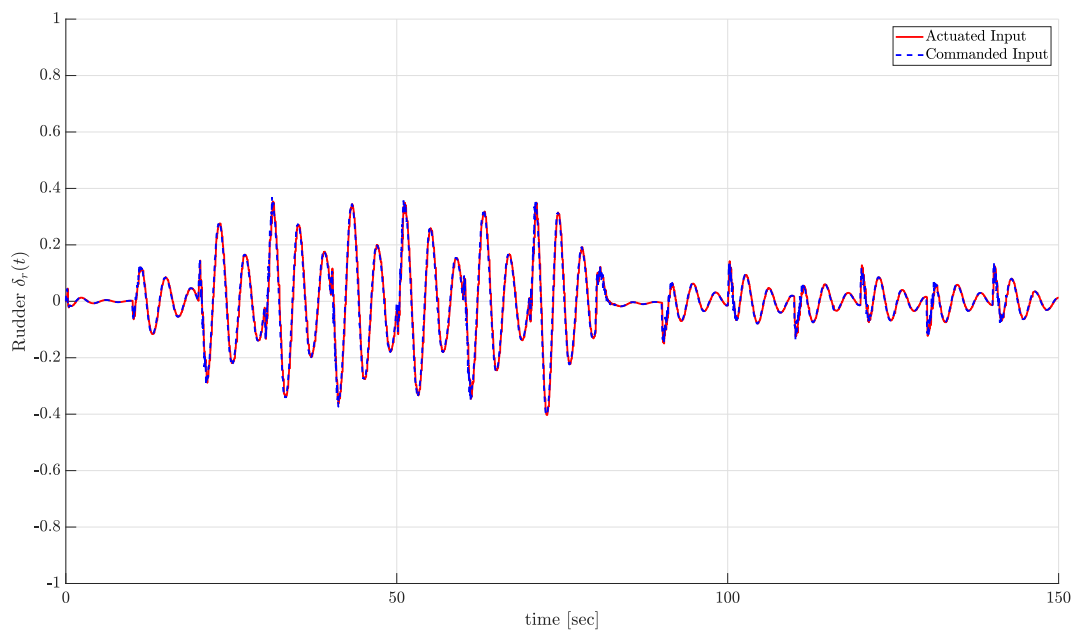
Figure 3.12: Rudder Control for X-Plane SITL Simulation with $\Gamma = 2I_{n \times n}$, $\gamma_m = 20$, $\gamma_1 = 1$, and $\gamma_2 = 20$

CHAPTER 4

EXTENSION TO SYSTEMS WITH UNKNOWN CONTROL EFFECTIVENESS

4.1   Problem Definition

In Chapter 3, an information recovery method in filter-based model reference adaptive controllers is introduced for a class of uncertain nonlinear systems. The information lost during filtering is recovered by including the high-frequency content in the adaptation. Furthermore, a time-varying learning rate is proposed as stability augmentation to suppress the undesired high-frequency oscillations in the adaptation. However, the offered solution assumes the perfect knowledge of the control effectiveness, which is not the case in general. In this chapter, the information recovery results are extended to cover the uncertain systems with unknown control effectiveness. Specifically, the following form of the uncertain dynamical systems with unknown control effectiveness is considered:

$$\dot{x}(t) = Ax(t) + B\Lambda\big[u(t) + \delta\big(x\big)\big], \quad x(t_0) = x_0 \tag{4.1}$$

where $x(t) \in \mathcal{D}_x \subset \mathbb{R}^n$ denotes the state vector, $u(t) \in \mathcal{D}_u \subset \mathbb{R}^m$ is the control input, system matrix $A \in \mathbb{R}^{n \times n}$ and input matrix $B \in \mathbb{R}^{n \times m}$ are known constant matrices. Unknown control effectiveness matrix $\Lambda \in \mathbb{R}^{m \times m}$ is assumed to be constant with $\Lambda = \Lambda^T \succ 0$. Furthermore, the pair (A, B) is assumed to be controllable and input matrix B has full column rank; i.e. $\text{rank}(B) = m$. $\mathcal{D}_x$ is sufficiently large compact set, $\mathcal{D}_u$ is admissible control set, and $\delta : \mathbb{R}^n \times \mathbb{R}_+ \to \mathbb{R}^m$ is the mapping for the unknown matched uncertainty. In addition, full state measurement is available for feedback control, and the plant is not over-actuated; that is, $n \geq m$.

The contol objective is to track the reference model in Eq 2.2 while achieving the

uniform ultimate boundedness of all the closed-loop system signals. Furthermore, the matched uncertainty $\delta(x)$ is assumed to structured as in Assumption 2.2 and expressed as the following:

$$\delta(x) = w^T \phi_w(x) \tag{4.2}$$

where $w \in \mathbb{R}^{s \times m}$ is constant unknown weight matrix, $\phi_w(x) \in \mathbb{R}^s$ is the known basis vector-function. Lastly, it should be stated that the arguments 't' and 'x' denoting time and state dependency (resp) are omitted from the equations whenever it is appropriate.

Remark 4.1. *The uncertain systems in the form of*

$$\dot{x}(t) = Ax(t) + B\big[\Lambda u(t) + \delta(x)\big]$$

can be expressed as in Eq 4.1 by replacing $\delta(x)$ with $\bar{\delta}(x) \triangleq \Lambda^{-1}\delta(x)$, which yields

$$\dot{x}(t) = Ax(t) + B\Lambda\big[u(t) + \bar{\delta}(x)\big]$$

4.2 System Description

Adding and subtracting '$K_x x(t)$' and '$K_r r(t)$' to the uncertain system dynamics in Eq 4.1 results in:

$$
\begin{aligned}
\dot{x} &= \big(A - BK_x\big)x + BK_r r + B\Lambda\big[u + \Lambda^{-1}K_x x - \Lambda^{-1}K_r r + \delta(x)\big] \\
&= A_r x + B_r r + B\Lambda\big[u + \Lambda^{-1}K_x x - \Lambda^{-1}K_r r + \delta(x)\big] \\
&= A_r x + B_r r + B\Lambda\big[u + \Lambda^{-1}K_x x - \Lambda^{-1}K_r r + w^T\phi_w(x)\big]
\end{aligned}
$$

which can be re-written as

$$\dot{x} = A_r x + B_r r + B\Lambda\big[u + \Delta(x)\big] \tag{4.3}$$

where the aggregated uncertainty $\Delta(x)$ is defined as

$$
\begin{aligned}
\Delta(x) &= \begin{bmatrix} \Lambda^{-1}K_x & -\Lambda^{-1}K_r & w^T \end{bmatrix}\begin{bmatrix} x^T(t) & r^T(t) & \phi_w^T(x) \end{bmatrix}^T \\
&\triangleq W^T\phi(x,t)
\end{aligned} \tag{4.4}
$$

with $W^T \triangleq \begin{bmatrix} \Lambda^{-1}K_x & -\Lambda^{-1}K_r & w^T \end{bmatrix}$ and $\phi(x,t) \triangleq \begin{bmatrix} x^T & r^T & \phi_w^T \end{bmatrix}^T$.

Reference model that characterizes the desired closed-loop performance is given by

$$\dot{x}_r(t) = A_r x_r(t) + B_r r(t), \qquad x_r(t_0) = x_{r0} \tag{4.5}$$

where Hurwitz reference system matrix A_r and input matrix B_r satisfy the matching conditions in Assumption 2.1, and $r(t)$ is an exogenous bounded reference tracking command. The control input is chosen to be

$$u(t) = -\hat{W}^T(t)\phi(x) \tag{4.6}$$

with $\hat{W}$ being an online estimation of unknown weight matrix W. Then, denoting the state tracking error $e \triangleq x_r - x$, the tracking error dynamics can be obtained using Eq 4.3, Eq 4.5, and Eq 4.6 as follows:

$$\dot{e}(t) = A_r e(t) - B\Lambda \tilde{W}^T \phi(x) \tag{4.7}$$

Next, low-pass filters in Eq 2.12 are applied to the uncertain system in Eq 4.3:

$$\dot{x}_f = A_r x_f + B_r r_f + B\Lambda\big[u_f + \Delta_f\big] \tag{4.8}$$

with filtered uncertainty being $\Delta_f(x,t) = W^T\phi_f(x,t)$. Rearranging the equation by collecting all the known terms on the same side results in

$$\begin{aligned}
Y(x,t) &\triangleq \Lambda\big[u_f(t) + W^T\phi_f(x,t)\big] \\
&= B^\dagger\big[\dot{x}_f(x,t) - A_r x_f(x,t)\big] - K_r r_f(t)
\end{aligned} \tag{4.9}$$

Eq 4.9 can also be written as

$$Y = \begin{bmatrix} \Lambda & \Lambda W^T \end{bmatrix}\begin{bmatrix} u_f^T & \phi_f^T \end{bmatrix}^T \triangleq \Theta^T \Phi_f(x,t) \tag{4.10}$$

Note that filtered aggregated basis function Φ_f is low-pass filtered form of the basis function $\Phi \triangleq \begin{bmatrix} u^T & \phi^T \end{bmatrix}^T$. Next, following the idea in Ref [11], the estimated form $\hat{Y}$ is introduced as follows

$$\begin{aligned}
\hat{Y}(t) &\triangleq \hat{\Lambda}(t)\big[u_f(t) + \hat{W}^T(t)\phi_f(x,t)\big] \\
&= \hat{\Theta}^T\Phi_f
\end{aligned} \tag{4.11}$$

The estimation error $e_Y \triangleq Y - \hat{Y}$ is expressed as

$$\begin{aligned}
e_Y &= B^\dagger\big[\dot{x}_f(x,t) - A_r x_f(x,t)\big] - K_r r_f(t) - \hat{\Lambda}(t)\big[u_f(t) + \hat{W}^T(t)\phi_f(x,t)\big] \\
&= \Lambda\big[u_f(t) + W^T\phi_f(x,t)\big] - \hat{\Lambda}(t)\big[u_f(t) + \hat{W}^T(t)\phi_f(x,t)\big] \\
&= \Lambda u_f - \hat{\Lambda}u_f + \Lambda W^T\phi_f - \hat{\Lambda}\hat{W}^T\phi_f + \Lambda\hat{W}^T\phi_f - \Lambda\hat{W}^T\phi_f \\
&= \tilde{\Lambda}\big[u_f + \hat{W}^T\phi_f\big] + \Lambda\tilde{W}^T\phi_f = \tilde{\Theta}^T\Phi_f
\end{aligned} \tag{4.12}$$

51

where the error signals $\tilde{W}, \tilde{\Lambda}$, and $\tilde{\Theta}$ are defined as

$$\tilde{W} \triangleq W - \hat{W}$$

$$\tilde{\Lambda} \triangleq \Lambda - \hat{\Lambda}$$

$$\tilde{\Theta} \triangleq \Theta - \hat{\Theta}$$

4.2.1 Secondary (Indirect) Weight Update Law

Assumption 4.1. *Aggregated basis function $\Phi \in \mathbb{R}^{\bar{s}}$ is a sufficiently exciting signal with $\bar{s} = s + n + q + m$. Hence, there exists positive constants $\tau, \alpha, T_e \in \mathbb{R}_+$ such that the following inequality holds:*

$$\int_{t_0}^{t} \Phi(\tau)\Phi^T(\tau)d\tau \succeq \alpha I_{\bar{s} \times \bar{s}}, \qquad t = T_e$$

Remark 4.2. *Assumption 4.1 ensures that aggregated basis function Φ contains as many spectral lines as there are unknown parameters. Note that basis function Φ is an exogenous signal to the low-pass filter system in Eq 2.12 with the transfer function of $\mathcal{G}(s) \triangleq \frac{\omega_f}{s+\omega_f}$. Then, filtered basis function ϕ_f has also the same number of spectral lines with less energy than that of the original basis ϕ since $\mathcal{G}(s)$ is stable, minimum phase, and strictly proper transfer function [87]. This implies the following:*

$$\int_{t_0}^{t} \Phi_f(\tau)\Phi_f^T(\tau)d\tau \succeq \beta I_{\bar{s} \times \bar{s}}, \qquad t = T_e$$

with $0 < \beta \leq \alpha$. The degradation in the richness of the signal (which is equivalent to how small is β than α) depends on the cutoff frequency ω_f and spectrum of the basis Φ. Let the spectral measure of ϕ is given by $S_\phi([\omega_1 \; \omega_2])$ with $\omega_1 < \omega_2$. Choosing the filter design parameter ω_f to be larger than ω_2 leads to relatively small degradation in the richness of Φ_f with β being closer to α.

Multiplying Eq 4.10 from the right by aggregated filtered basis Φ_f yields

$$Y\Phi_f^T = \Theta^T \Phi_f \Phi_f^T$$

$$\mathcal{M}^T \triangleq \int_{t_0}^{t} Y\Phi_f^T d\xi = \int_{t_0}^{t} \Theta^T \Phi_f \Phi_f^T d\xi = \Theta^T \int_{t_0}^{t} \Phi_f \Phi_f^T d\xi$$

52

Note that the signal $\mathcal{M}$ is accessible as the signal Y is available from Eq 4.9. Then, estimated form $\hat{\mathcal{M}}$ and corresponding error $\tilde{\mathcal{M}}$ are defined as:

$$\hat{\mathcal{M}}^T \triangleq \hat{\Theta}^T \int_{t_0}^t \Phi_f \Phi_f^T d\xi$$

$$\tilde{\mathcal{M}} \triangleq \mathcal{M} - \hat{\mathcal{M}} = \underbrace{\left(\int_{t_0}^t \Phi_f \Phi_f^T d\xi \right)}_{\triangleq \mathscr{M}} \tilde{\Theta} = \mathscr{M} \tilde{\Theta} \tag{4.13}$$

It should also be noted that the signal $\tilde{\mathcal{M}}$ is also available since both $\mathcal{M}$ and $\hat{\mathcal{M}}$ are accessible through Eq 4.9 and Eq 4.13, respectively. Having defined the error signal $\tilde{\mathcal{M}}$, the secondary weight update law is proposed to have the following form:

$$\dot{\hat{\Theta}} = \left(\Gamma_\Theta^{-1} + \gamma_y \Phi_f \Phi_f^T \right)^{-1} \left(\gamma_y \dot{\Phi}_f e_Y^T + \gamma_1 \Phi_f e_Y^T + \gamma_2 \tilde{\mathcal{M}} \right) \tag{4.14}$$

where $\gamma_1, \gamma_2, \gamma_y \in \mathbb{R}_+$ are user-defined scalar design parameters, and $\Gamma_\Theta = \Gamma_\Theta^T \succ 0$ is the positive definite learning rate.

Theorem 4.1. *Consider the unknown signal Y in Eq 4.9-4.10 and its estimation $\hat{Y}$ in Eq 4.11. Assume Assumption 4.1 holds. Then, weight update law in Eq 4.14 results in global exponential stability of the zero solution $\left(e_Y, \tilde{\Theta} \right)(t) \equiv 0$.*

Proof. Consider the following Lyapunov function

$$\mathcal{V}(e_Y, \tilde{\Theta}) = \frac{\gamma_y}{2} e_Y^T e_Y + \frac{1}{2} \mathrm{tr}\left(\tilde{\Theta}^T \Gamma_\Theta^{-1} \tilde{\Theta} \right) \tag{4.15}$$

Its time derivative becomes:

$$\begin{aligned}
\dot{\mathcal{V}} &= e_Y^T \gamma_y \dot{e}_Y - \mathrm{tr}\left(\tilde{\Theta}^T \Gamma_\Theta^{-1} \dot{\tilde{\Theta}} \right) \\
&= \mathrm{tr}\left(e_Y^T \gamma_y \dot{e}_Y \right) - \mathrm{tr}\left(\tilde{\Theta}^T \Gamma_\Theta^{-1} \dot{\tilde{\Theta}} \right) \\
&= \mathrm{tr}\left[e_Y^T \gamma_y \left(\dot{\tilde{\Theta}}^T \Phi_f + \tilde{\Theta}^T \dot{\Phi}_f \right) \right] - \mathrm{tr}\left(\tilde{\Theta}^T \Gamma_\Theta^{-1} \dot{\tilde{\Theta}} \right) \\
&= \mathrm{tr}\left(e_Y^T \gamma_y \dot{\tilde{\Theta}}^T \Phi_f \right) + \mathrm{tr}\left(e_Y^T \gamma_y \tilde{\Theta}^T \dot{\Phi}_f \right) - \mathrm{tr}\left(\tilde{\Theta}^T \Gamma_\Theta^{-1} \dot{\tilde{\Theta}} \right) \\
&= -\mathrm{tr}\left(e_Y^T \gamma_y \dot{\hat{\Theta}}^T \Phi_f \right) + \mathrm{tr}\left(e_Y^T \gamma_y \tilde{\Theta}^T \dot{\Phi}_f \right) - \mathrm{tr}\left(\tilde{\Theta}^T \Gamma_\Theta^{-1} \dot{\hat{\Theta}} \right) \\
&= -\mathrm{tr}\left(\Phi_f^T \dot{\hat{\Theta}} \gamma_y e_Y \right) + \mathrm{tr}\left(e_Y^T \gamma_y \tilde{\Theta}^T \dot{\Phi}_f \right) - \mathrm{tr}\left(\tilde{\Theta}^T \Gamma_\Theta^{-1} \dot{\hat{\Theta}} \right) \\
&= -\gamma_y \mathrm{tr}\left(\tilde{\Theta}^T \Phi_f \Phi_f^T \dot{\hat{\Theta}} \right) + \gamma_y \mathrm{tr}\left(\tilde{\Theta}^T \dot{\Phi}_f e_Y^T \right) - \mathrm{tr}\left(\tilde{\Theta}^T \Gamma_\Theta^{-1} \dot{\hat{\Theta}} \right) \\
&= \gamma_y \mathrm{tr}\left(\tilde{\Theta}^T \dot{\Phi}_f e_Y^T \right) - \mathrm{tr}\left[\tilde{\Theta}^T \left(\Gamma_\Theta^{-1} + \Phi_f \Phi_f^T \right) \dot{\hat{\Theta}} \right]
\end{aligned}$$

Substituting the secondary update law in Eq 4.14 results in

$$\dot{\mathcal{V}}(e_Y, \tilde{\Theta}) = -\gamma_1 e_Y^T e_Y - \gamma_2 \mathrm{tr}\left(\tilde{\Theta}^T \mathscr{M} \tilde{\Theta} \right)$$

Using Assumption 4.1 and Remark 4.2, time derivative of the Lyapunov function can be bounded as:

$$\dot{\mathcal{V}}(e_Y, \tilde{\Theta}) \leq -\gamma_1 \|e_Y\|^2 - \beta\gamma_2 \|\tilde{\Theta}\|_2^2 \leq -\mu \mathcal{V}(e_Y, \tilde{\Theta}) < 0$$

with $\mu \triangleq \min\{\gamma_1, -\beta\gamma_2\} > 0$. Positive definite Lyapunov function with its negative definite derivative ensures the exponential stability of the zero solution $(e_y, \tilde{\Theta}) \equiv 0$. Since the Lyapunov function is radially unbounded, this result holds globally.

∎

Remark 4.3. *If Assumption 4.1 does not hold (i.e. $\beta = 0$), time derivative of the Lyapunov function becomes negative semi-definite:*

$$\dot{\mathcal{V}}(e_Y, \tilde{\Theta}) = -\gamma_1 e_Y^T e_Y \leq 0$$

which ensures the asymptotic stability of the error signal e_Y; i.e. $e_Y(t) \to 0$ as $t \to \infty$. However, asymptotic stability e_Y does not ensure the convergence of the estimated weight matrix $\hat{\Theta}$ to its ideal value.

Lemma 4.1. *Given $\Gamma_\Theta = \Gamma_\Theta^T \succ 0$ is positive definite matrix, $\gamma_y \in \mathbb{R}_+$ is a positive constant, and $\Phi_f \in \mathbb{R}^{\bar{s}}$, the matrix $(\Gamma_\Theta^{-1} + \gamma_y \Phi_f \Phi_f^T)$ is invertible and its inverse is:*

$$\left(\Gamma_\Theta^{-1} + \gamma_y \Phi_f \Phi_f^T\right)^{-1} = \Gamma_\Theta - \frac{\gamma_y}{1 + tr\left(\gamma_y \Phi_f \Phi_f^T \Gamma_\Theta\right)} \Gamma_\Theta \Phi_f \Phi_f^T \Gamma_\Theta \succ 0$$

Proof. The proof can be constructed by following the same steps in proof of Lemma 3.3. Hence, it is omitted here.

Remark 4.4. *If Assumption 4.1 does not hold (i.e. $\beta = 0$), the boundedness of $\hat{\Theta}$ may not be guaranteed in the presence of external disturbances. This is also the case if the structure of the uncertainty is not known and universal approximators are employed in the unstructured uncertainty framework. Hence, the Projection operator is utilized as a robust modification to prevent the parameter drift:*

$$\dot{\hat{\Theta}} = Proj\left\{\hat{\Theta}, \left(\Gamma_\Theta^{-1} + \gamma_y \Phi_f \Phi_f^T\right)^{-1}\left(\gamma_y \dot{\Phi}_f e_Y^T + \gamma_1 \Phi_f e_Y^T + \gamma_2 \tilde{\mathcal{M}}\right)\right\} \quad (4.16)$$

It can be shown that the results of Theorem 4.1 are not affected by the projection.

Remark 4.5. *Assuming the aggregated basis function Φ is sufficiently exciting, as stated in Assumption 4.1, estimated parameters $\hat{\Theta}$ converge to their ideal values Θ*

exponentially. That is, $\hat{\Theta}(t) \to \Theta$ as $t \to \infty$. From $\Theta = \begin{bmatrix} \Lambda & \Lambda W^T \end{bmatrix}^T$, it is clear that the parameter convergence is also equivalent to the identification of the unknown control effectiveness matrix Λ. Thus, one can obtain the online estimation of the unknown control effectiveness matrix by taking the first m row of the estimated weight matrix $\hat{\Theta}$. This linear operation is simply denoted as follows:

$$\hat{\Lambda} = \mathcal{H}_\Lambda(\hat{\Theta})$$

where the extraction operator $\mathcal{H}_\Lambda : \mathbb{R}^{\bar{s} \times m} \to \mathbb{R}^{m \times m}$ returns the first m row of its input argument. Once can also identify the product $N_1 \triangleq W\Lambda^T$ in a similar manner using the operator $\mathcal{H}_W : \mathbb{R}^{\bar{s} \times m} \to \mathbb{R}^{(\bar{s}-m) \times m}$ with $N_1 = \mathcal{H}_W(\Theta)$. Hence, the estimation $\hat{N}_1$ is reachable from the following:

$$\hat{N}_1 = \mathcal{H}_W(\hat{\Theta}) \tag{4.17}$$

One can produce a gradient-descent based adaptive weight update law using the estimation $\hat{N}_1$ as follows:

$$\dot{\hat{N}}_W = -\Gamma_W \text{Proj}\{\hat{N}_W, (\hat{N}_1 - \hat{N}_W \hat{\Lambda}^T)\hat{\Lambda}\} \tag{4.18}$$

where $\Gamma_W = \Gamma_W^T \succ 0$ is a user-defined positive definite learning rate. With this update law, the estimated weight matrix $\hat{N}_W$ is updated in the direction that minimizes the following cost function:

$$\mathcal{J} = \|\hat{N}_1 - \hat{N}_W \hat{\Lambda}^T\|_2^2$$

Lemma 4.2. *Consider the results of Theorem 4.1, linear operator $\mathcal{H}_W$ in Eq 4.17, and update law in Eq 4.18. If Assumption 4.1 is satisfied, then the zero solution $(\hat{N}_W(t) - W) \equiv 0$ is asymptotically stable.*

Proof. Consider the following Lyapunov function:

$$\mathcal{V} = \frac{1}{2}\text{tr}\big[(W - \hat{N}_W)^T \Gamma_W^{-1}(W - \hat{N}_W)\big]$$

Let $\tilde{\Lambda} \triangleq \Lambda - \hat{\Lambda}$, $\tilde{N}_1 \triangleq N_1 - \hat{N}_1$. Then, time derivative of the Lyapunov function

along the trajectory in Eq 4.18 (with Lemma 2.3 being incorporated) results in:

$$
\begin{aligned}
\dot{\mathcal{V}} \leq & - \left(W - \hat{N}_W\right)^T \left(\hat{N}_1 - \hat{N}_W \hat{\Lambda}^T\right) \hat{\Lambda} \\
= & - \left(W - \hat{N}_W\right)^T \left(\hat{N}_1 - N_1 + N_1 - \hat{N}_W \hat{\Lambda}^T + \hat{N}_W \Lambda^T - \hat{N}_W \Lambda^T\right) \hat{\Lambda} \\
= & \left(W - \hat{N}_W\right)^T \tilde{N}_1 \hat{\Lambda} + \left(W - \hat{N}_W\right)^T \hat{N}_W \tilde{\Lambda}^T \hat{\Lambda} - \left(W - \hat{N}_W\right)^T \left(N_1 - \hat{N}_W \Lambda^T\right) \hat{\Lambda}
\end{aligned}
$$

Now, consider the last term only:

$$
\begin{aligned}
\left(W - \hat{N}_W\right)^T \left(N_1 - \hat{N}_W \Lambda^T\right) \hat{\Lambda} &= \left(W - \hat{N}_W\right)^T \left(W \Lambda^T - \hat{N}_W \Lambda^T\right) \hat{\Lambda} \\
&= \left(W - \hat{N}_W\right)^T \left(W \Lambda^T - \hat{N}_W \Lambda^T\right) \left(\Lambda - \tilde{\Lambda}\right) \\
&= \left(W - \hat{N}_W\right)^T \left(W - \hat{N}_W\right) \left(\Lambda^T \Lambda - \Lambda^T \tilde{\Lambda}\right)
\end{aligned}
$$

Combining the results gives:

$$
\begin{aligned}
\dot{\mathcal{V}} \leq & \left(W - \hat{N}_W\right)^T \tilde{N}_1 \hat{\Lambda} + \left(W - \hat{N}_W\right)^T \hat{N}_W \tilde{\Lambda}^T \hat{\Lambda} \\
& - \left(W - \hat{N}_W\right)^T \left(W - \hat{N}_W\right) \Lambda^T \Lambda + \left(W - \hat{N}_W\right)^T \left(W - \hat{N}_W\right) \Lambda^T \tilde{\Lambda}
\end{aligned}
\tag{4.19}
$$

It is important to note that $\hat{N}_W$ is uniformly ultimately bounded due to projection operator (see Lemma 2.2). Hence, adaptive law for $\hat{\Lambda}$ (will be stated later in Eq 4.21) ensures the boundedness of $\hat{\Lambda}$ from well-known $\sigma-$modification [3]. Since unknown matrices W and Λ are constant, corresponding error matrices $\tilde{W}$ and $\tilde{\Lambda}$ are also constant. Thus, one can always find a constant upper-bound $\bar{\vartheta} \in \mathbb{R}_+$ that satisfies

$$
\operatorname{tr}\left[\left(W - \hat{N}_W\right)^T \left(\tilde{N}_1 \hat{\Lambda} + \hat{N}_W \tilde{\Lambda}^T \hat{\Lambda} + \left(W - \hat{N}_W\right) \Lambda^T \tilde{\Lambda}\right)\right] \triangleq \vartheta(t) \leq \bar{\vartheta}
$$

which yields:

$$
\begin{aligned}
\dot{\mathcal{V}} &\leq -\operatorname{tr}\left[\left(W - \hat{N}_W\right)^T \left(W - \hat{N}_W\right) \Lambda^T \Lambda\right] + \vartheta \\
&= -\operatorname{tr}\left[\Lambda \left(W - \hat{N}_W\right)^T \left(W - \hat{N}_W\right) \Lambda^T\right] + \vartheta
\end{aligned}
\tag{4.20}
$$

Boundedness of ϑ ensures the boundedness of the error signal $\left(W - \hat{N}_W\right) \Lambda^T$, as well. Furthermore, if Assumption 4.1 is satisfied, $\vartheta \to 0$ as $t \to \infty$ from the results of Theorem 4.1; that is,

$$
\tilde{\Theta}(t) \to 0 \quad \Rightarrow \quad \tilde{\Lambda}(t) \to 0, \quad \tilde{N}_1(t) \to 0 \quad \Rightarrow \quad \vartheta(t) \to 0 \qquad \text{as} \quad t \to \infty
$$

Asymptotic stability of the error signal $\left(W - \hat{N}_W\right) \Lambda^T$ ensures $\hat{N}_W(t) \to W$ as $t \to 0$ since positive definite diagonal matrix Λ has full column rank. Finally, this result constructs the asymptotic stability of the zero solution $\left(\hat{N}_W(t) - W\right) \equiv 0$.

■

4.2.2 Primary (Direct) Weight Update Law

In this section, the results from secondary weight update law is integrated into a direct adaptation to suppress the effects of matched uncertainty $\Delta(x, t)$ and unknown control effectiveness Λ. With the secondary adaptive law in Eq 4.16, an online estimation $\hat{\Lambda}$ of unknown control effectiveness Λ can be achieved by extracting the first m row as stated in Remark 4.5. However, an online estimation of unknown weight matrix W is not available from the indirect adaptation. Although an estimation for the product ΛW^T is available from $\hat{\Theta}^T = \begin{bmatrix} \hat{\Lambda} & \widehat{\Lambda W^T} \end{bmatrix}$, one cannot reach the estimation $\hat{W}^T = \hat{\Lambda}^{-1}\widehat{\Lambda W^T}$ since $\hat{\Lambda}$ is not guaranteed to be invertible for $\forall t \geq t_0$. Hence, a direct-indirect hybrid adaptive law is introduced to construct the control input in Eq 4.6 with estimated weight $\hat{W}$ and ensure the closed-loop stability of the uncertain dynamical system in Eq 4.3.

The following weight update laws are proposed for online estimations $\hat{W}$ and $\hat{\Lambda}$:

$$
\begin{aligned}
\dot{\hat{W}} &= -\Gamma \text{Proj}\big\{\hat{W}, \phi e^T P B - \gamma_\lambda \phi_f e_Y^T - \gamma_4\big(\hat{N}_W - \hat{W}\big)\big\} \\
\dot{\hat{\Lambda}} &= \gamma_\lambda \Gamma_\Lambda \big[e_Y\big(u_f + \hat{W}^T \phi_f\big)^T - \gamma_3\big(\hat{\Lambda} - \hat{N}_\Lambda\big)\big] \\
\dot{\hat{N}}_W &= -\Gamma_W \text{Proj}\big\{\hat{N}_W, \big(\hat{N}_1 - \hat{N}_W \hat{\Lambda}^T\big)\hat{\Lambda}\big\}
\end{aligned}
\tag{4.21}
$$

where $\gamma_\lambda, \gamma_3, \gamma_4 \in \mathbb{R}_+$ being scalar design parameters, $\Gamma = \Gamma^T \succ 0$, $\Gamma_\Lambda = \Gamma_\Lambda^T \succ 0$, and $\Gamma_W = \Gamma_W^T \succ 0$ are user-defined positive definite learning rates, basis function ϕ is as in Eq 4.4, error signal e_Y is as in Eq 4.12, filtered signals u_f, ϕ_f are available from Eq 2.12, $P \succ 0$ is the symmetric positive definite solution to Lyapunuv equation 2.3, $\hat{N}_\Lambda \triangleq \mathcal{H}_\Lambda\big(\hat{\Theta}\big)$ is obtained using the extraction operator $\mathcal{H}_\Lambda(\cdot)$ defined in Remark 4.5, and $\hat{N}_1$ is given by Eq 4.17.

Theorem 4.2. *Consider the uncertain dynamical system in Eq 4.1, reference model in Eq 4.5, control input in Eq 4.6, secondary weight update law in Eq 4.14, and primary weight update laws in Eq 4.21. Then, all the system signals are uniformly ultimately bounded. Furthermore, the zero solution $\big(e, e_Y, \tilde{W}, \tilde{\Lambda}\big) \equiv \big(0, 0, 0, 0\big)$ is semi-globally asymptotically stable if Assumption 4.1 holds.*

Proof. Consider the following Lyapunov function

$$
\begin{aligned}
\mathcal{V}(e, \tilde{W}, \tilde{\Lambda}) =& \frac{1}{2} e^T P e + \frac{1}{2} \text{tr}\left[\left(\tilde{W} \Lambda^{1/2}\right)^T \Gamma^{-1} \left(\tilde{W} \Lambda^{1/2}\right)\right] + \frac{1}{2} \text{tr}\left(\tilde{\Lambda}^T \Gamma_\Lambda^{-1} \tilde{\Lambda}\right) \\
=& \frac{1}{2} \eta^T \bar{P} \eta
\end{aligned}
\tag{4.22}
$$

where $\eta \triangleq \begin{bmatrix} e^T & \text{vec}\left(\tilde{W} \Lambda^{1/2}\right)^T & \text{vec}\left(\tilde{\Lambda}\right)^T \end{bmatrix}^T$ denotes the aggregated error vector and corresponding positive definite matrix is $\bar{P} \triangleq \text{diag}\left(P, I_1 \otimes \Gamma^{-1}, I_2 \otimes \Gamma_\Lambda^{-1}\right)$ with I_1 and I_2 being identity matrices of appropriate dimensions. Let $\hat{N}_W \triangleq W - \Delta \hat{N}_W$. Then, time derivative of the Lyapunov function along the system trajectories in Eq 4.7 and Eq 4.21 yields:

$$
\begin{aligned}
\dot{\mathcal{V}} =& e^T P \left(A_r e - B \Lambda \tilde{W}^T \phi\right) - \text{tr}\left(\tilde{W}^T \Gamma^{-1} \dot{\hat{W}} \Lambda\right) - \text{tr}\left(\tilde{\Lambda}^T \Gamma_\Lambda^{-1} \dot{\hat{\Lambda}}\right) \\
=& - \frac{1}{2} e^T Q e - \text{tr}\left(\tilde{W}^T \phi e^T P B \Lambda\right) - \text{tr}\left(\tilde{W}^T \Gamma^{-1} \dot{\hat{W}} \Lambda\right) - \text{tr}\left(\tilde{\Lambda}^T \Gamma_\Lambda^{-1} \dot{\hat{\Lambda}}\right) \\
=& - \frac{1}{2} e^T Q e - \gamma_\lambda \text{tr}\left(\tilde{W}^T \phi_f e_Y^T \Lambda\right) - \gamma_4 \text{tr}\left(\tilde{W}^T \tilde{W}\right) + \gamma_4 \text{tr}\left(\tilde{W}^T \Delta \hat{N}_W\right) - \text{tr}\left(\tilde{\Lambda}^T \Gamma_\Lambda^{-1} \dot{\hat{\Lambda}}\right) \\
=& - \frac{1}{2} e^T Q e - \gamma_\lambda \text{tr}\left(e_Y e_Y^T\right) - \gamma_4 \text{tr}\left(\tilde{W}^T \tilde{W}\right) + \gamma_4 \text{tr}\left(\tilde{W}^T \Delta \hat{N}_W\right) + \gamma_\lambda \gamma_3 \text{tr}\left[\tilde{\Lambda}^T \left(\hat{\Lambda} - \hat{N}_\Lambda\right)\right]
\end{aligned}
$$

Now, consider the last term, only:

$$
\begin{aligned}
\text{tr}\left[\tilde{\Lambda}^T \left(\hat{\Lambda} - \hat{N}_\Lambda\right)\right] =& \text{tr}\left[\tilde{\Lambda}^T \left(\hat{\Lambda} - \hat{N}_\Lambda - \Lambda + \Lambda\right)\right] \\
=& - \text{tr}\left(\tilde{\Lambda}^T \tilde{\Lambda}\right) + \text{tr}\left[\tilde{\Lambda}^T \left(\Lambda - \hat{N}_\Lambda\right)\right]
\end{aligned}
$$

Substituting results in

$$
\begin{aligned}
\dot{\mathcal{V}} =& - \frac{1}{2} e^T Q e - \gamma_\lambda \text{tr}\left(e_Y e_Y^T\right) - \gamma_4 \text{tr}\left(\tilde{W}^T \tilde{W}\right) - \gamma_\lambda \gamma_3 \text{tr}\left(\tilde{\Lambda}^T \tilde{\Lambda}\right) \\
& + \gamma_\lambda \gamma_3 \text{tr}\left[\tilde{\Lambda}^T \left(\Lambda - \hat{N}_\Lambda\right)\right] + \gamma_4 \text{tr}\left(\tilde{W}^T \Delta \hat{N}_W\right) \\
\leq& - \frac{1}{2} \lambda_{\min}(Q) \|e\|_2^2 - \gamma_\lambda \|e_Y\|_2^2 - \gamma_4 \|\tilde{W}\|_2^2 - \gamma_\lambda \gamma_3 \|\tilde{\Lambda}\|_2^2 \\
& + \gamma_\lambda \gamma_3 \|\tilde{\Lambda}\|_2 \|\Lambda - \hat{N}_\Lambda\|_2 + \gamma_4 \|\tilde{W}\|_2 \|\Delta \hat{N}_W\|_2
\end{aligned}
$$

From Young's inequality [96],

$$
\|\tilde{\Lambda}\|_2 \|\Lambda - \hat{N}_\Lambda\|_2 \leq k_1 \|\tilde{\Lambda}\|_2^2 + \frac{1}{4 k_1} \|\Lambda - \hat{N}_\Lambda\|_2^2
$$

Similarly,

$$
\|\tilde{W}\|_2 \|\Delta \hat{N}_W\|_2 \leq k_2 \|\tilde{W}\|_2^2 + \frac{1}{4 k_2} \|\Delta \hat{N}_W\|_2^2
$$

Next, consider the term '$\|\Lambda - \hat{N}_\Lambda\|_2$' only:

$$
\|\Lambda - \hat{N}_\Lambda\|_2 = \|\mathcal{H}_\Lambda(\Theta) - \mathcal{H}_\Lambda(\hat{\Theta})\|_2 = \|\mathcal{H}_\Lambda(\tilde{\Theta})\|_2
$$

58

Combining these results gives

$$\dot{\mathcal{V}} \leq -\frac{1}{2}\lambda_{\min}(Q)\|e\|_2^2 - \gamma_\lambda\|e_Y\|_2^2 - \gamma_\lambda\gamma_3(1-k_1)\|\tilde{\Lambda}\|_2^2 - \gamma_4(1-k_2)\|\tilde{W}\|_2^2$$
$$+ \frac{\gamma_\lambda\gamma_3}{4k_1}\|\mathcal{H}_\Lambda(\tilde{\Theta})\|_2^2 + \frac{\gamma_4}{4k_2}\|\Delta\hat{N}_W\|_2^2$$

which ensures the boundedness of errors $e, e_Y, \tilde{W}$, and $\tilde{\Lambda}$ for $k_1, k_2 \in (0,1)$. Furthermore, these error signals asymptotically converge to compact sets as summarized in Table 4.1.

Table 4.1: Compact Sets at which the Error Signals Converge Asymptotically

Error	Compact Set
e	$\mathcal{D}_e := \left\{e(t) : \|e\|_2^2 < \frac{2\gamma_\lambda\gamma_3}{4k_1\lambda_{\min}(Q)}\|\mathcal{H}_\Lambda(\tilde{\Theta})\|_2^2 + \frac{2\gamma_4}{4k_2\lambda_{\min}(Q)}\|\Delta\hat{N}_W\|_2^2\right\}$
e_Y	$\mathcal{D}_Y := \left\{e_Y(t) : \|e_Y\|_2^2 < \frac{\gamma_\lambda\gamma_3}{4k_1\gamma_\lambda}\|\mathcal{H}_\Lambda(\tilde{\Theta})\|_2^2 + \frac{\gamma_4}{4k_2\gamma_\lambda}\|\Delta\hat{N}_W\|_2^2\right\}$
$\tilde{\Lambda}$	$\mathcal{D}_\Lambda := \left\{\tilde{\Lambda}(t) : \|\tilde{\Lambda}\|_2^2 < \frac{\gamma_\lambda\gamma_3}{4k_1\gamma_\lambda\gamma_3(1-k_1)}\|\mathcal{H}_\Lambda(\tilde{\Theta})\|_2^2 + \frac{\gamma_4}{4k_2\gamma_4(1-k_2)}\|\Delta\hat{N}_W\|_2^2\right\}$
$\tilde{W}$	$\mathcal{D}_W := \left\{\tilde{W}(t) : \|\tilde{W}\|_2^2 < \frac{\gamma_\lambda\gamma_3}{4k_1\gamma_4(1-k_2)}\|\mathcal{H}_\Lambda(\tilde{\Theta})\|_2^2 + \frac{\gamma_4}{4k_2\gamma_4(1-k_2)}\|\Delta\hat{N}_W\|_2^2\right\}$

It should be noted from Theorem 4.1 that $\|\mathcal{H}_\Lambda(\tilde{\Theta})\|_2$ and $\|\Delta\hat{N}_W\|_2$ asymptotically converge to the origin if Assumption 4.1 holds. Hence, compacts sets $\mathcal{D}_e, \mathcal{D}_Y, \mathcal{D}_\Lambda$, and $\mathcal{D}_W$ asymptotically shrink to the set $\{0\}$, which ensures the asymptotic stability of $e, e_Y, \tilde{\Lambda}$, and $\tilde{W}$. That concludes the asymptotic stability of the zero solution $(e, e_Y, \tilde{\Lambda}, \tilde{W}) \equiv (0, 0, 0, 0)$.

■

4.3 Numerical Examples

4.3.1 Uncertain Roll Dynamics with Loss of Aileron Control

In this example, the first order roll dynamics of an aircraft [97] is considered:

$$\dot{p}(t) = L_p p(t) + L_\delta \Lambda \big[u(t) + \Delta(p)\big], \quad p(t_0) = p_0 \tag{4.23}$$

where $p(t)$ is the roll rate, $u(t)$ is the aileron input, dynamic stability derivative L_p denoting the roll damping is $L_p = -1$, input matrix is $L_\delta = 1$, and the uncertainty

is given by $\Delta(p) = 0.2 + p|p|$, which yields $\phi(p) = \begin{bmatrix} 1 & p|p| \end{bmatrix}^T$ and $w = \begin{bmatrix} 0.2 & 1 \end{bmatrix}^T$. Unknown control effectiveness is represented by Λ. This numerical example can be regarded as incorrect characterization of the roll mode time constant and existence of constant wind disturbance trying to roll the aircraft. Unknown control effectiveness is chosen to be $\Lambda = 0.2$ meaning that the aircraft experiences 80% loss in aileron control. Reference model is constructed with $A_r = -2$ and $B_r = 2$. Positive definite solution P is determined using $Q = 2$. Low-pass filter cutoff frequency is $\omega_f = 1$ rad/s. Sampling frequency is 100 Hz. In this example, 4 controllers are applied:

  - (Nominal) Nominal controller in Eq 2.4
  - (Std-MRAC) Standard MRAC in Eq 2.10
  - (CMRAC) CMRAC in Eq 2.19
  - (IR-CMRAC) Proposed CMRAC with Information Recovery in Eq 4.21

where the controller parameters are summarized in Table 4.2.

Table 4.2: Controller Parameters (N/A: Not Available)

	Nominal	Std-MRAC	CMRAC	IR-CMRAC
K_x	1	1	1	1
K_r	2	2	2	2
Γ	N/A	1	1	1
Γ_Θ	N/A	N/A	N/A	$I_{5\times5}$
γ_y	N/A	N/A	N/A	1
γ_1	N/A	N/A	N/A	1
γ_2	N/A	N/A	N/A	1
γ_3	N/A	N/A	N/A	1
γ_4	N/A	N/A	N/A	1
γ_λ	N/A	N/A	10	10
Γ_Λ	N/A	N/A	1	1
Γ_W	N/A	N/A	N/A	10

Figure 4.1 illustrates the response of nominal controller in Eq 2.4. As seen in the figure, nominal controller is not able to track the command as desired.
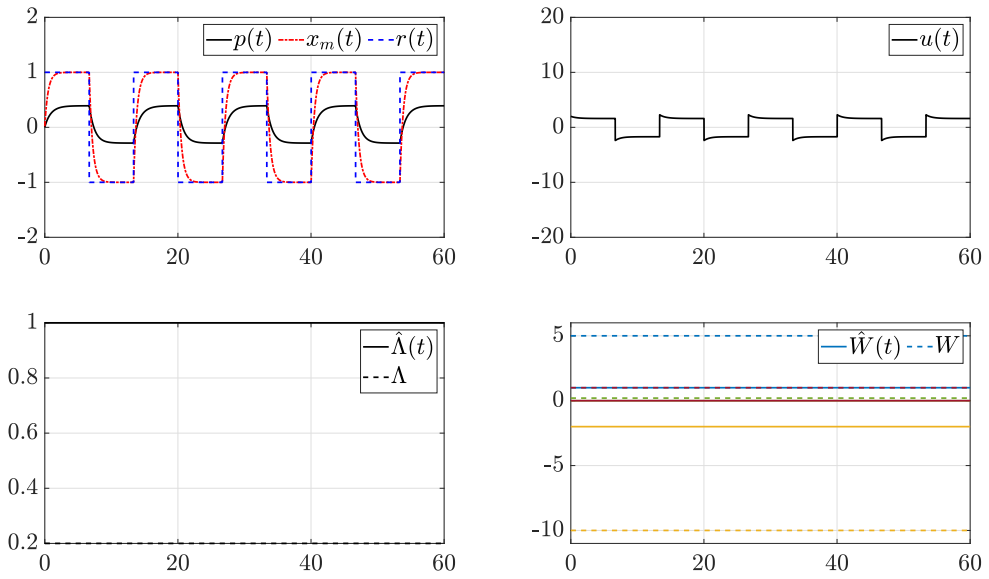
Figure 4.1: Example 1: Response of Nominal Controller in Eq 2.4

Then, adaptation is activated with standard MRAC law in Eq 2.10. Figure 4.2 shows that better tracking performance is achieved with standard MRAC law. Although parameters slowly converge to their ideal values, online estimation of unknown control effectiveness is not available with standard MRAC. It is important to note that this convergence is because of the persistent excitation of the regressor signal ϕ.
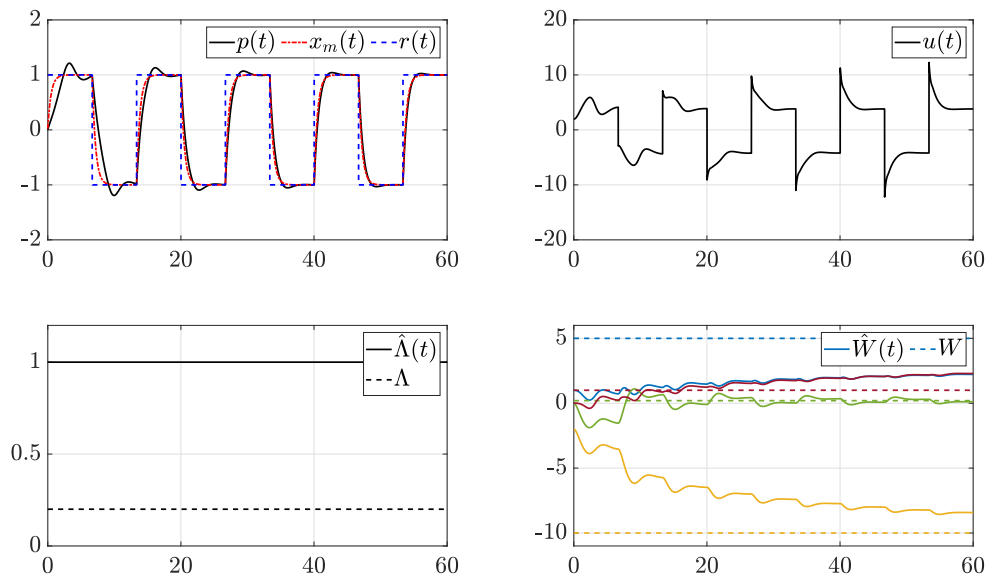
Figure 4.2: Example 1: Response of Standard MRAC in Eq 2.10

In Figure 4.3, adaptation is achieved with CMRAC update law in Eq 2.19. As denoted by Remark 2.7, error signal e_Y asymptotically converges to zero (see Figure 4.4). It is important to note that main contribution of CMRAC law over standard MRAC vanishes as e_Y converges to zero. That is, evolution of $\hat{\Lambda}$ freezes and CMRAC modification term becomes trivial with $e_Y \cong 0$ (see update laws in Eq 2.19). It is also important to highlight that $\hat{\Lambda}$ evolves completely in the wrong direction.
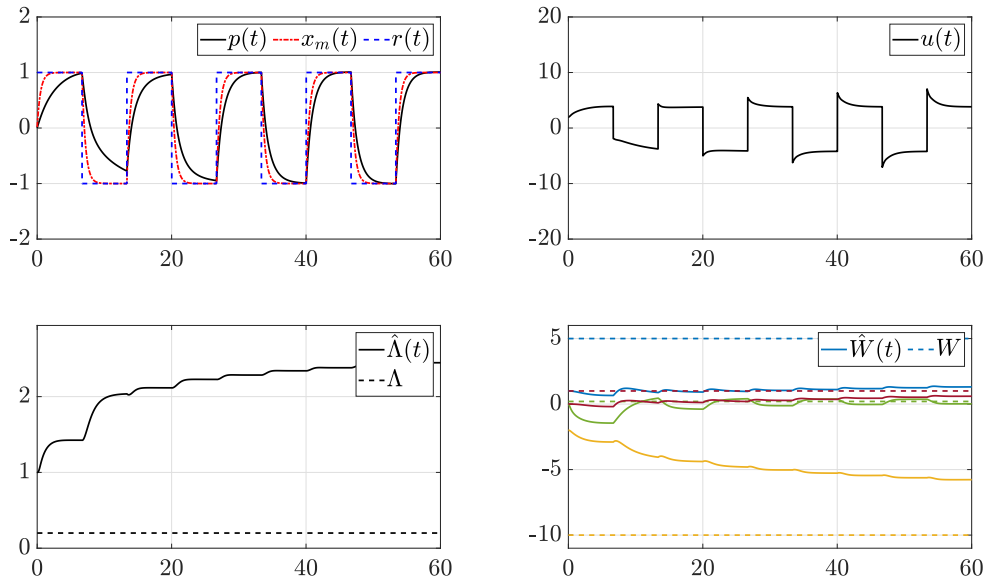
Figure 4.3: Example 1: Response of CMRAC in Eq 2.19
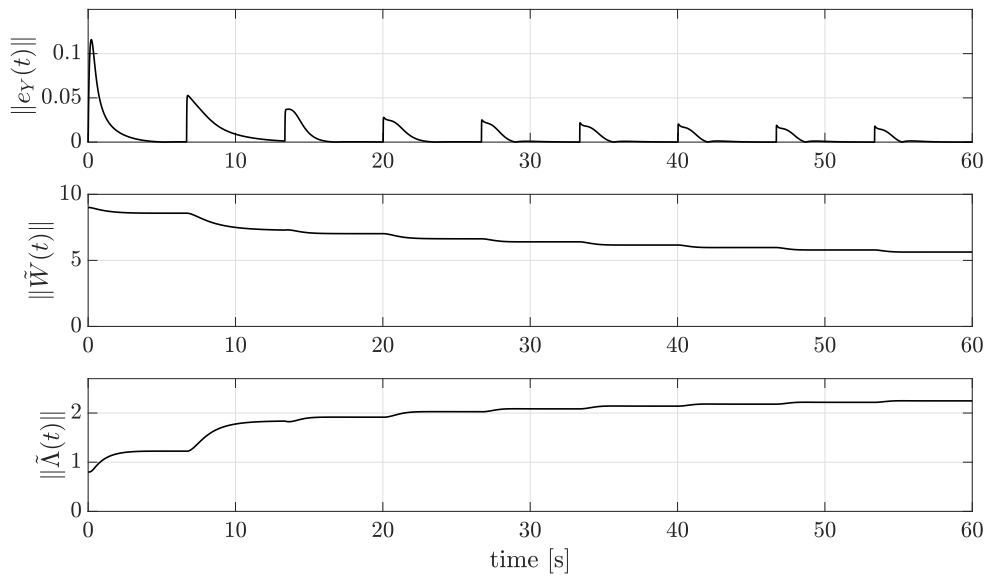
Figure 4.4: Example 1: Parameter Estimation Error with CMRAC in Eq 2.19

62

Next, the proposed adaptive law in Eq 4.21 is employed. Figure 4.5 shows the ideal state tracking performance (top left) and ideal parameter characterization (bottom two subfigures) with the proposed method. As opposed to CMRAC framework, asymptotic convergence of e_Y does not prevent the estimated parameter to evolve in the desired direction.
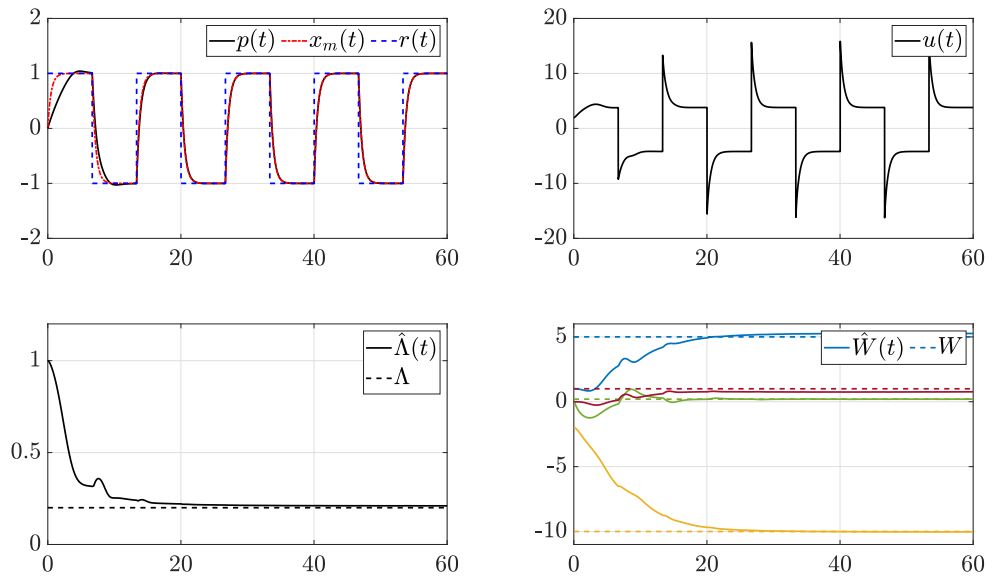
Figure 4.5: Example 1: Response of the Proposed Controller in Eq 4.21
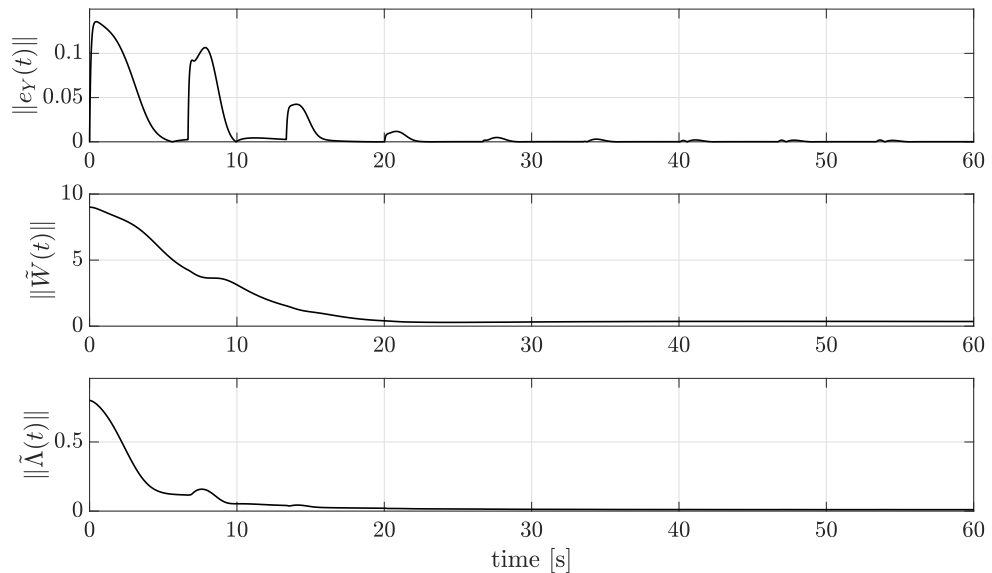
Figure 4.6: Example 1: Weight Estimation Error with Proposed Controller in Eq 4.21

4.3.2 Systems with Integrator Dynamics

It is well-known that the standard MRAC suffers from degraded performance if the system has an augmented integrator dynamics. In this example, the first order roll dynamics in Eq 4.23 is considered with the following uncertainty:

$$\Delta(p) = 0.2 + p|p| \tag{4.24}$$

The integrator state $x_i(t)$ is augmented to the system as follows:

$$\begin{bmatrix} \dot{p}(t) \\ \dot{x}_i(t) \end{bmatrix} = \begin{bmatrix} L_p & 0 \\ -1 & 0 \end{bmatrix} \begin{bmatrix} p(t) \\ x_i(t) \end{bmatrix} + \begin{bmatrix} L_\delta \\ 0 \end{bmatrix} \Lambda \big[u(t) + \Delta(p) \big] + \begin{bmatrix} 0 \\ 1 \end{bmatrix} r(t)$$

The nominal controller is designed to be:

$$u_n(t) = -K_x p(t) + K_i x_i(t) = -\begin{bmatrix} K_x & -K_i \end{bmatrix} x(t) \triangleq -K x(t)$$

with $K_x = 1.5$ being a feedback gain and $K_i = 3$ being an integral gain. 80% loss of aileron control is assumed with $\Lambda = 0.2$. Reference model is designed by applying the nominal controller to the nominal system without any uncertainty:

$$\dot{x}_r(t) = \begin{bmatrix} L_p - L_\delta K_x & L_\delta K_i \\ -1 & 0 \end{bmatrix} x_r(t) + \begin{bmatrix} 0 \\ 1 \end{bmatrix} r(t) \tag{4.25}$$

Figure 4.7 presents the simulation results obtained through Standard MRAC with two difference gains; $\Gamma = 10$ and $\Gamma = 1000$. As clearly seen, increasing the learning rate Γ does not improve the tracking performance, instead it induces high frequency oscillations to the system. This result supports the initial statement that the standard MRAC has poor adaptation performance for the systems having an augmented integrator.

Figure 4.8 illustrates the tracking response of the nominal controller in Eq 2.4. Compared to the nominal controller response in Figure 4.1, adding an integrator slowly eliminates the steady state error, as expected. Yet, the command following performance is still not acceptable.
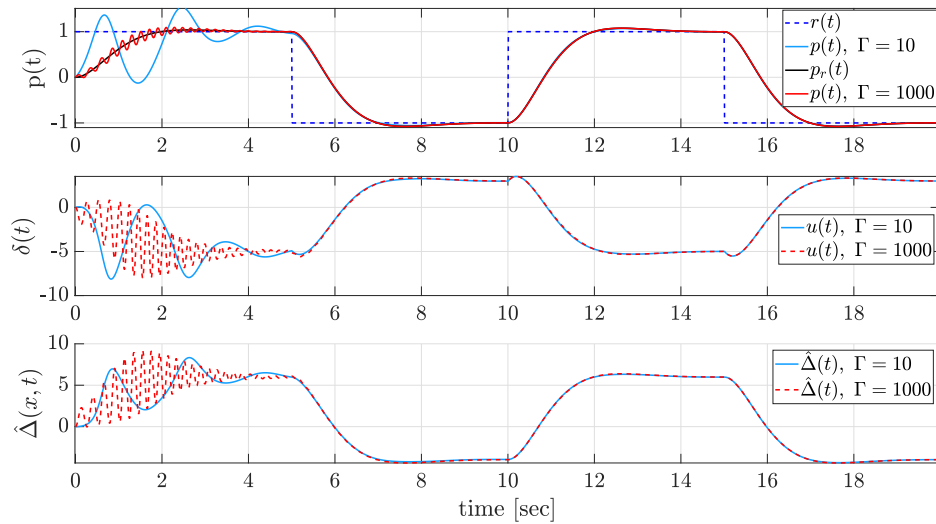
Figure 4.7: Example 2: Performance Comparison for Standard MRAC
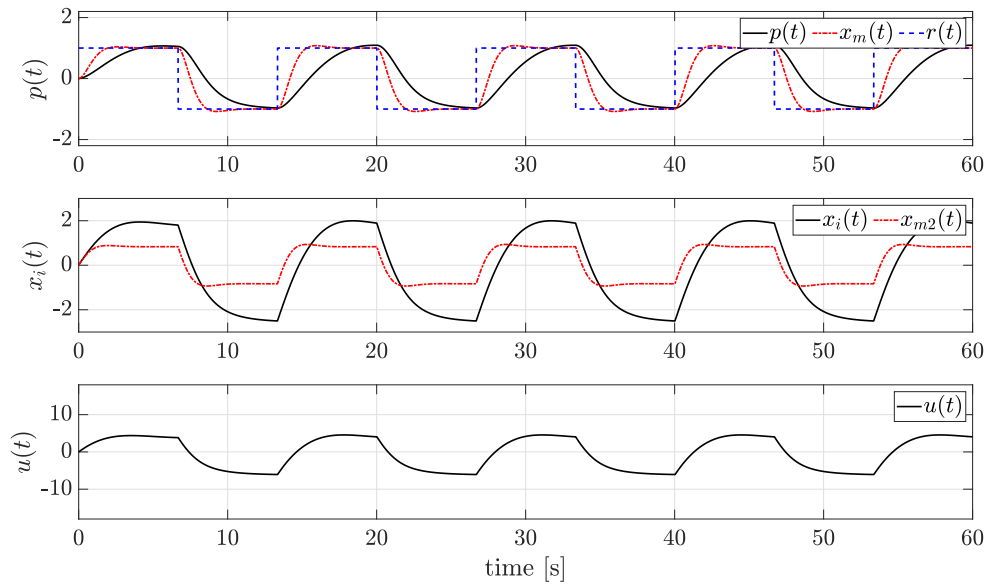
Figure 4.8: Example 2: Response of Nominal Controller in Eq 2.4

Next, standard MRAC is employed for the integrator augmented uncertain system. It has been previously shown in Figure 4.7 that large learning rates induces high-frequency oscillations in system states and control input. Hence, a relatively small learning rate of $\Gamma = 1$ is applied as indicated in Table 4.2. Figure 4.9 presents the state tracking performance with standard MRAC. As seen in the figure, command following performance is improved compared to nominal controller. However, it is not possible to reach an estimation of unknown control effectiveness. In addition, fast

adaptation is not achieved as the overshoot in the response vanishes slowly.
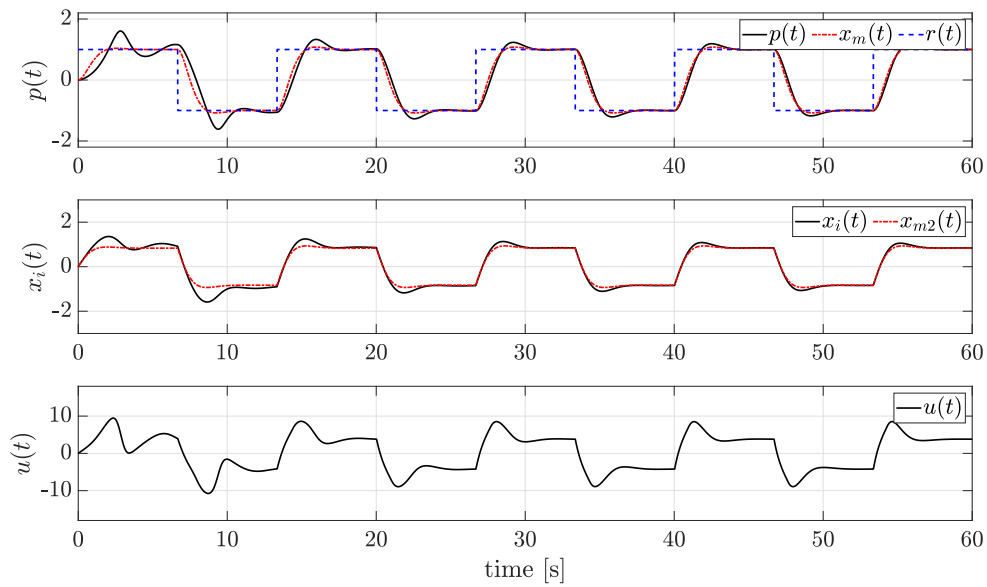
Figure 4.9: Example 2: Response of Standard MRAC in Eq 2.10

Slow adaptation can also be visualized from Figure 4.10 as the estimated parameters converge to their ideal values slowly. It is important to note that parameter convergencec with standard MRAC is achieved in this example, just because the regressor Φ is persistently exciting.
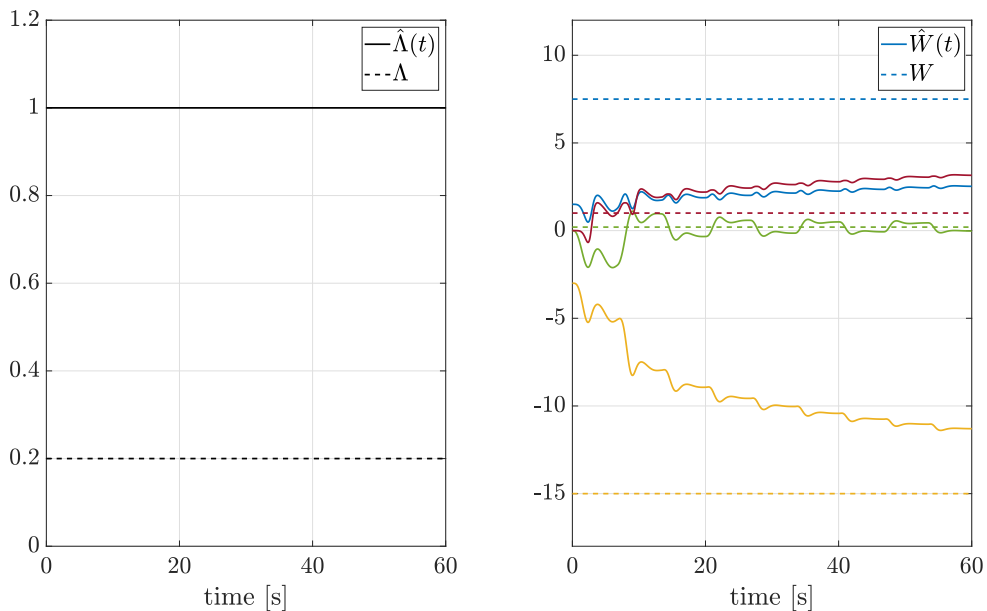
Figure 4.10: Example 2: Response of Standard MRAC in Eq 2.10

Next, CMRAC is applied to the integrator augmented uncertain system. Low-pass filter cutoff frequency is chosen to be ω_f on purpose. This is to show CMRAC suffers from losing information due to filtering. As clearly seen from Figure 4.11, CMRAC slightly improves the damping in the response. However, not much improvement is achieved in terms of command following performance.
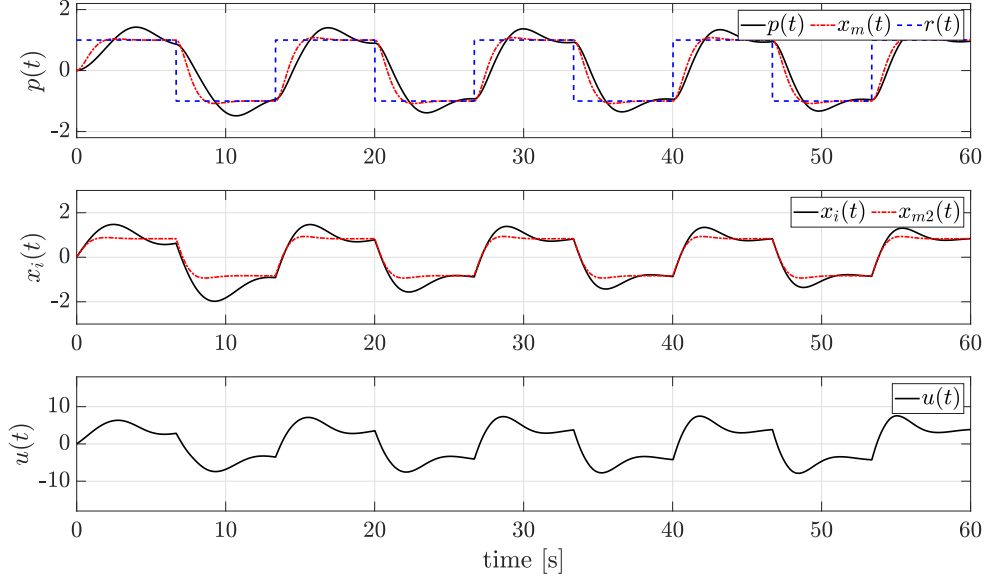
Figure 4.11: Example 2: Response of CMRAC in Eq 2.19

In addition, parameter estimation performance is also far away from the desired one (see Figure 4.12). As aforementioned, CMRAC update law in Eq 2.19 turns into standard MRAC law in Eq 2.10 as the error signal $e_Y(t)$ converges to zero as $t \to \infty$. Note that $e_Y(t) \cong 0$ for $t \geq 10$ as seen from Figure 4.15.

Then, the numerical simulation results are presented with the proposed information recovery-based adaptive controller. Figure 4.13 illustrates the state tracking performance. As seen, ideal command following is achieved with fast-adaptation feature of the proposed controller. In Figure 4.13, evolution of the adaptive weights is shown. Both estimated parameters $\hat{W}$ and $\hat{\Lambda}$ converge to their ideal values as theoretically shown by Theorem 4.2.
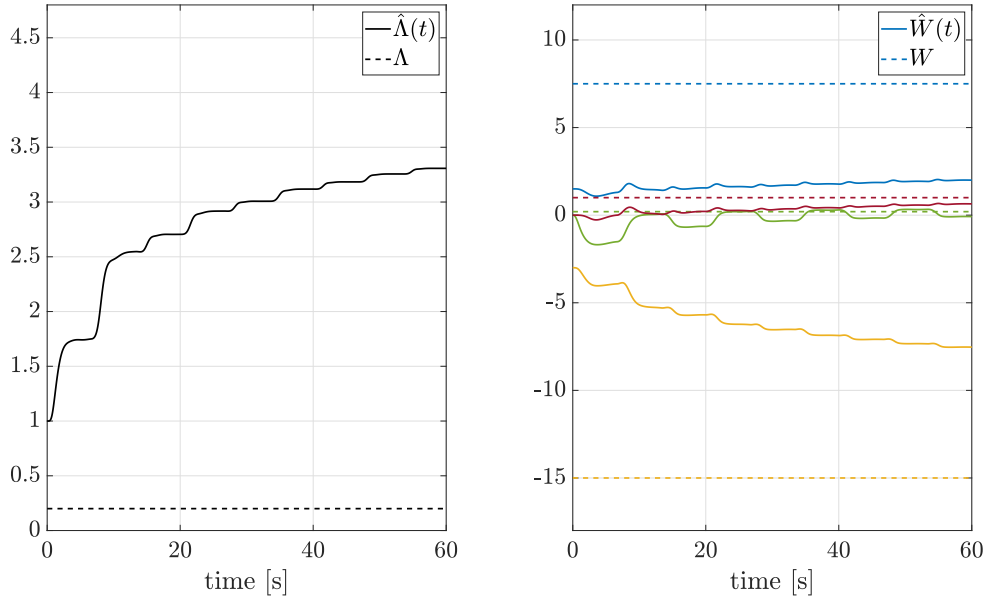
Figure 4.12: Example 2: Response of CMRAC in Eq 2.19
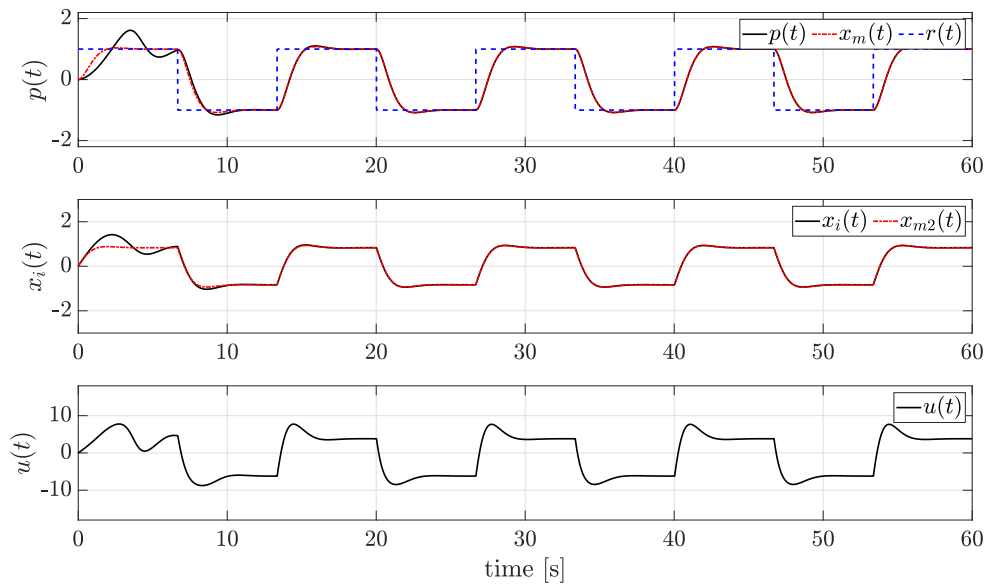
Figure 4.13: Example 2: Response of Proposed Controller in Eq 4.21

Lastly, Figure 4.15 highlights the improved parameter estimation performance of the proposed controller against Composite MRAC. It is obvious from the figure that Information Recovery-based CMRAC (IR-CMRAC) outperforms the conventional CMRAC by achieving the parameter convergence even in the presence of small LPF cutoff frequency of $\omega_f = 1$ rad/s.
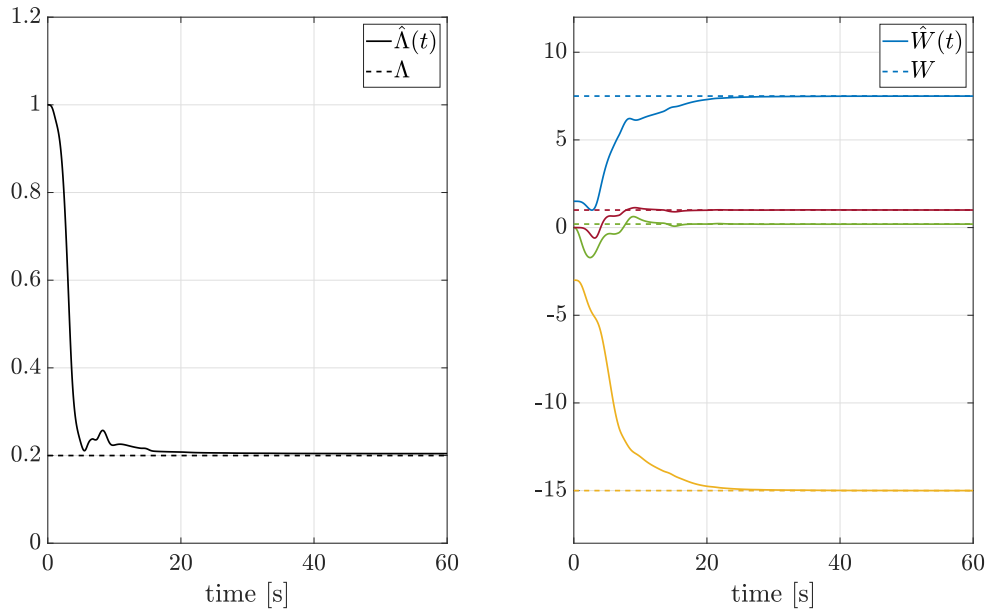
Figure 4.14: Example 2: Response of Proposed Controller in Eq 4.21
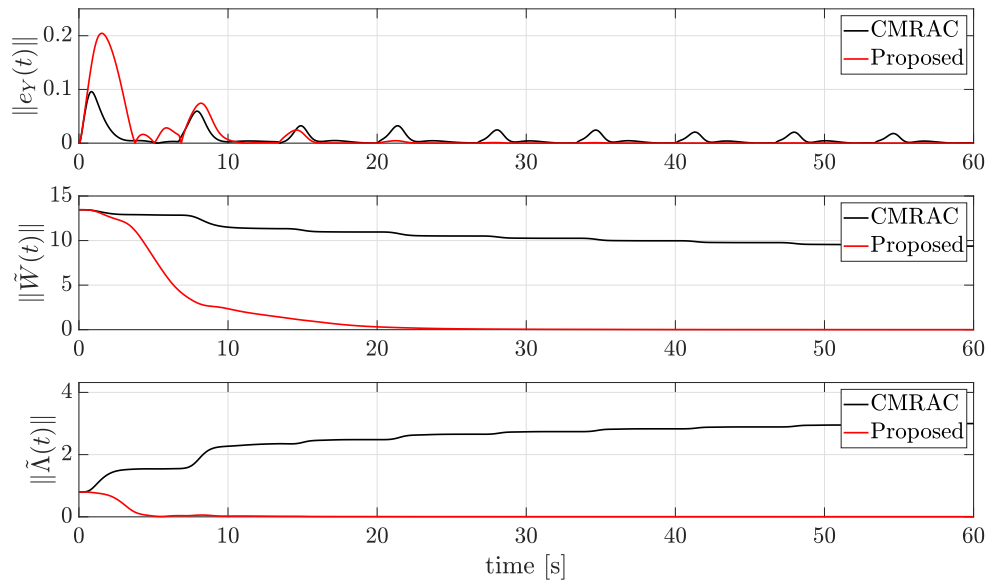
Figure 4.15: Example 2: Response of Proposed Controller in Eq 4.21

69

CHAPTER 5

COMMAND GOVERNOR-BASED ADAPTIVE CONTROL FOR THE SYSTEMS WITH MATCHED AND UNMATCHED UNCERTAINTIES

5.1   Introduction

In this chapter, a command governor-based adaptive control architecture is proposed for stabilizing uncertain dynamical systems with not only matched but also unmatched uncertainties and achieving desired command following performance of a user-defined subset of the accessible states. In the proposed solution, composite model reference adaptive control with information recovery is employed to attenuate the effects of matched and unmatched uncertainties. Specifically, the matched uncertainty is identified and its effect upon the system behavior is entirely suppressed. Moreover, using the unmatched uncertainty approximation obtained through radial basis function neural networks, the command governor signal is designed to achieve the desired command following performance of the user-defined subset of the accessible states. With this command governor-based Model Reference Adaptive Control architecture, the tracking error of the selected states can be made arbitrarily small by judiciously tuning the design parameters. In addition to the analysis of the closed-loop system stability using methods from Lyapunov theory, the findings are also illustrated through numerical examples.

Model Reference Adaptive Control (MRAC) architectures achieve a desired level of closed-loop stability and performance for uncertain dynamical systems with online adaptive weight update laws. Many MRAC frameworks rely on the matching assumption between the reference model and plant to track the desired reference command. Without restrictive persistent excitation (PE) of system signals, standard

MRAC framework cannot guarantee closed-loop stability in the presence of bounded perturbations using only instantaneous data [1, 2]. To increase the robustness of standard MRAC and/or guarantee stability without PE, well-established robust modifications are introduced in literature [3]- [9]. Yet, these MRAC frameworks have been restricted to uncertainties lying on the span of the control input, which are called *matched* uncertainties. However, this assumption may not hold for many practical systems with unmatched uncertainties, unmodeled dynamics and external disturbances (e.g. magnetic levitation [26]). In this chapter, the motivation is to guarantee the desired tracking performance in the presence of uncertainties lying outside the span of the control input.

5.2 Problem Formulation

In this chapter, the following uncertain dynamical systems are considered:

$$\dot{x}(t) = Ax(t) + B\big[u(t) + \Delta\big(x(t)\big)\big] + D\Delta_u\big(x(t)\big), \quad x(t_0) = x_0 \qquad (5.1)$$

where $x(t) \in \mathcal{D}_x \subset \mathbb{R}^n$ is the state vector where $\mathcal{D}_x$ is sufficiently large compact set, system matrix $A \in \mathbb{R}^{n\times n}$ and input matrix $B \in \mathbb{R}^{n\times m}$ are *known*, control input is $u(t) \in \mathcal{U} \subset \mathbb{R}^m$ where $\mathcal{U}$ is the admissible control set, $\Delta\big(x(t)\big) \in \mathbb{R}^m$ and $\Delta_u\big(x(t)\big) \in \mathbb{R}^{m_u}$ are the Lipschitz continuous functions representing the unknown matched and unmatched uncertainties, respectively. $D \in \mathbb{R}^{n\times m_u}$ lies in the left null space of B; that is, $D \in \mathcal{N}(B^T)$, $B^T D = D^T B = 0$. Note that D may not necessarily be the orthogonal complement of B; i.e. $1 \leq m_u \leq (n-m)$.

Assumption 5.1. *Throughout this chapter, the following assumptions are made:*

a. *The structure of the matched uncertainty is known. Hence, it can be parameterized by the linear combinations of known basis functions as*

$$\Delta\big(x(t)\big) = W^T\phi\big(x(t)\big),$$

where $W \in \mathbb{R}^{s\times m}$ is the unknown constant weight matrix, the known vector-function $\phi\big(x(t)\big) \in \mathbb{R}^s$ is Lipschitz continuous over $\mathcal{D}_x$.

b. *The structure of the unmatched uncertainty is unknown. But, it can be*

approximated by an RBF NN as [77]

$$\Delta_u\big(x(t)\big) = W_u^T \psi\big(x(t)\big) + \varepsilon\big(x(t)\big),$$

where $W_u \in \mathbb{R}^{s_u \times m_u}$ is the unknown constant weight matrix, the known basis vector-function $\psi\big(x(t)\big) \in \mathbb{R}^{s_u}$ is Lipschitz continuous over $\mathcal{D}_x$, and $\varepsilon\big(x(t)\big)$ is the residual error with $\big\|\varepsilon\big(x(t)\big)\big\| \leq \varepsilon_0$, $\forall x(t) \in \mathcal{D}_x$.

As standard [77], the basis vector-function $\psi(x)$ is constructed using RBFs as

$$\psi(x) = \begin{bmatrix} \psi_1(x) & \psi_2(x) & \dots & \psi_{s_u}(x) \end{bmatrix}^T,$$

where $\psi_i(x) \in \mathbb{R}$ for $i = 1, \dots, s_u$ is given by

$$\psi_i(x) = \begin{cases} 1 & , \text{ for } i = 1 \\ \exp\big(-\frac{\|x(t)-\bar{c}_i\|^2}{2\bar{\mu}_i^2}\big) & , \text{ for } i = 2, \dots, s_u \end{cases}$$

with $\bar{c}_i \in \mathbb{R}^n$ being the center of an RBF unit and $\bar{\mu}_i \in \mathbb{R}_+$ being the width of the ith kernel node. Under Assumption 5.1, uncertain system in Eq 5.1 can be re-written as:

$$\dot{x}(t) = Ax(t) + B\big[u(t) + W^T\phi(x)\big] + DW_u^T\psi(x) + D\varepsilon(x,t) \qquad (5.2)$$

Assumption 5.2. *Basis function ϕ is sufficiently exciting signals. Hence, there exist positive constants $\alpha, T_e \in \mathbb{R}_+$ that satisfies:*

$$\int_{t_0}^t \phi(\tau)\phi^T(\tau)d\tau \succeq \alpha I, \qquad t = T_e$$

As elaborated in Remark 3.2, filtered signal ϕ_f is also sufficiently exciting with the following inequality:

$$\int_{t_0}^t \phi_f(\tau)\phi_f^T(\tau)d\tau \succeq \beta I, \qquad t = T_e, \qquad 0 < \beta \leq \alpha$$

The ideal reference model that captures the desired closed-loop command following performance is given by

$$\dot{x}_r(t) = A_r x_r(t) + B_r r(t), \qquad x_r(t_0) = x_{r_0}, \qquad (5.3)$$

where $x_r(t) \in \mathbb{R}^n$ is the ideal reference state vector, $A_r \in \mathbb{R}^{n \times n}$ is the Hurwitz system matrix, $B_r \in \mathbb{R}^{n \times k}$ is the input matrix, and $r(t) \in \mathbb{R}^k$ is a bounded and piecewise continuous reference signal with $k \leq m$, $\|r(t)\| \leq r_0$, $\forall t \geq t_0$.

In order to analyze the effects of unmatched uncertainty upon the system behavior, an auxiliary reference model is designed based on unmatched uncertainty estimation. To this end, better unmatched uncertainty estimation allows better understanding the effects of unmatched uncertainty on the control response. Hence, the information recovery-based adaptive control architecture (proposed in Chapter 3) is employed for fast adaptation with improved transient response. Next, the auxiliary reference model is defined as the following:

$$\dot{x}_m(t) = A_r x_m(t) + B_r\big[r(t) + z(t)\big] + D\hat{W}_u^T(t)\psi(x) - k_\lambda e(t), \qquad (5.4)$$

where $x_m(t) \in \mathbb{R}^n$ is the auxiliary reference state vector, $\hat{W}_u(t) \in \mathbb{R}^{s_u \times m_u}$ is the online estimation of W_u, $z(t) \in \mathbb{R}^r$ is the command governor signal, $k_\lambda \in \mathbb{R}_+$ is a constant, and $e(t) \triangleq x_m(t) - x(t)$ is the tracking error signal. Reference model system matrix A_r and input matrix B_r are chosen such that $A_r = A - BK_x$ and $B_r = BK_r$. The error feedback term in the auxiliary reference model in Eq 5.4 improves the transient performance (see, for example, [81, 83, 98–100] that employ similar reference model modifications).

Assumption 5.3. *Unknown weight matrix W_u lies inside the convex set Ω_c on which unmatched estimations $\hat{W}_u(t)$ are constrained by the projection operator [88].*

Remark 5.1. *Let $\overline{\gamma} \in \mathbb{R}_+$ be the projection norm bound to be used in projection operator. Then, by Assumption 5.3, the existence of following bound is ensured:*

$$\big\|\hat{W}_u(t)\big\| \leq \big\|\hat{W}_u(t)\big\|_F \leq rank\big(\hat{W}_u(t)\big)\big\|\hat{W}_u(t)\big\| \leq rank\big(\hat{W}_u(t)\big)\overline{\gamma} \leq \min\big(s_u, m_u\big)\overline{\gamma}$$
$$thus \rightarrow \ W_u, \big\|\hat{W}_u(t)\big\|, \big\|\hat{W}_u(t)\big\|_F \leq \min\big(s_u, m_u\big)\overline{\gamma} \triangleq \gamma_0.$$

The nominal control input consisting of a feedback part $u_{\text{fb}}(t) \triangleq K_x x(t)$ and a feedforward part $u_{\text{ff}}(t) \triangleq K_r r(t)$ is given by

$$u_n(t) = -K_x x(t) + K_r r(t) \qquad (5.5)$$

The overall control input with an adaptive part $u_{\text{ad}}(t) \triangleq \hat{W}^T(t)\phi(x)$ and a command governor part $u_g(t) \triangleq K_r z(t)$ is given by

$$u(t) = u_n(t) - \hat{W}^T(t)\phi(x) + K_r z(t)$$
$$u(t) = -K_x x(t) + K_r r(t) - \hat{W}^T(t)\phi(x) + K_r z(t). \qquad (5.6)$$

Using Eq 5.6 with the matched weight estimation error $\tilde{W}(t) \triangleq W - \hat{W}(t)$, uncertain dynamical system Eq 5.1 can be written as

$$\dot{x}(t) = A_r x(t) + B_r\big[r(t) + z(t)\big] + B\tilde{W}^T(t)\phi(x) + D\big[W_u^T \psi(x) + \varepsilon(x, t)\big] \quad (5.7)$$

Now, let $e_m(t) \triangleq x_r(t) - x_m(t)$ be the auxiliary tracking error. Then, its dynamics can be obtained using Eq 5.3 and Eq 5.4 as

$$\dot{e}_m(t) = A_r e_m(t) - B_r z(t) - D\hat{W}_u^T(t)\psi(x) + k_\lambda e(t). \quad (5.8)$$

Furthermore, one can write the tracking error dynamics using Eq 5.4 and Eq 5.7 as

$$\dot{e}(t) = \big(A_r - k_\lambda I\big)e(t) - B\tilde{W}^T(t)\phi(x) - D\tilde{W}_u^T(t)\psi(x) - D\varepsilon(x) \quad (5.9)$$

Remark 5.2. *As the positive constant k_λ increases, robustness of the error dynamics in Eq 5.9 increases against uncertainty estimation. This is because of the fact that the eigenvalues of Hurwitz matrix A_r shift to the left by amount of k_λ.*

5.3   Filtering System Dynamics

In this section, a set of low-pass filters is applied to the system dynamic to reach the low-frequency content of matched and unmatched uncertainties separately. First, the uncertain system dynamics in Eq 5.1 is multiplied by the left pseudo inverse of input matrix B from the left:

$$B_{\text{left}}^{-1}\dot{x}(t) = B_{\text{left}}^{-1}Ax(t) + \big[u(t) + \Delta(x)\big] \quad (5.10)$$

Note that the left pseudo inverse of B is given by $B_{\text{left}}^{-1} = \big(B^T B\big)^{-1} B^T$, which yields $B_{\text{left}}^{-1}D = \big(B^T B\big)^{-1} B^T D = 0$ since $D^T B = B^T D = 0$. Next, the low-pass filters in Eq 2.12 is applied to get the following:

$$\Delta_f(x, t) = W^T\phi_f(x, t) = B_{\text{left}}^{-1}\dot{x}_f(t) - B_{\text{left}}^{-1}Ax_f(t) - u_f(t) \quad (5.11)$$

Similarly, multiplying the uncertain system by $D_{\text{left}}^{-1} = \big(D^T D\big)^{-1} D^T$ from the left and applying the same low-pass filters yield:

$$\Delta_{u,f}(x, t) = W_u^T\psi_f(x, t) + \varepsilon_f(x, t) = D_{\text{left}}^{-1}\dot{x}_f(t) - D_{\text{left}}^{-1}Ax_f(t) \quad (5.12)$$

5.4 Adaptive Laws

From this point forward, the information recovery in Chapter 3 is exploited to the adaptive law for the matched parameters:

$$\dot{\hat{W}} = \left(\Gamma^{-1} + \gamma_m \phi_f \phi_f^T\right)^{-1}\left(\gamma_m \dot{\phi}_f \tilde{\Delta}_f^T + \gamma_1 \phi_f \tilde{\Delta}_f^T + \gamma_2 \tilde{\mathcal{M}} - \phi e^T PB\right) \quad (5.13)$$

As it can be seen, weight update law for the matched parameters is kept the same as in Eq 3.4. Then, a new adaptive weight update law is introduced for the unmatched parameters as:

$$\dot{\hat{W}}_u = \text{Proj}\left\{\hat{W}_u, \left(\Gamma_u^{-1} + \mu_m \psi_f \psi_f^T\right)^{-1}\left(\mu_m \dot{\psi}_f \tilde{\Delta}_{u,f}^T + \mu_1 \psi_f \tilde{\Delta}_{u,f}^T - \psi e^T PD\right)\right\} \quad (5.14)$$

where $\Gamma_u = \Gamma_u^T \succ 0$ is positive definite learning rate, $\mu_m, \mu_1 \in \mathbb{R}_+$ are user-defined positive scalar design parameters, and $\hat{W}_u$ is the online estimation of unknown unmatched weight matrix W_u. In addition, $\tilde{\Delta}_{uf}$ is stated as follows:

$$\tilde{\Delta}_{uf} \triangleq \Delta_{uf} - \hat{\Delta}_{uf}$$

with $\hat{\Delta}_{uf}$ being defined as $\hat{\Delta}_{uf} \triangleq \hat{W}_u^T \psi_f$.

For the uncertain dynamical system Eq 5.1 subject to Assumption 5.1, the goal is to drive the user-defined subset of the accessible states $y(t) = Cx(t)$ to a close neighborhood of that of the reference model $y_r(t) = Cx_r(t)$; $y(t) \in N_\delta(y_r(t))$. To achieve this, both matched and unmatched uncertainties are estimated in the adaptive control framework and the command governor signal is designed based on backstepping technique using the unmatched estimations. The overall block diagram is given in Figure 5.1.

Theorem 5.1. *Consider the uncertain dynamical system in Eq 5.1, auxiliary reference model in Eq 5.4, weight update laws in Eq 5.13 and Eq 5.14, and control input in Eq 5.6. Then, the tracking error $e(t)$, and weight estimation errors $\tilde{W}(t)$ and $\tilde{W}_u(t)$ are uniformly ultimately bounded.*

Proof.

Let $\eta \triangleq \begin{bmatrix} e^T & \text{vec}(\tilde{W})^T & \text{vec}(\tilde{W}_u)^T & \tilde{\Delta}_f^T & \tilde{\Delta}_{uf}^T \end{bmatrix}^T$ be the aggregated error vector. Wherever appropriate, the arguments 't' for time dependency and 'x' for state dependency are dropped consistently over an entire for ease of exposition.

Figure 5.1: Block diagram for command governor-based adaptive control for unmatched uncertainties.

Consider the Lyapunov candidate

$$\mathcal{V}_1 = \frac{1}{2}e^T P e + \frac{1}{2}\text{tr}\big(\tilde{W}^T \Gamma_m^{-1} \tilde{W}\big) + \frac{1}{2}\text{tr}\big(\tilde{W}_u^T \Gamma_u^{-1} \tilde{W}_u\big) + \frac{1}{2}\tilde{\Delta}_f^T \gamma_m \tilde{\Delta}_f + \frac{1}{2}\tilde{\Delta}_{uf}^T \mu_m \tilde{\Delta}_{uf}$$
$$= \frac{1}{2}\eta^T \overline{P} \eta$$

where $\overline{P} \triangleq \text{diag}\big(I_1 \otimes P, I_2 \otimes \Gamma_m^{-1}, I_3 \otimes \Gamma_u^{-1}, \gamma_m, \mu_m\big)$ with I_1, I_2, I_3 being identity matrices of appropriate dimensions. Note that $\mathcal{V}_1(0) = 0$, $\mathcal{V}_1(\eta) > 0, \forall \eta \neq 0$, and $\mathcal{V}_1(\eta)$ is radially unbounded. Time derivative of the Lyapunov function along system trajectories in Eq 5.8, Eq 5.13, and Eq 5.14 is given by:

$$\dot{\mathcal{V}}_1 = -\frac{1}{2}e^T Q e - k_\lambda e^T P e + \text{tr}\big[\tilde{W}^T\big(-\phi e^T PB + \gamma_m \dot{\phi}_f \tilde{\Delta}_f^T\big)\big]$$
$$- \text{tr}\big[\tilde{W}^T\big(\Gamma^{-1} + \gamma_m \phi_f \phi_f^T\big)\dot{\hat{W}}\big] + \text{tr}\big[\tilde{W}_u^T\big(-\psi e^T PD + \mu_m \dot{\psi}_f \tilde{\Delta}_{u,f}^T\big)\big]$$
$$- \text{tr}\big[\tilde{W}_u^T\big(\Gamma_u^{-1} + \mu_m \psi_f \psi_f^T\big)\dot{\hat{W}}_u\big] + e^T PD\varepsilon$$

Substituting the adaptive laws in Eq 5.13-Eq 5.14 and applying Lemma 2.3 yields:

$$\dot{\mathcal{V}}_1 = -\frac{1}{2}e^T Q e - k_\lambda e^T P e - \gamma_1 \text{tr}\big(\tilde{\Delta}_f \tilde{\Delta}_f^T\big) - \gamma_2 \text{tr}\big(\tilde{W}^T \Phi \tilde{W}\big)$$
$$- \mu_1 \text{tr}\big(\tilde{\Delta}_{u,f} \tilde{\Delta}_{u,f}^T\big) + e^T PD\varepsilon$$
$$\leq -\left(\frac{1}{2}\lambda_{\min}(Q) + k_\lambda \lambda_{\min}(P)\right)\|e\|^2 - \gamma_1\|\tilde{\Delta}_f\|^2 - \gamma_2 \lambda_{\min}(\Phi)\|\tilde{W}\|^2$$
$$- \mu_1\|\tilde{\Delta}_{u,f}\|^2 + e^T PD\varepsilon$$

One can bound the last term by applying the Young's inequality [96] to get the

following:

$$e^T P D \varepsilon \leq \|e\| \|PD\| \varepsilon_0 \leq k_3 \|e\|^2 + \frac{1}{4k_3} \|PD\|^2 \varepsilon_0^2 \tag{5.15}$$

with $k_3 \in (a, b)$. Then, time derivative of the Lyapunov function can be bounded by:

$$\begin{aligned}
\dot{\mathcal{V}}_1 = & - \left(\frac{1}{2} \lambda_{\min}(Q) + k_\lambda \lambda_{\min}(P) - k_3 \right) \|e\|^2 - \gamma_2 \lambda_{\min}(\Phi) \|\tilde{W}\|^2 \\
& - \mu_1 \|\tilde{\Delta}_{u,f}\|^2 - \gamma_1 \|\tilde{\Delta}_f\|^2 + \frac{1}{4k_3} \|PD\|^2 \varepsilon_0^2
\end{aligned} \tag{5.16}$$

where positive constant k_3 is an arbitrary scalar with $k_3 \in \left(0, \frac{1}{2}\lambda_{\min}(Q) + k_\lambda \lambda_{\min}(P)\right)$. With this result, boundedness of error signals $e(t), \tilde{W}(t), \tilde{\Delta}_f(t)$, and $\tilde{\Delta}_{u,f}(t)$ is guaranteed. By the definition $\tilde{W}(t) = W - \hat{W}(t)$, matched parameter estimation $\hat{W}(t)$ becomes bounded since ideal weight matrix W is constant. Furthermore, unmatched parameter estimation $\hat{W}_u(t)$ is ensured to be bounded within a convex set due to projection operator, which results in boundedness of unmatched weight estimation error $\tilde{W}_u(t)$.

∎

Remark 5.3. *Theorem 5.1 ensures that the tracking error $e(t) = x_m(t) - x(t)$ is uniformly ultimately bounded. However, boundedness of the states $x(t)$ is not guaranteed since the auxiliary reference states $x_m(t)$ are not bounded, yet.*

5.5 Design of Command Governor

In Remark 5.3, it is noted that the auxiliary reference model states need to be bounded to ensure boundedness of the actual states. In this section, a command governor input procedure is systematically shown using backstepping technique to guarantee boundedness of the auxiliary reference model. In return, boundedness of all the system signals is established.

Let the unmatched uncertainty estimation be defined as $\hat{\Delta}_u(t, x) \triangleq \hat{W}_u^T(t)\psi(x)$.

Then, multi-level low-pass filter structure that is used in this chapter is given by

$$\dot{\hat{\Delta}}_{\text{uf},1}(t,x) = \Gamma_{\text{f}}\left[\dot{\hat{\Delta}}_u(t,x) - \hat{\Delta}_{\text{uf},1}(t,x)\right]$$

$$\dot{\hat{\Delta}}_{\text{uf},2}(t,x) = \Gamma_{\text{f}}\left[\dot{\hat{\Delta}}_{\text{uf},1}(t,x) - \hat{\Delta}_{\text{uf},2}(t,x)\right]$$

$$\dot{\hat{\Delta}}_{\text{uf},3}(t,x) = \Gamma_{\text{f}}\left[\dot{\hat{\Delta}}_{\text{uf},2}(t,x) - \hat{\Delta}_{\text{uf},3}(t,x)\right] \tag{5.17}$$

$$\vdots$$

$$\dot{\hat{\Delta}}_{\text{uf},\text{p}}(t,x) = \Gamma_{\text{f}}\left[\dot{\hat{\Delta}}_{\text{uf},\text{p-1}}(t,x) - \hat{\Delta}_{\text{uf},\text{p}}(t,x)\right]$$

where $\hat{\Delta}_{\text{uf},1}(t_0,x_0) = \hat{\Delta}_u(t_0,x_0)$, $\hat{\Delta}_{\text{uf},\text{i}}(t_0,x_0) = 0$ for $i = 2,\ldots,p$, diagonal matrix $\Gamma_{\text{f}} \succ 0$ is chosen such that $\lambda_{\max}(\Gamma_{\text{f}}) \le \Gamma_{\text{f,max}}$, with $\Gamma_{\text{f,max}}$ being a design parameter. This low-pass filter structure in command governor design allows to suppress the undesired high-frequency oscillations possibly contained in estimated unmatched signals which may cause problems if directly used in the control input such as rate saturation of actuators and/or exciting unmodeled dynamics.

5.5.1 Command Governor Design for Second Order Systems

Consistent with the existing literature (e.g., see chapter 10 of [101]), the backstepping design here starts with the second order system. Then, following the similar steps in [35, 36], it is extended to the higher order systems, recursively. Without loss of generality, it can be assumed that the reference model matrices A_r and B_r are in controllable canonical form. Hence,

$$A_r = \begin{bmatrix} 0 & 1 \\ -a_1 & -a_2 \end{bmatrix}, \quad B_r = \begin{bmatrix} 0 \\ b_r \end{bmatrix}, \quad D = \begin{bmatrix} d_1 \\ 0 \end{bmatrix},$$

where $a_1, a_2 \in \mathbb{R}_+$, and $b_r, d_1 \in \mathbb{R} \setminus \{0\}$. The objective is to drive the system state $x_1(t)$ to a close neighborhood of the reference state $x_{r_1}(t)$; i.e. $x_1(t) \to N_\delta(x_{r_1}(t))$. Hence, the matrix C pointing out the user-defined subset of accessible states becomes $C = \begin{bmatrix} 1 & 0 \end{bmatrix}$. Next, auxiliary tracking error dynamics Eq 5.8 in open-form is

$$\dot{e}_{m1}(t) = e_{m2}(t) - d_1\hat{\Delta}_u(t,x) + k_\lambda e_1(t) + \Gamma_0 e_{m1}(t) - \Gamma_0 e_{m1}(t) + d_1\hat{\Delta}_{\text{uf},1} - d_1\hat{\Delta}_{\text{uf},1}$$

$$\dot{e}_{m2}(t) = -a_1 e_{m1}(t) - a_2 e_{m2}(t) - b_r z(t) + k_\lambda e_2(t).$$

Remark 5.4. *Boundedness of unmatched weight estimations $\hat{W}_u(t)$ is guaranteed with Theorem 5.1. Furthermore, the basis vector-function $\psi(x)$ with Gaussian*

kernel units is bounded which results in boundedness of the unmatched uncertainty estimation $\hat{\Delta}_u(t, x)$. Since the low-pass filter given in Eq 5.17 is BIBO stable, the low-pass filtered signal $\hat{\Delta}_{uf,1}(t, x)$ is bounded. From Eq 5.17, it follows that its time derivative $\dot{\hat{\Delta}}_{uf,1}(t, x)$ is also bounded.

Let $\mathcal{E}_1(t) \triangleq e_{m2}(t) - d_1\hat{\Delta}_{uf,1} + \Gamma_0 e_{m1}(t)$ be the new state variable. Then, state dynamics for $\zeta(t) \triangleq \begin{bmatrix} e_{m1}(t) & \mathcal{E}_1(t) \end{bmatrix}^T$ can be written as

$$
\begin{aligned}
\dot{e}_{m1}(t) &= -\Gamma_0 e_{m1}(t) + \mathcal{E}_1(t) - d_1\widetilde{q}_1 \\
\dot{\mathcal{E}}_1(t) &= -a_1 e_{m1}(t) - a_2 e_{m2}(t) - b_r z(t) + k_\lambda e_2(t) \\
&\quad + \Gamma_0 \left(-\Gamma_0 e_{m1}(t) + \mathcal{E}_1(t) - d_1\widetilde{q}_1\right) - d_1\dot{\hat{\Delta}}_{uf,1} + \Gamma_1\mathcal{E}_1(t) - \Gamma_1\mathcal{E}_1(t)
\end{aligned}
\tag{5.18}
$$

where error $\widetilde{q}_1$ is $\widetilde{q}_1 \triangleq \left(\hat{\Delta}_u - \hat{\Delta}_{uf,1} - \frac{k_\lambda}{d_1}e_1(t)\right)$. Note that $\widetilde{q}_1$ is bounded since $\hat{\Delta}_u$ and $\hat{\Delta}_{uf,1}$ are bounded from Remark 4 and tracking error $e_1(t)$ is bounded from Theorem 5.1, $\forall t \geq t_0$. Choosing the command governor signal $z(t)$ as

$$
\begin{aligned}
z(t) \triangleq b_r^{-1}\Big\{ & e_{m1}(t)\left(-a_1 + a_2\Gamma_0 - \Gamma_0^2\right) + \mathcal{E}_1\left[\Gamma_0 + \Gamma_1 - a_2\right] \\
& + k_\lambda e_2(t) - d_1\left[\dot{\hat{\Delta}}_{uf,1} + a_2\hat{\Delta}_{uf,1} + \Gamma_0\widetilde{q}_1\right] \Big\}
\end{aligned}
\tag{5.19}
$$

simplifies Eq 5.18 to the compact form given by

$$
\dot{\zeta}(t) = \begin{bmatrix} \dot{e}_{m1}(t) \\ \dot{\mathcal{E}}_1(t) \end{bmatrix} = \begin{bmatrix} -\Gamma_0 & 1 \\ 0 & -\Gamma_1 \end{bmatrix} \begin{bmatrix} e_{m1}(t) \\ \mathcal{E}_1(t) \end{bmatrix} + \begin{bmatrix} d_1 \\ 0 \end{bmatrix} \widetilde{q}_1.
$$

Remark 5.5. *With suitable design parameters Γ_0 and Γ_1, boundedness of the state vector $\zeta(t)$ is guaranteed since the non-vanishing perturbation $\widetilde{q}_1$ is bounded [101]. With the bounded state $\zeta(t)$, boundedness of the auxiliary reference model states $x_m(t)$ is guaranteed. From Theorem 5.1, the tracking error $e(t) = x_m(t) - x(t)$ is bounded. Hence, with the command governor input Eq 5.19, boundedness of the actual system states $x(t)$ is established.*

5.5.2 Generalizations to Higher Order Systems

Command governor design can be recursively employed for the higher order systems as this is a standard procedure in backstepping technique. In the 3rd order system

case, for instance, the low-pass filter structure is employed up to 2nd level; i.e. $p = 2$.

Remark 5.6. *From Remark 5.4, the signal $\hat{\Delta}_{uf,1}$ is bounded. Then, cascaded low-pass filter signals $\hat{\Delta}_{uf,2}$ and $\dot{\hat{\Delta}}_{uf,2}$ are also bounded by following similar discussions made in Remark 4. Hence, recursive composition of low-pass filter signals to any level yields bounded filter signals.*

Now, consider the following matrices that characterizes the auxiliary tracking error dynamics Eq 5.8

$$A_r = \begin{bmatrix} 0 & 1 & 0 \\ 0 & 0 & 1 \\ -a_1 & -a_2 & -a_3 \end{bmatrix}, \ B_r = \begin{bmatrix} 0 \\ 0 \\ b_r \end{bmatrix}, \ D = \begin{bmatrix} d_1 \\ d_2 \\ 0 \end{bmatrix},$$

where $a_1, a_2, a_3 \in \mathbb{R}_+$, and $b_r, d_1, d_2 \in \mathbb{R} \setminus \{0\}$. Again, the goal is to drive $x_1(t)$ to a close neighborhood of $x_{r_1}(t)$; i.e. $x_1(t) \to N_\delta\left(x_{rm_1}(t)\right)$. Thus, $C = \begin{bmatrix} 1 & 0 & 0 \end{bmatrix}$.

Auxiliary tracking error dynamics in open-form is

$$\dot{e}_{m1}(t) = e_{m2}(t) - d_1\hat{\Delta}_u + k_\lambda e_1(t) + d_1\hat{\Delta}_{uf,1} - d_1\hat{\Delta}_{uf,1} + \Gamma_0 e_{m1}(t) - \Gamma_0 e_{m1}(t)$$

$$\dot{e}_{m2}(t) = e_{m3}(t) - d_2\hat{\Delta}_u + k_\lambda e_2(t)$$

$$\dot{e}_{m3}(t) = -a_1 e_{m1}(t) - a_2 e_{m2}(t) - a_3 e_{m3}(t) - b_r z(t) + k_\lambda e_3(t).$$

With the command governor signal $z(t)$

$$\begin{aligned}
z \triangleq b_r^{-1}\Big\{ &e_{m1}\left(-a_1 + a_2\Gamma_0 - a_3\Gamma_0^2 + \Gamma_0^3\right) + k_\lambda e_3 \\
&+ \mathcal{E}_1\left(-a_2 + a_3(\Gamma_0 + \Gamma_1) - \Gamma_0^2 - \Gamma_1(\Gamma_0 + \Gamma_1)\right) \\
&+ \mathcal{E}_2\left(-a_3 + (\Gamma_0 + \Gamma_1 + \Gamma_2)\right) + d_1\left(-a_2\hat{\Delta}_{uf,1} - a_3\hat{\Delta}_{uf,2} - \dot{\hat{\Delta}}_{uf,2}\right) \\
&+ d_2\left(-a_3\hat{\Delta}_{uf,1} - \dot{\hat{\Delta}}_{uf,1}\right) - \Gamma_0^2\tilde{q}_1 + (\Gamma_0 + \Gamma_1)\tilde{q}_2 \Big\}
\end{aligned}$$

and state choices

$$\mathcal{E}_1(t) \triangleq e_{m2}(t) - d_1\hat{\Delta}_{uf,1} + \Gamma_0 e_{m1}(t) \tag{5.20a}$$

$$\mathcal{E}_2(t) \triangleq e_{m3}(t) - d_2\hat{\Delta}_{uf,1} - d_1\hat{\Delta}_{uf,2} - \Gamma_0^2 e_{m1}(t) + (\Gamma_0 + \Gamma_1)\mathcal{E}_1(t), \tag{5.20b}$$

the dynamics for $\zeta(t) \triangleq \begin{bmatrix} e_{m1}(t) & \mathcal{E}_1(t) & \mathcal{E}_2(t) \end{bmatrix}^T$ becomes

$$\begin{aligned}
\dot{e}_{m1}(t) &= -\Gamma_0 e_{m1}(t) + \mathcal{E}_1(t) + \tilde{q}_1 \\
\dot{\mathcal{E}}_1(t) &= -\Gamma_1\mathcal{E}_1(t) + \mathcal{E}_2(t) + \tilde{q}_2 \\
\dot{\mathcal{E}}_2(t) &= -\Gamma_2\mathcal{E}_2(t).
\end{aligned} \tag{5.21}$$

In compact form, Eq 5.21 can be stated as

$$
\begin{bmatrix} \dot{e}_{m1}(t) \\ \dot{\mathcal{E}}_1(t) \\ \dot{\mathcal{E}}_2(t) \end{bmatrix} = \begin{bmatrix} -\Gamma_0 & 1 & 0 \\ 0 & -\Gamma_1 & 1 \\ 0 & 0 & -\Gamma_2 \end{bmatrix} \begin{bmatrix} e_{m1}(t) \\ \mathcal{E}_1(t) \\ \mathcal{E}_2(t) \end{bmatrix} + \begin{bmatrix} d_1 \widetilde{q}_1 \\ d_2 \widetilde{q}_2 \\ 0 \end{bmatrix},
$$

where the bounded errors $\widetilde{q}_1$ and $\widetilde{q}_2$ are

$$
\widetilde{q}_1 \triangleq - d_1 \left(\hat{\Delta}_u - \hat{\Delta}_{uf,1} \right) + k_\lambda e_1(t)
$$

$$
\widetilde{q}_2 \triangleq k_\lambda e_2(t) + \Gamma_0 \widetilde{q}_1 - d_2 \left(\hat{\Delta}_u - \hat{\Delta}_{uf,1} \right) - d_1 \left(\dot{\hat{\Delta}}_{uf,1} - \hat{\Delta}_{uf,2} \right).
$$

Remark 5.7. *With suitable design parameters Γ_0, Γ_1 and Γ_2, boundedness of state $\zeta(t)$ is guaranteed since perturbations $\widetilde{q}_1$ and $\widetilde{q}_2$ are bounded [101].*

Remark 5.8. *From Remark 5.7, $e_{m1}(t)$ is bounded. Boundedness of the signals $\mathcal{E}_1(t)$, $\hat{\Delta}_{uf,1}$, and $e_{m1}(t)$ guarantees the boundedness of the signal $e_{m2}(t)$ from Eq 5.20a. Furthermore, with the bounded signals $\mathcal{E}_2(t)$, $\hat{\Delta}_{uf,1}$, $\hat{\Delta}_{uf,2}$, $e_{m1}(t)$, and $\mathcal{E}_1(t)$, the signal $e_{m3}(t)$ is bounded from Eq 5.20b. Hence, boundedness of the auxiliary tracking error $e_m(t) = x_{rm}(t) - x_m(t)$ is established. Since $x_{rm}(t)$ is bounded, auxiliary states $x_m(t)$ are also bounded. From Theorem 1, the tracking error $e(t) = x_m(t) - x(t)$ is bounded. All in all, the system states $x(t)$ become bounded with bounded $x_m(t)$.*

5.6 Numerical Examples

5.6.1 A Second-Order System

Consider the uncertain nonlinear dynamical system

$$
\dot{x}(t) = \begin{bmatrix} 0 & 1 \\ 2 & 4 \end{bmatrix} x(t) + \begin{bmatrix} 0 \\ 1 \end{bmatrix} [u(t) + \Delta(x)] + \begin{bmatrix} 1 \\ 0 \end{bmatrix} \Delta_u(x) \tag{5.22}
$$

$$
y(t) = x_1(t),
$$

where the system uncertainties are characterized by

$$\Delta(x) = W^T \phi(x)$$

$$W = \begin{bmatrix} -1.23 & 0.78 & -0.62 & 1.02 \end{bmatrix}^T$$

$$\phi(x) = \begin{bmatrix} 1 & |x_1|x_2 & |x_2|x_2 & x_1^3 \end{bmatrix}^T$$

$$\Delta_u(x) = -0.65x_1^2 + 0.8sin(x_2) + 0.3x_1.$$

Ideal reference model that characterizes the desired closed-loop behavior with the natural frequency of $\omega_n = 2$ and damping ratio of $\xi = 1.4$ is designed as

$$\dot{x}_r(t) = \begin{bmatrix} 0 & 1 \\ -\omega_n^2 & -2\xi\omega_n \end{bmatrix} x_r(t) + \begin{bmatrix} 0 \\ \omega_n^2 \end{bmatrix} r(t)$$

$$y_r(t) = x_{r_1}(t).$$

Numerical simulation parameters are as follows. Adaptive learning rates are $\Gamma = \Gamma_u = 1$ and $\gamma_m = \gamma_1 = \gamma_2 = \mu_1 = 1$, low-pass filter gain is $\Gamma_f = 10$, command governor parameters are $\Gamma_0 = \Gamma_1 = 10$, and simulation sampling frequency is set to 100 Hz. Square reference command is passed through first order low-pass filter with the filter gain of 1. All the system states, ideal and modified reference model states, matched and unmatched weight estimations are initialized from zero.

Without command governor design, the system is unstable. This result emphasizes the significance of command governor signal. Thus, the effects of matched and unmatched weight estimations on the reference command following performance are investigated.

Nominal controller in Eq 5.5 exhibits an unstable behavior for the uncertain system as shown in Figure 5.2.

Figure 5.3 indicates the unstable response with standard MRAC in Eq 2.10. Hence, it is clear from the figure that the unmatched uncertainty should be handled properly to ensure the closed loop stability.

In order to suppress the effects of the unmatched uncertainty upon the system behavior, the proposed command governor-based method is employed. The unknown unmatched uncertainty $\Delta_u(x)$ is approximated by RBF NN. The centers $\bar{c}_i$ for RBF
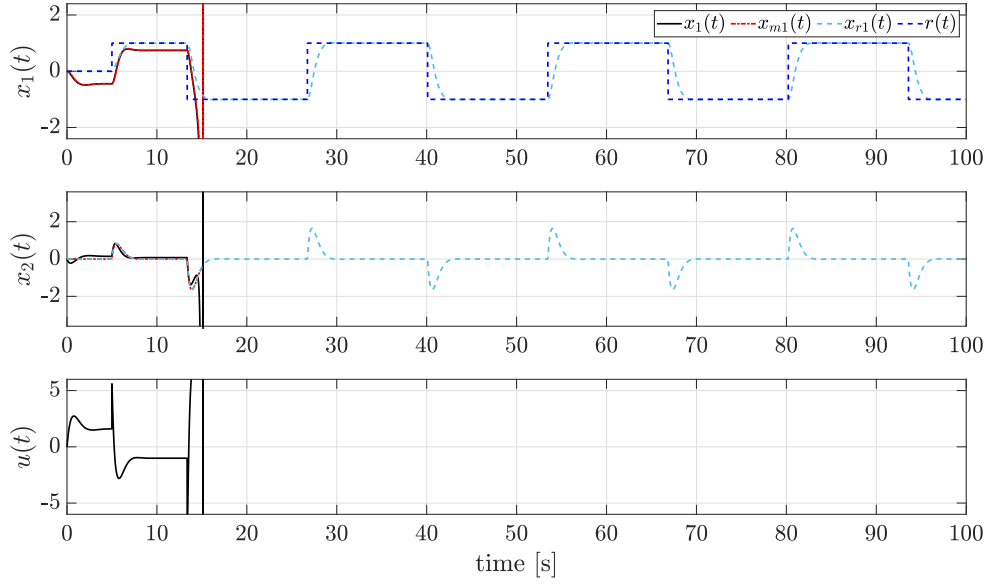
83

Figure 5.2: Unstable Closed-loop Response with the Nominal Controller in Eq 5.5
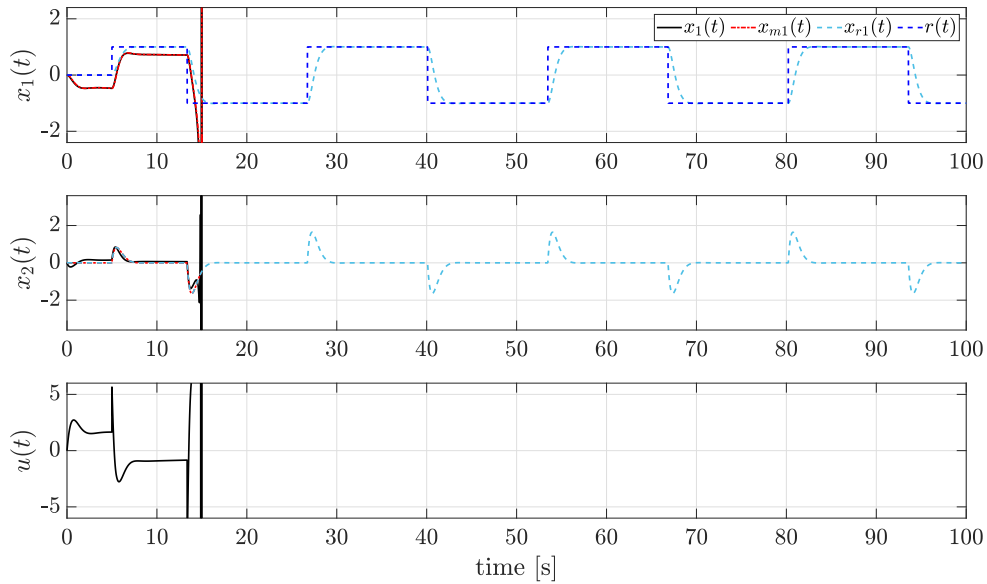

Figure 5.3: Unstable Closed-loop Response with Standard MRAC with Eq 2.10

are uniformly distributed over the space of $[-4, 4] \times [-4, 4]$, and width of the kernel unit is uniformly set to $\bar{\mu}_i = 0.5$, $i = 2, \ldots, s_u = 24$. Figure 5.4 illustrates the distribution with a 1D example. The first element $\psi_1(x)$ is reserved for the bias unit; i.e. $\psi_1(x) = 1$. Lastly, auxiliary reference model in Eq 5.4 is designed with $k_\lambda = 15$.

In Figure 5.5, reference command following performance is illustrated for the
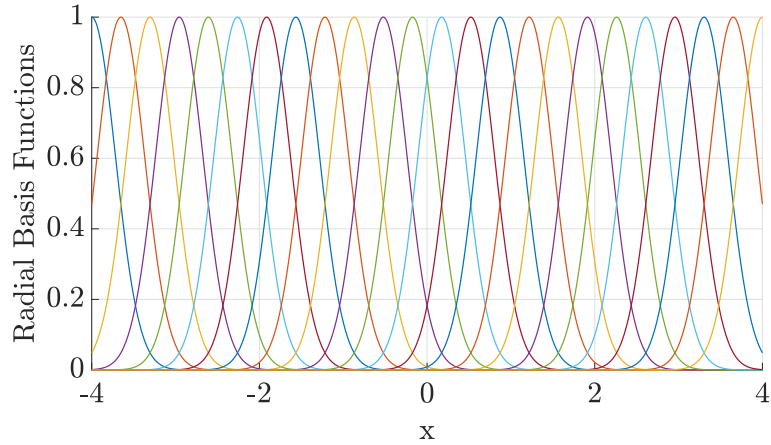
Figure 5.4: Visualization of Radial Basis Functions with $\bar{\mu} = 0.5$

proposed command governor-based adaptive control architecture. As it can be seen, the user-defined subset of accessible states $y(t) = x_1(t)$ can satisfactorily follow the reference signal $y_r(t) = x_{r_1}(t)$.
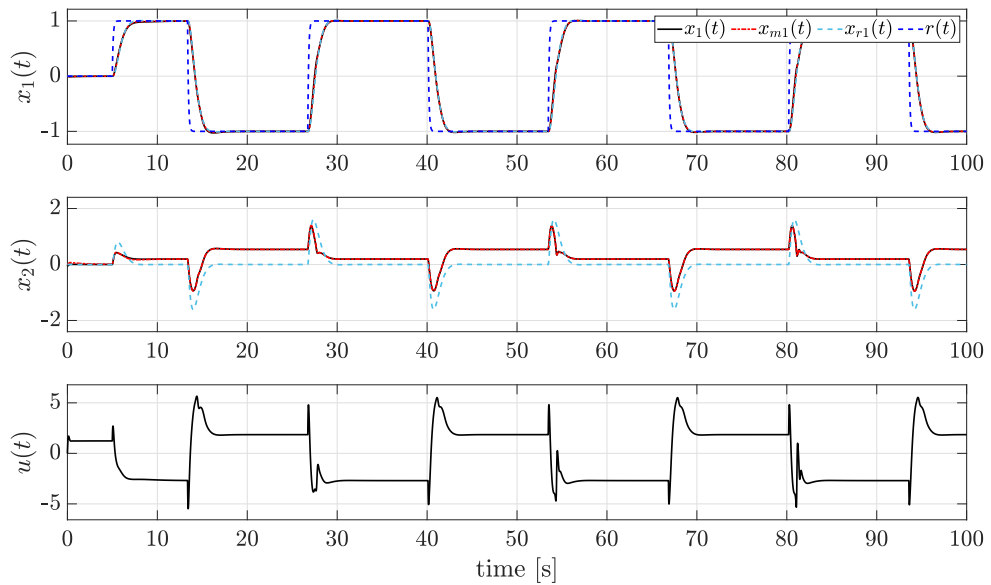
Figure 5.5: Tracking performance and control input $u(t)$ with the Proposed Command Governor-Based Adaptive Controller

The auxiliary tracking error $e_m(t)$ and tracking error $e(t)$ are given in Figure 5.6. The tracking error $e(t)$ stays in the close neighborhood of zero with the matched parameter identification and unmatched parameter approximation. Furthermore, reference command following error $e_{m1}(t)$ is in close neighborhood of zero. Hence,

85

reference command following is achieved satisfactorily; i.e. $y(t) \to N_\delta(y_r(t))$.
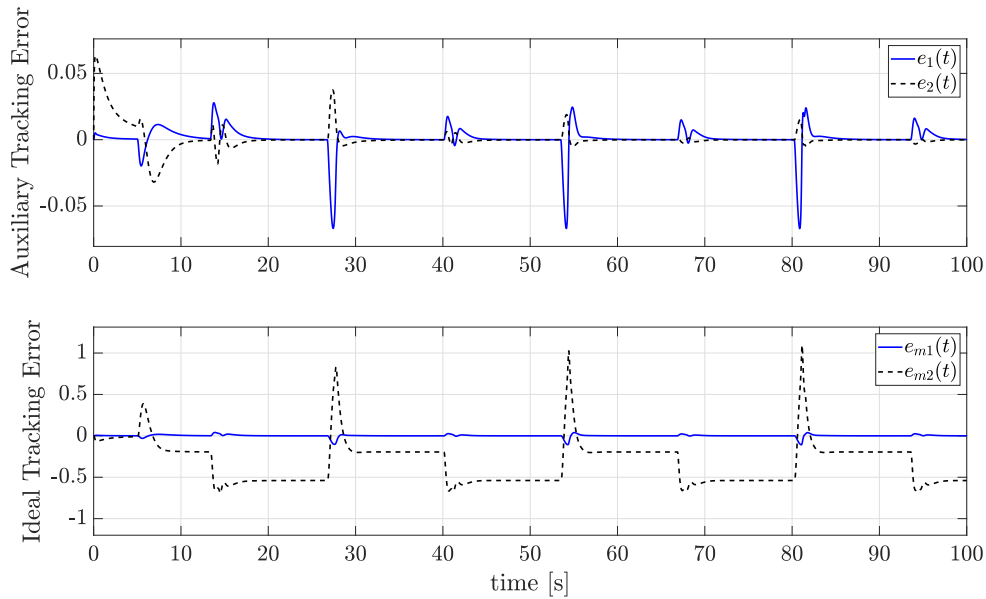

Figure 5.6: Tracking error $e(t)$ and auxiliary tracking error $e_m(t)$ with the Proposed Command Governor-Based Adaptive Controller

The evolution of the adaptive matched weights is given in Figure 5.7. Dashed lines indicate the ideal unknown matched parameters whereas the solid lines are the corresponding estimations. Figure 5.7 clearly illustrates that the estimated weights are closely bounded around their ideal values. From Theorem 5.1, this bound can be made arbitrarily small by decreasing the RBF residual bound ε_0, which can be achieved by increasing the size of basis function ψ.

Figure 5.8 illustrates the evolution of the unmatched weights. Since the unmatched uncertainty is parametrized by RBF, ideal weights are not known. Hence, only the adaptive weight evolution is shown in the figure. As seen, there is no high-frequency oscillation in the estimations while achieving the satisfactory uncertainty estimation as seen in Figure 5.9. With (almost) convergence in matched weights, matched uncertainty is identified and estimations overlap with the actual uncertainty.
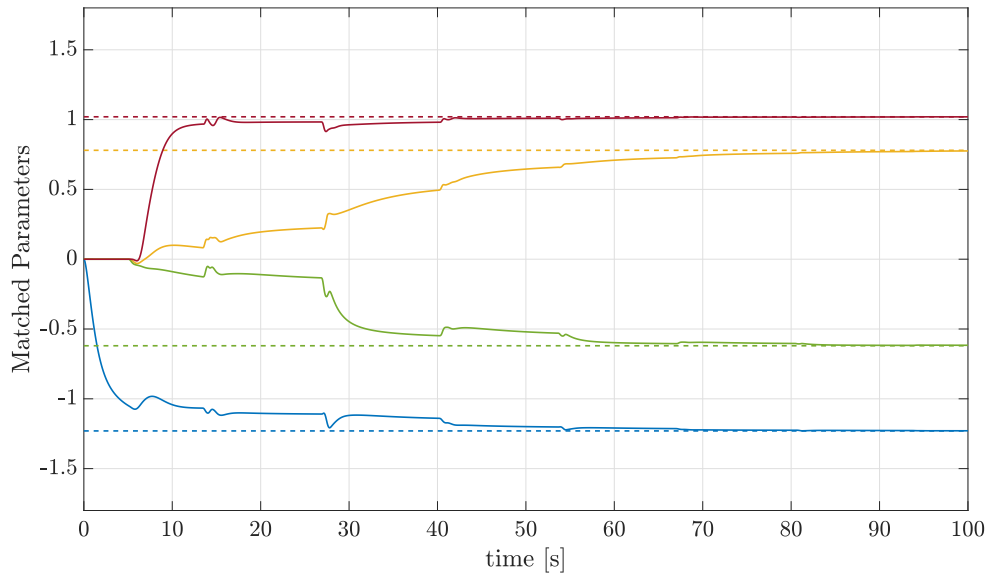
86
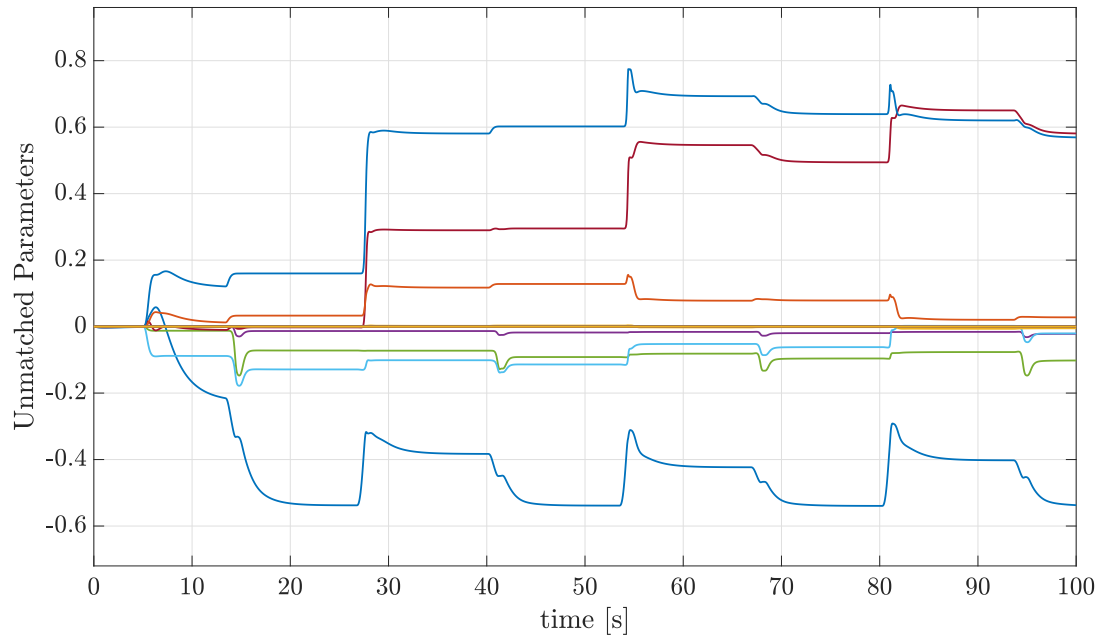
Figure 5.7: Adaptive matched weight evolution

Figure 5.8: Adaptive unmatched weight evolution
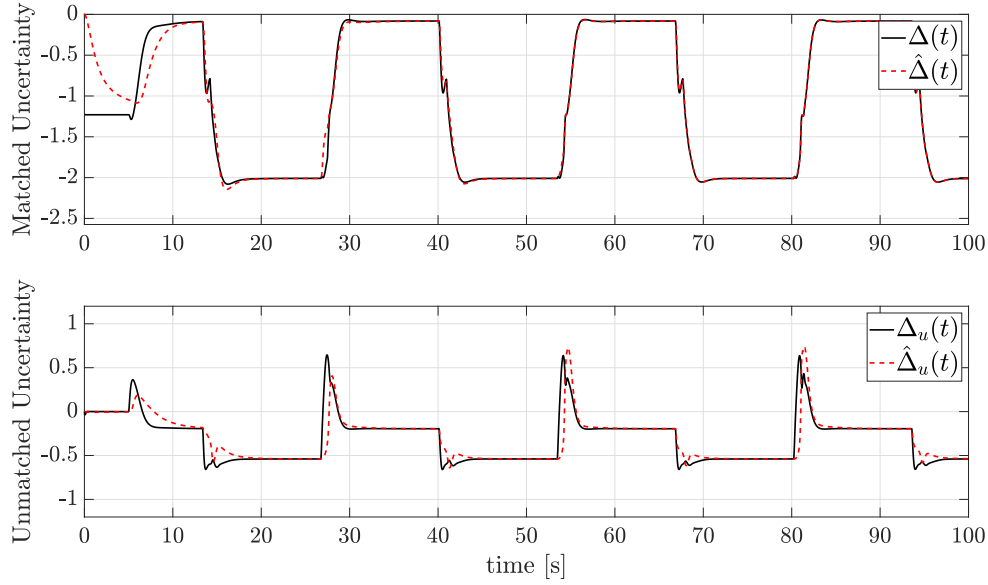
Figure 5.9: Adaptation performance for both matched and unmatched uncertainties

5.6.2 A Third-Order System Case

Consider the uncertain dynamical system given by

$$\dot{x}(t) = \begin{bmatrix} 0 & 1 & 0 \\ 0 & 0 & 1 \\ 2 & 1 & 1 \end{bmatrix} x(t) + \begin{bmatrix} 0 \\ 0 \\ 1 \end{bmatrix} [u(t) + \Delta(x)] + \begin{bmatrix} 1 \\ 0 \\ 0 \end{bmatrix} \Delta_u(x)$$

$$y(t) = x_1(t).$$

where the system uncertainties are characterized by

$$W = \begin{bmatrix} -1.2 & 0.8 & -0.6 & 1.0 & 0.4 \end{bmatrix}^T$$

$$\phi(x) = \begin{bmatrix} 1 & x_1 x_2 & x_2^2 & x_1^3 & x_2 x_3^2 \end{bmatrix}^T$$

$$\Delta_u(x) = -0.26x_1^2 - 0.32x_2 x_3 - 0.12x_1 x_3^2$$

Nominal controller gains are chosen to be $K_x = \begin{bmatrix} 12.2 & 16.2 & 7.6 \end{bmatrix}$ and $K_r = 10.2$, where the reference model matrices are $A_r = A - BK_x$, $B_r = BK_r$. Closed-loop reference model gain is chosen to be $k_\lambda = 25$.

Simulation parameters are as follows. Adaptive controller gains are $\Gamma = \Gamma_u = 1$, $\Gamma_0 = 2$, $\Gamma_1 = 5$, $\Gamma_2 = 10$, $\gamma_2 = \gamma_m = \mu_m = 0.1$, $\gamma_1 = \mu_1 = 1$. Furthermore, low-pass filter cut-off frequencies are $\omega_f = 4$, $\Gamma_f = 10$. Simulation sampling frequency is set

to $100\ Hz$. All the system states, ideal and modified reference model states, matched and unmatched weight estimations are initialized from zero. Centers $\bar{c}_i$ are uniformly distributed over $x_1 - x_2 - x_3$ space of $[-5,5] \times [-5,5] \times [-5,5]$, and width of kernel unit is uniformly set as $\bar{\mu}_i = 0.3$, $i = 1, \ldots, s_u = 38$. 1D visualization of the selected RBF structure is given in Figure 5.10. Bias unit is $\psi_1(x) = 1$.
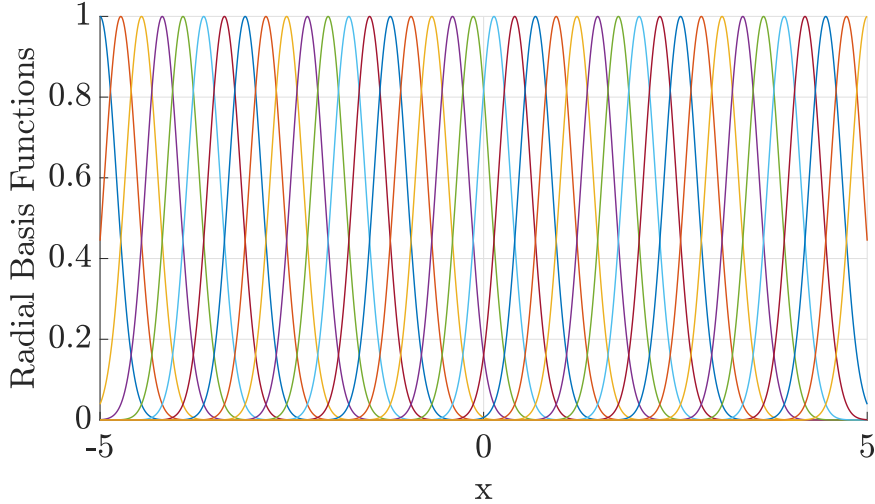

Figure 5.10: Visualization of Radial Basis Functions with $\bar{\mu} = 0.3$
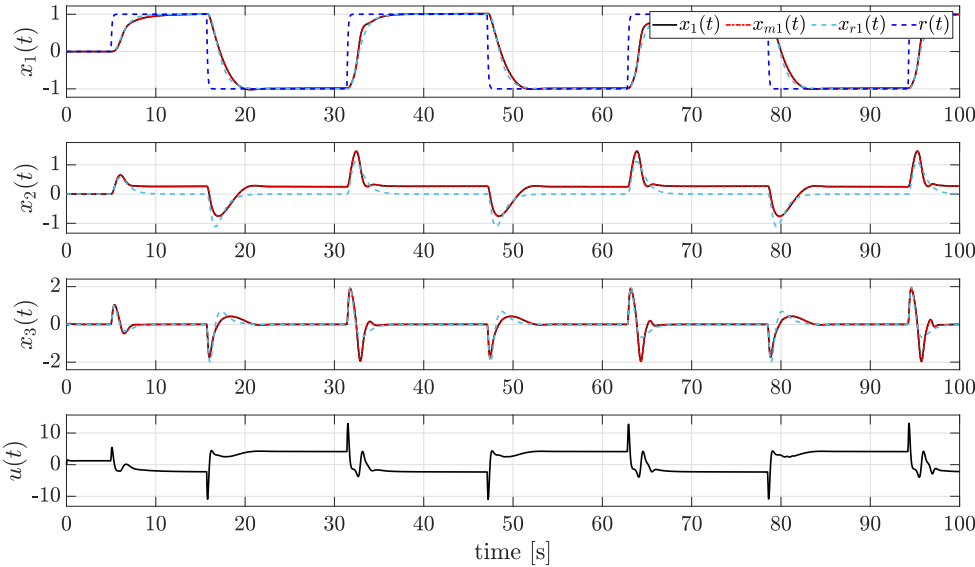

Figure 5.11: Tracking performance and control input $u(t)$.

Without command governor, the closed-loop system is unstable as in the 2nd order example. Thus, the simulation results are only given for the command governor

89

employed cases. In Figure 5.11, the tracking performance is illustrated. The selected system state $y(t) = x_1(t)$ can satisfactorily follow the desired one $y_r(t) = x_{r1}(t)$. The corresponding tracking errors are in Figure 5.12.
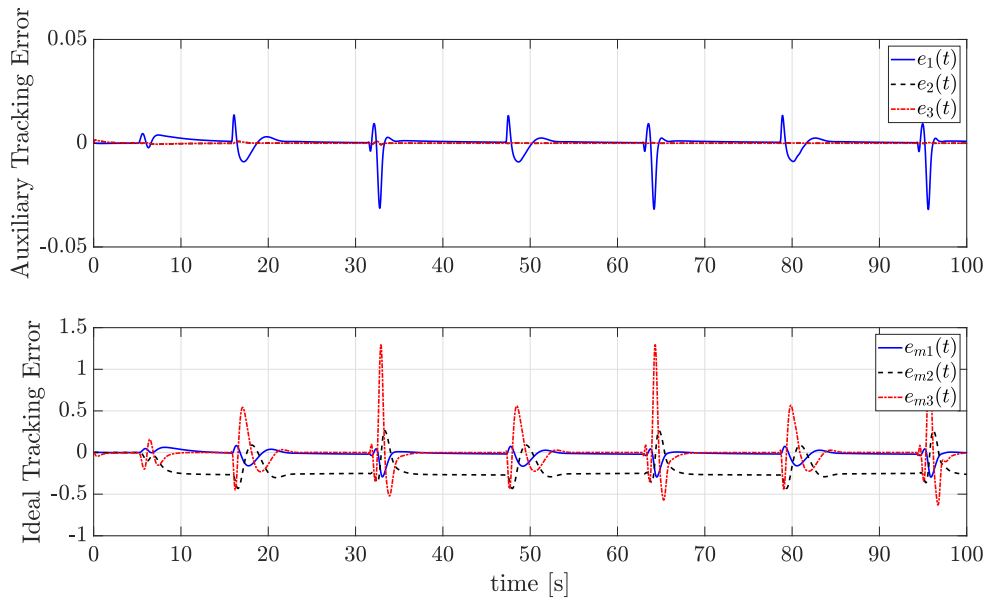
Figure 5.12: Tracking error $e(t)$ and auxiliary tracking error $e_m(t)$.

The evolution of the adaptive matched weights is given in Figure 5.13. Dashed lines indicate the ideal unknown matched parameters whereas the solid lines are the corresponding estimations. Figure 5.13 clearly illustrates that the estimated weights are closely bounded around their ideal values. From Theorem 5.1, this bound can be made arbitrarily small by decreasing the RBF residual bound ε_0, which can be achieved by increasing the size of basis function ψ. With (almost) convergence in matched weights, matched uncertainty is identified and estimations overlap with the actual uncertainty. This result can be seen in Figure 5.15.

Figure 5.14 illustrates the evolution of the unmatched weights. Since the unmatched uncertainty is parametrized by RBF, ideal weights are not known. Hence, only the adaptive weight evolution is shown in the figure. As seen, there is no high-frequency oscillation in the estimations while achieving the satisfactory uncertainty estimation as seen in Figure 5.15.
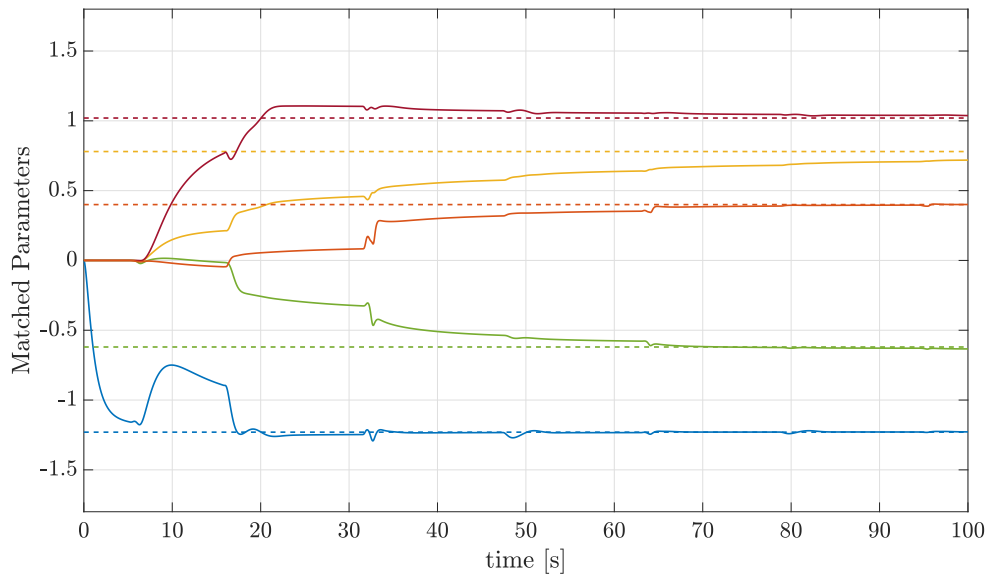
Figure 5.13: Adaptive matched weight evolution.
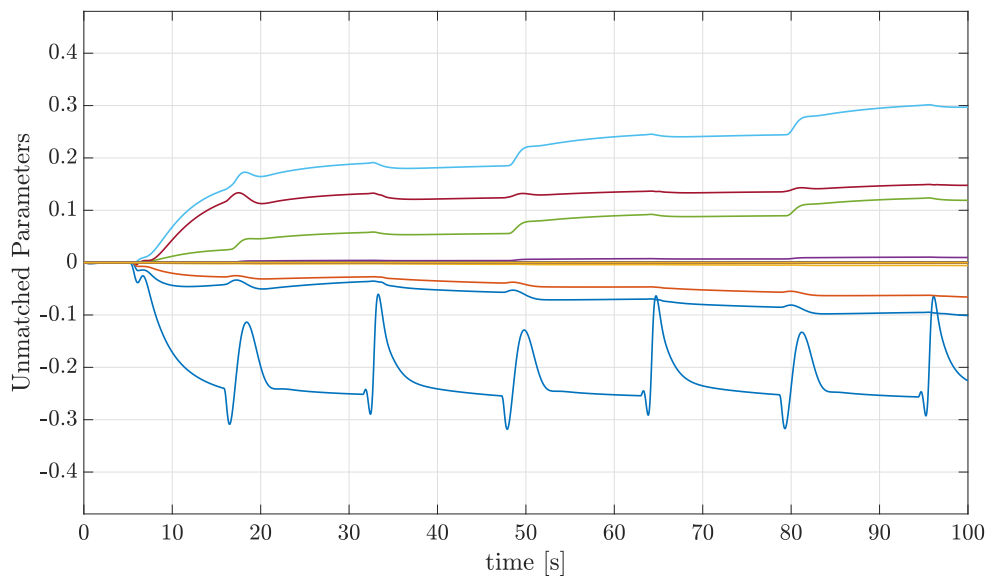
Figure 5.14: Adaptive unmatched weight evolution.
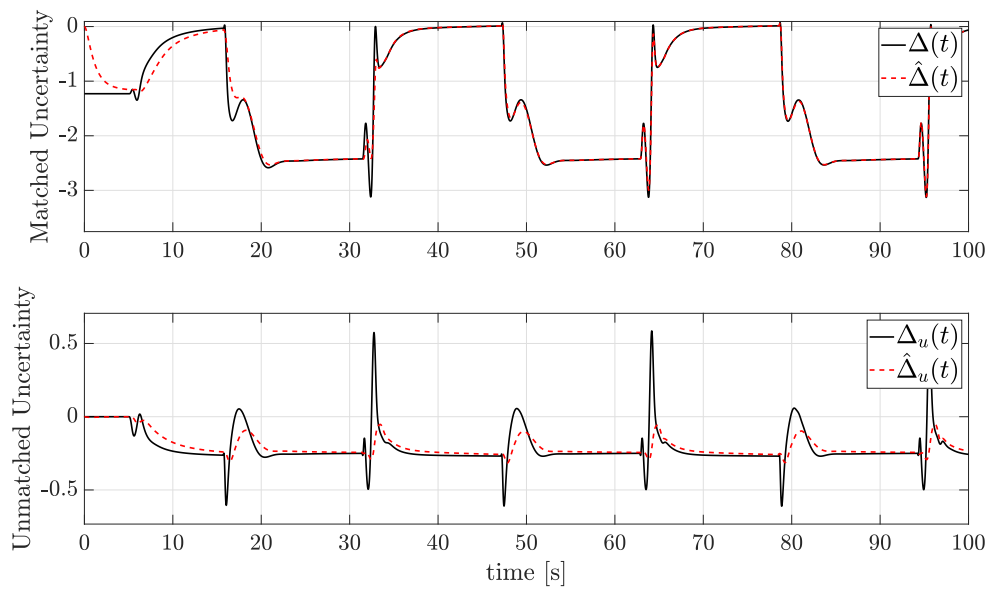
Figure 5.15: Adaptation performance for both matched and unmatched uncertainties.

CHAPTER 6

ENERGY-BASED ADAPTIVE FLIGHT CONTROLLER FOR IMPROVED COORDINATED LONGITUDINAL CONTROL

6.1 Introduction

In this chapter, an adaptive energy-based longitudinal flight control framework is proposed. Uncertainties on the Lagrangian channel is eliminated with an adaptive element in the pitch stability augmentation system, in which the fast system states are regulated. Thus, uncertainties in the energy distribution channel is successfully removed, and short period mode characteristics are improved. For the coordination between Hamiltonian and Lagrangian controls, an adaptive outer energy management loop is designed. Remaining uncertainties on the energy sources and/or energy draining components are addressed in this controller. Furthermore, bandwidth of both Lagrangian and Hamiltonian control loops are determined with a reference model. As a result, proper suppression of uncertainties immediately results in the desired decoupled airspeed and altitude responses. Block diagram of the proposed control architecture is given in Figure 6.1.
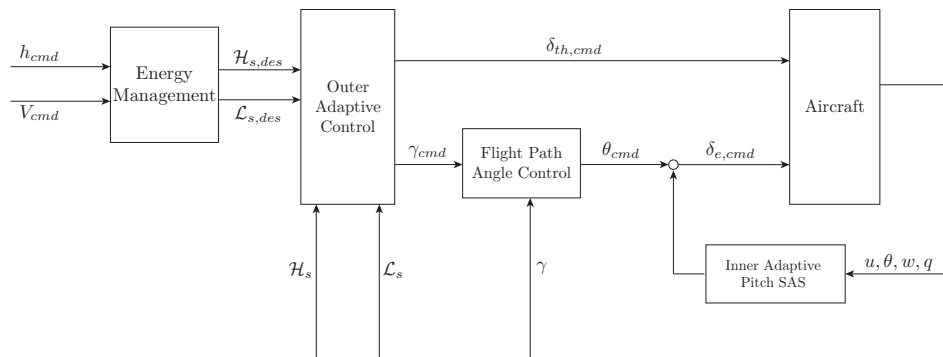
Figure 6.1: Block Diagram of the Proposed Longitudinal Flight Control Algorithm

6.2 System Description

Nonlinear equations of motion for the longitudinal dynamics of an aircraft written in its body frame are given by:

$$\dot{h} = V_\infty \sin(\gamma) = u \sin(\theta) - w \cos(\theta)$$

$$\dot{u} = \frac{1}{m} \left[T - D \cos(\alpha) + L \sin(\alpha) - W \sin(\theta) \right] - qw$$

$$\dot{\theta} = q \qquad\qquad (6.1)$$

$$\dot{w} = \frac{1}{m} \left[-D \sin(\alpha) - L \cos(\alpha) + W \cos(\theta) \right] + qu$$

$$\dot{q} = \frac{1}{I_{xx}} \left[M_{ctrl} + M_{pitch} \right]$$

where L is the lift force, D is the drag force, T is the thrust, M_{ctrl} is the pitching moment generated by the deflected elevator, M_{pitch} is the pitching moment when no control surfaces are deflected. These forces and moments are explicitly given as:

$$L = q_\infty S_{ref} C_L$$

$$D = q_\infty S_{ref} C_D$$

$$M_{ctrl} = q_\infty S_{ref} C_{m_{\delta_e}} \delta_e \bar{c}$$

$$M_{pitch} = q_\infty S_{ref} C_m \bar{c}$$

where q_∞ is the dynamic pressure, S_{ref} is the reference wing area, C_L, C_D, and C_m are lift, drag, and pitching moment coefficients (resp.), $C_{m_{\delta_e}}$ is the non-dimensional control derivative, δ_e is the elevator deflection, and $\bar{c}$ is the mean aerodynamic chord. Wind frame states such as angle of attack α, flight path angle γ, and airspeed V_∞ are given in terms of body frame states as follows:

$$\alpha = \operatorname{atan}_2(w, u), \qquad \gamma = \theta - \alpha, \qquad V_\infty = \sqrt{u^2 + w^2}$$

The objective is to design an energy-based flight control algorithm to enhance the coordination between the elevator and thrust controls so that the velocity and altitude responses are satisfactorily decoupled and desired command following performance is reached. First, an inner stability augmentation system (SAS) is designed to improve the short period mode characteristics. Next, flight path angle control loop is augmented. Finally, an energy-based velocity and altitude controllers close the loops.

94

6.3 Controller Design

6.3.1 Short Period Stability Augmentation

In the longitudinal dynamics of an aircraft, there are typically two oscillatory modes which are separated in terms of time scale by an order. The slow one is called the Phugoid mode whereas the faster one is the Short period. During the Phugoid oscillations, it is commonly assumed the angle of attack (α) of the aircraft remains constant while the pitch attitude (θ) and airspeed (V_∞) are changing. Since the oscillatory motion is slow, body pitch rate q stays considerably small. On the other hand, short period oscillations result in large body pitch rate q which needs to be damped by an external stability augmentation system (SAS), namely pitch SAS. In the 2nd order approximation of the short period mode, the states can be chosen as body pitch rate and angle of attack. One may also add the pitch attitude to short period mode approximation to improve the quality of the pitch SAS [42]. In this thesis, a 3rd order approximated system is picked with the states $x_{sp} = \begin{bmatrix} \alpha & \theta & q \end{bmatrix}^T$, and outputs $y_{sp} = \begin{bmatrix} \theta & q \end{bmatrix}^T$:

$$\dot{x}_{sp} = A_{sp} x_{sp} + B_{sp} \delta_e$$
$$y_{sp} = C_{sp} x_{sp}$$

where the system matrix A_{sp}, input matrix B_{sp}, and output matrix C_{sp} are known matrices for approximated short period dynamical system with their appropriate dimensions. Note that for the given inputs, states, and outputs, the matrices B_{sp}, C_{sp}, and $C_{sp}B_{sp}$ are full rank matrices.

6.3.1.1 Nominal Controller Design

In the inner loop control, main concern is to achieve a desired damping and adequate natural frequency in the pitch motion of the aircraft which is expressed by the following dynamics:

$$\ddot{\theta}_d + 2\zeta_{sp,d}\omega_{sp,d}\dot{\theta}_d + \omega_{sp,d}^2\theta_d = \omega_{sp,d}^2\theta_{cmd} \tag{6.2}$$

In order to damp the short period mode oscillations effectively, it is important to select the desired natural frequency $\omega_{sp,d}$ to be larger than the natural frequency of the short

period mode. Then, the desired pitch dynamics is used to construct the reference model with its specific structure:

$$\dot{x}_{sp,d} = A_{sp,d}x_{sp,d} + B_{sp,d}\theta_{cmd}$$

$$y_{sp,d} = C_{sp,d}x_{sp,d}$$

$$A_{sp,d} = \begin{bmatrix} \cdot & \cdot & \cdot \\ 0 & 0 & 1 \\ 0 & -\omega_{sp,d}^2 & -2\zeta_{sp,d}\omega_{sp,d} \end{bmatrix}, \qquad B_d = \begin{bmatrix} \cdot \\ 0 \\ \omega_{sp,d}^2 \end{bmatrix} \qquad (6.3)$$

where $A_{sp,d}$ is a Hurwitz matrix, $y_{sp,d} = \begin{bmatrix} \dot{\theta}_d & \dot{q}_d \end{bmatrix}^T$ is the reference output, and unspecified entries in $A_{sp,d}$ and $B_{sp,d}$ are chosen to satisfy the following matching conditions:

$$A_{sp,d} = A_{sp} - B_{sp}K_{sp}, \qquad B_{sp,d} = B_{sp}k_r$$

Then, inner loop nominal elevator control is design through dynamic inversion of the short period dynamics:

$$\dot{y}_{sp} = C_{sp}\dot{x}_{sp} = C_{sp}\left[A_{sp}x_{sp} + B_{sp}\delta_e\right] = C_{sp}A_{sp}x_{sp} + C_{sp}B_{sp}\delta_e = \dot{y}_d$$

where $\dot{y}_d$ is generated according to the desired pitch dynamics in Eq 6.2. Solving for the elevator input results in nominal control:

$$\delta_{e,n} = \left(C_{sp}B_{sp}\right)^\dagger \left[\dot{y}_d - C_{sp}A_{sp}x_{sp}\right] \qquad (6.4)$$

with $(\cdot)^\dagger$ denoting the pseudo-inverse of its inner argument. The matrix $\left(C_{sp}B_{sp}\right)^T \left(C_{sp}B_{sp}\right)$ is nonsingular and $\left(C_{sp}B_{sp}\right)$ has a unique pseudo-inverse matrix. Note that with the designed elevator control in Eq 6.4, the unspecified entries in the reference model (Eq 6.3) are immediately determined.

6.3.1.2   Inner Loop Adaptive Controller Design

So far, the perfect knowledge of the system is assumed which results in the nominal control in Eq 6.4. Now, the system uncertainties and nonlinearities are introduced as follows:

$$\dot{x} = Ax + B\left[u + \Delta(x)\right]$$

where the system state is $x = \begin{bmatrix} u & w & \theta & q \end{bmatrix}^T$, $u = \begin{bmatrix} \delta_{th} & \delta_e \end{bmatrix}^T$ is the vector of control inputs, A and B are known matrices of appropriate dimensions, $B = \begin{bmatrix} B_1 & B_2 \end{bmatrix}$ with B_i's have full column rank for $i = 1, 2$, and $\Delta(x)$ is the Lipschitz continuous functions representing the unknown matched uncertainties. In the adaptive controller design, the altitude is excluded from the system states as the heave mode of the aircraft is negligibly slow compared to Phugoid and short period modes.

Assumption 6.1. *The uncertainty $\Delta(x)$ can be expressed as linear combination of known basis functions:*

$$\Delta(x) = \mathbb{W}^T \Phi(x)$$

where $\mathbb{W} \in \mathbb{R}^{s \times 2}$ is unknown constant weight matrix, and $\Phi(x) \in \mathbb{R}^{s \times 1}$ is known basis vector function.

Remark 6.1. *Many nonlinear matched uncertainties can be parametrized as in Assumption 6.1 (e.g. nonlinear wing-rock dynamics [102]). However, for the case where the basis vector-function $\phi(x)$ is unknown, the matched uncertainty parametrization in Assumption 6.1 could be relaxed by considering $\Delta(x) = W_{nn}^T \phi_{nn}(x) + \varepsilon_{nn}(x), \quad \forall x(t) \in \mathcal{D}_x$ with $\mathcal{D}_x$ being sufficiently large compact set. Thus, the proposed algorithm can be readily extended for unstructured uncertainties.*

Since the engine actuators are considerably slow compared to pitch dynamics, the elevator input is going to be used to adapt all the system uncertainties as long as they are reachable by the elevator control. So, the control inputs are separated as follows:

$$\dot{x} = Ax + B_1 \big[\delta_{th} + \delta_1(x) \big] + B_2 \big[\delta_e + \delta_2(x) \big]$$

Some part of the uncertainty in the throttle channel $\delta_1(x)$ can be suppressed directly by the elevator as the same uncertainty may lie in the range space of B_2. Further decomposition of the uncertainty $\delta_1(x)$ yields

$$B_1 \delta_1(x) = B_2 \delta_{12}(x) + B_2^{\perp} \delta_{11}(x) \tag{6.5}$$

where $B_2^{\perp} = B_{2u}$ is the orthogonal complement of the elevator input matrix B_2; i.e. $B_2^T B_{2u} = 0$. Note that there may exists an uncertainty $\delta_{12}(x)$ where the source is the throttle, but the effect can directly be suppressed by the elevator. An example could be the misalignment of the vertical position of the engine and center of gravity of the

aircraft. In such a case, the thrust will cause a pitch up/down motion which can be directly controlled with the elevator control. Then, the uncertainty decomposition in Eq 6.5 is substituted into system dynamics as follows:

$$\dot{x} = Ax + B_1 \delta_{th} + B_2 \big[\delta_e + \delta_2(x) + \delta_{12}(x) \big] + B_{2u} \delta_{11}(x)$$

Next, the elevator control is designed with nominal control $\delta_{e,n}$ in Eq 6.4 and an adaptive part v_{ad}:

$$\delta_e = \delta_{e,n} + v_{ad}$$

Applying the elevator control the system yields

$$\dot{x} = A_m x + B_1 \delta_{th} + B_{2,m} \theta_{cmd} + B_2 \big[v_{ad} + \Delta_2(x) \big] + B_{2u} \Delta_1(x)$$
$$= A_m x + B_m r + B_2 \big[v_{ad} + \Delta_2(x) \big] + B_{2u} \Delta_1(x) \tag{6.6}$$

where the reference command is $r = \begin{bmatrix} \delta_{th} & \theta_{cmd} \end{bmatrix}^T$, and the uncertainties are $\Delta_2(x) \triangleq \delta_2(x) + \delta_{12}(x)$ and $\Delta_1(x) \triangleq \delta_{11}(x)$. From now on, the uncertainties $\Delta_1(x)$ and $\Delta_2(x)$ are called as unmatched and matched uncertainties with respect to elevator control, respectively. This is because the uncertainty $\Delta_1(x)$ lies in the null space of B_2^T which means it cannot be suppressed directly via elevator control. Due to Assumption 6.1, the uncertainties $\Delta_1(x)$ and $\Delta_2(x)$ can be expressed by

$$\Delta_1(x) = W_u^T \psi(x)$$
$$\Delta_2(x) = W^T \phi(x)$$

where $W \in \mathbb{R}^{s_2 \times 1}$ and $W_u \in \mathbb{R}^{s_1 \times 1}$ represents the constant weight matrices for matched and unmatched uncertainties, respectively. Next, consider the following reference model that characterizes the desired closed-loop performance:

$$\dot{x}_m = A_m x_m + B_m r \tag{6.7}$$

where the Hurwitz system matrix A_m and input B_m satisfy the following relations:

$$A_m = A - B_2 K_x^*$$
$$B_m = B_2 K_r^*$$

for some unknown matrices K_x^* and K_r^*. Note that this relations is well-known matching condition in model reference adaptive control literature [74]. In the inner

loop stability augmentation control, the objective is to design an inner loop adaptive controller so that the desired command following performance of the pitch response of the uncertain system is achieved. That is, a subset of the system states $y = Cx = \theta$ is desired to track the subset of the reference model states $y_m = Cx_m = \theta_d$ in the presence of uncertainties.

The adaptive input v_{ad} is designed to suppress the undesired effects of matched uncertainty $\Delta_2(x)$ as follows:

$$v_{ad}(t) = -\hat{W}^T(t)\phi(x) \tag{6.8}$$

where $\hat{W}(t)$ is the online estimation of unknown matched parameters W. The tracking error $e(t)$, weight estimation errors $\tilde{W}(t)$ and $\tilde{W}_u(t)$, and an auxiliary error $e_2(t)$ are defined as follows:

$$e \triangleq x_m - x$$
$$\tilde{W} \triangleq W - \hat{W}$$
$$\tilde{W}_u \triangleq W_u - \hat{W}_u$$
$$e_2 \triangleq B_2^T e$$

Then, the tracking error dynamics can be expressed using Eq 6.6 - 6.8 as:

$$\dot{e}(t) = A_m e(t) - B_2 \tilde{W}^T(t)\phi(x) - B_{2u}\Delta_1(x)$$

Multiplying from the left by B_2^T yields the auxiliary error dynamics

$$B_2^T \dot{e}(t) = B_2^T A_m e(t) - B_2^T B_2 \tilde{W}^T(t)\phi(x) \tag{6.9}$$

Now, consider the following Lyapunov candidate:

$$\mathcal{V}(t) = \frac{1}{2}e_2^T P_2 e_2 + \frac{1}{2}tr\left(\tilde{W}^T \Gamma^{-1}\tilde{W}\right) \tag{6.10}$$

where $P_2 = P_2^T \succ 0$ is a positive definite constant matrix of appropriate dimensions. In addition, consider the following Lyapunov equation:

$$A_m^T P + P A_m = -Q \tag{6.11}$$

with $P = P^T \succ 0$ being the unique solution for any $Q = Q^T \succ 0$. Positive definite matrix P_2 in Eq 6.10 is chosen to satisfy the following:

$$B_2 P_2 B_2^T = P \tag{6.12}$$

Note that B_2 has full column rank. Hence, the unique P_2 can be obtained using left pseudo inverse of B_2 and right pseudo-inverse of B_2^T using Eq 6.11 and Eq 6.12. Time derivative of Lyapunov candidate in Eq 6.10 becomes:

$$\dot{\mathcal{V}}(t) = e^T P A_m e - e^T P B_2 \tilde{W}^T \phi(x) - tr\big(\tilde{W}^T \Gamma^{-1} \dot{\tilde{W}}\big) \qquad (6.13)$$

Choosing the adaptive weight update law as

$$\dot{\hat{W}} = -\Gamma \phi(x) e^T P B_2$$

result in the following inequality:

$$\dot{\mathcal{V}}(t) \leq -\frac{1}{2}\lambda_{min}(Q)\|e\|^2 \preceq 0$$

Remark 6.2. *With positive definitive Lyapunov function having a negative semi-definite time derivative, asymptotic stability of the auxiliary error is ensured, i.e. $e_2 \to 0$ as $t \to \infty$. However, boundedness of the adaptive parameters is not guaranteed, yet. In order to bound the matched adaptive parameters, a robust modification can be applied from the literature such as σ-modification [3], e-modification [4], projection operator [5, 80], and optimal control based modification [6]. Well-known optimal control modification is chosen as it allows to use high adaptation gains without causing high-frequency oscillations. Hence, the adaptive weight update law becomes*

$$\dot{\hat{W}} = -\Gamma \phi(x) \big[e^T P - \nu \phi^T \hat{W} B_2^T P A_m^{-1}\big] B_2$$

where the optimal control modification term adds a damping to the update law, and $\nu > 0$ is a tuning parameter.

6.3.2 Outer Loop Control

As shown in the block diagram in Figure 6.1, reference altitude and velocity commands are converted to flight path angle and throttle commands using the energy principles. In this control loop, the objective is to design a control augmentation system to track the desired flight path angle using the transfer function $\frac{\gamma(s)}{\gamma_{cmd}(s)}$. For this purpose, PI-controller is designed as follows:

$$\theta_{cmd} = \left(K_p + \frac{K_i}{s}\right)\tilde{\gamma}, \qquad \tilde{\gamma} \triangleq \gamma_{cmd} - \gamma.$$

With the proposed outer control loop for flight path tracking, a zero is introduced in the closed loop dynamics at the location $z = -\frac{K_i}{K_p}$. Controller gains K_i and K_p should be chosen such that the introduced zero cancels a slow pole (if any), and outer loop dynamics have a loop frequency at least five times smaller than that of pitch dynamics $\omega_{sp,d}$ [103].

6.3.3 Energy Management and Outer-most Loop Control

6.3.3.1 PI Navigation Controller

In traditional SISO control architectures, altitude hold controller is closed over the flight path angle loop, and velocity control loop is connected to the throttle channel. As aforementioned, such a SISO assignment of the elevator and thrust may cause catastrophic failures in aircraft operation. So far, only elevator channel is used by closing the flight path angle control loop over the pitch SAS augmented plant dynamics. Different from the SISO classical theory based literature, the altitude and velocity loops are closed considering them together in an energy-based control framework.

Regarding the aircraft as a point mass, the Hamiltonian function $\mathcal{H}$ becomes the total mechanical energy of the aircraft if the generalized coordinates are expressed in the inertial frame. Then, the Hamiltonian function coincides the total mechanical energy function E_{tot} of the aircraft, and it is defined as the summation of kinetic energy E_{kin} and potential energy E_{pot}:

$$\mathcal{H} = E_{tot} = \frac{1}{2}mV^2 + mgh$$

Since the energy consuming and contributing factors in an aircraft are related to aerial conditions, the velocity V can be replaced with airspeed V_∞.

Specific total energy (also known as energy height) is given by:

$$\mathcal{H}_s \triangleq \frac{\mathcal{H}}{mg} = \frac{V_\infty^2}{2g} + h$$

Furthermore, the Lagrangian is expressed as the difference between kinetic energy

and potential energy:

$$\mathcal{L} = \frac{1}{2}mV^2 - mgh$$

Similar to the Hamiltonian, the specific Lagrangian is defined as:

$$\mathcal{L}_s \triangleq \frac{\mathcal{L}}{mg} = \frac{V_\infty^2}{2g} - h$$

Note that for a conservative system, total time-derivative of the Lagrangian along the generalized coordinates is constant. Kinetic energy and potential energy may change, but the Lagrangian remains the same. This fact implies that the aircraft cannot change its energy height without adding or subtracting energy. Under the mild assumption that the elevator deflection does not consume any energy, the Lagrangian can readily be related to the elevator control as the system remains conservative. With flight path angle control loop being closed, γ_{cmd} becomes available to distribute the existing total energy between kinetic energy and potential energy. Next, the specific total energy rate and specific energy distribution rate are obtained as:

$$\dot{\mathcal{H}}_s = mV_\infty \dot{V}_\infty + mg\dot{h}$$
$$\dot{\mathcal{L}}_s = mV_\infty \dot{V}_\infty - mg\dot{h}$$

where

$$\dot{h} = V_\infty \sin(\gamma)$$
$$\dot{V}_\infty = \frac{1}{m}\left[T\cos(\alpha) - D\right] - g\sin(\gamma) \tag{6.14}$$

Now, having stated some necessary terminology, the navigation loop controller design is initiated in which the flight path angle command and throttle command are generated. First, the airspeed and altitude commands are converted to the specific total energy and and specific Lagrangian commands as follows:

$$\mathcal{H}_{s,cmd} = \frac{V_{cmd}^2}{2g} + h_{cmd}$$
$$\mathcal{L}_{s,cmd} = \frac{V_{cmd}^2}{2g} - h_{cmd}$$

Using small perturbations around the equilibrium point and Eq 6.14, one can obtain the linear dynamics for the specific total energy rate and specific total energy

102

distribution rate as the following:

$$\dot{\mathcal{H}}_s \cong \frac{V_0}{mg}\Delta T = k_{th}V_0\delta_{th}$$

$$\dot{\mathcal{L}}_s \cong \frac{V_0}{mg}\Delta T - 2V_0\Delta\gamma = k_{th}V_0\delta_{th} - 2V_0\Delta\gamma$$

(6.15)

where

$$T = T_0 + \Delta T, \qquad \gamma = \gamma_0 + \Delta\gamma, \qquad V_\infty = V_0 + \Delta V, \qquad \Delta T = k_{th}\delta_{th}(mg)$$

For simplicity, the perturbed thrust is expressed as $\Delta T = k_{th}\delta_{th}(mg)$ where k_{th} is the ratio of the maximum achievable thrust to aircraft weight, and δ_{th} denotes the percent usage of the available thrust. This relation indicates that the additional thrust ΔT is equal to δ_{th} percent of the available thrust.

Eq 6.15 will be the starting point of the energy-based navigation loop controller design. Re-writing the Eq 6.15 in compact form yields:

$$\dot{x}_{out} = \begin{bmatrix} \dot{\mathcal{H}}_s \\ \dot{\mathcal{L}}_s \end{bmatrix} = \begin{bmatrix} 0 & 0 \\ 0 & 0 \end{bmatrix} x_{out} + \begin{bmatrix} k_{th}V_0 & 0 \\ k_{th}V_0 & -2V_0 \end{bmatrix} \begin{bmatrix} \delta_{th,cmd} \\ \Delta\gamma_{cmd} \end{bmatrix}$$

(6.16)

$$\dot{x}_{out} = A_{out}x_{out} + B_{out}u_{out}$$

where the state x_{out} consists of the desired specific energy rate and specific energy rate distribution states.

Remark 6.3. *The system in Eq 6.16 indicates a few important features:*

- *Total energy of the aircraft can only be increased or decreased with the throttle command $\delta_{th,cmd}$.*

- *If the existing total energy is going to be distributed without adding or subtracting any energy, it can be achieved by flight path angle command $\Delta\gamma_{cmd}$.*

- *If the energy is going to be added or subtracted, and simultaneously distributed between altitude and airspeed channels, they need to take place through identical loop dynamics. This is because the throttle appears in both control channels, but only responsible for changing the energy height of the aircraft. Hence, the flight path angle command should work in synchronization with throttle command.*

In order to achieve a desired coordinated longitudinal control, an outer reference model is introduced to be tracked by the outer system states. Consider the following reference model:

$$\dot{x}_r = \begin{bmatrix} \dot{\mathcal{H}}_{s,des} \\ \dot{\mathcal{L}}_{s,des} \end{bmatrix} = \underbrace{\begin{bmatrix} -\omega_H & 0 \\ 0 & -\omega_L \end{bmatrix}}_{\triangleq A_r} \begin{bmatrix} \mathcal{H}_{s,des} \\ \mathcal{L}_{s,des} \end{bmatrix} + \underbrace{\begin{bmatrix} \omega_h & 0 \\ 0 & \omega_L \end{bmatrix}}_{\triangleq B_r} \underbrace{\begin{bmatrix} \Delta\mathcal{H}_{s,cmd} \\ \Delta\mathcal{L}_{s,cmd} \end{bmatrix}}_{\triangleq r_{out}} \qquad (6.17)$$

where $\Delta\mathcal{H}_{s,cmd}$ and $\Delta\mathcal{L}_{s,cmd}$ are given by:

$$\Delta\mathcal{H}_{s,cmd} = \mathcal{H}_{s,cmd} - \mathcal{H}_0$$

$$\Delta\mathcal{L}_{s,cmd} = \mathcal{L}_{s,cmd} - \mathcal{L}_0$$

One can immediately realize that the outer reference model is an aggregated two distinct low-pass filters with cutoff frequencies ω_H and ω_L. Ideally, these cutoff frequencies should be equal to ensure the coordinated control of elevator and throttle. However, if there exists a difference between specific energy rate and specific energy distribution rate loop frequencies, ω_H and ω_L may be set different than each other to compensate that difference. As it is a rule of thumb in successive loop closure control design method, cutoff frequencies ω_H and ω_L should be at least five times smaller than that of engine dynamics and flight path angle control loop.

Using the outer system model in Eq 6.16 and reference model in Eq 6.17, one can generate the throttle command and flight path angle command as follows:

$$\begin{bmatrix} \delta_{th,cmd} \\ \Delta\gamma_{cmd} \end{bmatrix} = -K_{x,out} \begin{bmatrix} \mathcal{H}_s \\ \mathcal{L}_s \end{bmatrix} + K_{r,out} \begin{bmatrix} \Delta\mathcal{H}_{s,cmd} \\ \Delta\mathcal{L}_{s,cmd} \end{bmatrix} + K_{i,z}z \qquad (6.18)$$

with the integrator state z being

$$\dot{z} = e_{out}$$

$$e_{out} \triangleq \begin{bmatrix} \mathcal{H}_{s,des} \\ \mathcal{L}_{s,des} \end{bmatrix} - \begin{bmatrix} \mathcal{H}_s \\ \mathcal{L}_s \end{bmatrix}$$

and integral gain $K_{i,z}$ is given by:

$$K_{i,z} = (P_{out}B_{out})^{\dagger} K_z$$

It should be noted that $K_z = K_z^T \succ 0$ is a symmetric positive definite design matrix with diagonal entries, and P_{out} is the unique symmetric positive definite solution to

the Lyapunov equation

$$A_r^T P_{out} + P_{out} A_r = -Q_{out}$$

for any $Q_{out} = Q_{out}^T \succ 0$. Furthermore, feedback controller gain $K_{x,out}$ and feedforward controller gain $K_{r,out}$ should satisfy the following matching conditions:

$$A_r = A_{out} - B_{out} K_{x,out}$$
$$B_r = B_{out} K_{r,out}$$

6.3.3.2 Outer Loop Adaptive Control

In the inner loop, an adaptive controller is employed only for the elevator channel to adjust the short period mode characteristics as desired. It is also shown that some uncertainties in the throttle channel can be projected onto elevator channel and can be effectively suppressed by the elevator control. It should also be noted that such uncertainties have relatively faster effects on the system response. Since the elevator servo actuation takes place much faster than that of the throttle, it is effective to suppress these uncertainties with elevator. However, there still exists an uncertainty that is orthogonal to the elevator control. In this section, an outer loop adaptive controller is designed to address the solution to eliminate these uncertainties.

Unsuppressed uncertainty is mainly acting on the velocity channel since the remaining portion is handled in the inner loop adaptive controller. Hence, effect of the uncertainty in the velocity channel will directly be visible in the total specific energy and specific energy distribution states.

Considering the outer loop system model in Eq 6.16 and outer reference model in Eq 6.17, the uncertainty is introduced in the following manner:

$$\dot{x}_{out} = A_{out} x_{out} + B_{out} \left[\Lambda u_{out} + \Delta(x_{out}) \right]$$

where the matrix Λ represents the unknown control effectiveness matrix with diagonal entries $\lambda_i \in \mathbb{R}_+$, and $\Delta_{out}(x_{out})$ denotes the system uncertainty. Adding and subtracting $B_{out} K_{x,out} x_{out}$ and $B_{out} K_{r,out} r_{out}$ yields:

$$\dot{x}_{out} = A_r x_{out} + B_r r_{out} + B_{out} \Lambda \left[u_{out} + \Delta_{out}(x_{out}) \right] \tag{6.19}$$

where $\Delta_{out}(x_{out}) = \Theta^T \sigma(x_{out}, r_{out})$ with unknown matrix of $\Theta^T = [\Lambda^{-1} W_{out}^T, \Lambda^{-1} K_{x,out}, -\Lambda^{-1} K_{r,out}]^T$ and known basis vector function of $\sigma(x_{out}, r_{out}) = [\psi^T(x_{out}), x_{out}^T, r_{out}^T]^T$. Note that the outer uncertain system dynamics in Eq 6.19 and outer reference model in Eq 6.17 form the standard adaptive control structure [74]. Similar to the inner loop adaptive controller, the weight update law is applied with optimum control modification as follows:

$$\dot{\hat{\Theta}} = -\Gamma_o \sigma \left[e_{out}^T P_{out} - \nu \sigma^T \hat{\Theta} B_{out}^T P_{out} A_r^{-1} \right] B_{out}$$

where $\Gamma_o \succ 0$ is the adaptation gain, and $\nu > 0$ is a design parameter.

Remark 6.4. *Proposed outer energy control loop can be applied to any flight control architectures that takes the commanded pitch/flight path angle and commanded throttle as inputs. Such a control architecture covers a large class of longitudinal flight controllers. To give examples; in a typical SISO architecture, error in the altitude response converted either into flight path angle command or into pitch command in the inner loops. Furthermore, the error in the airspeed is converted into commanded throttle (see [41–43]). Similarly, TECS architecture generates a commanded pitch and a commanded thrust as inputs to the pitch SAS augmented inner loop (see Figure 1.1). Hence, the proposed architecture can easily be connected as an outer-most loop for these flight control architectures.*

Remark 6.5. *Although the proof for the closed loop system stability is omitted in this work, readers may refer to references [104–108] for the necessary tools and strategies to design a stable hierarchical nonlinear adaptive controller.*

6.4   Numerical Simulation

In the simulations, the nonlinear equations in Eq 6.1 are applied with the following non-dimensional aerodynamic coefficients:

$$C_L = a_0 + a_1 \alpha + a_2 \alpha^2 + a_3 \alpha^3 + a_4 q$$
$$C_D = b_0 + b_1 \alpha + b_2 \alpha^2$$
$$C_m = c_0 + c_1 \alpha + c_2 \alpha^2 + c_3 q$$

with $a_i = \{0.65, \ 6.03, \ -0.56, \ -20.9, \ -0.18\}$ for $i = 0, \ldots, 4$, $b_i = \{0.05, \ 0.13, \ 1.42\}$ for $i = 0, \ldots, 2$, and $c_i = \{-0.07, \ -1.18, \ -1.32, \ 0.17\}$ for $i = 0, \ldots, 3$ being constant parameters which are obtained by CFD simulations. The aircraft is trimmed at steady, straight, and level flight conditions at $V_\infty = 28$ m/s and flight level of $h = 15000$ ft. Thrust perturbation is $\Delta T = \delta_{th} 500$ N. Resulting linear dynamical system is as follows:

$$\begin{bmatrix} \dot{u} \\ \dot{\theta} \\ \dot{w} \\ \dot{q} \\ \dot{h} \end{bmatrix} = \begin{bmatrix} -0.005 & -9.696 & 0.378 & -4.384 & 0 \\ 0 & 0 & 0 & 1.000 & 0 \\ -0.531 & -1.471 & -1.120 & 28.884 & 0 \\ 0.071 & 0 & -0.418 & -1.329 & 0 \\ 0.150 & 28.000 & -0.989 & 0 & 0 \end{bmatrix} \begin{bmatrix} u \\ \theta \\ w \\ q \\ h \end{bmatrix} + \begin{bmatrix} 4.91 & -0.33 \\ 0 & 0 \\ 0 & -0.05 \\ -0.64 & 14.41 \\ 0 & 0 \end{bmatrix} \begin{bmatrix} \delta_{th} \\ \delta_e \end{bmatrix}$$

In addition to linearization errors, additional uncertainty is introduced in the following form:

$$\Delta(x) = \begin{bmatrix} \beta_5 q + \beta_6 u \\ \beta_0 + \beta_1 q + \beta_2 \theta + \beta_3 \alpha + \beta_4 \alpha^2 \end{bmatrix} \tag{6.20}$$

with $\beta_i = \{0.016, \ 1.3, \ -1.2, \ 1.3, \ 4.1, \ -0.08, \ 0.12\}$ for $i = 0, \ldots, 6$ being constant uncertainty parameters. It is important to note that all the simulation results are presented as the difference between trim values. That is, the velocity response in Figure 6.3 is the additional velocity on the trim velocity of 28 m/s.

In Figure 6.2 and Figure 6.3, the performance of the nominal controllers in Eq 6.4 and Eq 6.18 is illustrated in the absence of the uncertainty function in Eq 6.20. Yet, uncertainties due to linearization still exist during the simulation with nonlinear plant model. As seen in the figure, outer loop controller cannot adequately decouple the velocity and altitude response, and an undesired motion is induced on the other channel. On the other hand, short period mode is satisfactorily damped by the inner control.

Once the uncertainty is introduced to the system, the closed-loop system becomes unstable as seen in Figure 6.4 and Figure 6.5.

Now, only inner loop adaptation is activated in Figure 6.6 and Figure 6.7. Altitude response is highly related to flight path angle management which is connected to
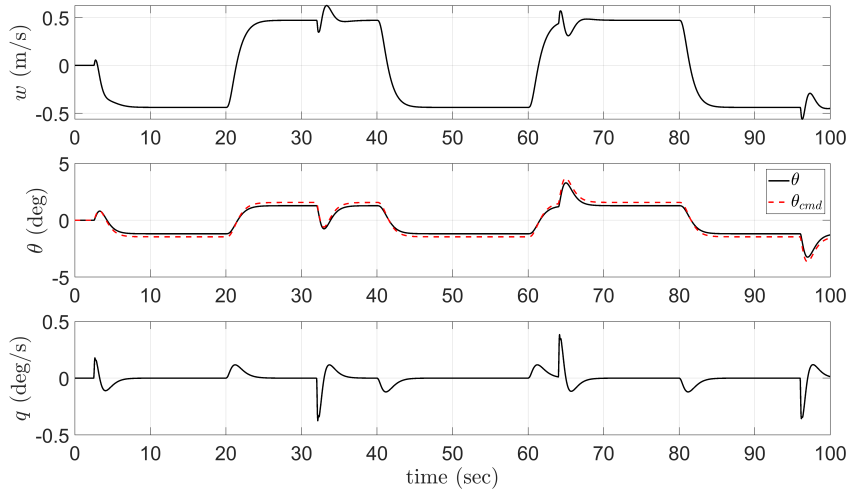
Figure 6.2: Inner Loop Short Period Mode States of the Nominal Closed Loop System without the Uncertainty
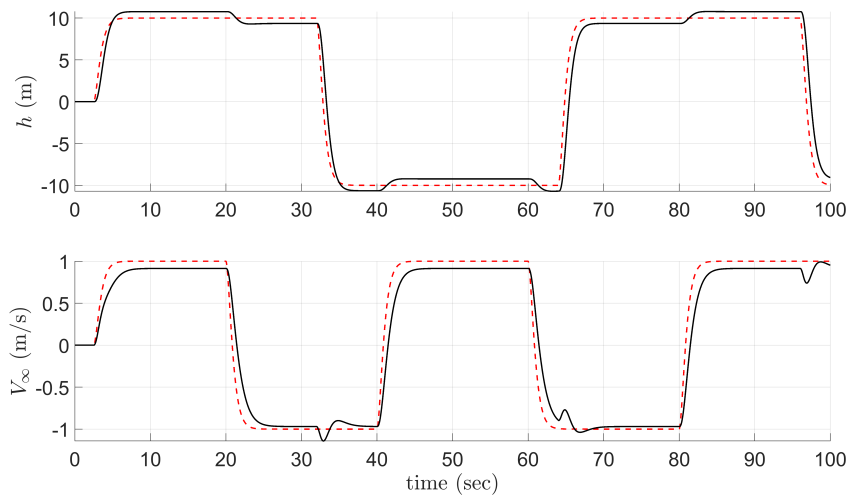
Figure 6.3: Outer Loop Command Tracking Performance of the Nominal Closed Loop System without the Uncertainty

the elevator channel. Since the inner loop adaptation successfully suppress the uncertainties that is achievable by the elevator, altitude response in Figure 6.7 gets pretty much closer to the nominal response in Figure 6.5. However, there exists a significant difference between velocity tracking performance as the uncertainty in the throttle channel is not completely addressed, yet. This is an expected result though, as the major effects of the uncertainty in throttle channel appears dominantly in the
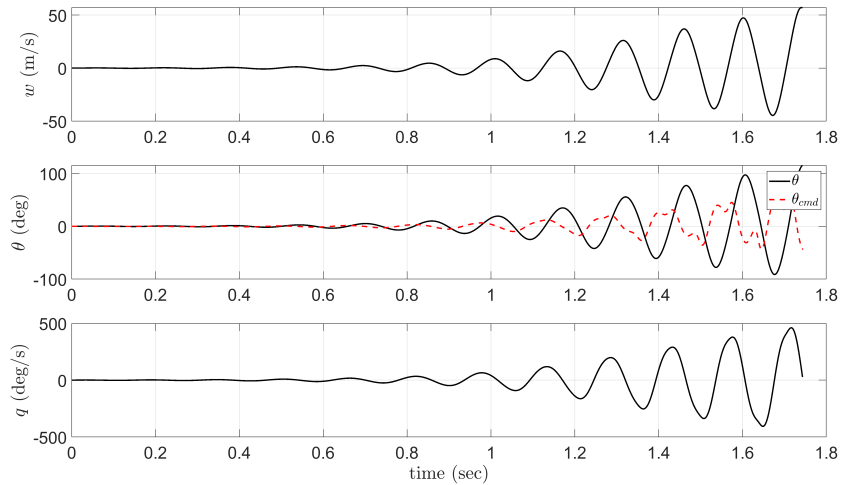
Figure 6.4: Unstable Response for the Inner Loop Short Period Mode States with the Nominal Controller in the Presence of the Uncertainty
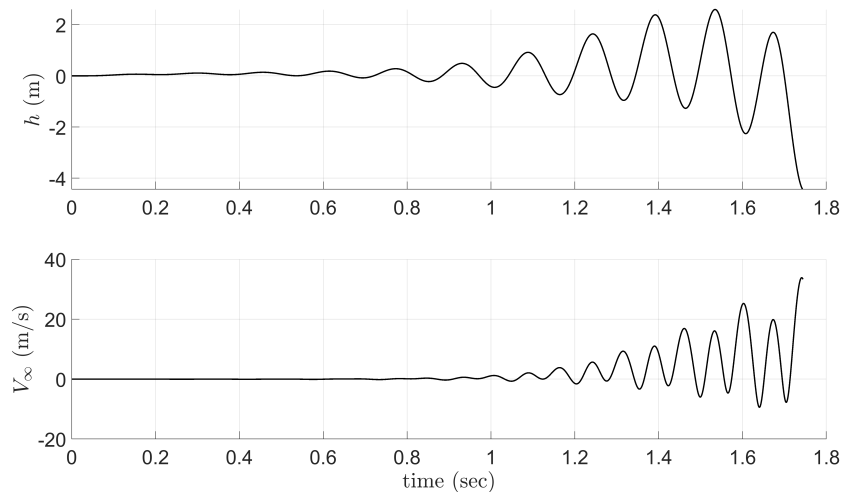
Figure 6.5: Unstable Outer Loop Command Tracking Performance with the Nominal Controller in the Presence of the Uncertainty

velocity response.

As the last case, both inner and outer loop adaptive controllers are activated. Corresponding tracking performance is illustrated in Figure 6.8 and Figure 6.9. As clearly seen, outer loop adaptive controller cancels out the uncertainty left over the throttle channel, and desired tracking performance is achieved at the outer loop states.
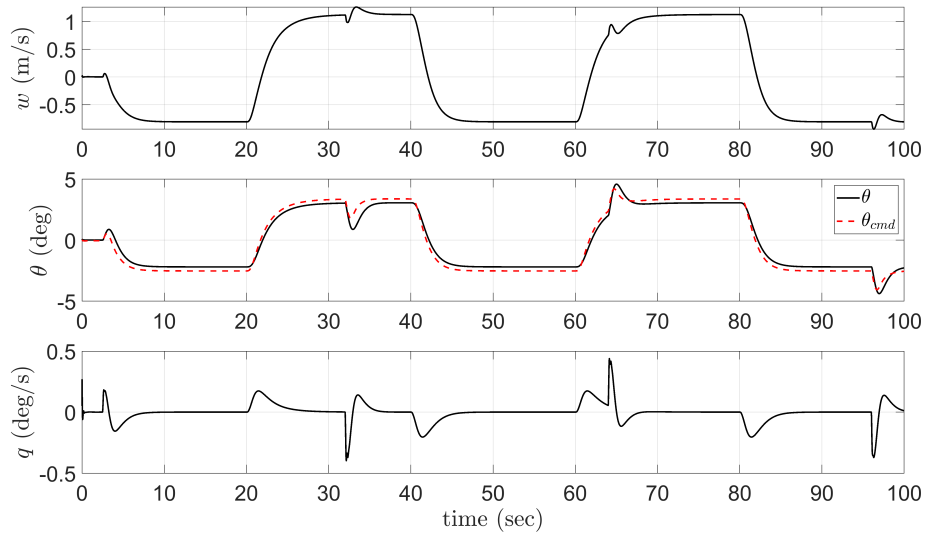
Figure 6.6: Inner Loop Short Period Mode States with Only Inner Loop Adaptation Activated in the Presence of the Uncertainty
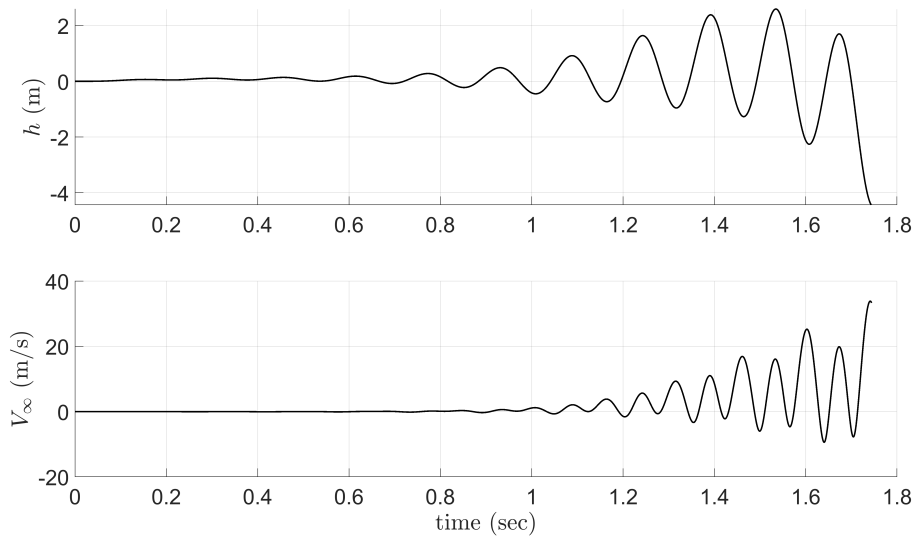
Figure 6.7: Outer Loop Command Tracking Performance with Only Inner Loop Adaptation Activated in the Presence of the Uncertainty

Furthermore, no high frequency short period oscillations are observed in the pitch response.

Figure 6.10 compares the control inputs between the following cases: i) nominal controller without the uncertainty in Eq 6.20, ii) only inner loop adaptation activated

110
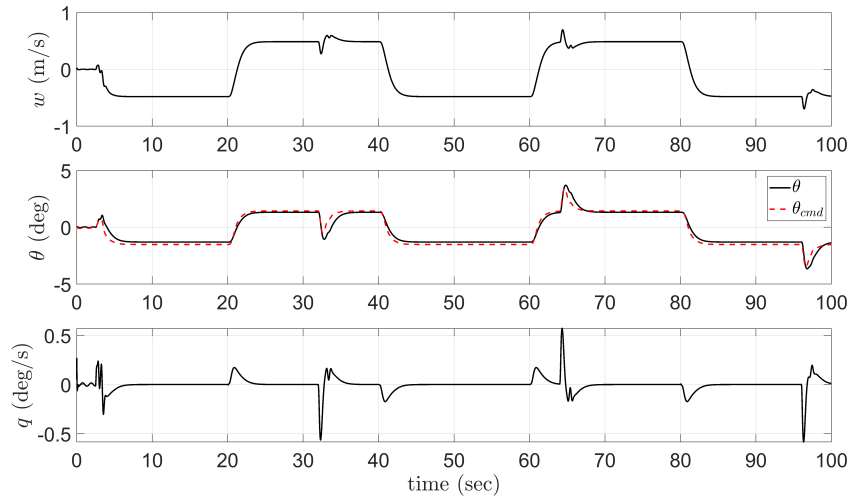
Figure 6.8: Inner Loop Short Period States with both Inner and Outer Adaptation
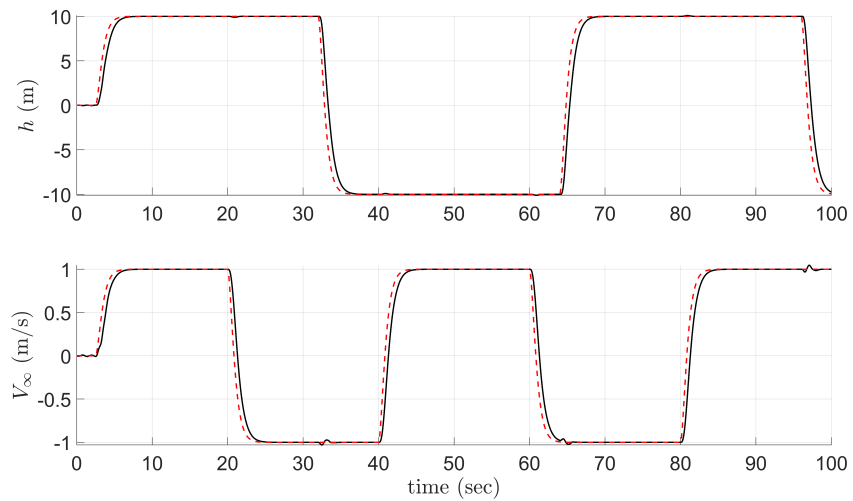
Figure 6.9: Outer Loop Tracking Performance with both Inner and Outer Adaptation

in the presence of uncertainty in Eq 6.20, iii) both inner and outer adaptations activated in the presence of uncertainty in Eq 6.20.

6.5 Conclusion

In this chapter, an adaptive longitudinal flight control architecture is proposed based on the energy principles. In the proposed flight control solution, elevator and

111
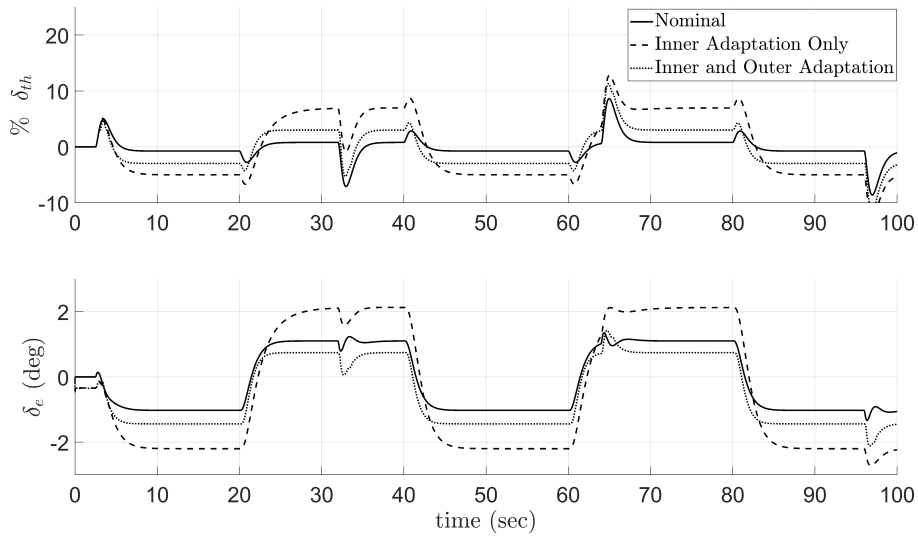
Figure 6.10: Input comparison between nominal control, inner adaptation only, and both inner and outer adaptation

thrust controls used together in a MIMO framework to control the energy state of the aircraft in the presence of uncertainties. Eventually, satisfactory velocity and altitude command following and decoupling performances are achieved. Specifically, an outer loop adaptive controller is designed to regulate the energy state of the aircraft. In the energy management module, commanded velocity and altitude are converted into total specific energy and specific energy distribution states. Then, the outer adaptive controller ensures that the aircraft energy state is able to track the reference model that enforces the Hamiltonian and Lagrangian control loops operate at the same bandwidth. Also, adaptation in the outer loop enhances the closed loop system stability by eliminating the uncertainties on the Hamiltonian state of the aircraft. Then, in order to distribute the total specific energy effectively over the velocity and altitude channels, a sequence of flight path angle controller and inner adaptive controller are designed. With these controllers, first, the commanded flight path angle is converted to pitch attitude command. Then, adaptive pitch stability augmentation system is utilized to track the commanded pitch despite the plant uncertainties. Eventually, satisfactory velocity and altitude command following performance is achieved with coordinated elevator and throttle control, short period mode characteristics are improved, and effects of uncertainties upon the system

112

behavior is effectively suppressed. Numerical simulations illustrate the efficacy of the proposed control algorithm in terms of command following and decoupling performances.

CHAPTER 7

ADAPTIVE CONTROLLER DESIGN WITH IMPROVED TRANSIENTS FOR THE LATERAL DYNAMICS OF A FIXED WING AIRCRAFT

7.1 Introduction

In this chapter, the gain scheduled lateral flight control problem is revisited in the presence of system uncertainties. Basically, the gain scheduling control is a powerful method to control nonlinear and/or parameter varying systems using well-developed linear controller design tools. Gain scheduling makes it possible to respond quickly to the variations in the operating conditions. However, typical gain scheduling approach is not suitable for uncertain nonlinear systems as the linearization carry little information about the plant dynamics [109]. A few notable contributions are available in the literature [110–113]. Specifically, Fujimori et al [110] proposes a fuzzy gain scheduled controller based on LMI optimization of an observer-based dynamic controller. The authors of [111] eigenvalue assignment problem is revisited for linear parameter varying systems in the context of gain scheduling. In both studies [110] and [111], a linear system is considered without any uncertainty, which makes them inapplicable to nonlinear systems with arbitrarily large uncertainties. To address this, Jang et al [112] propose an adaptive gain scheduling controller for time-varying systems. In their study, adaptive element is introduced to suppress the undesired effects of unknown control effectiveness matrix. Other than control anomalies that are captured by unknown control effectiveness matrix, no uncertainty exists upon the system dynamics. Furthermore, plant dynamics is assumed to be known for the nominal control effectiveness. Lastly, Zhang et al [113] propose an indirect adaptive controller to solve the online identification of gain scheduling coefficients and controller design problem. In their study, uncertain effects of structural damage

115

and external disturbances are assumed to be bounded and independent from the system states. This assumption restricts the class of applicable systems. In this study, the variations in the plant dynamics are allowed to be state and parameter dependent, time-varying, and switching. It is important to note that this chapter focuses on the gain scheduling problem. However, re-formulated system dynamics can readily be applied to parameter varying systems and switching systems.

7.2 Problem Formulation

Consider the uncertain nonlinear dynamical systems of the form

$$\dot{x}(t) = A(x,t)x(t) + B\big[u(t) + \delta(x)\big], \quad x(t_0) = x_0 \tag{7.1}$$

where $x(t) \in \mathcal{D}_x \subset \mathbb{R}^n$ is the state vector where $\mathcal{D}_x$ is sufficiently large compact set, the system matrix $A(x,t) \in \mathbb{R}^{n \times n}$ and input matrix $B \in \mathbb{R}^{n \times m}$ are *unknown*. System matrix $A(x,t)$ is Lipschitz continuous in x and $\mathcal{C}^1$ continuous in time, and input matrix B is constant. The control input is $u(t) \in \mathcal{U} \subset \mathbb{R}^m$ where $\mathcal{U}$ is admissible control set. The system is assumed to be underactuated; hence, $m < n$. $\delta(x) \in \mathbb{R}^m$ representing the unknown matched uncertainty is Lipschitz continuous in x. The pair (A, B) is assumed to be controllable $\forall x \in \mathcal{D}_x$, and full state measurement is available for feedback. Input matrix B has full column rank.

Unknown system and input matrices are decomposed as the following:

$$A(x,t) = A_0 + \delta A(x,t)$$
$$B = B_0 \Lambda \tag{7.2}$$

where $A_0 \in \mathbb{R}^{n \times n}$ and $B_0 \in \mathbb{R}^{n \times n}$ are known nominal values of system matrix $A(x,t)$ and input matrix B, respectively. $\delta A(x,t)$ represents the unknown part of the system matrix. In addition, $\Lambda = \text{diag}\big(\lambda_1 \quad \lambda_2 \quad \cdots \quad \lambda_m\big)$ denotes the unknown control effectiveness matrix with $\lambda_i \in \mathbb{R}_+$.

Then, the uncertain dynamical system in Eq 7.1 can be re-written as follows:

$$\dot{x}(t) = A_0 x(t) + \delta A(x,t)x(t) + B_0 \Lambda\big[u(t) + \delta(x)\big] \tag{7.3}$$

Furthermore, the term '$\delta A(x,t)x(t)$' is decomposed as follows:

$$\delta A(x,t)x(t) = B_0 v_1(x,t) + D_0 v_2(x,t)$$

with D_0 denoting the orthogonal complement of nominal input matrix B_0; that is, $B_0^T D_0 = D_0^T B_0 = 0$. Manipulating yields:

$$B_0^T B_0 v_1(x,t) = B_0^T \delta A(x,t)x(t) \quad \Rightarrow \quad v_1(x,t) = \left(B_0^T B_0\right)^{-1} B_0^T \delta A(x,t)x(t)$$

$$D_0^T D_0 v_2(x,t) = D_0^T \delta A(x,t)x(t) \quad \Rightarrow \quad v_2(x,t) = \left(D_0^T D_0\right)^{-1} D_0^T \delta A(x,t)x(t)$$

It should be noted that $B_0^T B_0$ is an invertible matrix since B_0 has full column rank. In addition, its orthogonal complement $D_0 \in \mathbb{R}^{n \times (n-m)}$ also has full column rank with $\text{rank}(D_0) = n - m > 0$. Hence, $D_0^T D_0$ is also invertible. One can realize that $\left(B_0^T B_0\right)^{-1} B_0^T$ and $\left(D_0^T D_0\right)^{-1} D_0^T$ are equivalent to left pseudo inverses of B_0 and D_0, respectively. For the rest of this chapter, the Moore Penrose inverses of B_0 and D_0 are defined as $B_0^\dagger = \left(B_0^T B_0\right)^{-1} B_0^T$ and $D_0^\dagger = \left(D_0^T D_0\right)^{-1} D_0^T$, respectively. Substituting these into Eq 7.3 yields:

$$\dot{x} = A_0 x + B_0 \Lambda \left[u + \delta(x) + \Lambda^{-1} B_0^\dagger \delta A(x,t)x\right] + D_0 D_0^\dagger \delta A(x,t)x \qquad (7.4)$$

Nominal control input $u_n(t)$ is designed to be

$$u_n(t) = -K_x x(t) + K_r r(t) + K_r z(t) \qquad (7.5)$$

where K_x is constant feedback gain, K_r is constant feedforward gain, $z(t)$ is the command governor signal (generated by following Section 5.5), and $r(t)$ is bounded piecewise continuous reference signal with $\|r(t)\| \leq r_0$, $\forall t \geq t_0$. Overall control input consisting a nominal part $u_n(t)$ and an adaptive part $u_{\text{ad}}(t)$ is given by

$$u(t) = u_n(t) + u_{\text{ad}}(t) \qquad (7.6)$$

Reference model that characterizes the ideal tracking performance is defined as

$$\dot{x}_r(t) = A_r x_r(t) + B_r r(t), \qquad x_r(t_0) = x_{r0} \qquad (7.7)$$

where the reference system and input matrices are designed using feedback gain K_x and feedforward gain K_r as:

$$A_r = A_0 - B_0 K_x$$

$$B_r = B_0 K_r$$

117

with A_r being Hurwitz reference system matrix and B_r being reference input matrix of appropriate dimensions. Manipulating uncertain system dynamics in Eq 7.4 by adding and subtracting '$B_0 u_n(t)$' results in:

$$\dot{x}(t) = A_0 x(t) + B_0 u_n(t) + B_0 \Lambda \big[u_{\mathrm{ad}}(t) + \big(I - \Lambda^{-1} \big) u_n(t) + \delta(x) +$$
$$\Lambda^{-1} B_0^\dagger \delta A(x,t) x(t) \big] + D_0 D_0^\dagger \delta A(x,t) x(t) \tag{7.8}$$

Defining the matched uncertainty Δ_m and unmatched uncertainty Δ_u as

$$\Delta_m(x,t) \triangleq \delta(x) + \big(I - \Lambda^{-1} \big) u_n(t) + \Lambda^{-1} B_0^\dagger \delta A(x,t) x(t)$$
$$\Delta_u(x,t) \triangleq D_0^\dagger \delta A(x,t) x(t) \tag{7.9}$$

simplifies the uncertain dynamical system representation as

$$\dot{x}(t) = A_0 x(t) + B_0 u_n(t) + B_0 \Lambda \big[u_{\mathrm{ad}}(t) + \Delta_m(x,t) \big] + D_0 \Delta_u(x,t) \tag{7.10}$$

Assumption 7.1. *Uncertainty component '$\Lambda^{-1} B_0^\dagger \delta A(x,t) x(t)$' can be approximated by linear combinations of RBFs as*

$$\Lambda^{-1} B_0^\dagger \delta A(x,t) x(t) = \theta^T(t) \phi_\theta(x) + \varepsilon_m(x,t)$$

where $\theta(t)$ is unknown time-varying weight matrix with appropriate dimensions and satisfying the following bounds: $\|\theta(t)\|_F \leq \bar{\theta}, \|\dot{\theta}(t)\|_F \leq \dot{\bar{\theta}}, \forall t \geq t_0$ for unknown positive scalars $\bar{\theta}, \dot{\bar{\theta}} \in \mathbb{R}_+$. Nonlinear mapping $\phi_\theta : \mathbb{R}^n \to \mathbb{R}^{s_\theta}$ is known and consists of the following RBF elements:

$$\phi_\theta(x) = exp \left(-\frac{\|x(t) - \bar{c}_{\theta,i}\|^2}{2 \bar{\mu}_{\theta,i}^2} \right)$$

with $\bar{c}_{\theta,i} \in \mathbb{R}^n$ being the center of an RBF unit and $\bar{\mu}_{\theta,i} \in \mathbb{R}_+$ being the width of the ith kernel node for $i = 1, 2, \ldots, s_m$. For the residual $\varepsilon_m(x,t)$, it holds that $\|\varepsilon_m(x,t)\| \leq \varepsilon_{m0} \in \mathbb{R}_+, \forall x \in \mathcal{D}_x, \forall t \geq t_0$, where the residual bound ε_{m0} can be made arbitrarily small by increasing the size of the RBF. Furthermore, matched uncertainty $\delta(x)$ is assumed to be structured, and has the following form:

$$\delta(x) = W_\delta^T \phi_\delta(x)$$

where W_δ is constant unknown weight matrix and $\phi_\delta : \mathbb{R}^n \to \mathbb{R}^{s_\delta}$ is known basis vector-function of appropriate dimensions.

With Assumption 7.1, aggregated uncertainty Δ_m in Eq 7.9 can be expressed as:

$$\Delta_m(x, t) = W_m^T(t)\phi_m(x) + \varepsilon_m(x, t)$$

with unknown weight and known basis being $W_m^T(t) \triangleq \begin{bmatrix} W_\delta^T & (I - \Lambda^{-1}) & \theta^T(t) \end{bmatrix}$ and $\phi_m(x) \triangleq \begin{bmatrix} \phi_\delta^T & u_n^T & \phi_\theta^T \end{bmatrix}^T$, respectively.

Assumption 7.2. *Unmatched uncertainty $\Delta_u(x, t)$ in Eq 7.9 can be approximated by linear combinations of known radial basis functions (RBF) as*

$$\Delta_u(x, t) = W_u^T(t)\phi_u(x) + \varepsilon_u(x, t)$$

where $W_u(t) \in \mathbb{R}^{s_u \times m}$ is unknown time-varying weight matrix satisfying the bounds $\|W_u(t)\|_F \leq \bar{w}_u$, $\|\dot{W}_u(t)\|_F \leq \dot{\bar{w}}_u$ with $\bar{w}_u, \dot{\bar{w}}_u \in \mathbb{R}_+$ being unknown positive scalars. Known nonlinear mapping $\phi_u : \mathbb{R}^n \to \mathbb{R}^{s_u}$ consists of following RBF elements:

$$\phi_u(x) = exp\left(-\frac{\|x(t) - \bar{c}_{u,i}\|^2}{2\bar{\mu}_{u,i}^2}\right)$$

with $\bar{c}_{u,i} \in \mathbb{R}^n$ being the center of an RBF unit and $\bar{\mu}_{u,i} \in \mathbb{R}_+$ being the width of the ith kernel node for $i = 1, 2, \ldots, s_u$. For the residual $\varepsilon_u(x, t)$, it holds that $\|\varepsilon_u(x, t)\| \leq \varepsilon_{u0} \in \mathbb{R}_+$, $\forall x \in \mathcal{D}_x$, $\forall t \geq t_0$, where the residual bound ε_{u0} can be made arbitrarily small by increasing the size of the RBF.

With Assumption 7.1 and Assumption 7.2, uncertain dynamical system in Eq 7.10 can be re-written as:

$$\dot{x} = A_0 x + B_0 u_n + B_0 \Lambda \left[u_{\text{ad}} + W_m^T \phi_m + \varepsilon_m \right] + D_0 \left[W_u^T \phi_u + \varepsilon_u \right] \tag{7.11}$$

Then, adaptive controller $u_{\text{ad}}(t)$ is designed to be:

$$u_{\text{ad}}(t) = -\hat{W}_m^T(t)\phi_m(x)$$

Applying the control input in Eq 7.6 to uncertain system in Eq 7.11 results in:

$$\dot{x} = A_r x + B_r \left[r + z \right] + B_0 \Lambda \left[\tilde{W}_m^T \phi_m + \varepsilon_m \right] + D_0 \left[W_u^T \phi_u + \varepsilon_u \right] \tag{7.12}$$

where $\tilde{W}_m(t) \triangleq W_m - \hat{W}_m(t)$ is the matched parameter estimation error. Next, the auxiliary reference model is defined similar to Eq 5.4 as the following:

$$\dot{x}_m(t) = A_r x_m(t) + B_r \left[r(t) + z(t) \right] + D_0 \hat{W}_u^T(t)\phi_u(x) - k_\lambda e(t), \tag{7.13}$$

119

Let $e(t) \triangleq x_m(t) - x(t)$ be the auxiliary tracking error. Then, its dynamics becomes:

$$\dot{e} = \left(A_r - k_\lambda I\right)e - B_0 \Lambda \tilde{W}_m^T \phi_m - B_0 \Lambda \varepsilon_m - D_0 \tilde{W}_u^T \phi_u - D\varepsilon_u \qquad (7.14)$$

where $I \in \mathbb{R}^{n \times n}$ is the identity matrix, $\tilde{W}_u(t) \triangleq W_u - \hat{W}_u(t)$ is the unmatched weight estimation error. In addition, the tracking error is defined as $e_m(t) \triangleq x_r(t) - x_m(t)$. Then, one can write the corresponding error dynamics as:

$$\dot{e}_m(t) = A_r e_m(t) - B_r z(t) - D_0 \hat{W}_u^T(t)\phi_u(x) + k_\lambda e(t). \qquad (7.15)$$

7.2.1 Adaptive Laws

Following the similar steps in Section 5.3, applying low-pass filter to uncertain system dynamics in Eq 7.10 gives

$$\begin{aligned} B_0^\dagger \dot{x}_f(t) &= B_0^\dagger A_0 x_f(t) + u_{n,f}(t) + \Lambda\left[u_{\text{ad},f}(t) + \Delta_{m,f}(x,t)\right] \\ D_0^\dagger \dot{x}_f(t) &= D_0^\dagger A_0 x_f(t) + \Delta_{u,f}(x,t) \end{aligned} \qquad (7.16)$$

yielding

$$\begin{aligned} Y &\triangleq \Lambda\left[u_{\text{ad,f}}(t) + \Delta_{m,f}(x,t)\right] = B_0^\dagger \dot{x}_f(t) - B_0^\dagger A_0 x_f(t) - u_n(t) \\ \Delta_{u,f}(x,t) &= D_0^\dagger \dot{x}_f(t) - D_0^\dagger A_0 x_f(t) \end{aligned} \qquad (7.17)$$

where the filtered signals are available from Eq 2.12 and followings:

$$\begin{aligned} \dot{\phi}_{m,f} &= \omega_f\left(\phi_m - \phi_{m,f}\right) \\ \dot{\phi}_{u,f} &= \omega_f\left(\phi_u - \phi_{u,f}\right) \\ \dot{u}_{n,f} &= \omega_f\left(u_n - u_{n,f}\right) \\ \dot{u}_{\text{ad},f} &= \omega_f\left(u_{\text{ad}} - u_{\text{ad},f}\right) \end{aligned} \qquad (7.18)$$

Assumption 7.3. *Let $\mathcal{F}(s)$ be the transfer function for the low-pass filter in Eq 7.18. Let $\Delta_{m,f} = \mathcal{F}(s)\{\Delta_m\}$ where $\Delta_m = W_m^T \phi_m + \varepsilon_m$ as given in Assumption 7.1. Then, the following entity is bounded:*

$$\|\Delta_{m,f} - W_m^T \phi_{m,f}\|_F = \|\varrho_m\|_F \leq \bar{\delta}_m$$

where $\bar{\delta}_m \in \mathbb{R}_+$ is an unknown positive scalar constant. Similarly, the following bound for the filtered unmatched uncertainty holds with unknown constant $\bar{\delta}_u \in \mathbb{R}_+$:

$$\|\Delta_{u,f} - W_u^T \phi_{u,f}\|_F = \|\varrho_u\|_F \leq \bar{\delta}_u$$

Remark 7.1. *Assumption 7.3 implies that time-varying learning weight matrices $W_m(t)$ and $W_u(t)$ have relatively low frequency content. Although it sounds restrictive, Assumption 7.3 generally holds in many practical systems. For a gain scheduling problem in aircraft flight control, for instance, scheduling parameters are usually velocity, altitude, and mass of the aircraft [ref], which are varying slowly. Furthermore, if the unknown weight matrices W_m and W_u were to be constant, the inequalities in Assumption 7.3 become equalities with $\bar{\delta}_m = 0$ and $\bar{\delta}_u = 0$. Hence, presented assumption already covers the uncertain systems that are parametrized by unknown constant parameters.*

Under the Assumption 7.3, Eq 7.17 can be re-written as:

$$Y \triangleq \Lambda\big[u_{\text{ad,f}} + W_m^T \phi_{m,f} + \varrho_m\big] = B_0^\dagger \dot{x}_f - B_0^\dagger A_0 x_f - u_n$$
$$W_u^T \phi_{u,f} + \varrho_u = D_0^\dagger \dot{x}_f - D_0^\dagger A_0 x_f \tag{7.19}$$

Next, the estimations of Y and $W_u^T \phi_{u,f}$ are defined as the followings:

$$\hat{Y} \triangleq \hat{\Lambda}\big[u_{\text{ad,f}} + \hat{W}_m^T \phi_{m,f}\big]$$
$$\hat{W}_u^T \phi_{u,f} \triangleq D_0^\dagger \dot{x}_f - D_0^\dagger A_0 x_f \tag{7.20}$$

where $\hat{Y}, \hat{\Lambda}, \hat{W}_m$, and $\hat{W}_u$ are online estimations of Y, Λ, W_m, and W_u, respectively. Adaptive laws for $\hat{\Lambda}, \hat{W}_m$, and $\hat{W}_u$ are given by:

$$\dot{\hat{W}}_m = \Gamma_m \text{Proj}\left\{\hat{W}_m, -\phi_m e^T PB + \gamma_1 \phi_{m,f} e_Y^T\right\}$$
$$\dot{\hat{W}}_u = \Gamma_u \text{Proj}\left\{\hat{W}_u, -\phi_u e^T PD + \mu_1 \phi_{u,f} \tilde{\Delta}_{u,f}^T\right\} \tag{7.21}$$
$$\dot{\hat{\Lambda}} = \gamma_1 \Gamma_\Lambda \text{Proj}\left\{\hat{\Lambda}, \big[e_Y \big(u_{\text{ad,f}} + \hat{W}_m^T \phi_{m,f}\big)^T\big]\right\}$$

where the error signals e_Y and $\tilde{\Delta}_{u,f}$ are defined as

$$e_Y \triangleq Y - \hat{Y} = \tilde{\Lambda}\big(u_{\text{ad,f}} + \hat{W}_m^T \phi_{m,f}\big) + \Lambda \tilde{W}_m^T \phi_{m,f} + \Lambda \varrho_m$$
$$\tilde{\Delta}_{u,f} \triangleq \Delta_{u,f} - \hat{W}_u^T \phi_{f,u} = \tilde{W}_u^T \phi_{f,u} + \varrho_u \tag{7.22}$$

Theorem 7.1. *Consider the uncertain dynamical system in Eq 7.1 with decomposition in Eq 7.2, control input in Eq 7.6, ideal reference model in Eq 7.7, auxiliary reference model in Eq 7.13, and adaptive laws in Eq 7.21. Then, under Assumption 7.1, system*

signals $e(t), e_Y(t), \hat{W}_m(t), \tilde{W}_m(t), \hat{W}_u(t), \tilde{W}_u(t), \hat{\Lambda}(t), \tilde{\Lambda}(t),$ and $\tilde{z}_u \triangleq \tilde{W}_u^T \phi_{f,u}$ are uniformly ultimately bounded.

Proof. Consider the following Lyapunov function:

$$\mathcal{V} = \frac{1}{2} e^T P e + \frac{1}{2} \text{tr}\big(\tilde{W}_m^T \Gamma_m^{-1} \tilde{W}_m \Lambda\big) + \frac{1}{2} \text{tr}\big(\tilde{W}_u^T \Gamma_u^{-1} \tilde{W}_u\big) \qquad (7.23)$$

Its time derivative along the system trajectories in Eq 7.14 and Eq 7.21 can be bounded as

$$\dot{\mathcal{V}} \leq -\left(\frac{1}{2}\lambda_{\min}(Q) + k_\lambda \lambda_{\min}(P) - k_1 - k_2\right)\|e\|^2 - \gamma_1\|e_Y\|^2 - \mu_1\big(1 - k_3\big)\|\tilde{z}_u\|^2$$
$$+ \frac{\|PB_0\Lambda\|_F^2 \varepsilon_{m0}^2}{4k_1} + \frac{\|PD_0\|_F^2}{4k_2}\varepsilon_{u0}^2 + \frac{\bar{\delta}_u^2}{4k_3} + w_m^* \dot{\bar{\theta}}\|\Gamma_m^{-1}\|_F\|\Lambda\|_F + w_u^* \dot{\bar{w}}\|\Gamma_u^{-1}\|_F\|\Lambda\|_F$$

with $\tilde{z}_u \triangleq \tilde{W}_u^T \phi_{f,u}$, $\|\tilde{W}_m\|_F \leq w_m^*$, $\|\tilde{W}_u\|_F \leq w_u^*$. which can be simplified as

$$\dot{\mathcal{V}} \leq -\left(\frac{1}{2}\lambda_{\min}(Q) + k_\lambda \lambda_{\min}(P) - k_1 - k_2\right)\|e\|^2 - \gamma_1\|e_Y\|^2 - \mu_1\big(1 - k_3\big)\|\tilde{z}_u\|^2 + c$$

where positive scalar constant c is $c \triangleq \frac{\|PB_0\Lambda\|_F^2 \varepsilon_{m0}^2}{4k_1} + \frac{\|PD_0\|_F^2}{4k_2}\varepsilon_{u0}^2 + \frac{\bar{\delta}_u^2}{4k_3} + w_m^* \dot{\bar{\theta}}\|\Gamma_m^{-1}\|_F\|\Lambda\|_F + w_u^* \dot{\bar{w}}\|\Gamma_u^{-1}\|_F\|\Lambda\|_F$. In addition, $k_3 \in (0, 1)$ and positive scalars $k_1, k_2 \in \mathbb{R}_+$ satisfy $k_1 + k_2 < \frac{1}{2}\lambda_{\min}(Q) + k_\lambda \lambda_{\min}(P)$. This result ensures the boundedness of error signals $e(t)$, $e_Y(t)$, and $\tilde{z}_u(t)$.

∎

Remark 7.2. *Theorem 7.1 ensures that the tracking error $e(t) = x_m(t) - x(t)$ is uniformly ultimately bounded. However, boundedness of the states $x(t)$ cannot be guaranteed since the auxiliary reference state $x_m(t)$ is not bounded, yet. This is also the case in Chapter 5. In order to guarantee the boundedness of system states $x(t)$, it is necessary to bound auxiliary state vector $x_m(t)$. Hence, the command governor input is designed as in Section 5.5. It is important to note that the command governor signal is designed using ideal reference model in Eq 7.7 and auxiliary reference model in Eq 7.13, which are exactly the same as the ones in Chapter 5. It means the command governor input design will be the same as in Section 5.5, as well. Thus, the details of command governor design is omitted to avoid the repetitions.*

7.3 Linearized Aircraft Lateral Dynamics

Linearized equations of motion for lateral dynamics of an aircraft can be stated as [42]

$$
\underbrace{\begin{bmatrix} \dot{\beta} \\ \dot{r} \\ \dot{\phi} \\ \dot{p} \end{bmatrix}}_{\triangleq \dot{x}_p} = \underbrace{\begin{bmatrix} Y_\beta & -1 & \frac{g}{U_0} & 0 \\ N'_\beta & N'_r & 0 & N'_p \\ 0 & \tan\theta_0 & 0 & 1 \\ L'_\beta & L'_r & 0 & L'_p \end{bmatrix}}_{\triangleq A_p} \underbrace{\begin{bmatrix} \beta \\ r \\ \phi \\ p \end{bmatrix}}_{\triangleq x_p} + \underbrace{\begin{bmatrix} Y^*_{\delta_r} & 0 \\ N'_{\delta_r} & N'_{\delta_a} \\ 0 & 0 \\ L'_{\delta_r} & L'_{\delta_a} \end{bmatrix}}_{\triangleq B_p} \underbrace{\begin{bmatrix} \delta_r \\ \delta_a \end{bmatrix}}_{\triangleq u} \tag{7.24}
$$

with

$$
Y^*_{\delta_r} = \frac{Y_{\delta_r}}{U_0}
$$

$$
L'_\beta = L_\beta + \frac{I_{xz}}{I_{zz}} N_\beta \qquad\qquad N'_\beta = N_\beta + \frac{I_{xz}}{I_{xx}} L_\beta
$$

$$
L'_p = L_p + \frac{I_{xz}}{I_{zz}} N_p \qquad\qquad N'_p = N_p + \frac{I_{xz}}{I_{xx}} L_p
$$

$$
L'_r = L_r + \frac{I_{xz}}{I_{zz}} N_r \qquad\qquad N'_r = N_r + \frac{I_{xz}}{I_{xx}} L_p
$$

$$
L'_{\delta_a} = L_{\delta_a} + \frac{I_{xz}}{I_{zz}} N_{\delta_a} \qquad\qquad N'_{\delta_a} = N_{\delta_a} + \frac{I_{xz}}{I_{xx}} L_{\delta_a}
$$

$$
L'_{\delta_r} = L_{\delta_r} + \frac{I_{xz}}{I_{zz}} N_{\delta_r} \qquad\qquad N'_{\delta_r} = N_{\delta_r} + \frac{I_{xz}}{I_{xx}} L_{\delta_r}
$$

where β is sideslip angle $[rad]$, r is angular velocity about body z_b-axis $[rad/s]$, ϕ is roll angle $[rad]$, p is angular velocity about body x_b-axis, θ_0 is pitch angle $[rad]$ at trim condition, U_0 is body velocity along x_b-axis $[m/s]$, δ_a is aileron control input $[rad]$, δ_r is rudder control input $[rad]$, I_{xz}, I_{xx}, I_{zz} are components of inertia matrix, and Y_*, L_*, N_* are dimensional stability derivatives. It is important to note that both static and dynamic stability derivatives vary with respect to system states and scheduling parameters such as airspeed, altitude, dynamic pressure, weight, etc. Hence, matrices A_p and B_p vary with the flight condition. These variations are considered unknown, and only constant nominal system matrix A_{p0} and input matrix B_{p0} are known for controller synthesis. In addition, actual nonlinear plant dynamics involve nonlinear uncertainties such as modeling errors, linearization, etc. Hence, the matched uncertainty δ is introduced to represent these nonlinearities:

$$
\dot{x}_p(t) = A_p(x_p, t) x_p(t) + B_p \big[u(t) + \delta(x_p) \big] \tag{7.25}
$$

with $\delta(x_p) = W_\delta^T \phi_\delta$, where the matched uncertainty $\delta(x_p)$ is defined as

$$\delta(x_p) = \begin{bmatrix} -0.31 & -0.03 \\ -0.09 & 0.056 \\ 0.23 & 0.018 \\ 0.17 & -0.023 \\ 0.04 & -0.19 \\ -0.013 & 0.11 \\ 0.036 & 0.14 \\ 0.09 & -0.23 \end{bmatrix}^T \begin{bmatrix} |\beta|r \\ |r|r \\ |\phi|r \\ \sin\beta \\ |\phi|p \\ |p|p \\ |\phi|r \\ \sin\phi \end{bmatrix} \tag{7.26}$$

7.3.1 State Transformation

In Chapter 5, command governor-based adaptive controller is designed assuming the reference model is in controllable canonical form. In this way, backstepping control implementation becomes more straight-forward due to integral chain structure of the controllable canonical form (CCF). However, the pair (A_p, B_p) in Eq 7.24 is not in CCF. Thus, it is challenging to find a reference model in CCF that still satisfies the matching condition in Assumption 2.1.

Applying the matrix decomposition in Eq 7.2 and using the uncertainty definitions in Eq 7.9 yields:

$$\dot{x}_p(t) = A_{p0}x_p(t) + B_{p0}u_n(t) + B_{p0}\Lambda\big[u_{\text{ad}}(t) + \Delta_m(x_p, t)\big] + D_0'\Delta_u(x_p, t) \tag{7.27}$$

which is equivalent to uncertain system representation in 7.10. Next, the state transformation $x \triangleq Tx_p$ is applied to get CCF representation [114]:

$$\dot{x} = \underbrace{TA_{p0}T^{-1}}_{\triangleq A_0}x + \underbrace{TB_{p0}}_{\triangleq B_0}u_n + \underbrace{TB_{p0}}_{\triangleq B_0}\Lambda\big[u_{\text{ad}} + \Delta_m(x_p, t)\big] + \underbrace{TD_0'}_{\triangleq D_0}\Delta_u(x_p, t) \tag{7.28}$$

where A_0, B_0, and D_0 are in the following forms:

$$A_0 = \begin{bmatrix} 0 & 1 & 0 & 0 \\ -a_{21} & -a_{22} & -a_{23} & -a_{24} \\ 0 & 0 & 0 & 1 \\ -a_{41} & -a_{42} & -a_{43} & -a_{44} \end{bmatrix}, \quad B_0 = \begin{bmatrix} 0 & 0 \\ 1 & 0 \\ 0 & 0 \\ 0 & 1 \end{bmatrix}, \quad D_0 = \begin{bmatrix} 0 & 1 \\ 0 & 0 \\ 1 & 0 \\ 0 & 0 \end{bmatrix}$$

Ideal reference model is designed to be in the following form:

$$A_r = \begin{bmatrix} 0 & 1 & 0 & 0 \\ -\omega_1^2 & -2\xi_1\omega_1 & 0 & 0 \\ 0 & 0 & 0 & 1 \\ 0 & 0 & -\omega_2^2 & -2\xi_2\omega_2 \end{bmatrix}, \qquad B_r = \begin{bmatrix} 0 & 0 \\ \omega_1^2 & 0 \\ 0 & 0 \\ 0 & \omega_2^2 \end{bmatrix} \qquad (7.29)$$

where $\omega_1, \omega_2 \in \mathbb{R}_+$ are desired natural frequencies and $\zeta_1, \zeta_2 \in \mathbb{R}_+$ are desired damping coefficients.

One can realize that the reference model selection in Eq 7.29 results in two decoupled tracking error dynamics from Eq 7.15:

$$\text{Subsys 1.} \quad \dot{\xi}_1 = \begin{bmatrix} 0 & 1 \\ -\omega_1^2 & -2\zeta_1\omega_1 \end{bmatrix} \xi_1 - \begin{bmatrix} 0 \\ \omega_1^2 \end{bmatrix} z_1 - \begin{bmatrix} 1 \\ 0 \end{bmatrix} \hat{\Delta}_{u2} + k_\lambda \begin{bmatrix} e_1 \\ e_2 \end{bmatrix}$$

$$\text{Subsys 2.} \quad \dot{\xi}_2 = \begin{bmatrix} 0 & 1 \\ -\omega_2^2 & -2\zeta_2\omega_2 \end{bmatrix} \xi_2 - \begin{bmatrix} 0 \\ \omega_2^2 \end{bmatrix} z_2 - \begin{bmatrix} 1 \\ 0 \end{bmatrix} \hat{\Delta}_{u1} + k_\lambda \begin{bmatrix} e_3 \\ e_4 \end{bmatrix} \qquad (7.30)$$

Hence, command governor input design for 2nd order systems in Section 5.5.1 is directly applied for $z(t) = \begin{bmatrix} z_1 & z_2 \end{bmatrix}^T$.

7.4 Numerical Simulation

7.4.1 System Description

For a typical flight control problem, forces and moments acting on the aircraft are highly dependent on the dynamic pressure, which is a function of airspeed and air density. Neglecting the effects of humidity, it is mostly possible to replace the air density with flight altitude using standard atmosphere model [115]. Hence, one can safely pick the airspeed and altitude as the scheduling variables to reflect the changes in the plant dynamics as operating conditions change. In this example, the flight altitude is kept (almost) constant at 2000 m. Nonlinear model of the aircraft shown in Figure 7.1 is trimmed and linearized at steady, straight, level flight conditions for different velocities ranging from 24 m/s to 38 m/s with a velocity increment of 1 m/s. Hence, there exist 15 different linear models for the shown aircraft. Corresponding system and input matrices are given in Appendix A.
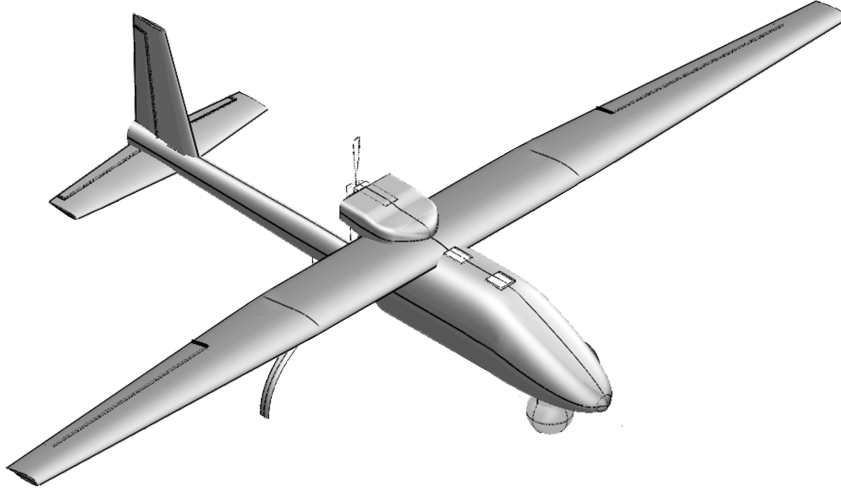
Figure 7.1: Isometric View of Simulation Aircraft

Nominal linear model is chosen to be the middle one, which is obtained at calibrated airspeed (CAS) of 30 m/s. Corresponding matrices A_{p0} and B_{p0} are as follows:

$$
A_{p0} = \begin{bmatrix} -0.2 & -1.0 & 0.3 & 0.03 \\ 3.5 & -0.89 & 0 & -2.2 \\ 0 & 0.03 & 0 & 1 \\ -1.9 & 4.2 & 0 & -9.9 \end{bmatrix}, \quad B_{p0} = \begin{bmatrix} -0.11 & -0.004 \\ 10.2 & 0.74 \\ 0.0 & 0.0 \\ -3.94 & 24.83 \end{bmatrix}
$$

Transformation matrix T for $x = T x_p$ is given by

$$
T = \begin{bmatrix} -0.0964 & -0.0010 & -0.0021 & 0.0 \\ 0.0156 & 0.0973 & -0.0289 & -0.0029 \\ -0.0141 & -0.0002 & 0.0399 & 0.0 \\ 0.0023 & 0.0154 & -0.0042 & 0.0398 \end{bmatrix}
$$

yielding

$$
A_0 = \begin{bmatrix} 0.0 & 1.0 & 0.0 & 0.0 \\ -3.61 & -0.38 & -0.92 & -5.39 \\ 0.0 & 0.0 & 0.0 & 1.0 \\ 0.32 & 3.24 & 1.26 & -10.62 \end{bmatrix}, \quad B_0 = \begin{bmatrix} 0 & 0 \\ 1 & 0 \\ 0 & 0 \\ 0 & 1 \end{bmatrix}, \quad D_0 = \begin{bmatrix} 0 & 1 \\ 0 & 0 \\ 1 & 0 \\ 0 & 0 \end{bmatrix}
$$

Reference model design parameters that determine the desired closed-loop behavior are chosen as $\omega_1 = \omega_2 = 1.6$ rad/s, and $\zeta_1 = \zeta_2 = 0.86$. Then, feedback gain K_x and

126

feedforward gain K_r become:

$$K_x = \begin{bmatrix} -1.05 & 2.37 & -0.92 & -5.39 \\ 0.32 & 3.24 & 3.82 & -7.87 \end{bmatrix}$$

$$K_r = \begin{bmatrix} 2.56 & 0.0 \\ 0.0 & 2.56 \end{bmatrix}$$

Adaptive control gains utilized in the numerical simulations are as follows: $k_\lambda = \Gamma_f = \Gamma_m = \gamma_1 = \mu_1 = 10$, $\omega_f = \Gamma_0 = 5$, $\Gamma_1 = 15$, and $\Gamma_u = \Gamma_\Lambda = 1$. Simulation sampling frequency is set to 100 Hz. All the estimated and filtered signals are initialized from zero.

7.4.2 Results

In this part, a fighter aircraft performing successive bank maneuvers to the left and right while experiencing an undamped Phugoid oscillations with period of $T_{\text{phugoid}} = 30$ seconds is considered. Corresponding velocity profile is illustrated in Figure 7.2. Since the velocity of the aircraft varies during Phugoid oscillations, linearized model will differ at each velocity since aircraft velocity is one of the scheduling parameters.
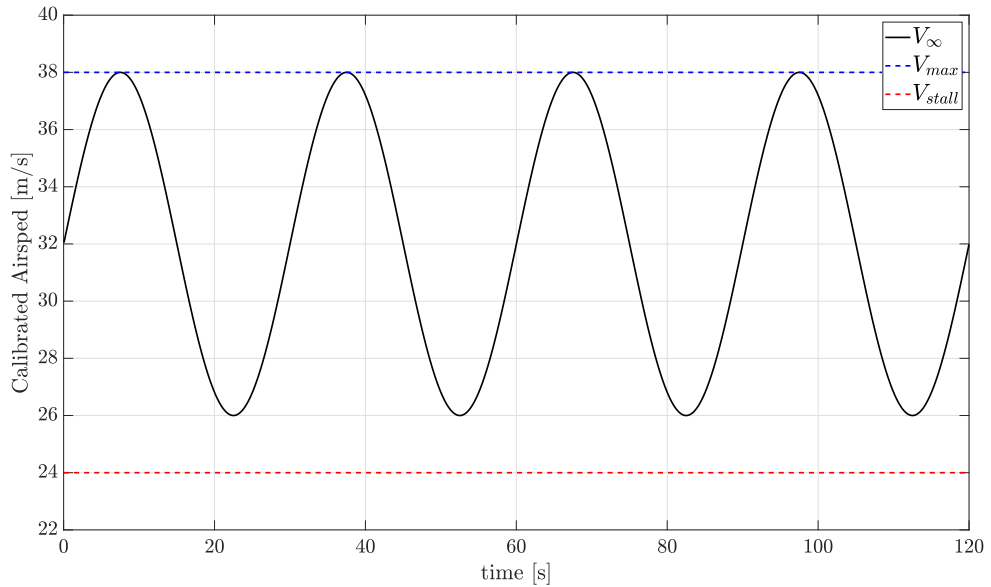

Figure 7.2: Velocity Variation during Phugoid Oscillations

127

Nominal controller tracking response to roll commands is given in Figure 7.3. As seen from the figure, the roll tracking performance is not acceptable.
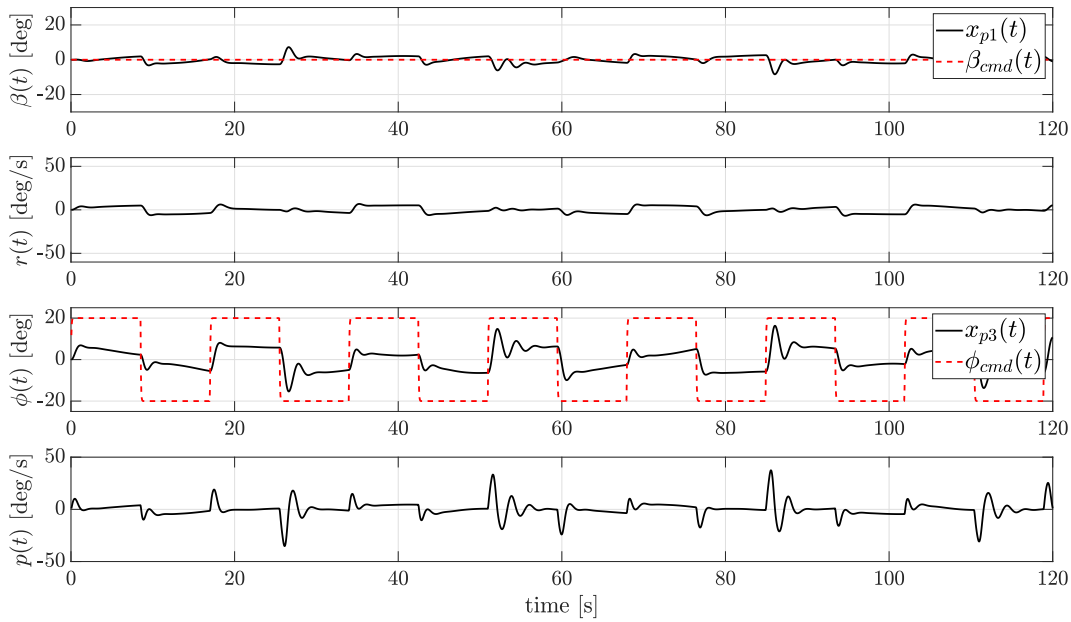

Figure 7.3: Command Tracking Performance of the Nominal Controller

Next, the standard MRAC is applied to suppress the effects of matched uncertainties, while leaving the unmatched part of the uncertainty as it is. Figure 7.4 presents the corresponding command tracking performance. Although the roll state tracks the command better, it is not still within the acceptable limits. Furthermore, excessive sideslip angles are encountered during bank maneuvers, which results in uncoordinated turn maneuvers.

In Figure 7.5, estimated matched uncertainty is illustrated with Standard MRAC. It is clear from the figure that estimated matched uncertainty is considerably aligned with the actual matched uncertainty (see top two plots). However, undesired high-frequency variations appear here and there in the matched uncertainty estimation with Standard MRAC. In the presence of time-delays and/or actuation constraints, these high-frequency variations may result in instability.

As the third controller, CMRAC is applied to the problem of interest. Corresponding command tracking results and matched uncertainty estimation performance are illustrated in Figure 7.6 and Figure 7.7, respectively. High-frequency oscillations that
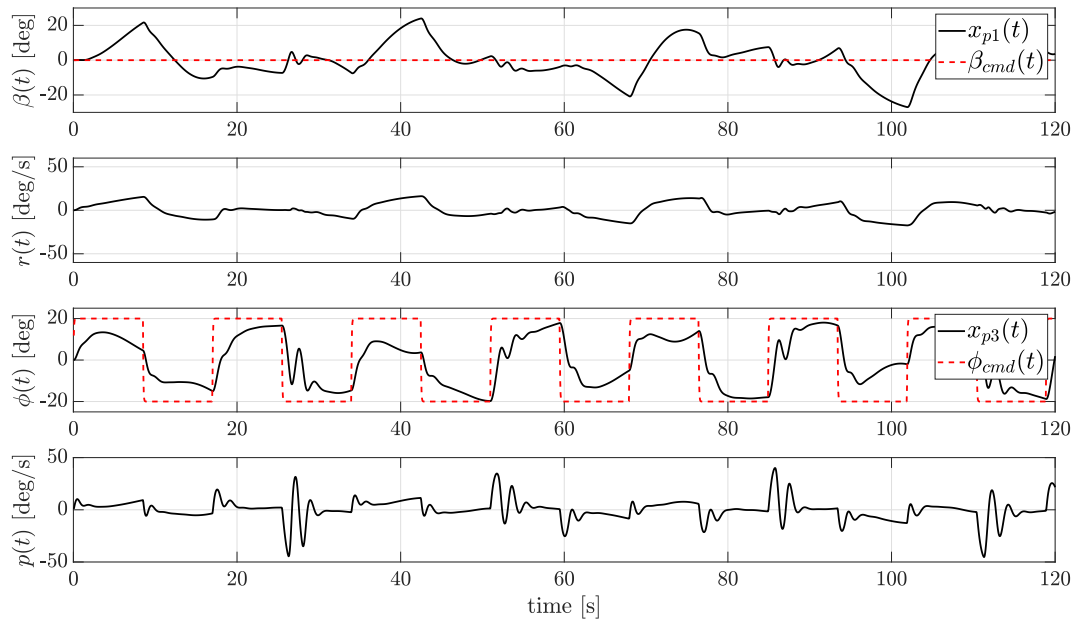
Figure 7.4: Command Tracking Performance of the Standard MRAC
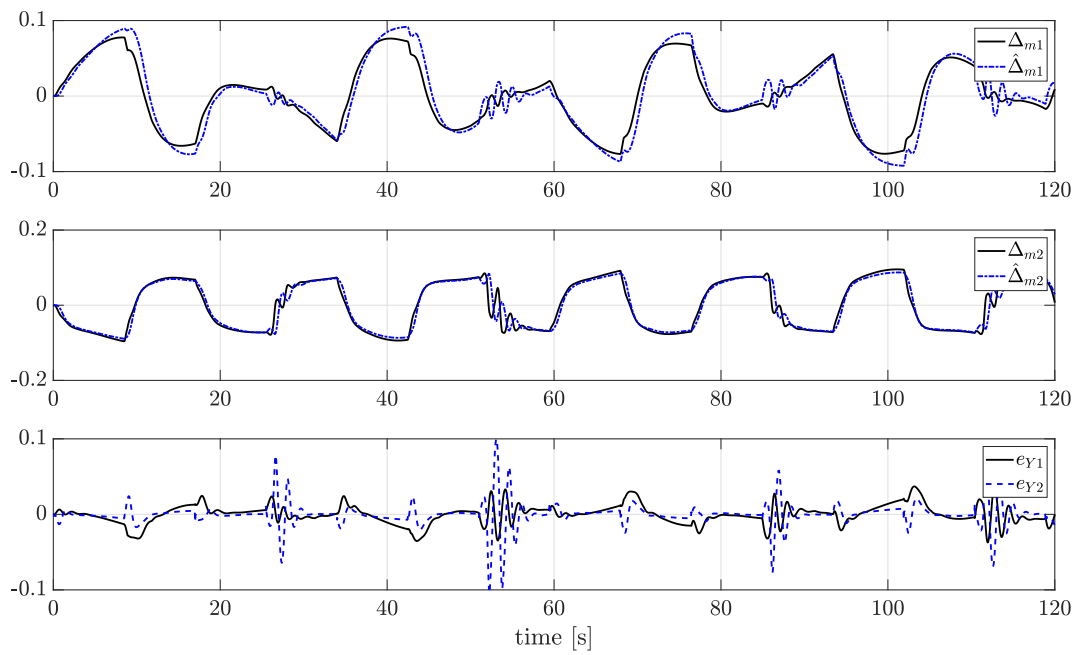
Figure 7.5: Matched Uncertainty Estimation for the Standard MRAC

are encountered in Standard MRAC are gone with the CMRAC as seen in Figure 7.7. In addition, it is clear from the figure that estimated matched uncertainty overlaps with the actual unknown uncertainty in CMRAC, which yields smooth systems signals. As opposed to Standard MRAC, the success of CMRAC in suppressing the error signal

129

e_Y is evident from the figure. However, the tracking performance is not acceptable even with (almost) perfect estimation of the matched uncertainty due to presence of unmatched uncertainties. Furthermore, bank maneuvers still induce unacceptably large sideslip angles (see Figure 7.6).

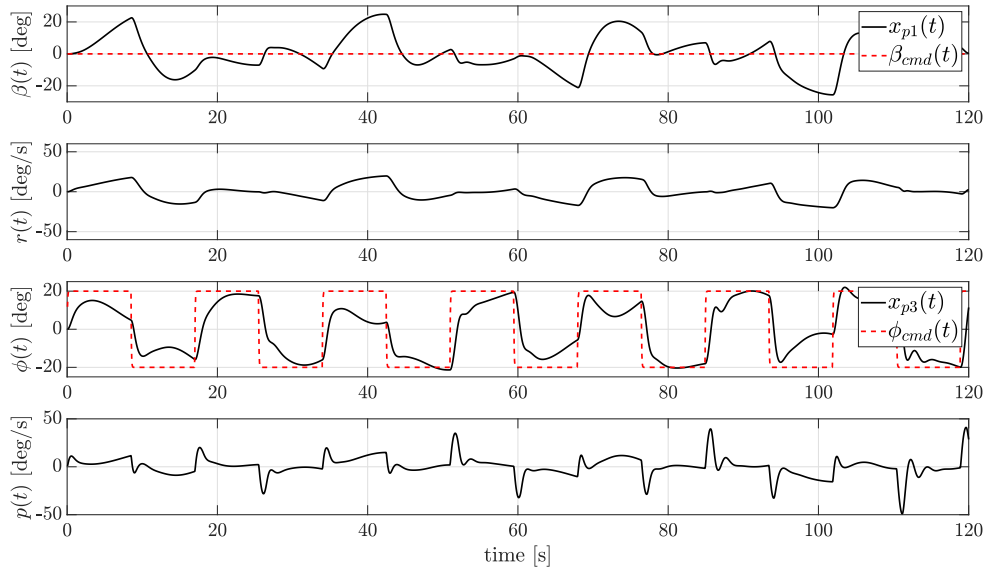
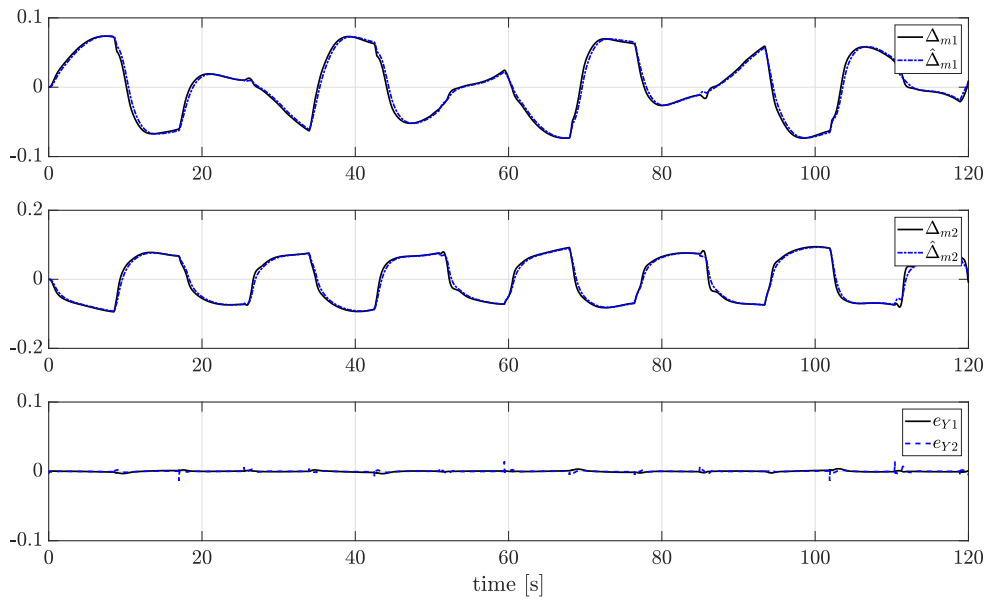Figure 7.6: Command Tracking Performance of the CMRAC

Figure 7.7: Matched Uncertainty Estimation for the CMRAC

130

Lastly, the simulation results for the proposed Command Governor-based MRAC (CG-MRAC) framework are presented. Figure 7.8 illustrates the corresponding command tracking performance. As seen from the figure, desired tracking is achieved as soon as the unmatched uncertainties are taken into account with command governor. In addition, one can immediately observe that induced sideslip angles are drastically decreased compared to aforementioned controllers.
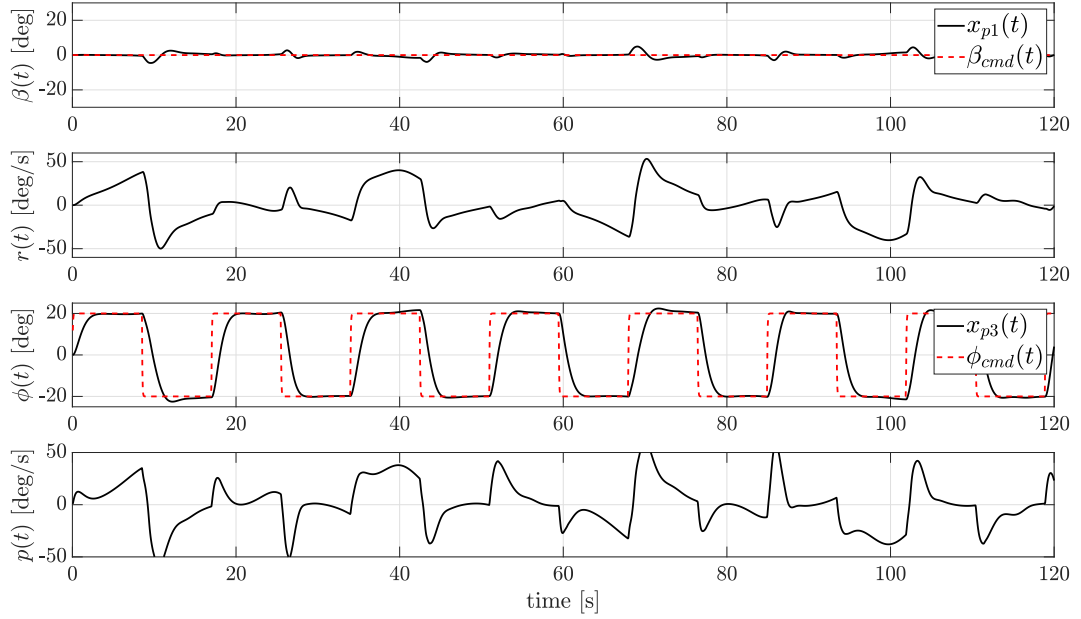
Figure 7.8: Command Tracking Performance of the Proposed CG-MRAC

Figure 7.9 compares the transformed states x, auxiliary reference model states x_m, and ideal reference model states x_r. As seen from the figure, transformed system states overlap with the auxiliary reference model states. Additionally, auxiliary reference model satisfactorily follows the ideal reference model in the controlled output channels (sideslip and roll). Figure 7.10 illustrates the matched uncertainty estimation performance of the Command Governor-based MRAC. One of the driving errors for the weight update law in Eq 7.21 is the error signal e_Y. Hence, it is expected from the adaptive law that error e_Y successfully suppressed. Indeed, this is the case as seen in Figure 7.10. However, matched uncertainty estimation performance is relatively degraded. Because, the driving tracking error in the adaptive law is the difference between auxiliary reference states and system states where it was the ideal reference model in standard MRAC and CMRAC. Yet,
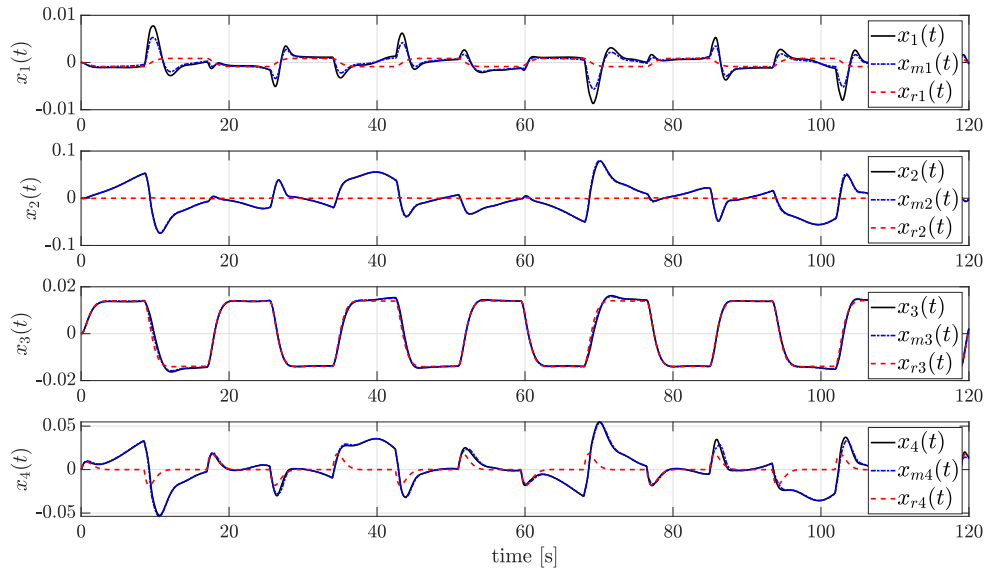
Figure 7.9: Transformed State Tracking Performance of the Proposed CG-MRAC

having relatively small error e_Y, $e_Y \cong 0$, is sufficient to reach the desired tracking response. Figure 7.11 presents the unmatched uncertainty estimation performance for CG-MRAC. Estimated unmatched uncertainty is almost aligned with the actual unmatched uncertainty. In fact, the success in the unmatched uncertainty estimation is the main reason to obtain the desired command tracking in Figure 7.8.
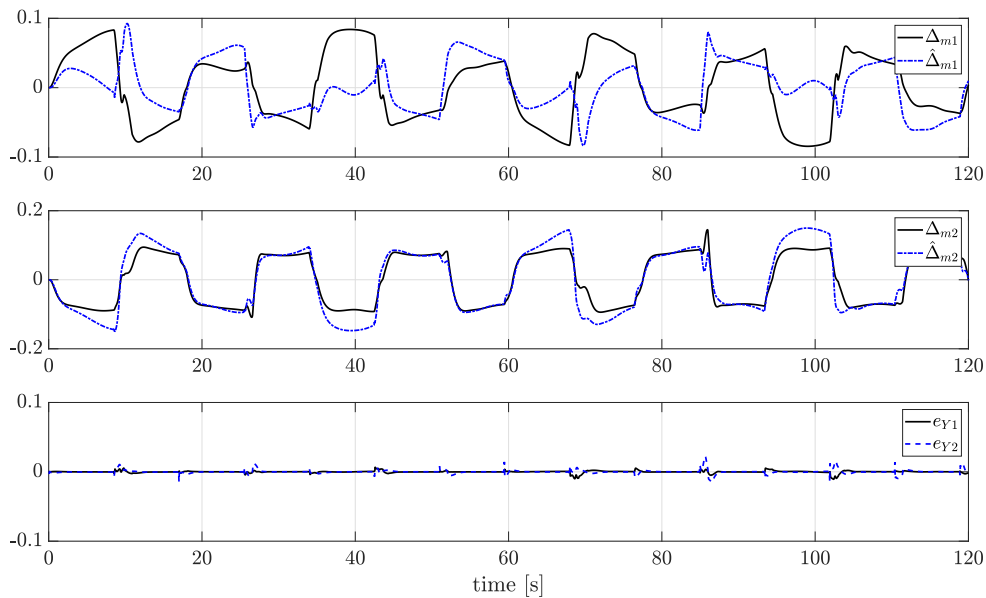
Figure 7.10: Matched Uncertainty Estimation for the Proposed CG-MRAC
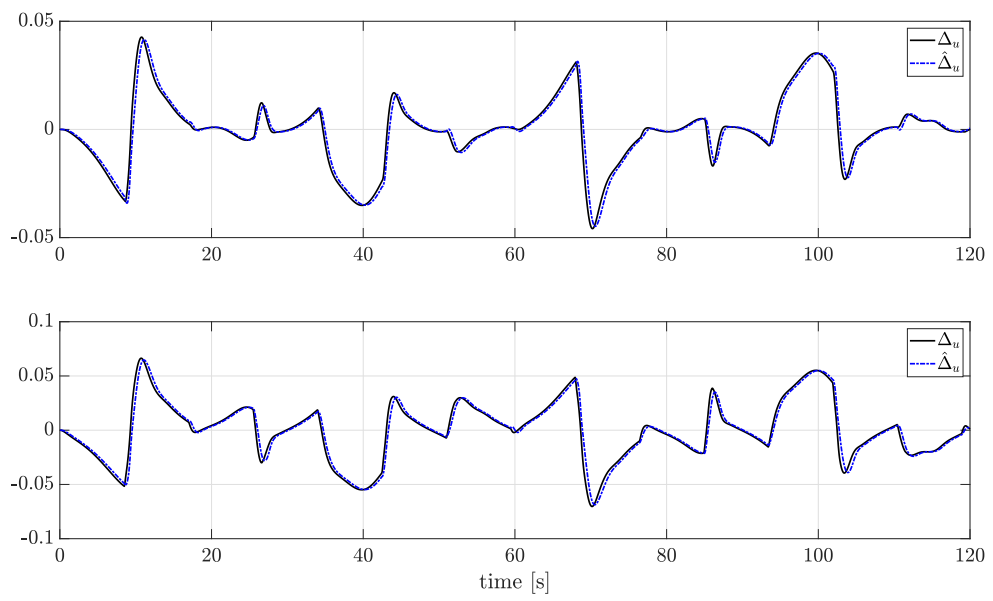
Figure 7.11: Unmatched Uncertainty Estimation for the Proposed CG-MRAC

CHAPTER 8

CONCLUSION

8.1 Concluding Remarks

The intent of this thesis is to introduce improvements to filter-based adaptive controllers and novel adaptive control architectures. For this purpose, first an information recovery system is presented in Chapter 3 for Combined/Composite Model Reference Adaptive Controllers (CMRAC), called Information Recovery-based Model Reference Adaptive Control (IR-MRAC). In the presence of a poorly designed low-pass filter with an inappropriate bandwidth, command tracking performance of CMRAC is degraded as the low-pass filter suppresses the useful content for adaptation. With the proposed method, adverse effects of excessive filtering is eliminated by including the high-frequency signals in the adaptation. Furthermore, a time-varying learning rate is introduced to the adaptive laws that works as stability augmentation systems for the uncertainty estimation dynamics. Hence, undesired effects of included high-frequency signals are attenuated by the time-varying gain. In addition, new directions are added to weight update laws to achieve faster adaptation and parameter convergence without persistency of excitation. In order to show the efficacy of IR-MRAC, both numerical and software in-the-loop simulations are conducted, showing that it is practical and tractable in real applications. Then, IR-MRAC is extended to cover the underactuated systems with unknown control effectiveness in Chapter 4. Asymptotic stability of tracking error and parameter estimation error is ensured by separate identification of unknown control effectiveness and uncertain weight matrices with an indirect-direct adaptive control architecture. Chapter 5 introduces a new adaptive control framework to deal with systems having not only matched but also unmatched uncertainties. Specifically,

a command governor input is designed for the command tracking performance recovery that is affected by the unmatched uncertainty. Unlike the examples from the literature, the proposed Command Governor-based MRAC (CG-MRAC) is capable of dealing with arbitrary state-dependent matched and unmatched uncertainties, which is much harder and general case than bounded unmatched time-varying perturbations. CG-MRAC can also address the model reference adaptive control problems with ideal reference models that does not satisfy the matching condition. In this way, desired command tracking performance can be defined with more flexible reference systems. Chapter 6 highlights the major issues in energy-based longitudinal flight control problems. Specifically, energy management of the aircraft should be properly carried out to achieve the desired and decoupled airspeed and altitude responses. Contributions from the previous chapters to filter-based adaptive controllers are applied to energy-based longitudinal flight control problem to ensure both Hamiltonian and Lagrangian dynamics operate at the same bandwidth. As a result, desired tracking performance is achieved in the presence of uncertainties. Improvements with the proposed energy-based adaptive controller is illustrated through high-fidelity nonlinear simulations of an unmanned aircraft (UAV). Lastly, contributions to unmatched systems in Chapter 5 are exploited to solve the gain scheduled lateral flight control problem in the presence of uncertainties in Chapter 7. Mathematical representation of nonlinear uncertain system dynamics is re-formulated assuming very little information is available for the aircraft model. In fact, the only assumption appears to be known sign of the control gain. With CG-MRAC being applied to the re-formulated uncertain system dynamics, the desired command following performance is achieved. Although the chapter is mainly concentrated on gain scheduling problem, new formulation of the system dynamics allows that the proposed method can readily be extended for parameter varying nonlinear systems and switched systems. The proposed lateral flight controller is also applied to a nonlinear parameter varying dynamics of a UAV to emphasize the contributions of the chapter. As a result, this dissertation has contributed a few improvements to filter-based adaptive control theory for fast adaptation and parameter convergence, and exemplified the contributions with real applications from the aerospace industry. Efficacy of the proposed methods are illustrated through numerical simulations, and rigorous closed-loop stability is established by Lyapunov's stability theorem.

8.2 Future Research Directions

Following studies could be the future research directions:

- The results can be extended to output feedback adaptive control.

- A rigorous mathematics can be carried out to tune newly introduced design parameters. For instance, to what extend the high-frequency content should be involved in the adaptation? With further transient analysis, the choice of newly introduced learning rates can be clarified.

- An immediate extension to presented works becomes the adaptive control uncertain systems with time-varying ideal parameters. In that regard, Swapping Lemma can be used to extract more information about the time-varying weights.

- Efficacy of the proposed method in the presence of unknown control effectiveness is illustrated with several examples. These results can be extended to cover the overactuated systems. This extensions opens new research directions in the adaptive control allocation field.

- Results of Chapter 5 on unmatched systems can be extended to cover nonlinear parameter varying systems and switching systems. A real world example could be a damage in the aircraft structure.

REFERENCES

[1] G. Tao, *Adaptive Control Design and Analysis*. New York, NY, USA: John Wiley & Sons, Inc., 2003.

[2] S. Boyd and S. S. Sastry, "Necessary and sufficient conditions for parameter convergence in adaptive control," *Automatica*, vol. 22, no. 6, pp. 629–639, 1986.

[3] P. A. Ioannou and P. V. Kokotovic, "Instability analysis and improvement of robustness of adaptive control," *Automatica*, vol. 20, no. 5, pp. 583–594, 1984.

[4] K. S. Narendra and A. Annaswamy, "A new adaptive law for robust adaptation without persistent excitation," *IEEE Transactions on Automatic control*, vol. 32, no. 2, pp. 134–145, 1987.

[5] J.-B. Pomet and L. Praly, "Adaptive nonlinear regulation: estimation from the lyapunov equation," *IEEE Transactions on Automatic Control*, vol. 37, no. 6, pp. 729–740, 1992.

[6] N. Nguyen, K. Krishnakumar, and J. Boskovic, "An optimal control modification to model-reference adaptive control for fast adaptation," *AIAA Guidance, Navigation and Control Conference*, 2008.

[7] A. J. Calise, T. Yucelen, J. A. Muse, and B.-J. Yang, "A loop recovery method for adaptive control," *AIAA Guidance, Navigation and Control Conference*, 2009.

[8] K. Kim, T. Yucelen, and A. J. Calise, "K-modification in adaptive control," *AIAA Infotech Conference*, 2010.

[9] T. Yucelen and A. J. Calise, "Kalman filter modification in adaptive control," *Journal of Guidance, Control, and Dynamics*, vol. 33, no. 2, pp. 426–439, 2010.

[10] J.-J. E. Slotine and W. Li, "Composite adaptive control of robot manipulators," *Automatica*, vol. 25, no. 4, pp. 509–519, 1989.

[11] E. Lavretsky, "Combined/composite model reference adaptive control," *IEEE Transactions on Automatic Control*, vol. 54, no. 11, pp. 2692–2697, 2009.

[12] G. Chowdhary, T. Yucelen, M. Mühlegg, and E. N. Johnson, "Concurrent learning adaptive control of linear systems with exponentially convergent bounds," *International Journal of Adaptive Control and Signal Processing*, vol. 27, no. 4, pp. 280–301, 2013.

[13] K. Volyanskyy, A. J. Calise, B.-J. Yang, and E. Lavretsky, "An error minimization method in adaptive control," *AIAA Guidance Navigation and Control Conference*, 2006.

[14] A. I. Glushchenko, V. A. Petrov, and K. A. Lastochkin, "Adaptive control system with a variable adjustment law gain based on the recursive least squares method," *Automation and Remote Control*, vol. 82, no. 4, pp. 619–633, 2021.

[15] V. Adetola and M. Guay, "Performance improvement in adaptive control of linearly parameterized nonlinear systems," *IEEE Transactions on Automatic Control*, vol. 55, no. 9, pp. 2182–2186, 2010.

[16] L. Höcht, A. Maity, and F. Holzapfel, "Frequency selective learning model reference adaptive control," *IET Control Theory & Applications*, vol. 9, no. 15, pp. 2257–2265, 2015.

[17] J. Na, J. Yang, and G. Gao, "Reinforcing transient response of adaptive control systems using modified command and reference model," *IEEE Transactions on Aerospace and Electronic Systems*, vol. 56, no. 3, pp. 2005–2017, 2019.

[18] Y. Pan, S. Aranovskiy, A. Bobtsov, and H. Yu, "Efficient learning from adaptive control under sufficient excitation," *International Journal of Robust and Nonlinear Control*, vol. 29, no. 10, pp. 3111–3124, 2019.

[19] D.-D. Zheng, Y. Pan, K. Guo, and H. Yu, "Identification and control of nonlinear systems using neural networks: A singularity-free approach," *IEEE Transactions on Neural Networks and Learning Systems*, vol. 30, no. 9, pp. 2696–2706, 2019.

[20] S. Basu Roy and S. Bhasin, "Novel model reference adaptive control architecture using semi-initial excitation-based switched parameter estimator," *International Journal of Adaptive Control and Signal Processing*, vol. 33, no. 12, pp. 1759–1774, 2019.

[21] T. Ma, "Filtering adaptive neural network controller for multivariable nonlinear systems with mismatched uncertainties," *International Journal of Robust and Nonlinear Control*, vol. 30, no. 12, pp. 4565–4583, 2020.

[22] K. W. Lee and S. Singh, "Composite adaptive attitude control of asteroid-orbiting spacecraft with regressor integral excitation," *IEEE Transactions on Aerospace and Electronic Systems*, 2022.

[23] X. Shao, Q. Hu, D. Li, Y. Shi, and B. Yi, "Composite adaptive control for anti-unwinding attitude maneuvers: An exponential stability result without persistent excitation," *IEEE Transactions on Aerospace and Electronic Systems*, 2022.

[24] T. Yucelen and W. M. Haddad, "Low-frequency learning and fast adaptation in model reference adaptive control," *IEEE Transactions on Automatic Control*, vol. 58, no. 4, pp. 1080–1085, 2012.

[25] N. Nguyen, J. Burken, and C. Hanson, "Optimal control modification adaptive law with covariance adaptive gain adjustment and normalization," in *AIAA Guidance, Navigation, and Control Conference*, p. 6606, 2011.

[26] H.-J. Shieh, J.-H. Siao, and Y.-C. Liu, "A robust optimal sliding-mode control approach for magnetic levitation systems," *Asian Journal of Control*, vol. 12, no. 4, pp. 480–487, 2010.

[27] M. L. Fravolini and G. Campa, "Integrated design of a linear/neuro-adaptive controller in the presence of norm-bounded uncertainties," *International Journal of Control*, vol. 84, no. 10, pp. 1664–1677, 2011.

[28] C. D. Heise and F. Holzapfel, "Uniform ultimate boundedness of a model reference adaptive controller in the presence of unmatched parametric uncertainties," *IEEE International Conference on Automation, Robotics and Applications*, 2015.

[29] B.-J. Yang, T. Yucelen, J.-Y. Shin, and A. Calise, "LMI-based analysis of an adaptive flight control system with unmatched uncertainty," *AIAA Infotech Aerospace*, 2010.

[30] A. J. Koshkouei, A. Zinober, and K. J. Burnham, "Adaptive sliding mode backstepping control of nonlinear systems with unmatched uncertainty," *Asian Journal of Control*, vol. 6, no. 4, pp. 447–453, 2004.

[31] S. Wang, D. Yu, and D. Yu, "Compensation for unmatched uncertainty with adaptive rbf network," *International Journal of Engineering, Science and Technology*, vol. 3, no. 6, pp. 35–43, 2011.

[32] E. Xargay, N. Hovakimyan, and C. Cao, "$\mathcal{L}_1$ adaptive controller for multi-input multi-output systems in the presence of nonlinear unmatched uncertainties," *American Control Conference, 2010*, 2010.

[33] V. Stepanyan and K. Krishnakumar, "State and output feedback certainty equivalence m-mrac for systems with unmatched uncertainties," *Asian Journal of Control*, vol. 17, no. 6, pp. 2041–2054, 2015.

[34] M. Yayla and A. T. Kutay, "Adaptive control algorithm for linear systems with matched and unmatched uncertainties," *IEEE Conference on Decision and Control*, 2016.

[35] A. Arabi, T. Yucelen, and B. C. Gruenwald, "Model reference adaptive control for uncertain dynamical systems with unmatched disturbances: A command governor-based approach," *Robotics and Mechatronics for Agriculture*, 2017.

[36] M. Yayla, E. Arabi, A. T. Kutay, and T. Yucelen, "Command governor-based adaptive control for dynamical systems with matched and unmatched uncertainties," *International Journal of Adaptive Control and Signal Processing*, vol. 32, no. 8, pp. 1124–1144, 2018.

[37] H. R. Shafei, M. Bahrami, and H. A. Talebi, "Disturbance observer-based two-layer control strategy design to deal with both matched and mismatched uncertainties," *International Journal of Robust and Nonlinear Control*, vol. 31, no. 5, pp. 1640–1656, 2021.

[38] M. Pan, Y. Xu, B. Gu, J. Huang, and Y.-H. Chen, "Fuzzy-set theoretic control design for aircraft engine hardware-in-the-loop testing: mismatched uncertainty and optimality," *IEEE Transactions on Industrial Electronics*, vol. 69, no. 7, pp. 7223–7233, 2021.

[39] J. Yang, J. Na, and G. Gao, "Robust adaptive control for unmatched systems with guaranteed parameter estimation convergence," *International Journal of Adaptive Control and Signal Processing*, vol. 33, no. 12, pp. 1868–1884, 2019.

[40] J. D. Boskovic and Z. Han, "Certainty equivalence adaptive control of plants with unmatched uncertainty using state feedback," *IEEE Transactions on Automatic Control*, vol. 54, no. 8, pp. 1918–1924, 2009.

[41] J. Reiner, G. J. Balas, and W. L. Garrard, "Flight control design using robust dynamic inversion and time-scale separation," *Automatica*, vol. 32, no. 11, pp. 1493–1504, 1996.

[42] D. McLean, *Automatic flight control systems(Book)*. Englewood Cliffs, NJ, Prentice Hall, 1990, 606, 1990.

[43] W. Durham, *Aircraft flight dynamics and control*. John Wiley & Sons, 2013.

[44] M. V. Cook, *Flight dynamics principles: a linear systems approach to aircraft stability and control*. Butterworth-Heinemann, 2012.

[45] F. Gavilan, J. Acosta, and R. Vazquez, "Control of the longitudinal flight dynamics of an uav using adaptive backstepping," *IFAC Proceedings Volumes*, vol. 44, no. 1, pp. 1892–1897, 2011.

[46] D. Karagiannis and A. Astolfi, "Nonlinear and adaptive flight control of autonomous aircraft using invariant manifolds," *Proceedings of the Institution of Mechanical Engineers, Part G: Journal of Aerospace Engineering*, vol. 224, no. 4, pp. 403–415, 2010.

[47] A. Kurdjukov, G. Natchinkina, and A. Shevtchenko, "Energy approach to flight control," in *Guidance, Navigation, and Control Conference and Exhibit*, p. 4211, 1998.

[48] A. Lambregts, "Functional integration of vertical flight path and speed control using energy principles," tech. rep., NASA Langley Research Center, 1984.

[49] L. F. Faleiro and A. Lambregts, "Analysis and tuning of a total energy control system control law using eigenstructure assignment," *Aerospace science and technology*, vol. 3, no. 3, pp. 127–140, 1999.

[50] B. of Inquiry, "Preliminary report on the accident on june 30, 1994 in toulouse-blagnac (31) to airbus a330 no 42 of airbus industry, registration fwwkh," 1994.

[51] A. Lambregts, "Total energy based flight control system," Aug. 1985. US Patent 4,536,843.

[52] A. Lambregts, "Vertical flight path and speed control autopilot design using total energy principles," in *Guidance and Control Conference*, p. 2239, 1983.

[53] A. Lambregts, "Integrated system design for flight and propulsion control using total energy principles," in *Aircraft design, systems and technology meeting*, p. 2561, 1983.

[54] A. Lambregts, "Operational aspects of the integrated vertical flight path and speed control system," *SAE Transactions*, pp. 29–41, 1983.

[55] R. Akmeliawati and I. M. Mareels, "Nonlinear energy-based control method for aircraft automatic landing systems," *IEEE Transactions on Control Systems Technology*, vol. 18, no. 4, pp. 871–884, 2009.

[56] P. Jimenez, P. Lichota, D. Agudelo, and K. Rogowski, "Experimental validation of total energy control system for uavs," *Energies*, vol. 13, no. 1, p. 14, 2020.

[57] K. Bruce, "Nasa b737 flight test results of the total energy control system," tech. rep., Boeing Commercial Airplane Company, Seattle, WA, 1987.

[58] S. Wang, Z. Zhen, J. Jiang, and X. Wang, "Flight tests of autopilot integrated with fault-tolerant control of a small fixed-wing uav," *Mathematical Problems in Engineering*, vol. 2016, 2016.

[59] J. Brigido-González and H. Rodriguez-Cortes, "Adaptive energy based control for the longitudinal dynamics of a fixed-wing aircraft," in *2014 American Control Conference*, pp. 715–720, IEEE, 2014.

[60] J. Brigido-González and H. Rodríguez-Cortés, "Experimental validation of an adaptive total energy control system strategy for the longitudinal dynamics of a fixed-wing aircraft," *Journal of Aerospace Engineering*, vol. 29, no. 1, p. 04015024, 2016.

[61] M. Lamp and R. Luckner, "The total energy control concept for a motor glider," in *2nd CEAS Specialist Conference on Guidance, Navigation and Control*, pp. 1344–1363, 2013.

[62] P. Chudy and P. Rzucidlo, "Tecs/thcs based flight control system for general aviation," in *AIAA modeling and simulation technologies conference*, p. 5689, 2009.

[63] M. Lamp and R. Luckner, "Automatic landing of a high-aspect-ratio aircraft without using the thrust," in *Advances in Aerospace Guidance, Navigation and Control*, pp. 549–567, Springer, 2015.

[64] Y.-C. Lai and W. O. Ting, "Design and implementation of an optimal energy control system for fixed-wing unmanned aerial vehicles," *Applied Sciences*, vol. 6, no. 11, p. 369, 2016.

[65] A. M. Shevchenko, "Energy-based approach for flight control systems design," *Automation and Remote Control*, vol. 74, no. 3, pp. 372–384, 2013.

[66] T. Giusti Degaspare and K. Kienitz, "More integrated total energy control law for longitudinal automatic flight control system design," in *AIAA Scitech Forum*, p. 0606, 2020.

[67] M. E. Argyle and R. W. Beard, "Nonlinear total energy control for the longitudinal dynamics of an aircraft," in *American Control Conference*, pp. 6741–6746, IEEE, 2016.

[68] C. Voth and U.-L. Ly, "Design of a total energy control autopilot using constrained parameter optimization," *Journal of Guidance, Control, and Dynamics*, vol. 14, no. 5, pp. 927–935, 1991.

[69] R. Nuriwati and R. A. Sasongko, "Development flight path control for unmanned combat aerial vehicle (ucav) using total energy control system (tecs)," *IOP Conference Series: Materials Science and Engineering*, vol. 645, 2019.

[70] Viswanathan, A. Kale, G. K. Singhz, and V. V. Patel, "L1 adaptive-output feedback based energy control," in *2015 European Control Conference (ECC)*, pp. 2792–2797, IEEE, 2015.

[71] G. Looye and H.-D. Joos, "Design of autoland controller functions with multiobjective optimization," *Journal of guidance, control, and dynamics*, vol. 29, no. 2, pp. 475–484, 2006.

[72] G. H. Looye, *An Integrated Approach to Aircraft Modelling and Flight Control Law Design. 2008*. PhD thesis, Doctoral thesis Delft University of Technology, 2008.

[73] R. Rysdyk and R. Agarwal, "Nonlinear adaptive flight path and speed control using energy principles," in *AIAA Guidance, Navigation, and Control Conference and Exhibit*, p. 4440, 2002.

[74] P. A. Ioannou and J. Sun, *Robust Adaptive Control*. Control Theory, PTR Prentice-Hall, 1996.

[75] E. Lavretsky and K. Wise, *Robust and Adaptive Control: With Aerospace Applications*. Advanced Textbooks in Control and Signal Processing, Springer London, 2012.

[76] S. N. Singh, W. Yirn, and W. R. Wells, "Direct adaptive and neural control of wing-rock motion of slender delta wings," *Journal of Guidance, Control, and Dynamics*, vol. 18, no. 1, pp. 25–30, 1995.

[77] J. Park and I. W. Sandberg, "Universal approximation using radial basis function networks," *Neural computation*, vol. 3, no. 2, pp. 246–257, 1991.

[78] J. P. Hespanha, *Linear Systems Theory*. Princeton University Press, 2018.

[79] H. K. Khalil, *Nonlinear Systems*. Prentice Hall, 2002.

[80] E. Lavretsky, T. E. Gibson, and A. M. Annaswamy, "Projection operator in adaptive systems," 2011.

[81] T. Yucelen, G. De La Torre, and E. N. Johnson, "Improving transient performance of adaptive control architectures using frequency-limited system error dynamics," *International Journal of Control*, vol. 87, no. 11, pp. 2383–2397, 2014.

[82] J. Sun, "A modified model reference adaptive control scheme for improved transient performance," *IEEE Transactions on Automatic Control*, vol. 38, no. 8, pp. 1255–1259, 1993.

[83] E. Lavretsky, "Reference dynamics modification in adaptive controllers for improved transient performance," *AIAA guidance, navigation, and control conference*, p. 6200, 2011.

[84] T. Gibson, A. Annaswamy, and E. Lavretsky, "Improved transient response in adaptive control using projection algorithms and closed loop reference models," *AIAA Guidance, Navigation, and Control Conference*, p. 4775, 2012.

[85] J. Yang, J. Na, and G. Gao, "Robust model reference adaptive control for transient performance enhancement," *International Journal of Robust and Nonlinear Control*, vol. 30, no. 15, pp. 6207–6228, 2020.

[86] M. A. Duarte and K. S. Narendra, "Combined direct and indirect approach to adaptive control," *IEEE Transactions on Automatic Control*, vol. 34, no. 10, pp. 1071–1075, 1989.

[87] K. S. Narendra and A. M. Annaswamy, *Stable adaptive systems*. Courier Corporation, 2012.

[88] E. Lavretsky, T. E. Gibson, and A. M. Annaswamy, "Projection operator in adaptive systems," *arXiv preprint arXiv:1112.4232v6*, 2012.

[89] N. Cho, H.-S. Shin, Y. Kim, and A. Tsourdos, "Composite model reference adaptive control with parameter convergence under finite excitation," *IEEE Transactions on Automatic Control*, vol. 63, no. 3, pp. 811–818, 2017.

[90] A. Maity, L. Höcht, and F. Holzapfel, "Higher order direct model reference adaptive control with generic uniform ultimate boundedness," *International Journal of Control*, vol. 88, no. 10, pp. 2126–2142, 2015.

[91] J. Na, G. Herrmann, and K. Zhang, "Improving transient performance of adaptive control via a modified reference model and novel adaptation," *International Journal of Robust and Nonlinear Control*, vol. 27, no. 8, pp. 1351–1372, 2017.

[92] K. S. Miller, "On the inverse of the sum of matrices," *Mathematics magazine*, vol. 54, no. 2, pp. 67–72, 1981.

[93] G. Dahlquist and Å. Björck, *Numerical methods*. Courier Corporation, 2003.

[94] Laminar Research, "X-plane: Flight simulator," *X-Plane Version 11*, 2022.

[95] Drela, M. and Youngren, H., "Athena vortex lattice," *AVL 3.6*, 2022.

[96] D. S. Bernstein, "Matrix mathematics: Theory, facts, and formulas," in *Matrix Mathematics*, Princeton university press, 2009.

[97] T. Yucelen and A. J. Calise, "Derivative-free model reference adaptive control," *Journal of Guidance, Control, and Dynamics*, vol. 34, no. 4, pp. 933–950, 2011.

[98] T. E. Gibson, A. M. Annaswamy, and E. Lavretsky, "Adaptive systems with closed-loop reference models: Stability, robustness and transient performance," *arXiv preprint arXiv:1201.4897*, 2012.

[99] V. Stepanyan and K. Krishnakumar, "Adaptive control with reference model modification," *Journal of Guidance, Control and Dynamics*, vol. 35, no. 4, pp. 1370–1374, 2012.

[100] T. Bierling, M. Muhlegg, F. Holzapfel, and R. Maier, "Reference model modification for robust performance conservation of model reference adaptive controllers," *AIAA Guidance, Navigation, and Control Conference*, 2013.

[101] W. M. Haddad and V. Chellaboina, *Nonlinear dynamical systems and control: A Lyapunov-based approach*. Princeton University Press, 2008.

[102] T. H. Go, *Aircraft wing rock dynamics and control*. PhD thesis, Massachusetts Institute of Technology, 1999.

[103] R. W. Beard and T. W. McLain, *Small unmanned aircraft: Theory and practice*. Princeton university press, 2012.

[104] Y. Yildiz, M. Unel, and A. E. Demirel, "Nonlinear hierarchical control of a quad tilt-wing uav: An adaptive control approach," *International journal of adaptive control and signal processing*, vol. 31, no. 9, pp. 1245–1264, 2017.

[105] D. P. Wiese, *Systematic adaptive control design using sequential loop closure*. PhD thesis, Massachusetts Institute of Technology, 2016.

[106] D. P. Wiese, A. M. Annaswamy, J. A. Muse, M. A. Bolender, and E. Lavretsky, "Sequential loop closure based adaptive output feedback," *IEEE Access*, vol. 5, pp. 23436–23451, 2017.

[107] E. Arabi, T. Yucelen, R. Sipahi, and Y. Yildiz, "Human-in-the-loop systems with inner and outer feedback control loops: Adaptation, stability conditions, and performance constraints," in *AIAA Scitech Forum*, p. 2183, 2019.

[108] L. Fiorentini, A. Serrani, M. A. Bolender, and D. B. Doman, "Nonlinear robust adaptive control of flexible air-breathing hypersonic vehicles," *Journal of guidance, control, and dynamics*, vol. 32, no. 2, pp. 402–417, 2009.

[109] W. J. Rugh and J. S. Shamma, "Research on gain scheduling," *Automatica*, vol. 36, no. 10, pp. 1401–1425, 2000.

[110] A. Fujimori, H. Tsunetomo, and Z.-Y. Wu, "Gain-scheduled control using fuzzy logic and its application to flight control," *Journal of guidance, control, and dynamics*, vol. 22, no. 1, pp. 175–178, 1999.

[111] C. H. Lee, M. H. Shin, and M. J. Chung, "A design of gain-scheduled control for a linear parameter varying system: an application to flight control," *Control Engineering Practice*, vol. 9, no. 1, pp. 11–21, 2001.

[112] J. Jang, A. M. Annaswamy, and E. Lavretsky, "Adaptive control of time-varying systems with gain-scheduling," in *2008 American Control Conference*, pp. 3416–3421, IEEE, 2008.

[113] J. Zhang, X. Xu, L. Yang, and X. Yang, "Lpv model-based multivariable indirect adaptive control of damaged asymmetric aircraft," *Journal of Aerospace Engineering*, vol. 32, no. 6, p. 04019095, 2019.

[114] D. Luenberger, "Canonical forms for linear multivariable systems," *IEEE Transactions on Automatic Control*, vol. 12, no. 3, pp. 290–293, 1967.

[115] R. Minzner, "The 1976 standard atmosphere and its relationship to earlier standards," *Reviews of geophysics*, vol. 15, no. 3, pp. 375–384, 1977.

Appendix A - Scheduled Lateral Matrices

$$
A_{p0,CAS24} = \begin{bmatrix} -0.17 & -1.0 & 0.37 & 0.12 \\ 3.0 & -1.35 & 0.0 & -2.35 \\ 0.0 & 0.12 & 0 & 1.0 \\ -0.05 & 6.4 & 0.0 & -6.04 \end{bmatrix}, \quad B_{p0,CAS24} = \begin{bmatrix} -0.08 & -0.003 \\ 6.42 & 0.79 \\ 0.0 & 0.0 \\ -2.48 & 13.34 \end{bmatrix}
$$

$$
A_{p0,CAS25} = \begin{bmatrix} -0.18 & -1.0 & 0.35 & 0.09 \\ 3.1 & -1.25 & 0.0 & -2.34 \\ 0.0 & 0.09 & 0.0 & 1.0 \\ -0.25 & 5.98 & 0.0 & -6.96 \end{bmatrix}, \quad B_{p0,CAS25} = \begin{bmatrix} -0.08 & -0.004 \\ 7.01 & 0.82 \\ 0.0 & 0.0 \\ -2.72 & 15.3 \end{bmatrix}
$$

$$
A_{p0,CAS26} = \begin{bmatrix} -0.19 & -1.0 & 0.34 & 0.08 \\ 3.17 & -1.17 & 0.0 & -2.32 \\ 0.0 & 0.08 & 0.0 & 1.0 \\ -0.51 & 5.56 & 0.0 & -7.93 \end{bmatrix}, \quad B_{p0,CAS26} = \begin{bmatrix} -0.09 & -0.004 \\ 7.58 & 0.82 \\ 0.0 & 0.0 \\ -2.95 & 17.2 \end{bmatrix}
$$

$$
A_{p0,CAS27} = \begin{bmatrix} -0.20 & -1.0 & 0.33 & 0.065 \\ 3.24 & -1.08 & 0.0 & -2.29 \\ 0.0 & 0.065 & 0.0 & 1.0 \\ -0.8 & 5.17 & 0.0 & -8.78 \end{bmatrix}, \quad B_{p0,CAS27} = \begin{bmatrix} -0.09 & -0.004 \\ 8.21 & 0.82 \\ 0.0 & 0.0 \\ -3.18 & 19.07 \end{bmatrix}
$$

$$
A_{p0,CAS28} = \begin{bmatrix} -0.20 & -1.0 & 0.32 & 0.052 \\ 3.32 & -1.02 & 0.0 & -2.26 \\ 0.0 & 0.05 & 0.0 & 1.0 \\ -1.14 & 4.79 & 0.0 & -9.42 \end{bmatrix}, \quad B_{p0,CAS28} = \begin{bmatrix} -0.1 & -0.004 \\ 8.85 & 0.80 \\ 0.0 & 0.0 \\ -3.44 & 20.97 \end{bmatrix}
$$

$$
A_{p0,CAS29} = \begin{bmatrix} -0.21 & -1.0 & 0.306 & 0.04 \\ 3.39 & -0.94 & 0.0 & -2.22 \\ 0.0 & 0.04 & 0.0 & 1.0 \\ -1.49 & 4.47 & 0.0 & -9.69 \end{bmatrix}, \quad B_{p0,CAS29} = \begin{bmatrix} -0.1 & -0.004 \\ 9.49 & 0.78 \\ 0.0 & 0.0 \\ -3.68 & 22.87 \end{bmatrix}
$$

$$A_{p0,CAS30} = \begin{bmatrix} -0.21 & -1.0 & 0.29 & 0.03 \\ 3.47 & -0.88 & 0.0 & -2.18 \\ 0.0 & 0.03 & 0.0 & 1.0 \\ -1.87 & 4.21 & 0.0 & -9.96 \end{bmatrix}, \quad B_{p0,CAS30} = \begin{bmatrix} -0.11 & -0.004 \\ 10.16 & 0.74 \\ 0.0 & 0.0 \\ -3.93 & 24.77 \end{bmatrix}$$

$$A_{p0,CAS31} = \begin{bmatrix} -0.22 & -1.0 & 0.29 & 0.02 \\ 3.55 & -0.83 & 0.0 & -2.15 \\ 0.0 & 0.02 & 0.0 & 1.0 \\ -2.27 & 3.98 & 0.0 & -10.2 \end{bmatrix}, \quad B_{p0,CAS31} = \begin{bmatrix} -0.11 & -0.004 \\ 10.85 & 0.71 \\ 0.0 & 0.0 \\ -4.19 & 26.75 \end{bmatrix}$$

$$A_{p0,CAS32} = \begin{bmatrix} -0.23 & -1.0 & 0.28 & 0.013 \\ 3.63 & -0.79 & 0.0 & -2.12 \\ 0.0 & 0.013 & 0.0 & 1.0 \\ -2.67 & 3.78 & 0.0 & -10.48 \end{bmatrix}, \quad B_{p0,CAS32} = \begin{bmatrix} -0.11 & -0.004 \\ 11.58 & 0.67 \\ 0.0 & 0.0 \\ -4.47 & 28.77 \end{bmatrix}$$

$$A_{p0,CAS33} = \begin{bmatrix} -0.23 & -1.0 & 0.27 & 0.005 \\ 3.71 & -0.76 & 0.0 & -2.10 \\ 0.0 & 0.005 & 0.0 & 1.0 \\ -3.07 & 3.63 & 0.0 & -10.75 \end{bmatrix}, \quad B_{p0,CAS33} = \begin{bmatrix} -0.12 & -0.004 \\ 12.34 & 0.64 \\ 0.0 & 0.0 \\ -4.75 & 30.82 \end{bmatrix}$$

$$A_{p0,CAS34} = \begin{bmatrix} -0.24 & -1.0 & 0.26 & -0.001 \\ 3.79 & -0.73 & 0.0 & -2.08 \\ 0.0 & -0.001 & 0.0 & 1.0 \\ -3.49 & 3.48 & 0.0 & -11.01 \end{bmatrix}, \quad B_{p0,CAS34} = \begin{bmatrix} -0.12 & -0.004 \\ 13.11 & 0.60 \\ 0.0 & 0.0 \\ -5.04 & 32.91 \end{bmatrix}$$

$$A_{p0,CAS35} = \begin{bmatrix} -0.24 & -1.0 & 0.25 & -0.001 \\ 3.87 & -0.71 & 0.0 & -2.07 \\ 0.0 & -0.001 & 0.0 & 1.0 \\ -3.91 & 3.37 & 0.0 & -11.27 \end{bmatrix}, \quad B_{p0,CAS35} = \begin{bmatrix} -0.12 & -0.004 \\ 13.89 & 0.56 \\ 0.0 & 0.0 \\ -5.32 & 35.02 \end{bmatrix}$$

$$A_{p0,CAS36} = \begin{bmatrix} -0.25 & -1.0 & 0.25 & -0.013 \\ 3.96 & -0.69 & 0.0 & -2.05 \\ 0.0 & -0.013 & 0.0 & 1.0 \\ -4.35 & 3.27 & 0.0 & -11.53 \end{bmatrix}, \quad B_{p0,CAS36} = \begin{bmatrix} -0.13 & -0.004 \\ 14.67 & 0.52 \\ 0.0 & 0.0 \\ -5.62 & 37.18 \end{bmatrix}$$

Metehan YAYLA

PERSONAL DATA

BIRTH:	Ankara, Turkey	26 Aug, 1990
EMAIL:	metehanyayla@gmail.com
WEBPAGE:	http://www.ae.metu.edu.tr/~ymetehan/

EDUCATION

FEB 2023	Ph.D. in AEROSPACE ENGINEERING, **METU**, Ankara
AUG 2016	M.Sc. in AEROSPACE ENGINEERING, **METU**, Ankara
JUNE 2013	B.Sc. in AEROSPACE ENGINEERING, **METU**, Ankara

SELECTED PUBLICATIONS

[1] M Yayla, M. Senipek, A. T. Kutay, and O. Tekinalp. Adaptive flight control for aerodynamic interactions in multicopter evtol concept. In *Joint EUCASS & CEAS Conference*, 2023 (submitted).

[2] M. Senipek, M Yayla, A. T. Kutay, and O. Tekinalp. Mid-fidelity investigation of aerodynamic interactions on stability and control of evtol distributed propulsion. In *Joint EUCASS & CEAS Conference*, 2023 (submitted).

[3] M. Yayla and A. T. Kutay. Improved transient performance in filter-based adaptive control with aerospace applications. *IEEE Transactions on Aerospace and Electronic Systems*, 2022 (submitted).

[4] M Yayla and A. T. Kutay. A modification to adaptive control with time-varying learning rate for improved transient performance. In *AIAA SciTech Forum*, 2022.

[5] M. Yayla, A. T. Kutay, and A. Kutlu. Energy-based adaptive flight controller for imroved coordinated longitudinal control. In *AIAA SciTech Forum*, 2021.

[6] M. Yayla, A. T. Kutay, M. Senipek, and O. Gungor. An adaptive flight controller design for a tilt-prop fixed wing uav for all flight modes. In *AIAA SciTech Forum*, 2020 (Invited Session).

[7] M. Yayla, I. O. Uzunlar, and A. T. Kutay. A path planning algorithm for loiter maneuver: A limit cycle approach. *Ankara International Aerospace Conference*, 2019.

[8] M. Yayla, E. Arabi, A. T. Kutay, and T. Yucelen. Command governor-based adaptive control for dynamical systems with matched and unmatched uncertainties. *Int Journal of Adaptive Control and Signal Processing*, 32(8):1124–1144, 2018.

[9] M. Yayla and A. T. Kutay. Adaptive model predictive control of uncertain systems with input constraints. In *AIAA SciTech Forum*, 2017 (Invited Session).

[10] M. Yayla and A. T. Kutay. Adaptive control algorithm for linear systems with matched and unmatched uncertainties. In *2016 IEEE 55th Conference on Decision and Control (CDC)*, pages 2975–2980, . IEEE, 2016.

Work Experience

CURRENT MAY 2022	**Esen System Integration Ltd. Co.**, Ankara SENIOR FLIGHT MECHANICS AND CONTROL ENGINEER
MAY 2022 AUG 2019	**Esen System Integration Ltd. Co.**, Ankara RESEARCH SCIENTIST & ACADEMIC CONSULTANT
MAY 2022 NOV 2014	**Aerospace Engineering (AE), METU**, Ankara GRADUATE RESEARCH & TEACHING ASSISTANT
JUNE 2014 JUNE 2012	**Turkish Aerospace Industries Inc. (TAI)**, Ankara FLIGHT TEST ENGINEER

Miscellaneous Information

Memberships

AIAA Student Member
IEEE Student Member
IEEE Young Professionals
IEEE Control System Society (CSS)

Hobbies

Advanced Open Water Diver (PADI License #: 2205UV7981)
Skiing
Playing Chess
Playing Tennis

For the detailed CV including list of publications and detailed research experience,
please contact me.